

University of KwaZulu-Natal

**Metal Catalysed Cross-coupling Reactions of
Nitrogen and Fluorine containing Heterocyclic
compounds**

2016

Saba Alapour

**Metal Catalysed Cross-coupling Reactions of Nitrogen and
Fluorine containing Heterocyclic compounds**

A Thesis

Submitted in partial fulfillment for the requirements
for the award of the degree of

Doctor of Philosophy

in the

School of Chemistry and Physics

College of Agriculture, Engineering & Science,

By

Saba Alapour

2016

Supervisor: Prof. N.A. Koorbanally

Metal Catalysed Cross-coupling Reactions of Nitrogen and Fluorine containing Heterocyclic compounds

by

Saba Alapour

2016

A thesis submitted to the School of Chemistry, College of Agriculture, Engineering and Science, University of KwaZulu-Natal, for the degree of Doctor of Philosophy.

This thesis has been prepared according to **Format 4** as outlined in the guidelines from the College of Agriculture, Engineering and Science which states:

This is a thesis in which chapters are written as a set of discrete research papers, with an overall introduction and final discussion, where one (or all) of the chapters have either been submitted for publication or already been published. Typically these chapters will have been published in internationally recognized, peer- reviewed journals.

Preface

I hereby declare that the thesis entitled “**Metal Catalysed Cross-coupling Reactions of Nitrogen and Fluorine containing Heterocyclic compounds**” submitted to the University of KwaZulu-Natal for the award of degree of Doctor of Philosophy in Chemistry under the supervision of Professor Neil A. Koorbanally represents original work by the author and has not been submitted in full or part for any degree or diploma at this or any other University. Where use was made of the work of others it has been duly acknowledged in the text. This work was carried out at the School of Chemistry and Physics, University of KwaZulu-Natal, Westville campus, Durban, South Africa.

Signed: _____
Saba Alapour

As the candidate’s supervisor, I have approved this dissertation for submission

Signed: _____
Prof. Neil A. Koorbanally
Ph.D (Natal)

Declaration – Plagiarism

I, **Saba Alapour**, declare that:

1. The research reported in this thesis, except where otherwise indicated is my original research.
2. This thesis has not been submitted for any degree or examination at any other university.
3. This thesis does not contain other persons' data, pictures, graphs or other information, unless specifically acknowledged as being sourced from other persons.
4. This thesis does not contain other persons' writing, unless specifically acknowledged as being sourced from other researchers. Where other written sources have been quoted, then:
 - a) their words have been re-written but the general information attributed to them has been referenced.
 - b) or where their exact words have been used, then their writing has been placed in italics and inside quotation marks, and referenced.
5. This thesis does not contain text, graphics or tables copied and pasted from the internet, unless specifically acknowledged, and the source being detailed in the thesis and in the references sections.

Signed

"If you want to have good ideas you must have many ideas. Most of them will be wrong, and what you have to learn is which ones to throw away."

LINUS PAULING

Acknowledgements

Firstly, I would like to thank my parents. They were always here to support me and hear my complaints even though some years they did not see me. To my parents, Hassan Alapour and Fattaneh Dorri. No words can describe my gratitude in having your continued support (both emotionally and financially) in overcoming difficult stepping stones encountered through my PhD years as well as being a medium of comfort through the complaints heard. To my brother Pooya Alapour, thank you for your encouragement through the years.

I would also like to thank my undergraduate research advisor, Dr Bakhsha. He had taught me the principles of chemistry and at the same time portrayed chemistry as nature's rule to making beautiful molecules.

I also want to thank my supervisor, for the chance he gave me to work in his lab. He gave me a taste of research in chemistry and trusted me enough to give me my own project! He is a very special adviser and a very special friend that I will never forget. I learnt a lot from him. I learnt more important than anything else in the world, is respect, honour and patience. He not only helped me become a better scientist but also a better person. Through his mannerisms, he will be my role model in both academia and life.

I also want to thank my co-supervisor Prof. Ramjugernath. Thank you for taking me in your group and believing in my abilities to accomplish something in the group. Your encouragement and willingness to part knowledge was highly appreciable.

Special thanks to the National Research Foundation (NRF), South Africa for their support. This research was supported by grants from the National Research Foundation (NRF), South Africa and was supported by the South African Research Chairs Initiative of the Department of Science and Technology.

I also want to thank Chantal Koorbanally, for her inspiration in pursuing my studies through the years of organic chemistry.

I am thankful to the past and current members of NPRG, Asif Momin, Pramod Kadam, Adele Cheddie, Neha Manhas, Shirveen Sewpersad, Fitsum Tesfai, Mrs Patricia Govender, Suhas Shintre and Kimona Kisten, for the pleasant environment in the lab. All of their smiles, hugs and positive energy was a motivation throughout my work.

There were some of these colleagues that were always in the lab even at nights and weekends. Olumuyiwa Ogunlaja, Oluwole Aremu, Gbojubola Victoria Awolola, Ebenezer Omokorede, Olusola Bodede, Bongi Shelembe, Numfundo Mahlangeni. I will miss spending long nights in the lab, wearing my green lab coat and chatting to my colleagues whilst conducting my experiments.

I will miss playing soccer with my good friends Thrineshen Moodley, Christina Kannigadu, Kaalin Goupal, Siboniso Shezi, Thandokazi Ntshela, Lamla Thungatha...

I also want to convey my heartiest thanks to Mr Sizwe Zamisa for helping me with crystallography and imparting knowledge in this field in the last month of my PhD.

I would like to convey my sincerest thanks to my family in law who were always there to encourage me in hard times. MohammadReza, Sadighe, Maryam and Mojtaba Darestani Farahani. Their understanding and kindness were important to me.

Finally and more importantly, I would like to thank my husband Majid Darestani Farahani, for the years of sacrifice, encouragement and continued support that have led to my accomplishments. Completion of this PhD would have been difficult without him. All of the nights that we had lengthy talks about chemistry, lab sessions and reaction mechanisms written on the hand-made white board made of plastic. He was not only a husband but also a hard working colleague that always reminded me on being strong and unbeatable.

I would like to thank my God for endowing me with life, the blessing of having the ability to pursue a PhD, and for creating a wonderful world that one can find joy in only trying to understand it.

Abstract

Metal catalysed cross coupling reactions are important synthetic methods to synthesise heterocyclic organic molecules. Fluorinated nitrogen containing compounds have shown various medicinal importance in the pharmaceutical industry over the last few decades. This thesis contains the chemistry of two synthetic methods used to synthesise fluorinated nitrogenous heterocyclic compounds using Cu and Pd metal catalysed cross coupling reactions.

We have shown that a Smiles rearrangement occurs with a copper catalyst for the ring closure of Boc-protected phenoxypropanamine to benzoxazine and that the Boc group is instrumental in this mechanism as without it, direct nucleophilic substitution occurs and a different product results. Previously, only ring closure without Boc was reported in the literature and the Smiles rearrangement was not reported. As a follow up study to this work, we investigated the inter and intramolecular conventional and non-conventional hydrogen bond interactions by X-Ray diffraction (XRD) in the solid state and NMR spectroscopy at variable temperatures and different concentrations in the liquid state. In addition, we used computational data to verify the hydrogen bond interactions. Our studies have explained the three dimensional folding in the phenoxypropanamine precursors to benzoxazine.

In a second metal catalysed cross coupling reaction using Pd, a total of 19 quinoline derivatives, similar in structure to mefloquine were prepared by the Sonogashira cross coupling reaction. The synthesised compounds contained various alkyne derivatives with aromatic, aliphatic and cyclopropyl alkynyl side chains at C-4 and H, CH₃ and CF₃ at C-8 on the quinoline core skeleton. It was discovered that the different substituents at C-8 can change the charge distribution of the intermediates, resulting in different yields.

We have shown that the metal catalysed cross coupling reaction is a useful method to synthesise fluorinated nitrogen containing heterocyclic molecules. In addition, we have discussed the mechanism of one of these reactions as a novel mechanism for the conversion of phenoxypropanamines to benzoxazines.

List of Abbreviations

¹H NMR - Proton Nuclear Magnetic Resonance Spectroscopy
¹³C NMR - Carbon-13 Nuclear Magnetic Resonance Spectroscopy
¹⁹F NMR – Fluorine-19 Nuclear Magnetic Resonance Spectroscopy
°C - Degrees Celsius
Boc - *Tert*-butyloxycarbonyl protecting group
CDCl₃ - Deuterated chloroform
COSY - Correlated Nuclear Magnetic Resonance Spectroscopy
d- Doublet
dd – Doublet of doublets
DMSO - Dimethyl sulfoxide
DMF - Dimethylformamide
dt - Doublet of triplets
EtOAc - Ethyl acetate
FT-IR - Fourier Transform – Infrared Spectroscopy
HB - hydrogen bond
HCl - Hydrochloric acid
HMBC - Heteronuclear Multiple Bond Coherence
HPLC - High Pressure Liquid Chromatography
HRMS - High Resolution Mass Spectrometry
HSQC - Heteronuclear Multiple Quantum Coherence
Hyp - *Trans*-4-hydroxy-*L*-proline
Hz - Hertz
m – Multiplet
MS - Mass Spectrometry
NaCl - Sodium chloride
NMP - *N*-methyl-2-pyrrolidone
NMR- Nuclear Magnetic Resonance Spectroscopy
POCl₃ - Phosphorus oxychloride
PPA - Polyphosphoric acid
PR - Progesterone receptor
R_f - Retention factor
s – Singlet
SC-XRD - Single crystal X-ray diffraction
SR - Smiles rearrangement
t – Triplet
TBAB - Tetra-*n*-butylammonium bromide
TEA - Triethylamine
td - Triplet of doublets
THF - Tetrahydrofuran
TLC - Thin Layer Chromatography
UV - Ultraviolet spectroscopy
(VT) NMR - Variable temperature Nuclear Magnetic Resonance Spectroscopy

Table of contents

Chapter 1. Introduction.....	1
1.1 Coupling Reactions.....	2
1.2 Suzuki coupling.....	3
1.3 Heck coupling.....	4
1.4 Hiyama coupling.....	5
1.5 Negishi coupling.....	6
1.6 Stille Coupling.....	7
1.7 Buchwald Hartwig coupling.....	8
1.8 Sonogashira Coupling.....	8
1.9 History behind the Sonogashira coupling.....	9
1.10 Cu-catalysed cross-coupling: Ullmann reaction.....	10
1.11 Benzoxazines.....	11
1.12 Quinolines.....	15
1.13 The role of fluorinated precursors in metal catalysed cross-coupling reactions.....	17
1.14 Hypothesis.....	20
1.15 Aim.....	20
1.16 References.....	20
Chapter 2. Copper-catalysed cross-coupling affected by the Smiles rearrangement: A new chapter on diversifying the synthesis of chiral fluorinated 1,4-benzoxazine derivatives.....	26
2.1 Introduction.....	27
2.2 Results and discussion.....	29
2.3 Conclusion.....	37
2.4 Experimental Procedures.....	38
2.5 References.....	45
Chapter 3. How do hydrogen bonds affect the dynamic behaviour of an organic molecule?.....	49
3.1 Introduction.....	50
3.2 Results and discussion.....	53
3.3 Conclusion.....	61
3.4 Material and methods.....	61
3.5 References.....	63

Chapter 4. Copper-free Sonogashira coupling of 2-trifluoromethyl-4-chloroquinoline with alkynyl acetylene in the formation of fluorinated 4-(alkynyl)-quinolines using Pd(II) and xantphos	66
4.1 Introduction.....	67
4.2 Results and discussion	69
4.3 Conclusion	75
4.4 Experimental section.....	76
4.5 References.....	84
Chapter 5. Conclusion	87

List of Tables

Table 2-1 Optimization of conditions for formation of Boc-[1,4]benzoxazine.....	30
Table 2-2 Synthesis of different Boc-benzoxazine via SR copper catalyzed ring closure.. ..	32
Table 3-1 Effect of concentration variations on the available inter-molecular HB of compounds 1 and 2	55
Table 4-1 Optimization of conditions for the final step in the synthesis of 4-alkynyl quinolines 4	71

List of Figures

Figure 2-1 Crystal structure of 5e , 5f and 5h and the distances between the <i>ipso</i> carbon and nitrogen	36
Figure 2-2 (a) <i>Gauche</i> conformer (from crystal structure of 5g) (b) <i>anti</i> conformer (from crystal structure of 5d and 5e)	37
Figure 3-1 Hydrogen bonds detected by means of SC-XRD in compounds 1 and 2	53
Figure 3-2 VT-NMR studies of the NH group on dilute and concentrated solutions of compounds 1 and 2	55
Figure 3-3 VT-NMR studies of the CH and CH ₂ groups on dilute and concentrated solutions of compounds 1 and 2	57
Figure 3-4 The detection of inter-molecular non conventional HB in compounds 1 via SC-XRD.	58
Figure 3-5 Major and minor NH and methyl <i>t</i> -butyl resonances in the ¹ H NMR spectra of 1 and 2 at -40 °C.....	59
Figure 3-6 HOMO and LUMO plots	60
Figure 3-7 MEP plots for compounds 1 and 2 according to experimental and QM results...60	
Figure 4-1 Novel derivatives of quinoline by application of the Sonogashira coupling reaction under optimised conditions	73
Figure 4-2 Packing diagram of π -stacked compound 4s	75

List of Schemes

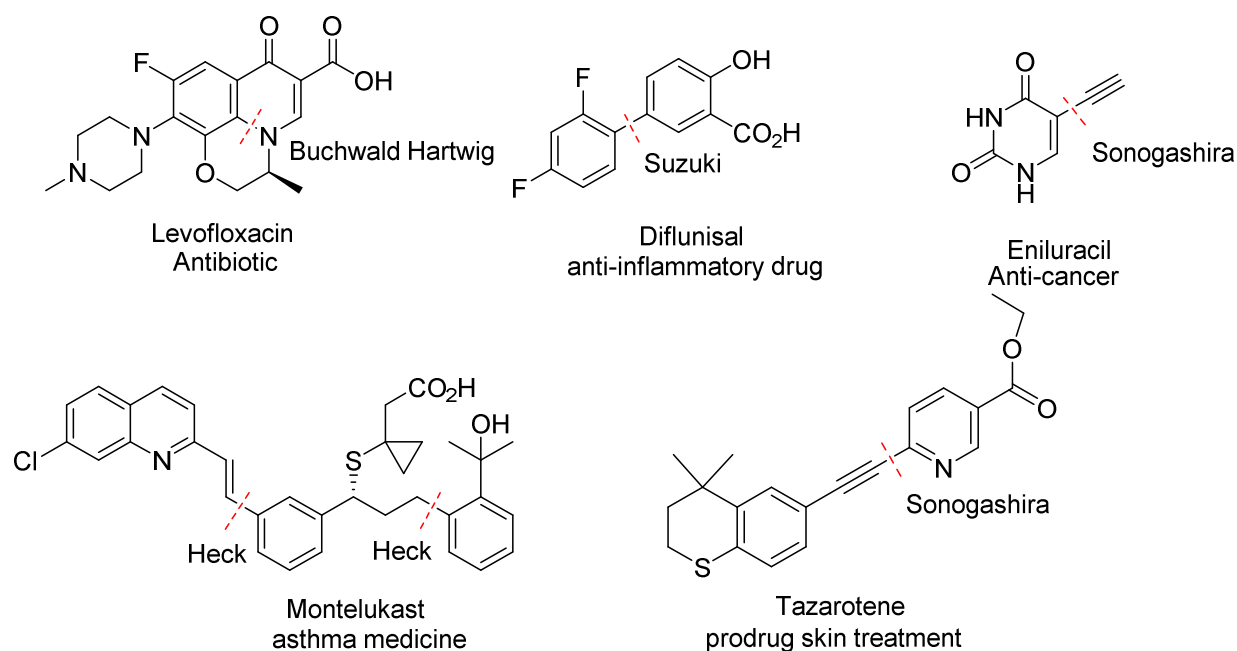
Scheme 1-1 Examples of drugs synthesised using cross coupling reactions	2
Scheme 1-2 A general scheme representing catalytic coupling reactions.....	3
Scheme 1-3 General Suzuki type catalytic reaction	4
Scheme 1-4 Pd-catalysed cross coupling of secondary alkylboron nucleophiles and aryl electrophiles	4
Scheme 1-5 General Heck type catalytic reaction.....	5
Scheme 1-6 Asymmetric intermolecular Heck reaction of cycloalkenes and aryl bromides...5	
Scheme 1-7 General procedure for a Hiyama coupling reaction	6
Scheme 1-8 The synthesis of stilbenes from silyl vinyl boronic esters using the Hiyama coupling.....	6
Scheme 1-9 General Negishi type catalytic reaction.....	6
Scheme 1-10 Monoselective α -arylation of sulfones and sulfonamides with 2,2,6,6- tetramethylpiperidine	7
Scheme 1-11 General procedure for Stille type catalytic reaction	7
Scheme 1-12 Palladium-catalyzed chemo-selective cross-coupling of acyl chlorides and organostannanes	7
Scheme 1-13 General Buchwald-Hartwig type catalytic reaction	8
Scheme 1-14 An example of Buchwald-Hartwig type catalytic reactions.....	8
Scheme 1-15 General Sonogashira type catalytic reaction	9
Scheme 1-16 Example of a Sonogashira cross-coupling reaction between a terminal alkyne and aryl bromide	9
Scheme 1-17 General Ullmann type catalytic reaction	10
Scheme 1-18 The synthetic reaction for enantiopure 1,4-benzoxazines via the Buchwald- Hartwig coupling reaction	12
Scheme 1-19 A copper catalysed method for the synthesis of chiral 1,4-benzoxazine.	13
Scheme 1-20 A biocatalytic method for the synthesis of an intermediate (14b) in the synthesis of chiral 1,4-benzoxazine	14
Scheme 1-21 Ring closing step for the synthesis of chiral 1,4-benzoxazine (<i>S</i>)- 8	14
Scheme 1-22 Sonogashira coupling at C-2 on the quinoline framework.....	15
Scheme 1-23 Sonogashira coupling on position 3 of quinoline	16
Scheme 1-24 Sonogashira coupling on position 2,4 of quinoline	16

Scheme 1-25 Palladium–phosphinous acid-catalyzed Sonogashira cross-coupling: Reactions of quinoline in position 4	17
Scheme 1-26 Diels–Alder reaction of dienophiles with cyclopentadiene.....	18
Scheme 1-27 Reduction of acetophenones and trifluoroacetophenone by the Corey–Bakshi–Shibata (CBS) method	18
Scheme 1-28 Ru-catalysed enantioselective hydrogenation of 2-fluoro-2-hexenoic acid	19
Scheme 1-29 Ring-opening fluoro- and chloromethylation of propylene oxide.....	19
Scheme 2-1 Synthesis of Boc-[1,4]-benzoxazine 6 procedure in comparison to the existing literature.	29
Scheme 2-2 Synthesis of Boc-[1,4]-benzoxazine 6 interrupted by SR	31
Scheme 2-3 Plausible catalytic cycle for formation of Boc-[1,4]-benzoxazine through the SR copper catalyzed ring closure reaction.....	34
Scheme 4-1 Synthesis of 4-alkynyl quinolines 4	70
Scheme 4-2 Plausible mechanism for formation of 4-alkynyl-2-quinolines through a Sonogashira copper-free coupling reaction.	74

Chapter 1. Introduction

The discovery of transition metal-mediated reactions for the synthesis of carbon-carbon and carbon-heteroatom bonds is important for synthetic chemists. Transition metal-catalysed reactions are important in the synthesis of many industrially important chemicals, including the pharmaceutical industry [Cho et al., 2011] and used extensively for large-scale preparation of active pharmaceutical ingredients. This method enables chemists to synthesise different functional groups, and high enantio-, diastereo-, and chemo-selective compounds creating libraries of compounds with particular backbones.

In the past few decades, a wide variety of transition metal-catalyzed carbon-carbon cross coupling reactions have been reported [Chinchilla and Najera, 2007], many of which have been used effectively in large-scale synthesis of small molecular drugs in the pharmaceutical industry such as levofloxacin [Bower et al., 2007], diflunisal [Kylmala et al., 2009], eniluracil [Cooke et al., 2001], montelukast [Bollikonda et al., 2015] and tazarotene [Kumar et al., 2007] (**Scheme 1-1**). These cross coupling reactions include the Suzuki reaction taking place between an organic boronic acid and either an aryl, alkyl or alkenyl halide or triflate, Heck coupling which involves the coupling of an alkyl, aryl halide or triflate with an alkene, Hiyama coupling in which organosilanes are coupled with aryl, alkenyl, alkyl halides or triflates, Negishi coupling that couples organozinc compounds and various aryl halides, Stille coupling between an organostannane and organohalide, Buchwald Hartwig coupling between alkyl or aryl amines and alkyl halides or triflates, Sonogashira coupling between terminal alkynes, and aryl or vinyl halide, and Ullmann coupling between alkyl or aryl amines and alkyl halides or triflates.

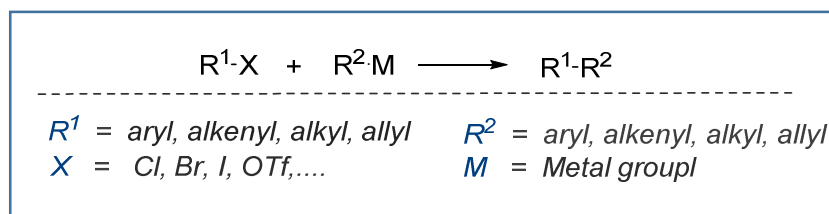


Scheme 1-1 Examples of drugs synthesised using cross coupling reactions

1.1 Coupling Reactions

A coupling reaction is a reaction that combines two organic substrates with the aid of a metal (**Scheme 1-2**). For example joining an organometallic substrate with an aryl or alkyl halide is known as a coupling reaction. In other words, the coupling reaction takes place between an organic nucleophile, and an aryl, vinyl, or alkyl halide, in the presence of a transition-metal catalyst (**Scheme 1-2**) [Yan et al., 2015].

Depending upon the nature of the reactants, coupling reactions are broadly classified into two types: (a) homo-coupling and (b) cross-coupling reactions. The term homo-coupling is reserved for a situation where two identical organic substrates are combined and cross-coupling is when two different organic reactants are joined into a single molecule [Yan et al., 2015].



Scheme 1-2 A general scheme representing catalytic coupling reactions

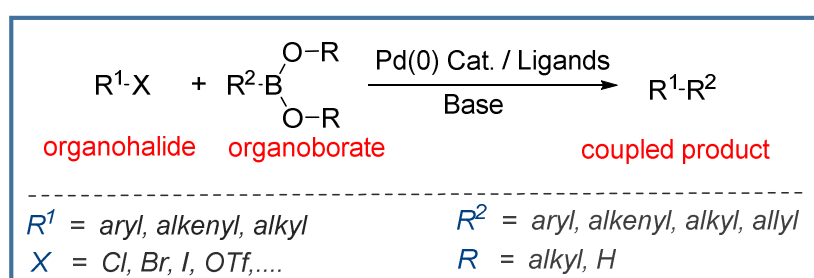
The coupling of organometallic reagents with organic electrophiles is widely used for C-C, C-N, C-O, C-S and C-P bond-forming processes. In 1963, Castro and Stephen discovered the synthesis of diarylacetylenes by cross coupling copper acetylides and aryl halides under reflux [Stephens and Castro, 1963]. Later, Sonogashira reported a coupling reaction of terminal alkynes and aryl halides in the presence of Pd and Cu [Sonogashira et al., 1975]. Subsequently, much work has been done in this area. Amongst the transition-metal based catalysts, Pd is the most common.

Reactions involving Pd however have a number of limitations such as (i) high cost, (ii) the need for ligands to enhance catalytic efficiency, (iii) concerns regarding toxicity, and (iv) extended reaction times [Bolm et al., 2004; Evano et al., 2008; Monnier and Taillefer, 2009]. From an industrial and environmental perspective Cu and Fe catalysts are preferred since they are cheaper and less toxic [Bolm et al., 2004; Evano et al., 2008; Monnier and Taillefer, 2009].

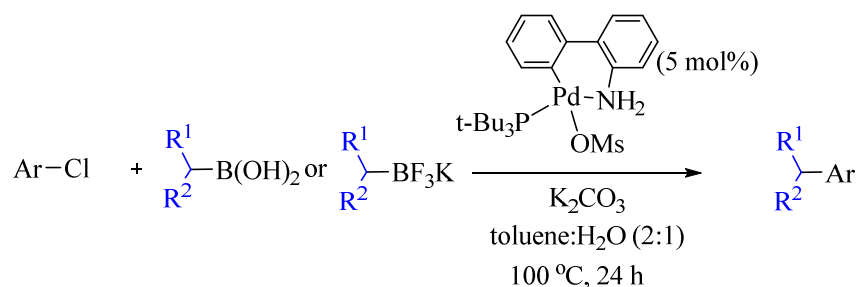
1.2 Suzuki coupling

The Suzuki reaction takes place between a boronic acid and either an aryl, alkyl or alkenyl halide or triflate, and is catalysed by a Pd(0) complex (**Scheme 1-3**) [Fihri et al., 2011]. This work was first reported by Akira Suzuki in 1979, who shared the 2010 Nobel Prize in chemistry with Heck and Negishi for discovering Pd-catalysed cross coupling reactions in

organic synthesis [Miyaura and Suzuki, 1979; Miyaura et al., 1979; Miyaura and Suzuki, 1995]. In his original work, Suzuki reported the cross-coupling between alkenyl boronates and alkenyl bromides [Miyaura et al., 1979]. Subsequently, these reactions grew to include reactions between boronic acids, boronate esters or organoboranes, and organic halides [Miyaura and Suzuki, 1995]. An example of a Suzuki reaction can be seen in Li et al. (2014), where a Pd-catalyst is used to couple aryl halides with secondary alkyl groups (**Scheme 1-4**).



Scheme 1-3 General Suzuki type catalytic reaction

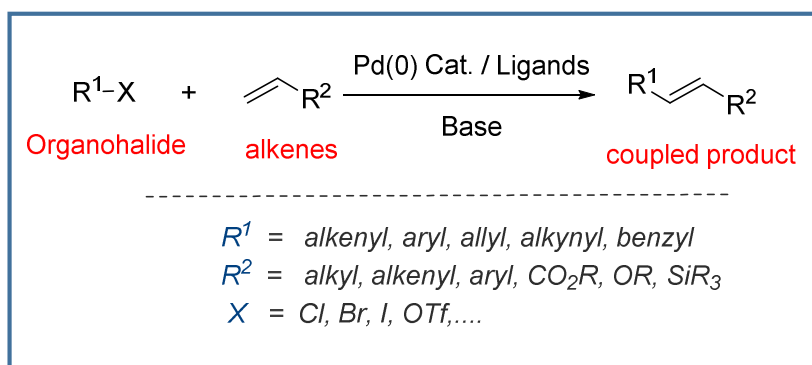


Scheme 1-4 Pd-catalysed cross coupling of secondary alkylboron nucleophiles and aryl electrophiles [Li et al., 2014]

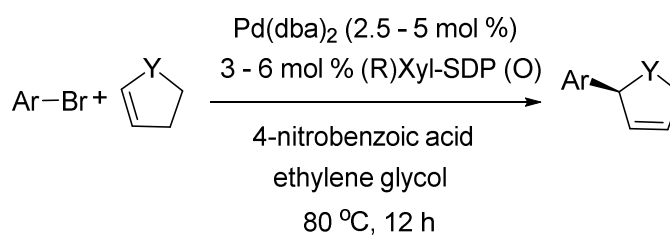
1.3 Heck coupling

The Heck cross-coupling reaction (also known as the Mizoroki-Heck reaction) involves the coupling of an alkyl or aryl halide or triflate with an alkene in the presence of a Pd(0) catalyst (**Scheme 1-5**) [Heck, 1968; Dieck and Heck, 1974; Heck, 1982; Lee, 2016]. An example of

this reaction can be seen in the coupling of aryl and vinyl bromides with cycloalkenes to produce asymmetric products (**Scheme 1-6**) [Wu and Zhou, 2014].



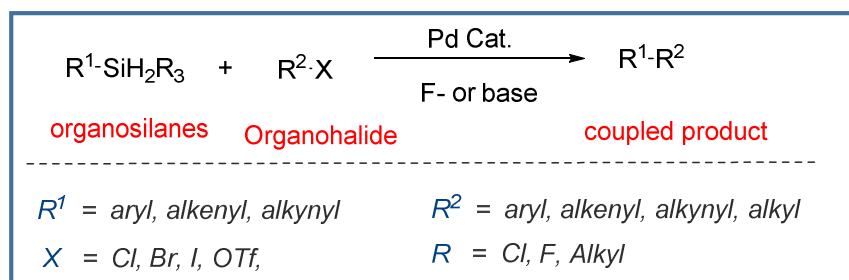
Scheme 1-5 General Heck type catalytic reaction



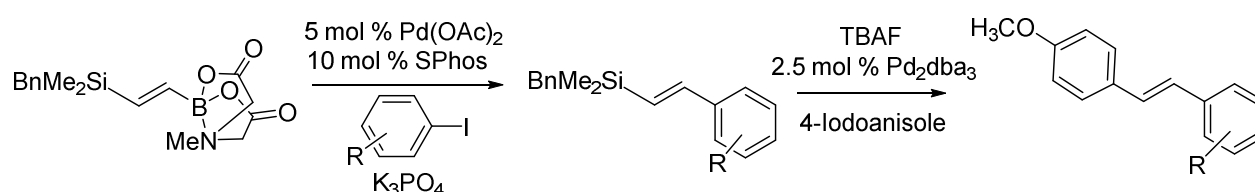
Scheme 1-6 Asymmetric intermolecular Heck reaction of cycloalkenes and aryl bromides [Wu and Zhou, 2014]

1.4 Hiyama coupling

The Hiyama Coupling is a Pd-catalysed reaction specifically suited to organosilanes coupled with aryl, alkenyl, alkyl halides or triflates. This reaction is comparable to Suzuki Coupling, but an activating agent, such as fluoride ion, or base is required. Organosilanes have low toxicity, are stable, and easy to prepare (**Scheme 1-7**) [Hiyama, 2002]. An example of this can be seen in the synthesis of stilbenes from silyl vinyl boronic esters and aryl halides (**Scheme 1-8**) [McLaughlin et al., 2015].



Scheme 1-7 General procedure for a Hiyama coupling reaction

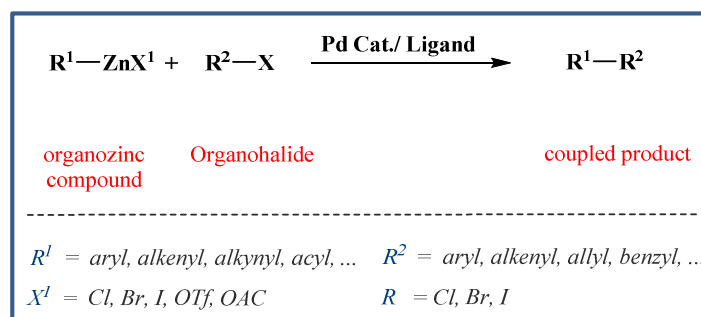


Scheme 1-8 The synthesis of stilbenes from silyl vinyl boronic esters using the Hiyama coupling [McLaughlin et al., 2015]

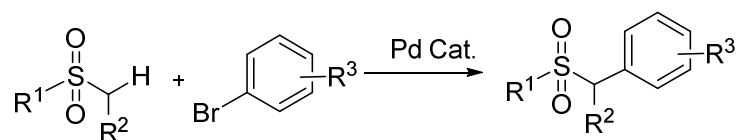
1.5 Negishi coupling

The Negishi coupling is used to prepare unsymmetrical biaryls from organozinc compounds and various aryl, vinyl, benzyl, allyl halides or triflates (**Scheme 1-9**) [Heravi et al., 2014].

An example of this can be seen in α -arylation of sulfones and sulfonamides with a broad range of aryl bromides (**Scheme 1-10**) [Knauber and Tucker, 2016].



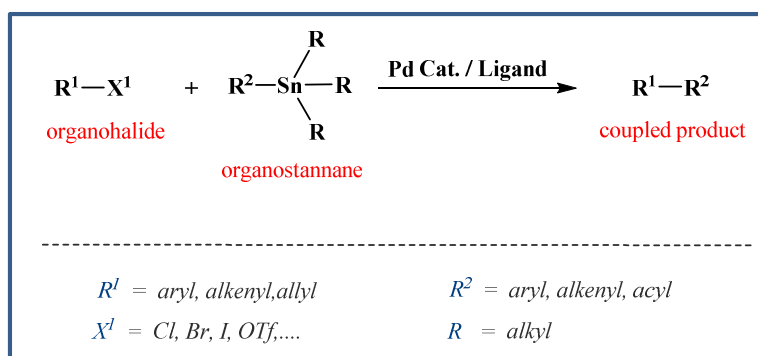
Scheme 1-9 General Negishi type catalytic reaction



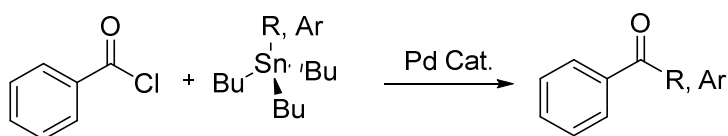
Scheme 1-10 Monoselective α -arylation of sulfones and sulfonamides with aryl halides

1.6 Stille Coupling

The Stille reaction is a cross-coupling reaction between an organohalide or triflate and an organostannane (**Scheme 1-11**). An example of this reaction is the Pd-catalysed cross-coupling of aromatic or aliphatic acyl chlorides and organostannanes (**Scheme 1-12**) [Lerebours et al., 2005].



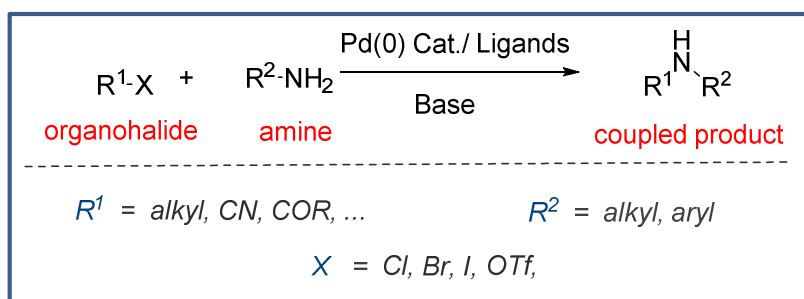
Scheme 1-11 General procedure for Stille type catalytic reaction [Lerebours et al., 2005]



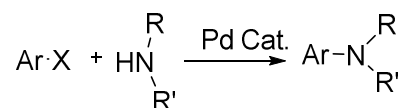
Scheme 1-12 Palladium-catalyzed chemo-selective cross-coupling of acyl chlorides and organostannanes [Lerebours et al., 2005]

1.7 Buchwald Hartwig coupling

The Buchwald-Hartwig coupling is the reaction of alkyl halides or triflates with alkyl or aryl amines in the presence of a Pd catalyst and strong base to form either secondary or tertiary amines (**Scheme 1-13**) [Guram and Buchwald, 1994; Paul et al., 1994; Schlummer and Scholz, 2004]. This reaction has been modified to synthesise aryl ethers from alcohols or phenols [Palucki et al., 1996; Aranyos et al., 1999]. An example of the Buchwald Hartwig coupling can be seen in a multiligand base Pd catalyst for C-N cross-coupling reactions (**Scheme 1-14**) [Fors and Buchwald, 2010].



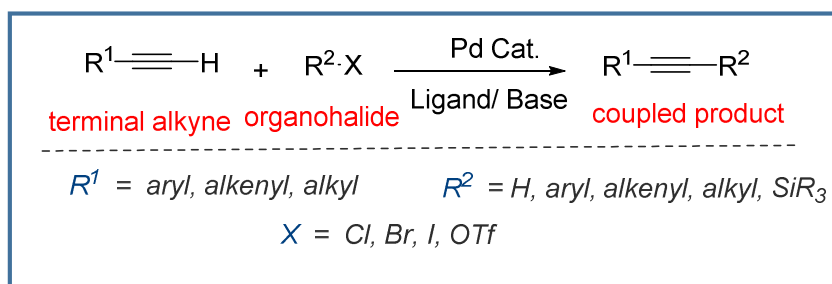
Scheme 1-13 General Buchwald-Hartwig type catalytic reaction



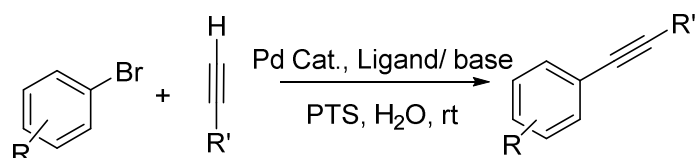
Scheme 1-14 An example of Buchwald-Hartwig type catalytic reactions

1.8 Sonogashira Coupling

The Sonogashira cross-coupling reaction takes place between a terminal alkyne, and an aryl, vinyl halide or triflate in the presence of a Pd catalyst to add an alkynyl moiety to an alkyl group (**Scheme 1-15**). For example, aryl or aliphatic terminal alkynes and aryl bromides formed alkynyl aromatic compounds in the presence of a Pd catalyst [Lipshutz et al., 2008] (**Scheme 1-16**).



Scheme 1-15 General Sonogashira type catalytic reaction



Scheme 1-16 Example of a Sonogashira cross-coupling reaction between a terminal alkyne and aryl bromide

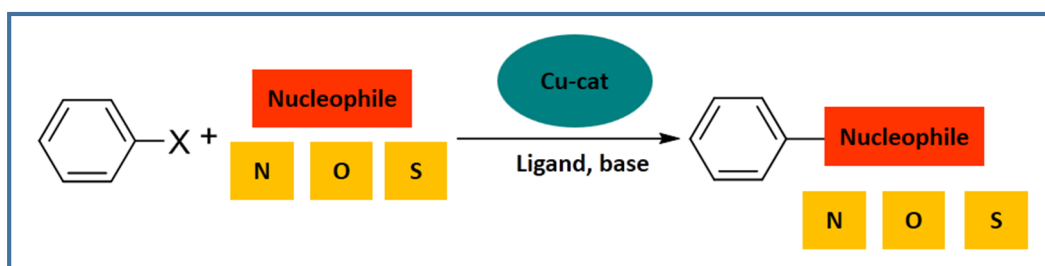
1.9 History behind the Sonogashira coupling

The first reports of Pd-catalysed cross coupling reactions of terminal acetylenes and alkyl halides were independently established by Heck, Cassar and Sonogashira in 1975 [Cassar, 1975; Dieck and Heck, 1975; Sonogashira et al., 1975]. Dieck and Heck (1975) and Cassar (1975) basically extended the Heck reaction to include alkynes instead of alkenes. Sonogashira et al. (1975) were the first to employ a Cu co-catalyst for this reaction and reported milder conditions. However, addition of copper salts as co-catalysts in Sonogashira type cross-coupling reactions has some disadvantages. Firstly, Cu is environmentally unfriendly and difficult to recover [Chinchilla and Najera, 2007] and secondly, copper acetylides generated *in situ* often generates homocoupled products from the terminal alkyne (the so-called Glaser coupling) [Siemsen et al., 2000]. The presence of side reactions is undesirable, especially when the terminal acetylene is expensive or difficult to synthesise.

The Sonogashira cross-coupling reaction discovered in 1975 has been used in a wide variety of areas due to its usefulness in the formation of carbon–carbon bonds [Sonogashira et al., 1975, Sonogashira, 2002]. The reaction has been modified to include various ligands, sources of Pd, solvents, bases, and amounts of catalysts used, [Sonogashira, 2002; Bakherad et al., 2010; Feng et al., 2010] as well as employing microwaves [Kabalka et al., 2000]. Furthermore, research into carrying out this procedure in the absence of copper salts was also investigated [Siemsen et al., 2000; Das et al., 2015; Dewan et al., 2016; Mandegani et al., 2016]. These methodologies are usually called copper-free Sonogashira couplings [Chinchilla and Najera, 2007].

1.10 Cu-catalysed cross-coupling: Ullmann reaction

Copper-catalysed Ullmann type coupling reactions have been extensively applied in both academia and industry in order to develop mild reaction conditions (**Scheme 1-17**) [Ley and Thomas, 2003; Evano et al., 2008; Monnier and Taillefer, 2009].



Scheme 1-17 General Ullmann type catalytic reaction

Ullmann and Goldberg discovered the copper mediated arylation of amines, or amides, to form new C-N bonds at the beginning of the 20th Century [Ullmann and Bielecki, 1901; Ullmann, 1903; Ullmann and Sponagel, 1905; Goldberg, 1906]. Their original reaction had some disadvantages, such as using stoichiometric amounts of copper, highly polar solvents, high temperatures (> 200 °C) and long reaction times. Ullmann condensation reactions have

reappeared in the literature with better procedures to synthesise aryl-heteroatom bonds [Ley and Thomas, 2003; Evano et al., 2008; Monnier and Taillefer, 2009]. At the beginning of the 21st century, several groups investigated various ligands to improve the performance of the copper catalyst in the Ullmann reaction [Strieter et al., 2005; Shafir and Buchwald, 2006].

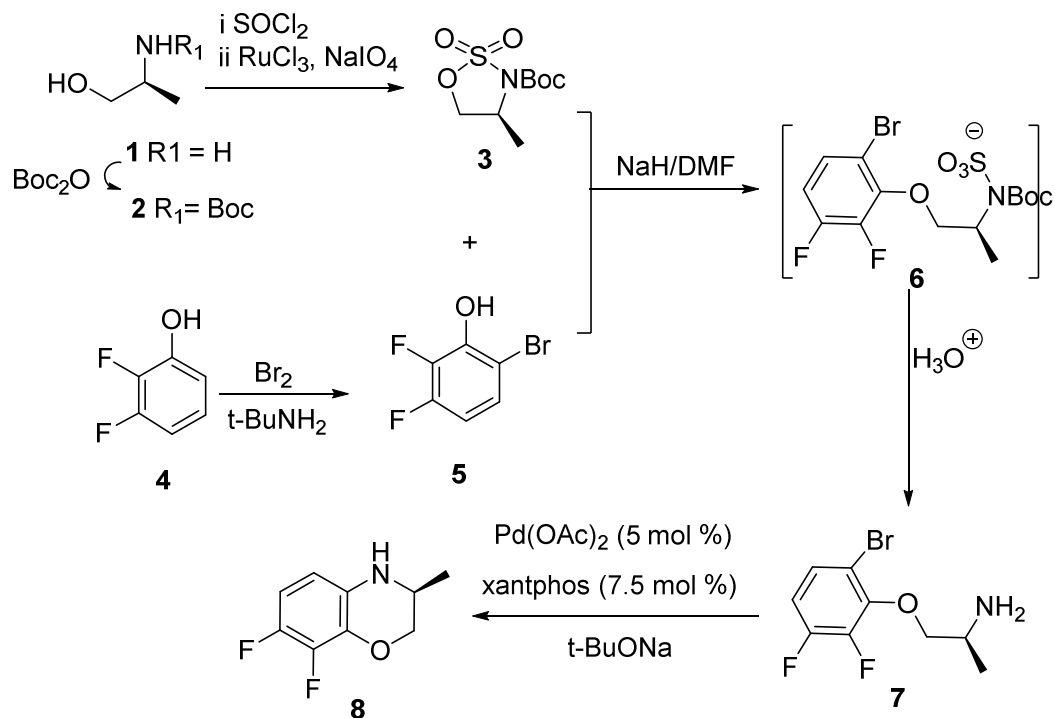
The most efficient catalytic transformations in Ullmann coupling reactions use low catalyst loadings (<1 mol% Cu), and the temperature may vary, from room temperature to $T > 130\text{ }^{\circ}\text{C}$ [Ribas and Gueell, 2014]. In general, a high concentration of base is required for the reaction. The mechanism of the reaction is still unclear and requires further investigation [Ribas and Gueell, 2014].

1.11 Benzoxazines

The benzoxazine core is a famous moiety in many biologically active compounds. It has interesting pharmaceutical applications, for example as progesterone receptor (PR) modulators, and for their activity in anti-anxiety, anti-HIV, agonist and antagonist assays [Hays et al., 1998; Zhang et al., 2002; Dias et al., 2005; Jana et al., 2015]. Chiral dihydrobenzo[1,4]oxazines find interesting application in the pharmaceutical industry [Achari et al., 2004] and in chemistry as a catalyst for the asymmetric transfer hydrogenation of α,β -unsaturated aldehydes [Ebner and Pfaltz, 2011].

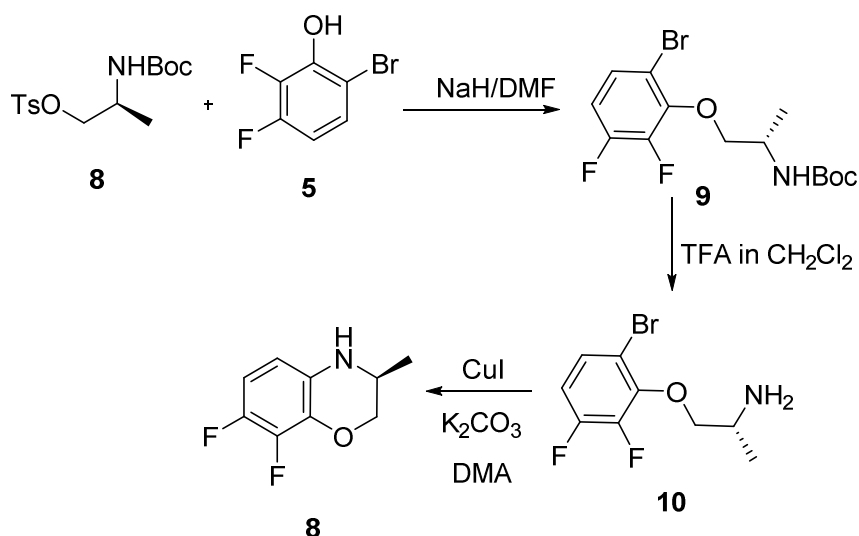
In 2007, Bower et al used chiral commercially available alaninol **1** protected under standard conditions, which was converted to a chiral cyclic sulfamidate **3** over three steps. This intermediate was then coupled with the fluorinated bromophenol **5** to produce the *N*-sulfate **6**. The Boc and sulfate groups were subsequently hydrolysed with acid, which afforded the phenoxy amine precursor **7**. This precursor was then cyclised with Pd(OAc)₂ and xantphos to

produce the chiral fluorinated benzoxazine **8**. This is an example of direct cyclization using a Pd catalyst in the Buchwald-Hartwig coupling reaction [Bower et al., 2007] (**Scheme 1-18**).



Scheme 1-18 The synthetic reaction for enantiopure 1,4-benzoxazines via the Buchwald-Hartwig coupling reaction [Bower et al., 2007]

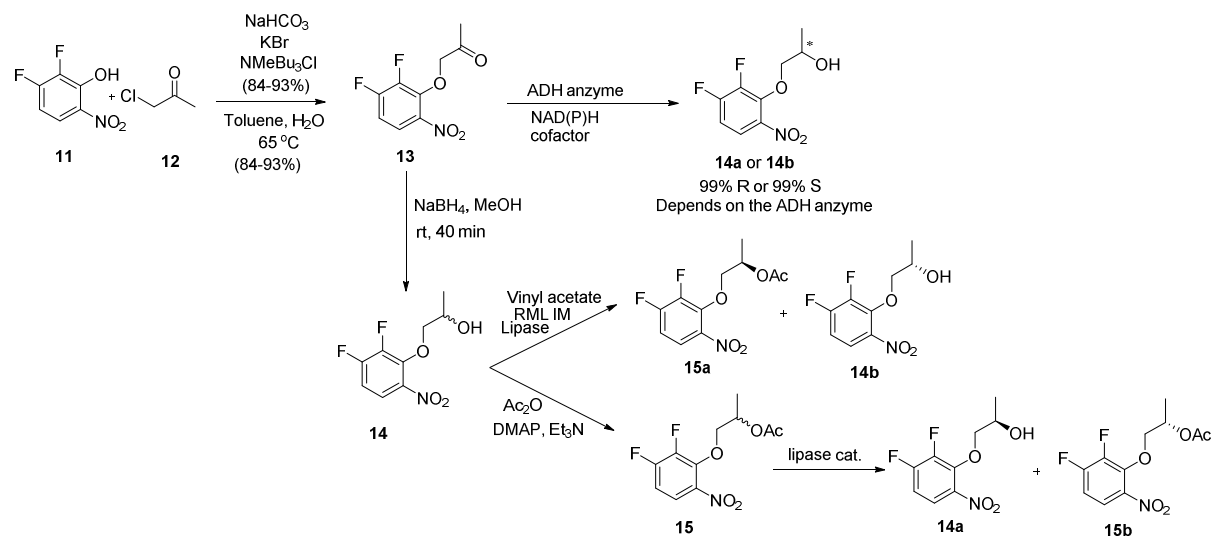
In 2009, Parai et al used a different method to synthesise the same product. They activated the Boc protected chiral alaninol with tosyl chloride and then reacted this with the fluorinated bromophenol **5** resulting in a Boc protected phenoxyamine intermediate **9**, which was never isolated in their method. They then deprotected the phenoxy amine **10** and cyclised this intermediate using a copper-catalysed intramolecular direct ring closure to produce chiral fluorinated benzoxazine **8** [Parai and Panda, 2009] (**Scheme 1-19**).



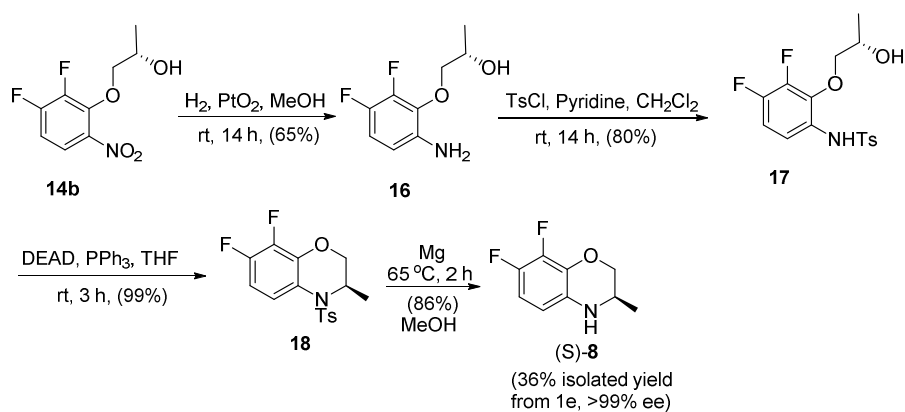
Scheme 1-19 A copper catalysed method for the synthesis of chiral 1,4-benzoxazine [Parai and Panda, 2009]

In 2015, a biocatalytic method was introduced by López-Iglesias et al. They used commercially available, 2,3-difluoro-6-nitrophenol (**11**) and *O*-alkylated it to **13** using 1-chloro-2-propanone (**12**) [López-Iglesias et al., 2015]. There were three different methods used to obtain enantiomerically pure **14b**, which was needed to obtain the final product **8**. In the first two methods, **13** was chemically reduced to the alcohol with NaBH₄, resulting in a racemic mixture of **14**. In the first method, using a lipase catalyst, **14** was enantiomerically converted to the acetate of one isomer only (**15a**), and not the other (**14b**). In the second method, the racemic compound **14** was first acetylated chemically, producing the acetylated racemic product **15**, which was then deacetylated with a lipase enzyme. This lipase enzyme selectively deacetylated one of the isomers (**14a**) and not the other (**15b**). In the third method, enantiomerically pure **14a** or **14b** could be produced from **13** directly using specific ADH enzymes with NADPH or NADH cofactors (**Scheme 1-20**). The **14b** intermediate was then reduced to the amine (**16**) with H₂ and PtO₂, the amine tosylated (**17**) and then cyclised

with PPh_3 and diethyl azidocarboxylate (**18**) and then the tosyl group removed to produce **8**, the levofloxacin intermediate (**Scheme 1-21**).



Scheme 1-20 A biocatalytic method for the synthesis of an intermediate (**14b**) in the synthesis of chiral 1,4-benzoxazine [López-Iglesias et al., 2015]



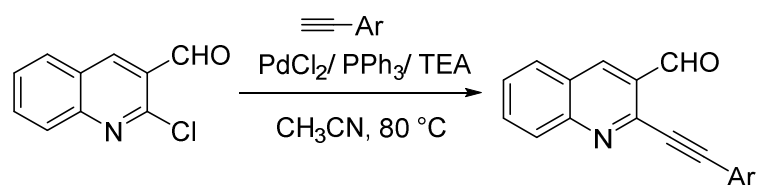
Scheme 1-21 Ring closing step for the synthesis of chiral 1,4-benzoxazine (*S*)-**8**

1.12 Quinolines

The quinoline core has found widespread application in the design and development of potential new drugs in pharmaceutical research [Ahmad and Li, 2003]. Amongst the quinolines, quinine and mefloquine are well known antimalarials [Bawa et al., 2010].

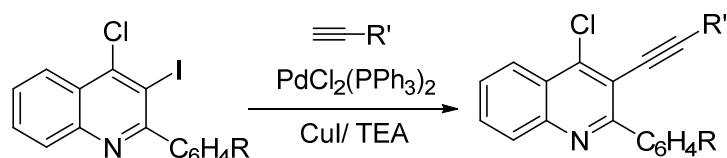
The Sonogashira coupling is one of the more attractive methods among cross-coupling reactions involving organometallic reagents used to synthesise quinoline fragments. It is well known that $I > Br > Cl$ when it comes to substitution of alkynes via the Sonogashira reaction [Mphahlele, 2010]. Therefore low yields of this coupling reaction can be improved by substituting the chloro and bromo group to iodine. There have been reports on selective cross-coupling reactions involving alkynes and quinolines at C-2, C-3, C-4 and C-2,4 on the quinoline framework.

Chandra et al. (2008) used $PdCl_2$ and PPh_3 as a catalyst, with TEA as a base to couple 2-chloroquinoline-3-carboxaldehyde with phenyl acetylene in a copper free Sonogashira reaction [Chandra et al., 2008]. In the same year, Reddy et al. reported the same reaction using typical Sonogashira reagents, 10% Pd/C, PPh_3 , CuI, Et_3N [Reddy et al., 2008] (**Scheme 1-22**).



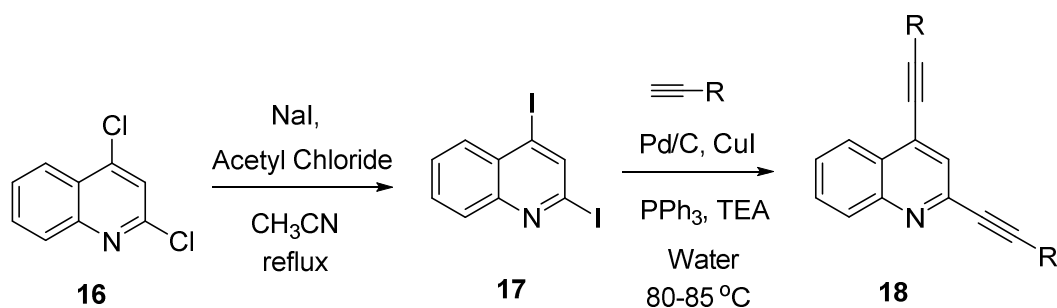
Scheme 1-22 Sonogashira coupling at C-2 on the quinoline framework [Chandra et al., 2008]

In 2010, Mphahlele demonstrated that alkynes replaced iodine under Sonogashira conditions [Mphahlele, 2010]. They used a dichlorobis(triphenylphosphine)palladium (II) ($\text{PdCl}_2(\text{PPh}_3)_2$) reagent with CuI to carry out the reaction (**Scheme 1-23**).



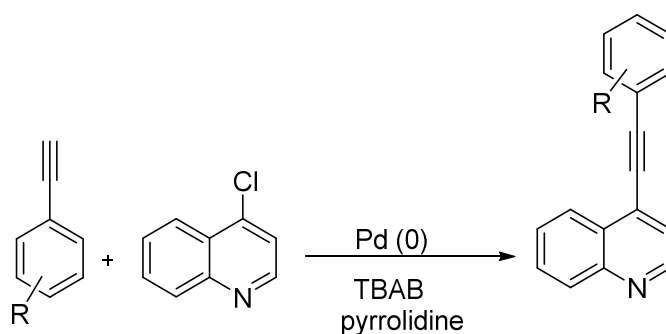
Scheme 1-23 Sonogashira coupling on position 3 of quinoline [Mphahlele, 2010]

2,4-Dialkynylquinolines were also synthesised under Sonogashira conditions using a Pd/C , CuI catalytic system [Reddy et al., 2010] (**Scheme 1-24**). In their work, they replaced the chloro leaving group with iodine, since the yields with 2,4-dichloroquinoline were low.



Scheme 1-24 Sonogashira coupling on position 2,4 of quinoline [Reddy et al., 2010]

Wolf and Lerebours (2003) has shown cross-coupling at C-4 with alkynes under Sonogashira conditions (**Scheme 1-25**). This was also seen in Reisch and Gunaherath (1993) and Nolan et al. (2003).



Scheme 1-25 Palladium–phosphinous acid-catalyzed Sonogashira cross-coupling: Reactions of quinoline at C-4

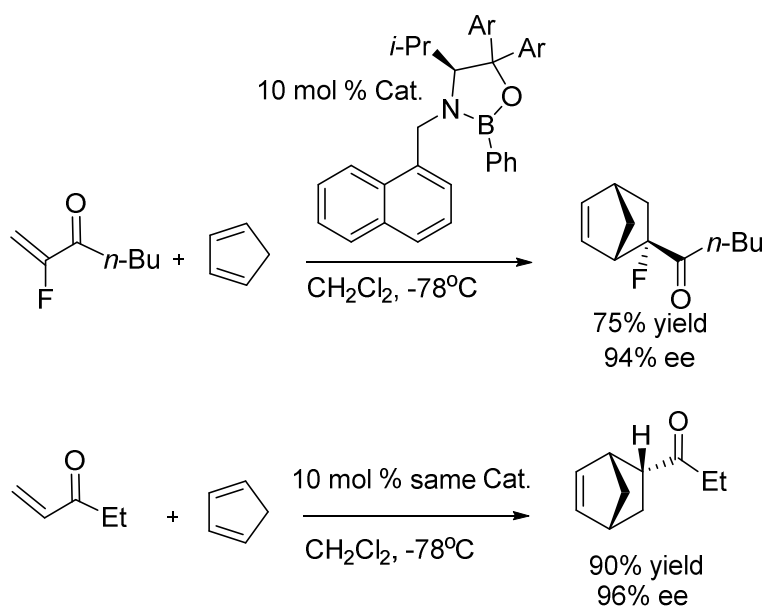
1.13 The role of fluorinated precursors in metal catalysed cross-coupling reactions

Introducing a fluorine atom into a molecule results in changes to its physico-chemical properties through steric, electronic and conformational effects. The partial negative charge of fluorine is responsible for intra- and intermolecular electrostatic interactions that are involved in determining the conformation the molecule adopts [Cahard and Bizet, 2014].

Electrostatic interactions in many cases force molecules with a fluorine atom to take on a *gauche* conformation in preference to *anti*. This *gauche* conformation results in better interaction with catalysts and increased reactivity of the organofluorine compounds [O'Hagan, 2008]. Furthermore, the fluorine atom is known to induce conformational control in cyclic intermediates [Bizet and Cahard, 2014]. Fluorine can also act as hydrogen bond acceptors that can influence inter- and intra- molecular interactions in the molecule [Bizet and Cahard, 2014].

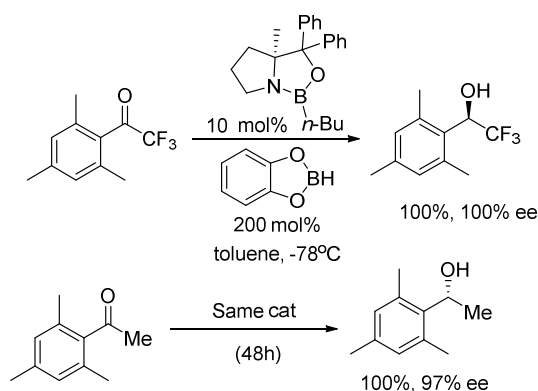
The Diels–Alder reaction with fluorinated dienophiles and cyclopentadiene has been shown to result in products with different regioselectivity (**Scheme 1-26**). This was attributed to fluorine increasing the π -electron density of the C=C bond by π - π interactions, which is an

example of a reverse electron demand Diels-Alder reaction [Essers et al., 2003; Shibatomi et al., 2010].



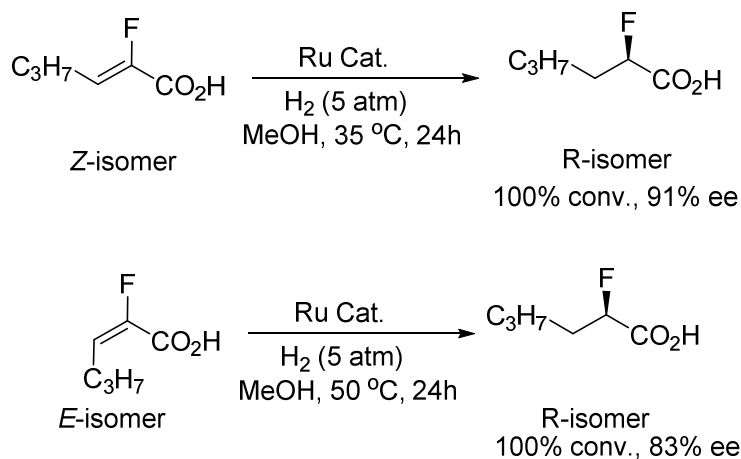
Scheme 1-26 Diels–Alder reaction of dienophiles with cyclopentadiene

Another example of fluorine influencing the product in the reaction can be seen in the Corey-Bakshi-Shibata (CBS) reduction where the fluorinated precursor was reduced to the (*R*)-alcohol, but its non-fluorinated analogue was reduced to the (*S*)-isomer (**Scheme 1-27**) [Kuroki et al., 2001].



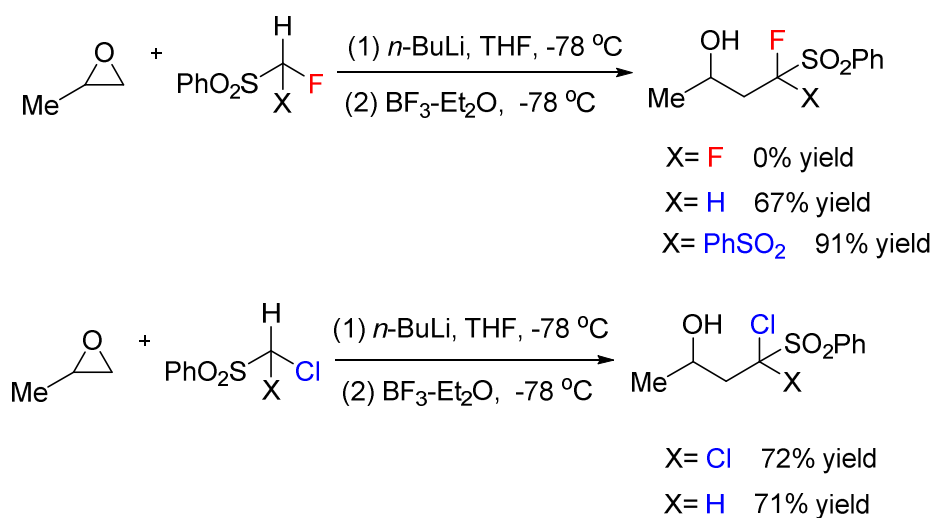
Scheme 1-27 Reduction of acetophenones and trifluoroacetophenone by the Corey-Bakshi-Shibata (CBS) method

It was observed that a slight increase in enantioselectivity occurred with the *Z*-fluorinated alkene compared to the *E*-isomer in the reduction of the alkene to the alkane using a ruthenium catalyst [Saburi et al., 1992] (**Scheme 1-28**). The reason for this is unknown.



Scheme 1-28 Ru-catalysed enantioselective hydrogenation of 2-fluoro-2-hexenoic acid

In 2006, Ni et al. showed that nucleophilic attack of alkylated sulfonyl phenyl compounds on epoxides occurred in all cases except when a difluorinated precursor was used in the reaction, in which case no product was observed (**Scheme 1-29**) [Netherton and Fu, 2001; Ni et al., 2006].



Scheme 1-29 Ring-opening fluoro- and chloromethylation of propylene oxide.

Thus, from the examples shown above, it can be clearly seen that the introduction of fluorine into a molecule at certain sites on precursors has a pronounced effect on the outcome of the reaction.

1.14 Hypothesis

It is hypothesised that fluorinated precursors influence the reactivity of organic reactions. We believe that fluorine and fluorinated groups on precursors can increase the reactivity of cross coupling reactions.

1.15 Aim

The effect of fluorine substituents in precursors which undergo cross coupling reactions has not been fully understood and explored. The aim of this work was to investigate the effect of fluorinated precursors in metal catalysed cross coupling reactions for the synthesis and substitution of fluorinated nitrogenous heterocyclic rings.

1.16 References

- Achari, B., Mandal, S.B., Dutta, P.K., Chowdhury, C., Perspectives on 1,4-benzodioxins, 1,4-benzoxazines and their 2,3-dihydro derivatives. *Synlett*, **2004**, No. 14, 2449-2467.
- Ahmad, N.M., Li, J.J., Palladium in quinoline synthesis. *Advances in Heterocyclic Chemistry*, **2003**, 84, 1-30.
- Aranyos, A., Old, D.W., Kiyomori, A., Wolfe, J.P., Sadighi, J.P., Buchwald, S.L., Novel electron-rich bulky phosphine ligands facilitate the palladium-catalyzed preparation of diaryl ethers. *Journal of the American Chemical Society*, **1999**, 121, 4369-4378.
- Bakherad, M., Amin, A.H., Keivanloo, A., Bahramian, B., Raeissi, M., Copper- and phosphine-free Sonogashira coupling reactions of aryl iodides catalyzed by an *N,N*-bis(naphthylideneimino)diethylenetriamine-functionalized polystyrene resin supported Pd(II) complex under aerobic conditions. *Tetrahedron Letters*, **2010**, 51, 5653-5656.
- Bawa, S., Kumar, S., Drabu, S., Kumar, R., Structural modifications of quinoline-based antimalarial agents: Recent developments. *Journal of Pharmacy & Bioallied Sciences*, **2010**, 2, 64-71.
- Bizet, V., Cahard, D., Fluorine as a control element in asymmetric synthesis, *Chimia*, **2014**, 68, 378-381.

- Bollikonda, S., Mohanarangam, S., Jinna, R.R., Kandirelli, V.K.K., Makthala, L., Sen, S., Chaplin, D.A., Lloyd, R.C., Mahoney, T., Dahanukar, V.H., Oruganti, S., Fox, M.E., An enantioselective formal synthesis of montelukast sodium. *Journal of Organic Chemistry*, **2015**, 80, 3891-3901.
- Bolm, C., Legros, J., Le Paih, J., Zani, L., Iron-catalyzed reactions in organic synthesis. *Chemical Reviews*, **2004**, 104, 6217-6254.
- Bower, J.F., Szeto, P., Gallagher, T., Enantiopure 1,4-benzoxazines via 1,2-cyclic sulfamidates. Synthesis of levofloxacin. *Organic Letters*, **2007**, 9, 3283-3286.
- Cahard, D., Bizet, V., The influence of fluorine in asymmetric catalysis. *Chemical Society Reviews*, **2014**, 43, 135-147.
- Chandra, A., Singh, B., Upadhyay, S., Singh, R.M., Copper-free sonogashira coupling of 2-chloroquinolines with phenyl acetylene and quick annulation to benzo[*b*]1,6-naphthyridine derivatives in aqueous ammonia. *Tetrahedron*, **2008**, 64, 11680-11685.
- Cassar, L., Synthesis of aryl- and vinyl-substituted acetylene derivatives by the use of nickel and palladium complexes. *Journal of Organometallic Chemistry*, **1975**, 93, 253-257.
- Chinchilla, R., Najera, C., The Sonogashira reaction: A booming methodology in synthetic organic chemistry. *Chemical Reviews*, **2007**, 107, 874-922.
- Cho, S.H., Kim, J.Y., Kwak, J., Chang, S., Recent advances in the transition metal-catalyzed twofold oxidative C-H bond activation strategy for C-C and C-N bond formation. *Chemical Society Reviews*, **2011**, 40, 5068-5083.
- Cooke, J.W.B., Bright, R., Coleman, M.J., Jenkins, K.P., Process research and development of a dihydropyrimidine dehydrogenase inactivator: Large-scale preparation of eniluracil using a Sonogashira coupling. *Organic Process Research & Development*, **2001**, 5, 383-386.
- Das, S., Samanta, S., Ray, S., Biswas, P., 3,6-Di(pyridin-2-yl)-1,2,4,5-tetrazine capped Pd(0) nanoparticles: A catalyst for copper-free Sonogashira coupling of aryl halides in aqueous medium. *RSC Advances*, **2015**, 5, 75263-75267.
- Dewan, A., Sarmah, M., Bora, U., Thakur, A.J., A green protocol for ligand, copper and base free Sonogashira cross-coupling reaction. *Tetrahedron Letters*, **2016**, 57, 3760-3763.
- Dias, N., Goossens, J.-F., Baldeyrou, B., Lansiaux, A., Colson, P., Di Salvo, A., Bernal, J., Turnbull, A., Mincher, D.J., Bailly, C., Oxoazabenz[*de*]anthracenes conjugated to amino acids: Synthesis and evaluation as DNA-binding antitumor agents. *Bioconjugate Chemistry*, **2005**, 16, 949-958.
- Dieck, H.A., Heck, R.F., Organophosphinepalladium complexes as catalysts for vinylic hydrogen substitution reactions. *Journal of the American Chemical Society*, **1974**, 96, 1133-1136.
- Dieck, H.A., Heck, R.F., Palladium catalyzed synthesis of aryl, heterocyclic, and vinylic acetylene derivatives. *Journal of Organometallic Chemistry*, **1975**, 93, 259-263.
- Ebner, C., Pfaltz, A., Chiral dihydrobenzo[1,4]oxazines as catalysts for the asymmetric transfer-hydrogenation of α,β -unsaturated aldehydes. *Tetrahedron*, **2011**, 67, 10287-10290.

- Essers, M., Ernet, T., Haufe, G., Enantioselective Diels-Alder reactions of alpha-fluorinated alpha,beta-unsaturated carbonyl compounds - part 5. Chemical consequences of fluorine substitution. *Journal of Fluorine Chemistry*, **2003**, 121, 163-170.
- Evano, G., Blanchard, N., Toumi, M., Copper-mediated coupling reactions and their applications in natural products and designed biomolecules synthesis, *Chemical Reviews*, **2008**, 108, 3054-3131.
- Feng, Y.-S., Li, Y.-Y., Tang, L., Wu, W., Xu, H.-J., Efficient ligand-free copper-catalyzed C-S cross-coupling of thiols with aryl iodides using KF/Al₂O₃ as base. *Tetrahedron Letters*, **2010**, 51, 2489-2492.
- Fihri, A., Bouhrara, M., Nekoueishahraki, B., Basset, J.M., Polshettiwar, V., Nanocatalysts for Suzuki cross-coupling reactions. *Chemical Society Reviews*, **2011**, 40, 5181-5203.
- Fors, B.P., Buchwald, S.L., A multiligand based Pd catalyst for C-N cross-coupling reactions. *Journal of the American Chemical Society*, **2010**, 132, 15914-15917.
- Goldberg, I., Phenylation in the presence of copper as catalyst. *Chemische Berichte*, **1906**, 39, 1691-1692.
- Guram, A.S., Buchwald, S.L., Palladium-catalyzed aromatic aminations with *in-situ* generated aminostannanes. *Journal of the American Chemical Society*, **1994**, 116, 7901-7902.
- Hays, S.J., Caprathe, B.W., Gilmore, J.L., Amin, N., Emmerling, M.R., Michael, W., Nadimpalli, R., Nath, R., Raser, K.J., Stafford, D., Watson, D., Wang, K., Jaen, J.C., 2-Amino-4*H*-3,1-benzoxazin-4-ones as inhibitors of c1r serine protease. *Journal of Medicinal Chemistry*, **1998**, 41, 1060-1067.
- Heck, R.F., Acylation, methylation, and carboxyalkylation of olefins by group VIII metal derivatives. *Journal of the American Chemical Society*, **1968**, 90, 5518-5526.
- Heck, R.F., Palladium-catalyzed vinylation of organic halides. *Organic Reactions*, **1982**, 27, 345-390.
- Heravi, M.M., Hashemi, E., Nazari, N., Negishi coupling: An easy progress for C-C bond construction in total synthesis. *Molecular Diversity*, **2014**, 18, 441-472.
- Hiyama, T., How I came across the silicon-based cross-coupling reaction. *Journal of Organometallic Chemistry*, **2002**, 653, 58-61.
- Jana, S., Ashokan, A., Kumar, S., Verma, A., Kumar, S., Copper-catalyzed trifluoromethylation of alkenes: Synthesis of trifluoromethylated benzoxazines. *Organic & Biomolecular Chemistry*, **2015**, 13, 8411-8415.
- Kabalka, G.W., Wang, L., Namboodiri, V., Pagni, R.M., Rapid microwave-enhanced, solventless sonogashira coupling reaction on alumina. *Tetrahedron Letters*, **2000**, 41, 5151-5154.
- Knauber, T., Tucker, J., Palladium catalyzed monoselective alpha-arylation of sulfones and sulfonamides with 2,2,6,6-tetramethylpiperidine•ZnCl•LiCl base and aryl bromides. *Journal of Organic Chemistry*, **2016**, 81, 5636-5648.
- Kuroki, Y., Sakamaki, Y., Iseki, K., Enantioselective Rhodium(I)-catalyzed hydrogenation of trifluoromethyl ketones. *Organic Letters*, **2001**, 3, 457-459.
- Kylmala, T., Tois, J., Xu, Y.J., Franzen, R., One step synthesis of diflunisal using a Pd-diamine complex. *Central European Journal of Chemistry*, **2009**, 7, 818-826.

- Lee, A.L., Enantioselective oxidative boron Heck reactions. *Organic & Biomolecular Chemistry*, **2016**, 14, 5357-5366.
- Lerebours, R., Camacho-Soto, A., Wolf, C., Palladium-catalyzed chemoselective cross-coupling of acyl chlorides and organostannanes. *Journal of Organic Chemistry*, **2005**, 70, 8601-8604.
- Ley, S.V., Thomas, A.W., Modern synthetic methods for copper-mediated C(aryl)-O, C(aryl)-N, and C(aryl)-S bond formation. *Angewandte Chemie, International Edition*, **2003**, 42, 5400-5449.
- Li, L., Zhao, S., Joshi-Pangu, A., Diane, M., Biscoe, M.R., Stereospecific Pd-catalyzed cross-coupling reactions of secondary alkylboron nucleophiles and aryl chlorides. *Journal of the American Chemical Society*, **2014**, 136, 14027-14030.
- Lipshutz, B.H., Chung, D.W., Rich, B., Sonogashira couplings of aryl bromides: Room temperature, water only, no copper. *Organic Letters*, **2008**, 10, 3793-3796.
- López-Iglesias, M., Busto, E., Gotor, V., Gotor-Fernández, V., Chemoenzymatic asymmetric synthesis of 1,4-benzoxazine derivatives: Application in the synthesis of a levofloxacin precursor. *Journal of Organic Chemistry*, **2015**, 80, 3815-3824.
- Mandegani, Z., Asadi, M., Asadi, Z., Nano tetraamine Pd(0) complex as an efficient catalyst for phosphine-free Suzuki reaction in water and copper-free Sonogashira reaction under aerobic conditions. *Applied Organometallic Chemistry*, **2016**, 30, 657-663.
- McLaughlin, M.G., McAdam, C.A., Cook, M.J., Mida-vinylsilanes: Selective cross-couplings and applications to the synthesis of functionalized stilbenes. *Organic Letters*, **2015**, 17, 10-13.
- Miyaura, N., Suzuki, A., Stereoselective synthesis of arylated (*E*)-alkenes by the reaction of alk-1-enylboranes with aryl halides in the presence of palladium catalyst. *Journal of the Chemical Society-Chemical Communications*, **1979**, 866-867.
- Miyaura, N., Suzuki, A., Palladium-catalyzed cross-coupling reactions of organoboron compounds. *Chemical Reviews*, **1995**, 95, 2457-2483.
- Miyaura, N., Yamada, K., Suzuki, A., A new stereospecific cross-coupling by the palladium-catalyzed reaction of 1-alkenylboranes with 1-alkenyl or 1-alkynyl halides. *Tetrahedron Letters*, **1979**, 3437-3440.
- Monnier, F., Taillefer, M., Catalytic C-C, C-N, and C-O Ullmann-type coupling reactions. *Angewandte Chemie, International Edition*, **2009**, 48, 6954-6971.
- Mphahlele, M.J., Regioselective alkynylation of 2-aryl-4-chloro-3-iodoquinolines and subsequent arylation or amination of the 2-aryl-3-(alkynyl)-4-chloroquinolines. *Tetrahedron*, **2010**, 66, 8261-8266.
- Netherton, M.R., Fu, G.C., Air-stable trialkylphosphonium salts: Simple, practical, and versatile replacements for air-sensitive trialkylphosphines. Applications in stoichiometric and catalytic processes. *Organic Letters*, **2001**, 3, 4295-4298.
- Ni, C.F., Li, Y., Hu, J.B., Nucleophilic fluoroalkylation of epoxides with fluorinated sulfones. *Journal of Organic Chemistry*, **2006**, 71, 6829-6833.

- Nolan, J.M., Comins, D.L., Regioselective Sonogashira couplings of 2,4-dibromoquinolines. A correction. *Journal of Organic Chemistry*, **2003**, 68, 3736-3738.
- O'Hagan, D., Understanding organofluorine chemistry. An introduction to the C-F bond. *Chemical Society Reviews*, **2008**, 37, 308-319.
- Palucki, M., Wolfe, J.P., Buchwald, S.L., Synthesis of oxygen heterocycles via a palladium-catalyzed C-O bond-forming reaction. *Journal of the American Chemical Society*, **1996**, 118, 10333-10334.
- Parai, M.K., Panda, G., A convenient synthesis of chiral amino acid derived 3,4-dihydro-2*H*-benzo[b][1,4]thiazines and antibiotic levofloxacin. *Tetrahedron Letters*, **2009**, 50, 4703-4705.
- Paul, F., Patt, J., Hartwig, J.F., Palladium-catalyzed formation of carbon-nitrogen bonds - reaction intermediates and catalyst improvements in the hetero cross-coupling of aryl halides and tin amides. *Journal of the American Chemical Society*, **1994**, 116, 5969-5970.
- Reddy, E.A., Barange, D.K., Islam, A., Mukkanti, K., Pal, M., Synthesis of 2-alkynylquinolines from 2-chloro and 2,4-dichloroquinoline via Pd/C-catalyzed coupling reaction in water. *Tetrahedron*, **2008**, 64, 7143-7150.
- Reddy, E.A., Islam, A., Mukkanti, K., Venu, B.K., Pal, M., Pd/C-mediated dual C-C bond forming reaction in water: Synthesis of 2,4-dialkynylquinoline. *Journal of the Brazilian Chemical Society*, **2010**, 21, 1681-1687.
- Reisch, J., Gunaherath, G.M.K.B., Acetylene chemistry. Part 27. Palladium catalyzed carbon-carbon bond formation between quinoline and mono-substituted alkynes: Synthesis of 4-alkynyl-2-bromoquinolines. *Journal of Heterocyclic Chemistry*, **1993**, 30, 1057-1059.
- Ribas, X., Gueell, I., Cu(I)/Cu(III) catalytic cycle involved in Ullmann-type cross-coupling reactions. *Pure and Applied Chemistry*, **2014**, 86, 345-360.
- Saburi, M., Shao, L., Sakurai, T., Uchida, Y., Asymmetric hydrogenation of 2-fluoro-2-alkenoic acids catalyzed by Ru-binap complexes: A convenient access to optically active 2-fluoroalkanoic acids. *Tetrahedron Letters*, **1992**, 33, 7877-7880.
- Schlummer, B., Scholz, U., Palladium-catalyzed C-N and C-O coupling - a practical guide from an industrial vantage point. *Advanced Synthesis & Catalysis*, **2004**, 346, 1599-1626.
- Shafir, A., Buchwald, S.L., Highly selective room-temperature copper-catalyzed C-N coupling reactions. *Journal of the American Chemical Society*, **2006**, 128, 8742-8743.
- Shibatomi, K., Futatsugi, K., Kobayashi, F., Iwasa, S., Yamamoto, H., Stereoselective construction of halogenated quaternary stereogenic centers via catalytic asymmetric Diels-Alder reaction. *Journal of the American Chemical Society*, **2010**, 132, 5625-5627.
- Siemsen, P., Livingston, R.C., Diederich, F., Acetylenic coupling: A powerful tool in molecular construction. *Angewandte Chemie, International Edition*, **2000**, 39, 2632-2657.
- Sonogashira, K., Development of Pd-Cu catalyzed cross-coupling of terminal acetylenes with sp²-carbon halides. *Journal of Organometallic Chemistry*, **2002**, 653, 46-49.

- Sonogashira, K., Tohda, Y., Hagihara, N., Convenient synthesis of acetylenes. Catalytic substitutions of acetylenic hydrogen with bromo alkenes, iodo arenes, and bromopyridines. *Tetrahedron Letters*, **1975**, 4467-4470.
- Stephens, R.D., Castro, C.E., The substitution of aryl iodides with cuprous acetylides. A synthesis of tolanes and heterocyclics. *Journal of Organic Chemistry*, **1963**, 28, 3313-3315.
- Strieter, E.R., Blackmond, D.G., Buchwald, S.L., The role of chelating diamine ligands in the Goldberg reaction: A kinetic study on the copper-catalyzed amidation of aryl iodides. *Journal of the American Chemical Society*, **2005**, 127, 4120-4121.
- Ullmann, F., Bielecki, J., Synthesis in the biphenyl series. I. *Chemische Berichte*, **1901**, 34, 2174-2185.
- Ullmann, F., A new path for preparing diphenylamine derivatives. *Chemische Berichte*, **1903**, 36, 2382-2384.
- Ullmann, F., Sponagel, P., Phenylation of phenols. *Chemische Berichte*, **1905**, 38, 2211-2212.
- Wolf, C., Lerebours, R., Palladium-phosphinous acid-catalyzed Sonogashira cross-coupling reactions in water. *Organic & Biomolecular Chemistry*, **2003**, 2, 2161-2164.
- Wu, C., Zhou, J., Asymmetric intermolecular Heck reaction of aryl halides. *Journal of the American Chemical Society*, **2014**, 136, 650-652.
- Yan, G.B., Borah, A.J., Wang, L.G., Yang, M.H., Recent advances in transition metal-catalyzed methylation reactions. *Advanced Synthesis & Catalysis*, **2015**, 357, 1333-1350.
- Zhang, P., Terefenko, E.A., Fensome, A., Zhang, Z., Zhu, Y., Cohen, J., Winneker, R., Wrobel, J., Yardley, J., Potent nonsteroidal progesterone receptor agonists: Synthesis and SAR study of 6-aryl benzoxazines. *Bioorganic & Medicinal Chemistry Letters*, **2002**, 12, 787-790.

Chapter 2. Copper-catalysed cross-coupling affected by the Smiles rearrangement: A new chapter on diversifying the synthesis of chiral fluorinated 1,4-benzoxazine derivatives

Abstract

Synthesis of different chiral fluorinated Boc-[1,4]-benzoxazine from their open chain precursors was investigated. The NMR spectra and crystallographic data showed the presence of the Smiles Rearrangement (SR) followed by copper catalysed coupling. The influence of the Boc protecting group, solvent, base, catalyst and the conformational changes of adducts was explored in detail by careful reaction optimization. No product was obtained in the absence of Boc, indicating its crucial role. Finally, a new mechanism for the SR copper catalysed ring closure was proposed.

2.1 Introduction

Benzoxazines exist in many drugs and herbicides, and are widely used as building blocks of bioactive molecules. They exhibit interesting biological and pharmaceutical properties such as progesterone receptor (PR) modulation, antianxiety, anti-HIV, agonist and antagonist activities [Hays et al., 1998; Zhang et al., 2002; Dias et al., 2005; Jana et al., 2015]. Particularly, chiral dihydrobenzo-[1,4]-oxazines attracted much attention due to their interesting biological activities [Achari et al., 2004; Feng et al., 2009]. Chiral dihydrobenzo-[1,4]-oxazines are also employed as catalysts for the asymmetric transfer hydrogenation of α,β -unsaturated aldehydes [Ebner and Pfaltz, 2011].

Fluorine atoms contained in the core structure of a drug results in enhancement of several biological properties such as solubility, lipophilicity, metabolic stability and binding selectivity [Purser et al., 2008]. Levofloxacin, Ciprofloxacin, Norfloxacin and Efavirenz are examples of pharmaceutical drugs containing a fluorine atom [Atarashi et al., 1987; Purser et al., 2008; Komnatnyy et al., 2014].

Consequently, a wide range of synthetic procedures have been developed for the synthesis of these fluorinated chiral benzoxazines. These procedures include direct cyclization using a metal catalyst such as Pd in the Buchwald-Hartwig coupling reaction [Bower et al., 2007] and the copper-catalysed intramolecular direct ring closure [Parai and Panda, 2009], a biocatalytic method [Lopez-Iglesias et al., 2015] and several other older methods [Mitscher et al., 1987; Atarashi et al., 1991; Kang et al., 1996; Satoh et al., 1998; Balint et al., 1999].

Rearrangement reactions are generally undesired, but in many instances can be favourable since they are able to facilitate the synthesis of synthetically complicated chemicals [Snape,

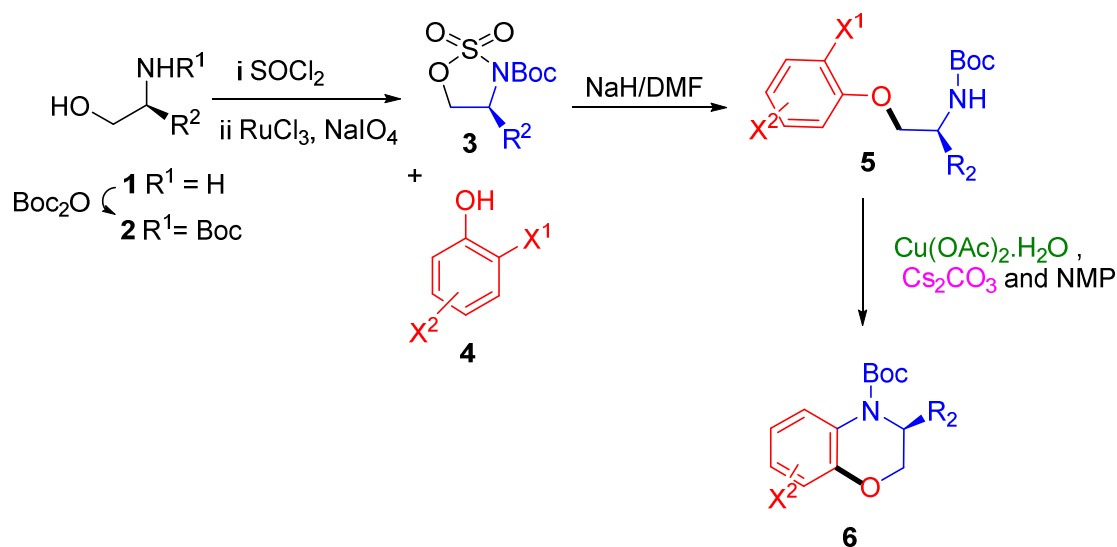
2008]. Additionally, these reactions provide an opportunity to synthesise organic molecules that were not possible previously.

The Smiles Rearrangement (SR) has been used in the synthesis of different benzoxazinones [Coutts and Southcott, 1990; Kang et al., 2008; Zuo et al., 2008; Xia et al., 2014]. To the best of our knowledge there have been no reports of this rearrangement in the synthesis of benzoxazines. In spite of the wealth of literature pertaining to SR, there is still a gap in the literature with regard to studies on the conformational effect on the copper catalysed ring closure via SR. It is well accepted that conformations of precursors can play a crucial role in chemical reactions and biological activity [Seeman, 1983; Agocs et al., 1997; Dobson, 2003; Wang et al., 2008; Nishizaka et al., 2010; Farahani et al., 2014; Lei et al., 2014]. As such, there is a need to explore this aspect further.

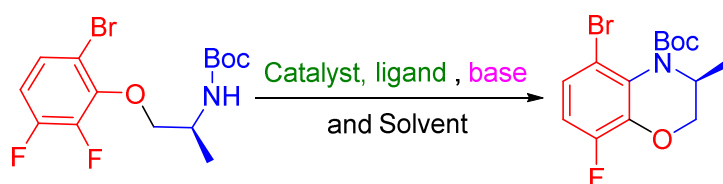
The initial aim of our work was to synthesise Levofloxacin's precursor (**6fi**) via a copper catalysed ring closure, but surprisingly the interruption by the SR was detected in all derivatives. Further investigation led us to provide a new insight to this rearrangement. The effects of conformational change as well as the presence of fluorine in novel derivatives of benzoxazines were investigated by NMR and X-ray crystallography. These studies helped us to propose a new mechanism for the one pot SR-ring closure reaction of benzoxazine type compounds. Herein we report an operationally simple and economic technique for the synthesis of enantiomerically pure fluorinated [1,4]-benzoxazines assisted by the SR and involving a copper mediated intramolecular ring closure, which can be considered as a novel procedure in comparison to the existing literature.

2.2 Results and discussion

Commercially available alaninol **1** was protected with Boc via standard procedures [Bower et al., 2007] to give **2**, which was transformed to a cyclic sulfamidate **3** over two steps with 90% overall yield [Bower et al., 2007]. The reaction of **3** and phenol **4** afforded the product **5** by nucleophilic cleavage in 98% yield [Bower et al., 2007]. The reaction of **5** with a catalytic amount of copper (II) acetate (20 mol %,) at 90 °C in (undried) NMP in the presence of Cs₂CO₃ (3 eq.) provided Boc-[1,4]-benzoxazine **6** by replacing the leaving group X¹ (either Br, I or F depending on the substrate) (Scheme 2-1).



Scheme 2-1 Synthesis of Boc-[1,4]-benzoxazine **6** procedure in comparison to the existing literature.

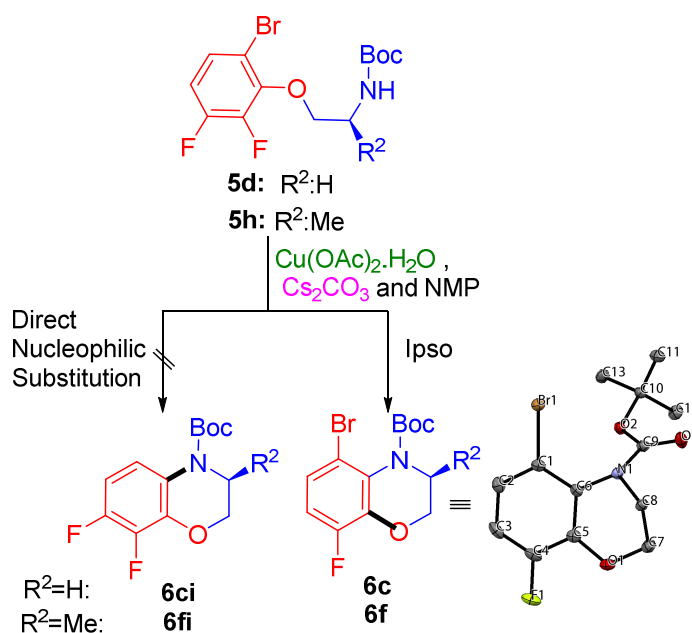
Table 2-1 Optimization of conditions for formation of Boc-[1,4]benzoxazine.

no.	cat.	ligand	base	solvent	temp. ^a	yield ^{b,c}
Solvent optimization						
1	Cu(OAc) ₂ .H ₂ O	none	Cs ₂ CO ₃	THF	90	trace
2	Cu(OAc) ₂ .H ₂ O	none	Cs ₂ CO ₃	toluene	90	trace
3	Cu(OAc) ₂ .H ₂ O	none	Cs ₂ CO ₃	Dioxane	90	75
4	Cu(OAc) ₂ .H ₂ O	none	Cs ₂ CO ₃	DMSO	90	75
5	Cu(OAc) ₂ .H ₂ O	none	Cs ₂ CO ₃	DMF	90	95
6	Cu(OAc) ₂ .H ₂ O	none	Cs ₂ CO ₃	NMP	90	98
Catalyst optimization						
7	CuBr	none	Cs ₂ CO ₃	NMP	90	60
8	CuI	none	Cs ₂ CO ₃	NMP	90	66
9	CuSO ₄	none	Cs ₂ CO ₃	NMP	90	79
10	Cu(OAc) ₂ .H ₂ O	none	Cs ₂ CO ₃	NMP	90	98
11	none	none	Cs ₂ CO ₃	NMP	90	None
Base optimization						
12	Cu(OAc) ₂ .H ₂ O	none	None	NMP	90	none
13	Cu(OAc) ₂ .H ₂ O	none	TEA ^d	NMP	90	trace
14	Cu(OAc) ₂ .H ₂ O	none	NaOC(CH ₃) ₃	NMP	90	73
15	Cu(OAc) ₂ .H ₂ O	none	KOH	NMP	90	80
16	Cu(OAc) ₂ .H ₂ O	none	K ₂ CO ₃	NMP	90	87
17	Cu(OAc) ₂ .H ₂ O	none	Cs ₂ CO ₃	NMP	90	98
Ligand optimization						
18	Cu(OAc) ₂ .H ₂ O	1,2-diamine	Cs ₂ CO ₃	NMP	90	80
19	Cu(OAc) ₂ .H ₂ O	Hyp ^e	Cs ₂ CO ₃	NMP	90	83
20	Cu(OAc) ₂ .H ₂ O	xantphos	Cs ₂ CO ₃	NMP	90	85
21	Cu(OAc) ₂ .H ₂ O	<i>L</i> -proline	Cs ₂ CO ₃	NMP	90	90
22	Cu(OAc) ₂ .H ₂ O	none	Cs ₂ CO ₃	NMP	90	98
Temperature optimization						
23	Cu(OAc) ₂ .H ₂ O	none	Cs ₂ CO ₃	NMP	25	90

^a Temperature (°C). ^b Isolated yield (%). ^c The reaction time for all reactions is 24 hours. ^d TEA: triethylamine ^e

Hyp: *trans*-4-Hydroxy-*L*-proline

On inspection of the ^{13}C and ^{19}F NMR data of the product **6f** from the precursor **5h**, it was apparent that the expected **6fi** (Scheme 2-2) did not form since there was a missing C-F resonance in the ^{13}C NMR spectrum and only a single fluorine resonance was observed in the ^{19}F NMR spectrum. The optimized reaction conditions (Table 2-1) were applied to **5d** and the same observation was found in the spectra of **6c**. Instead of **6ci** (Scheme 2-2), the rearranged compound (**6c**) was found to be the actual structure. This rearrangement, where the stronger F base acts as a leaving group, can be categorized as a SR that typically occurs in the presence of base in polar solvents [Snape, 2008b; Feng et al., 2009; Zhao et al., 2012]. Some reports have shown that Cu was essential for the SR ring closure to occur [Feng et al., 2009; Kitching et al., 2012; Sang et al., 2013; Ganguly et al., 2014; Hurst et al., 2015].

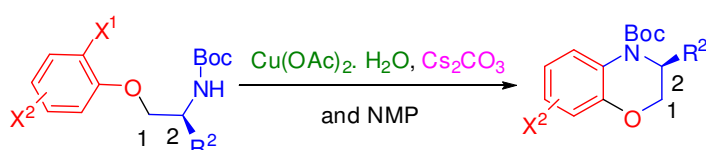


Scheme 2-2 Synthesis of Boc-[1,4]-benzoxazine **6** interrupted by SR

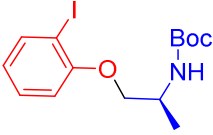
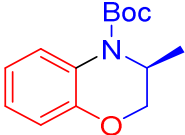
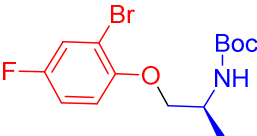
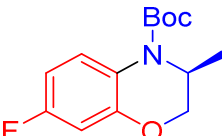
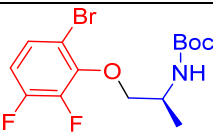
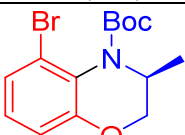
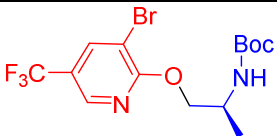
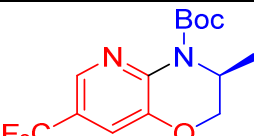
Considerable optimization showed that undried NMP (*N*-methyl-2-pyrrolidone) provided the best yield amongst other polar aprotic solvents. These results also indicated that $\text{Cu(OAc)}_2\cdot\text{H}_2\text{O}$ was the best catalyst amongst other copper sources. Control experiments in the absence of ligand revealed that $\text{Cu(OAc)}_2\cdot\text{H}_2\text{O}$ alone was capable of this catalytic

performance and application of an external ligand poisoned the reactions. In addition, no product was formed in the absence of copper, indicating its importance in the mechanism of the reaction. Various bases were also tested and amongst these, Cs₂CO₃ showed the best results. This was in agreement with other reports [Feng et al., 2009; Fang et al., 2011; Zhao et al., 2012; Ganguly et al., 2014].

Table 2-2 Synthesis of different Boc-benzoxazine via SR copper catalyzed ring closure



No.	Adduct (5) (Yield ^a %)	Boc-[1,4]-benzoxazine (yield ^a %) ^{b,c}
1	 5a (99%)	 6a (84%)
2	 5b (99%)	 6a (82%)
3	 5c (99%)	 6b (NR)
4	 5d (99%)	 6c (96%)
5	 5e (98%)	 6d (87%)

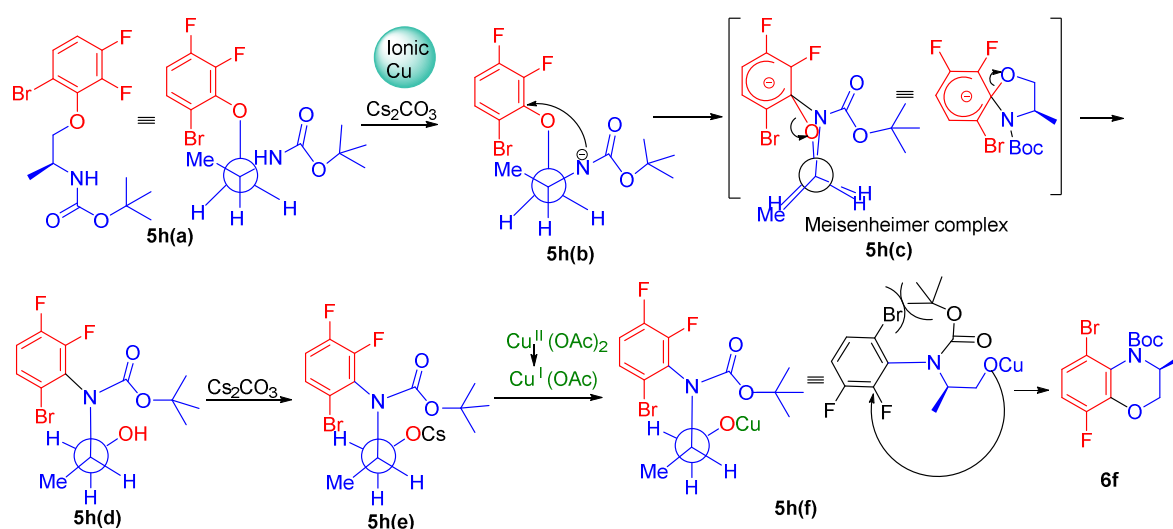
6	 <p>5f (98%)</p>	 <p>6d (82%)</p>
7	 <p>5g (99%)</p>	 <p>6e (NR)</p>
8	 <p>5h (99%)</p>	 <p>6f (98%)</p>
9	 <p>5i (99%)</p>	 <p>6g (NR)</p>

^a Isolated yield (%). ^b Temperature: 90 °C. ^c The reaction time for all reactions is 24 hours.

The reactions were repeated with the optimised conditions at room temperature instead of 90 °C. Surprisingly, the coupling reaction on **5d** and **5h** proceeded to **6c** and **6f** with 90 % yield at room temperature, while **5a** and **5b** proceeded to **6a**, and **5e** and **5f** to **6d** at 90 °C only and no product was observed at room temperature (Table 2-2). With the precursors **5c**, **5g** and **5i**, the products **6b**, **6e** and **6g** could not be formed even at 90 °C. This observation prompted us to study the conformation of adducts in the reaction in order to gain an insight into how the products were formed.

The presence of an iodine or bromine atom in the *ortho* position to the oxygenated side without further substitution (**5a**, **5b**, **5e** and **5f**) provided almost the same yield for the cyclized products **6a** and **6d** (~85 %) (Table 2-2). The highest yield was obtained for **6f** (98%) with the **5h** precursor. The other precursor with an *ortho* positioned F atom, **5d** also

had a similar yield of 96%. Therefore, it can be concluded that the electron-withdrawing effect of fluorine in the *ortho*-position of the aromatic ring stabilizes the formed intermediate (Meisenheimer complex **5h(c)** in **Scheme 2-3**) and therefore, the highest yields were obtained for **6c** and **6f**. Zhao et al. (2012) also showed that strong electron-withdrawing groups on the aromatic rings increase the yields of SR.



Scheme 2-3 Plausible catalytic cycle for formation of Boc-[1,4]-benzoxazine through the SR copper catalyzed ring closure reaction

It is likely that the SR copper catalyzed ring closure reaction in this study may follow the proposed mechanism in **Scheme 2-3**. In this proposed mechanism, the proton of the amide was removed from **5h(a)** in the presence of Cs_2CO_3 as a base (**Scheme 2-3**). This is followed by a nucleophilic substitution of the nitrogen onto the aromatic ring producing **5h(d)**. In the final step, the resulting nucleophilic oxygen in the side chain substitutes the *ortho* positioned F atom to yield the product **6f**.

The existence of different parameters seems to have a direct impact on the initiation of this reaction. The presence of the Boc protecting group seems to play a crucial role in the SR

[Bunnett and Zahler, 1951]. To prove this hypothesis, we applied the optimised reaction conditions on deprotected **5h** and observed that no cyclisation took place. Furthermore, it is suggested that the presence of a carbonyl group in the neighbouring NH (amide group) increases its nucleophilic effect in the SR [Bunnett and Zahler, 1951]. It is highly likely that this is the reason why there are no reports on the presence of SR for 1,4-benzoxazine, while this rearrangement was frequently reported for benzoxazinones.

Cu(OAc)₂ and Cs₂CO₃ are two other important reagents needed for this rearrangement to occur. The presence of ionic Cu plays a role in increasing the acidity of the amide proton and makes its deprotonation via Cs₂CO₃ easier [Ganguly et al., 2014].

It is also well accepted that the localized negative charge on the nitrogen in our study increases its nucleophilic strength [Bunnett and Zahler, 1951]. Polar aprotic solvents such as DMF and NMP are frequently used in the SR, which is in a good agreement with our optimized data [Ganguly et al., 2014; Hurst et al., 2015]. It is also suggested that these types of solvents stabilize the Meisenheimer complex and help improve the results [Ganguly et al., 2014].

This copper catalysed coupling reaction is known to occur through the presence of Cu(I). This is supported by literature, which reports that Cu(II) and Cu(0) as a source of Cu will be transformed to Cu(I) [Ribas and Gueell, 2014; Sambigioglio et al., 2014]. There are also reports that Cu(II) performed better than Cu(I) based on the selected conditions of the reaction [Li et al., 2012; Sang et al., 2013].

In addition, when there is competition between Br and F, the expected leaving group is assumed to be Br, the better of the two leaving groups. This did not occur in our experiments. The presence of steric hindrance between the Boc protecting group (**5h(f)** **Scheme 2-3**) and Br with a large atomic radius (in comparison to F) causes the oxygen to substitute the F instead of Br on the aromatic ring.

Based on the proposed mechanism in **Scheme 2-3**, this conformer (**5h**) facilitated the SR by shortening the distance between the nucleophile and the electrophile (ipso carbon) (**Figure 2-1**) for the occurrence of nucleophilic substitution. These desirable conformations of **5d** and **5h** assist these reactions, so much so that these reactions could proceed at room temperature with high yield.

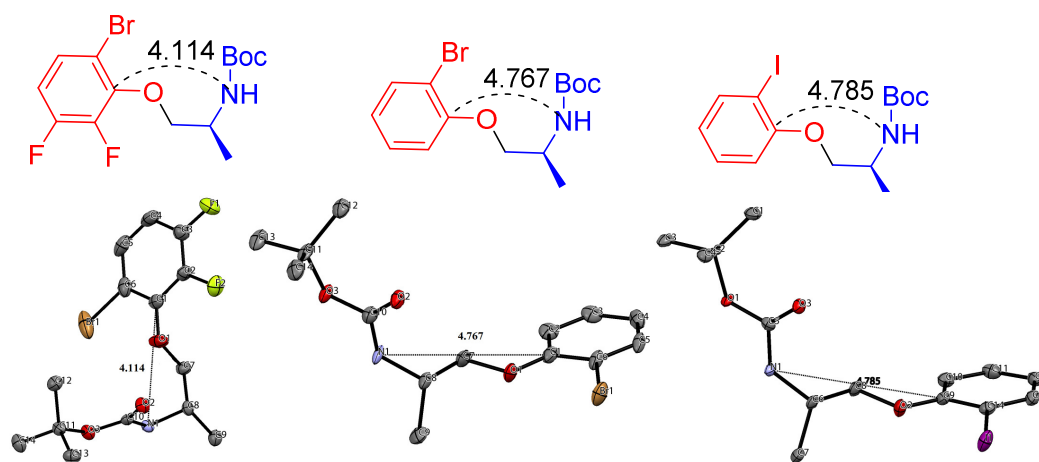


Figure 2-1 Crystal structure of **5e**, **5f** and **5h** and the distances between the *ipso* carbon and nitrogen

As can be seen from **Figure 2-1**, **5h** (and probably **5d**) possess a folded structure. Based on a review published by O'Hagan [O'Hagan, 2008], it can be proposed that the fluorine atoms in the aromatic ring of adduct **5g** (and **5d**) is situated in an ideal position for a dipole-dipole interaction, which results in the conformer shown in **Figure 2-1** and **Figure 2-2**. Since

fluorine atoms are well-known π donors, this interaction can be due to hyper-conjugation of the highly polarized C-F bonds, which is stabilized by the π system of the aromatic ring and provide the *gauche* conformer in **5h** (and **5d**) (**Figure 2-2**) [Rablen et al., 1999; Goodman et al., 2005; Sparr et al., 2011].

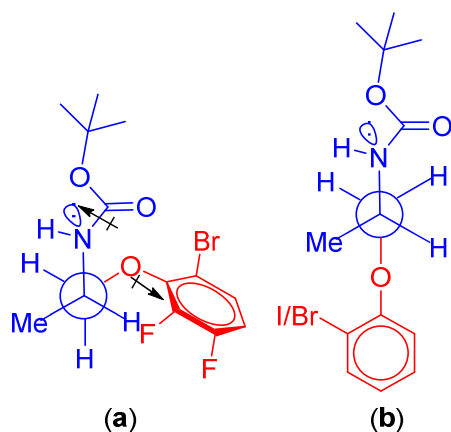


Figure 2-2 (a) *Gauche* conformer (from crystal structure of **5h**) (b) *anti* conformer (from crystal structure of **5e** and **5f**)

2.3 Conclusion

The new synthesis procedure for chiral [1,4]-benzoxazine derivatives containing F atoms as well as other halogens in different positions of the aromatic ring via the copper catalyzed SR ring closure provided valuable information about the effect of the SR on the synthesis and diversification of these valuable chemicals. The optimization reaction conditions as well as the proposed mechanism indicated the importance of the Boc protecting group, since this reaction could not proceed in its absence. Application of polar aprotic solvents seems to facilitate this reaction and enhances the final yield. In addition, presence of both a copper source and Cs_2CO_3 is crucial for this reaction to occur (**Scheme 2-3**). Finally, the reaction of adducts **5d** and **5h** (**Figure 1**) with folded structures in the *gauche* conformation (from crystallographic data) made it possible for these reactions to occur at room temperature.

2.4 Experimental Procedures

Compounds **2-4** were prepared according to standard procedures reported in the literature [Bower et al., 2007; Jangili et al., 2013].

General experimental procedure for the preparation of adduct 5: NaH (60 % dispersion in mineral oil, 40 mg, 1.01 mmol) was added to a solution of phenol **4** (211 mg, 1.01 mmol) in anhydrous DMF (10 mL) and the resultant mixture stirred at r.t. for 5 minutes. Cyclic sulfamidate **3** (200 mg, 0.84 mmol) was added and the mixture stirred at r.t. for 15 h prior to being concentrated in vacuo. The mixture was washed with saturated aq. NaCl and extracted with CH₂Cl₂ (3 × 20 mL). The combined organic extracts were concentrated in vacuo to afford amine **5**. This material was suitable for subsequent applications without any further purification. For analysis, a small portion was isolated by column chromatography (EtOAc/hexane: 5:95).

General experimental procedure for the preparation of dihydrobenzo[1,4]oxazines 6: In a 10 mL round bottom flask, Cu(OAc)₂ · H₂O (0.2 equiv), Cs₂CO₃ (3 equiv), and compound **5** (60 mg) were dissolved in NMP (5.0 mL). The mixture was stirred at 90 °C, and the progress of the reaction monitored by TLC. After 24 h the solvent was evaporated in vacuo and the residue diluted with CH₂Cl₂ (20 mL), washed with water (2×10 mL) and brine (2×10 mL), dried (Na₂SO₄) and concentrated in vacuo. The residue was purified by column chromatography (EtOAc/hexane: 10:90) to afford Boc-benzoxazine **6**.

Characterisation data for compounds 5a-i and 6a, 6c, 6d and 6f (For structures please refer to **Table 2-2**)

tert-butyl (2-(2-bromophenoxy)ethyl)carbamate (**5a**). colourless oil; ν_{\max} / cm^{-1} (film) 3441 (m), 2978 (m), 2934 (m), 1712 (s), 1587 (m), 1574 (m), 1509 (s), 1481 (s), 1278 (m), 1057 (s). ^1H NMR (400 MHz, CDCl_3) δ_{H} 1.41 (9H, s, $\text{NCO}_2\text{C}(\underline{\text{CH}_3})_3$), 3.51 (2H, m, 2C1-H), 4.00 (2H, t, 2C2-H, $J=5.2$), 5.24 (1H, br s, NH), 6.79 (2H, m, ArCH), 7.18 (1H, m, ArCH), 7.46 (1H, dd, $J=7.8, 1.5$ Hz, ArCH); ^{13}C NMR (100 MHz, CDCl_3) δ_{C} 28.4 ($\text{NCO}_2\text{C}(\underline{\text{CH}_3})_3$), 40.0 (C-1), 68.5 (C-2), 76.9 ($\text{NCO}_2\underline{\text{C}}(\text{CH}_3)_3$), 113.7 (ArCH), 122.3 (ArCH), 128.5 (ArCH), 133.2 (ArCH), 154.9 (s, C=O). The signals for the two aromatic quaternary carbons were not observed in the ^{13}C NMR spectrum. HRMS–ES⁺: m/z [M+Na] calcd for $\text{C}_{13}\text{H}_{18}\text{BrNO}_3$: 338.0368, found: 338.0376.

tert-butyl (2-(2-iodophenoxy)ethyl)carbamate (**5b**). colourless oil; ν_{\max} / cm^{-1} (film) 3355 (m), 2977 (m), 2934(m), 1711 (s), 1582(m), 1520 (s), 1475 (s), 1276 (m), 1247 (s), 1056 (s). ^1H NMR (400 MHz, CDCl_3) δ_{H} 1.37 (9H, s, $\text{NCO}_2\text{C}(\underline{\text{CH}_3})_3$), 3.49 (2H, m, 2C1-H), 3.96 (2H, t, 2C2-H, $J=5.1$ Hz), 5.08 (1H, br, s, NH), 6.63 (1H, td, ArCH, $J=7.6, 1.0$ Hz), 6.71 (1H, dd, ArCH, $J=7.3, 0.8$ Hz), 7.18 (1H, m, ArCH), 7.67 (1H, td, ArCH, $J=7.8, 1.5$ Hz); ^{13}C NMR (100 MHz, CDCl_3) δ_{C} 28.4 ($\text{NCO}_2\text{C}(\underline{\text{CH}_3})_3$), 40.0 (C-1), 68.6 (C-2), 79.5 ($\text{NCO}_2\underline{\text{C}}(\text{CH}_3)_3$), 86.8 (ArC-I), 112.5 (ArCH), 123.0 (ArCH), 129.6, (ArCH), 139.4 (ArCH), 155.9 (s, C=O), 157.0 (ArC). HRMS–ES⁺: m/z [M+Na] calcd for $\text{C}_{13}\text{H}_{18}\text{INO}_3$: 386.0229; found: 386.0230.

tert-butyl (2-(2-bromo-4-fluorophenoxy)ethyl)carbamate (**5c**). colourless oil; ν_{\max} / cm^{-1} (film) 3356 (m), 2979 (m), 2935 (m), 1712 (s), 1593 (m), 1493 (s), 1257 (m), 1171 (m), 1048 (s). ^1H NMR (400 MHz, CDCl_3) δ_{H} 1.37 (9H, s, $\text{NCO}_2\text{C}(\underline{\text{CH}_3})_3$), 3.47 (2H, m, 2C1-H), 3.95 (2H, t, 2C2-H, $J=5.0$ Hz), 5.06 (1H, br, s, NH), 6.76 (1H, dd, ArCH, $J=9.0, 4.7$ Hz), 6.88 (1H, m,

ArCH), 7.20 (1H, dd, ArCH, $J=7.8, 3.0$ Hz); ^{13}C NMR (100 MHz, CDCl_3) δ_{C} 28.4 ($\text{NCO}_2\text{C}(\underline{\text{C}}\text{H}_3)_3$), 40.0 (C-1), 69.4 (C-2), 79.6 ($\text{NCO}_2\text{C}(\underline{\text{C}}\text{H}_3)_3$), 114.3 (d, $J= 8.3$ Hz, ArCH), 114.8 (d, $J= 22.5$ Hz, ArCH), 120.4 (d, $J= 25.7$ Hz, ArCH), 151.6 (d, $J=2.9$ Hz, ArC), 156.0 (s, 2C, C=O, ArC-O), 156.9 (d, $J=243.5$ Hz, ArC). HRMS-ES⁺: m/z [M+Na] calcd for $\text{C}_{13}\text{H}_{17}\text{BrFNO}_3$: 356.0274; found: 356.0276.

tert-butyl (2-(6-bromo-2,3-difluorophenoxy)ethyl)carbamate (**5d**). colourless oil; $\nu_{\text{max}}/\text{cm}^{-1}$ (film) 3359 (m), 2979 (s), 2934 (s), 1705 (s), 1612 (m), 1584 (m), 1487 (s), 1292 (m), 1171 (s), 1054 (m). ^1H NMR (400 MHz, CDCl_3) δ_{H} 1.36 (9H, s, $\text{NCO}_2\text{C}(\text{CH}_3)_3$), 3.43 (2H, m, 2C1-H), 4.10 (2H, t, 2C2-H, $J=4.98$ Hz), 5.24 (1H, br, s, NH), 6.73 (1H, ddd, ArCH, $J=9.2, 9.1, 7.7$ Hz), 7.15 (1H, ddd, ArCH, $J=9.0, 5.4, 2.5$ Hz). ^{13}C NMR (100 MHz, CDCl_3) δ_{C} 28.4 ($\text{NCO}_2\text{C}(\text{CH}_3)_3$), 40.6 (C-1), 73.6 (C-2), 79.4 ($\text{NCO}_2\text{C}(\text{CH}_3)_3$), 112.6 (d, $J=18.3$ Hz, ArCH), 126.7 (dd, $J=7.5, 4.2$ Hz, ArCH), 144.9 (dd, $J= 250.9, 14.3$ Hz, ArC), 145.4 (d, $J=8.2$ Hz, ArC), 150.5 (dd, $J=250.2, 11.3$ Hz, ArC), 155.9 (ArC). HRMS-ES⁺: m/z [M+Na] calcd for $\text{C}_{13}\text{H}_{17}\text{BrFNO}_3$: 374.04; found: 374.017.

tert-butyl (*S*)-(1-(2-bromophenoxy)propan-2-yl)carbamate (**5e**). colourless crystal; mp 53-55 °C; $[\alpha]_{\text{D}}^{20}$ -32.20° ($c=0.35$, MeOH); $\nu_{\text{max}}/\text{cm}^{-1}$ (film) 3431 (m), 2978 (s), 2934 (m), 1715 (s), 1586 (m), 1574 (m), 1504 (s), 1483 (s), 1169 (m), 1053 (m). ^1H NMR (600 MHz, CDCl_3) δ_{H} 1.32 (3H, d, $J=6.8$ Hz, C1-CH₃), 1.43 (9H, s, $\text{NCO}_2\text{C}(\underline{\text{C}}\text{H}_3)_3$), 3.95 (1H, s, br, C1-H), 4.07 (2H, s, br, 2C2-H), 5.01 (1H, br, s, NH), 6.80 (1H, t, $J=7.6$ Hz, ArCH), 6.85 (1H, d, $J=8.2$ Hz, ArCH), 7.20 (1H, t, $J=7.7$ Hz, ArCH), 7.49 (1H, d, $J=7.8$ Hz, ArCH); ^{13}C NMR (100 MHz, CDCl_3) δ_{C} 17.9 (C1-CH₃), 28.4 ($\text{NCO}_2\text{C}(\underline{\text{C}}\text{H}_3)_3$), 45.8 (C-1), 72.1 (C-2), 113.4 (ArCH), 122.2 (ArCH), 122.4 (ArC), 128.5 (ArCH), 133.3 (ArCH), 155.0 (s, 2C, C=O, ArC-

O). The signal for the quaternary Boc carbon was not observed in the ^{13}C NMR spectrum. HRMS–ES⁺: m/z [M+Na] calcd for $\text{C}_{14}\text{H}_{20}\text{BrNO}_3$: 352.0524; found: 352.0529.

tert-butyl (*S*)-(1-(2-iodophenoxy)propan-2-yl)carbamate (**5f**). colourless crystal; mp 60-62 °C; $[\alpha]_{\text{D}}^{20}$ -33.7° (c=0.5, MeOH); $\nu_{\text{max}}/\text{cm}^{-1}$ (film) 3425 (m), 2977 (s), 2933 (m), 1715 (s), 1583 (m), 1571 (m), 1502 (m), 1366 (m), 1246 (s), 1051 (m). ^1H NMR (600 MHz, CDCl_3) δ_{H} 1.36 (3H, d, $J=6.9$ Hz, C1- $\underline{\text{CH}}_3$), 1.44 (9H, s, $\text{NCO}_2\text{C}(\underline{\text{CH}}_3)_3$), 3.94 (1H, s, br, C1- $\underline{\text{H}}$), 4.10 (2H, s, br, 2C2- $\underline{\text{H}}$), 5.0 (1H, br, s, $\underline{\text{NH}}$), 6.68 (1H, t, $J=7.5$ Hz, Ar $\underline{\text{CH}}$), 6.76 (1H, d, $J=8.2$ Hz, Ar $\underline{\text{CH}}$), 7.25 (1H, m, Ar $\underline{\text{CH}}$), 7.73 (1H, dd, $J=7.7, 1.3$, Ar $\underline{\text{CH}}$); ^{13}C NMR (100 MHz, CDCl_3) δ_{C} 18.2 (C1- $\underline{\text{CH}}_3$), 28.4 ($\text{NCO}_2\text{C}(\underline{\text{CH}}_3)_3$), 45.8 ($\underline{\text{C}}-1$), 72.1 ($\underline{\text{C}}-2$), 86.6 (ArC- $\underline{\text{I}}$), 112.2 (Ar $\underline{\text{CH}}$), 122.8 (Ar $\underline{\text{CH}}$), 129.6 (Ar $\underline{\text{CH}}$), 139.3 (Ar $\underline{\text{CH}}$), 155.3 (s, C=O), 157.0 (Ar $\underline{\text{C}}-\underline{\text{O}}$). The signal for the quaternary Boc carbon was not observed in the ^{13}C NMR spectrum. HRMS–ES⁺: m/z [M+Na] calcd for $\text{C}_{14}\text{H}_{20}\text{INO}_3$: 400.0386; found: 400.0396.

tert-butyl (*S*)-(1-(2-bromo-4-fluorophenoxy)propan-2-yl)carbamate (**5g**). colourless oil; $[\alpha]_{\text{D}}^{20}$ -28.25° (c=0.4, MeOH); $\nu_{\text{max}}/\text{cm}^{-1}$ (film) 3347 (m), 2978 (m), 2934 (m), 1699 (s), 1493 (s), 1470 (m), 1392 (m), 1367 (m), 1260 (s), 1191 (s), 1046 (s). ^1H NMR (400 MHz, CDCl_3) δ_{H} 1.25 (3H, d, $J=6.7$ Hz, C1- $\underline{\text{CH}}_3$), 1.37 (9H, s, $\text{NCO}_2\text{C}(\underline{\text{CH}}_3)_3$), 3.86 (2H, d, $J=3.6$ Hz, 2C2- $\underline{\text{H}}$), 3.98 (1H, s, C1- $\underline{\text{H}}$), 4.82 (1H, br, s, $\underline{\text{NH}}$), 6.75 (1H, dd, $J=9.0, 4.7$, Ar $\underline{\text{CH}}$), 6.87 (1H, m, Ar $\underline{\text{CH}}$), 7.19 (1H, dd, $J=7.8, 2.9$, Ar $\underline{\text{CH}}$); ^{13}C NMR (100 MHz, CDCl_3) δ_{C} 17.9 (C1- $\underline{\text{CH}}_3$), 28.4 ($\text{NCO}_2\text{C}(\underline{\text{CH}}_3)_3$), 50.5 (C-1), 72.8 (C-2), 114.0 (d, $J=8.6$ Hz, Ar $\underline{\text{CH}}$), 114.7 (d, $J=22.6$ Hz, Ar $\underline{\text{CH}}$), 120.4 (d, $J=25.8$ Hz, Ar $\underline{\text{CH}}$), 158.0 (s, C=O). The signals for the quaternary carbons were not observed in the ^{13}C NMR spectrum. HRMS–ES⁺: m/z [M+Na] calcd for $\text{C}_{14}\text{H}_{19}\text{BrFNO}_3$: 370.0430; found: 370.0419.

tert-butyl (*S*)-(1-(6-bromo-2,3-difluorophenoxy)propan-2-yl)carbamate (**5h**). colourless crystals; mp 55-57 °C; $[\alpha]_D^{20}$ -21.7° (c=0.35, MeOH). $\nu_{\max}/\text{cm}^{-1}$ (film) 3342 (m), 2979 (m), 2933 (m), 1713 (s), 1612 (m), 1584 (m), 1488 (s), 1391 (m), 1367 (m), 1170 (s), 1049 (s). ^1H NMR (400 MHz, CDCl_3) δ_{H} 1.28 (3H, d, $J=6.8$ Hz, C1- $\underline{\text{CH}}_3$), 1.37 (9H, s, $\text{NCO}_2\text{C}(\underline{\text{CH}}_3)_3$), 3.92 (1H, s, C1- $\underline{\text{H}}$), 4.40 (2H, s, 2C2- $\underline{\text{H}}$), 4.89 (1H, br, s, $\underline{\text{NH}}$), 6.74 (1H, m, Ar $\underline{\text{CH}}$), 7.18 (1H, m, Ar $\underline{\text{CH}}$); ^{13}C NMR (100 MHz, CDCl_3) δ_{C} 17.6 (C1- $\underline{\text{C}}\text{H}_3$), 28.5 ($\text{NCO}_2\text{C}(\underline{\text{C}}\text{H}_3)_3$), 46.5 (C-1), 77.0 (C-2), 79.4 ($\text{NCO}_2\underline{\text{C}}(\text{CH}_3)_3$), 111.5 (d, $J=3.6$ Hz, Ar $\underline{\text{C}}$), 112.5 (d, $J=18.4$ Hz, Ar $\underline{\text{CH}}$), 126.8 (dd, $J=7.6, 4.2$ Hz, Ar $\underline{\text{CH}}$), 144.9 (dd, $J=252.8, 14.3$ Hz, Ar $\underline{\text{C}}$), 145.6 (dd, $J=7.9, 2.2$ Hz, Ar $\underline{\text{C}}$), 150.8 (dd, $J=250.3, 11.4$ Hz, Ar $\underline{\text{C}}$), 155.3 (s, C=O). HRMS-ES⁺: m/z [M+Na] calcd for $\text{C}_{14}\text{H}_{18}\text{BrF}_2\text{NO}_3$: 388.0336; found: 388.0335.

tert-butyl (*S*)-(1-((3-bromo-5-(trifluoromethyl)pyridin-2-yl)oxy)propan-2-yl)carbamate (**5i**). white powder; mp 68-70 °C; $[\alpha]_D^{20}$ -21.83° (c=0.35, MeOH); $\nu_{\max}/\text{cm}^{-1}$ (film) 3348 (m), 2979 (m), 2934 (m), 1704 (s), 1604 (m), 1482 (s), 1367 (m), 1320 (m), 1162 (s), 1055 (s). ^1H NMR (400 MHz, CDCl_3) δ_{H} 1.22 (3H, d, $J=6.8$ Hz, C1- $\underline{\text{CH}}_3$), 1.37 (9H, s, $\text{NCO}_2\text{C}(\underline{\text{CH}}_3)_3$), 4.07 (1H, s, C1- $\underline{\text{H}}$), 4.31 (2H, m, 2C2- $\underline{\text{H}}$), 4.66 (1H, br, s, $\underline{\text{NH}}$), 7.94 (1H, d., $J=1.7$ Hz, Ar $\underline{\text{CH}}$), 8.27 (1H, s, Ar $\underline{\text{CH}}$); ^{13}C NMR (100 MHz, CDCl_3) δ_{C} 17.8 (C1- $\underline{\text{C}}\text{H}_3$), 28.4 ($\text{NCO}_2\text{C}(\underline{\text{C}}\text{H}_3)_3$), 45.5 (C-1), 70.7 (C-2), 107.4 (Ar $\underline{\text{C}}$), 121.4 (q, $J=33.4$ Hz, Ar $\underline{\text{C}}$), 123.0 (q, $J=271.6$ Hz, $\underline{\text{C}}\text{F}_3$), 138.6 (q, $J=3.1$ Hz, Ar $\underline{\text{CH}}$), 143.2 (q, $J=4.3$ Hz, Ar $\underline{\text{CH}}$), 155.2 (C=O), 161.7 (Ar $\underline{\text{C}}\text{-O}$). HRMS-ES⁺: m/z [M+Na] calcd for $\text{C}_{14}\text{H}_{18}\text{BrF}_3\text{N}_2\text{O}_3$: 421.0351; Found: 421.0363.

tert-butyl 2,3-dihydro-4*H*-benzo[*b*][1,4]oxazine-4-carboxylate (**6a**). colourless oil; $\nu_{\max}/\text{cm}^{-1}$ (film) 2977 (s), 2932 (s), 1705 (s), 1605 (m), 1586 (m), 1497 (m), 1380 (s), 1148 (s), 1062 (s); ^1H NMR (400 MHz, CDCl_3) δ_{H} 1.47 (9H, s, $\text{NCO}_2\text{C}(\underline{\text{CH}}_3)_3$), 3.78 (2H, t, $J=4.5$ Hz, 2C1-

H), 4.17 (2H, t, $J=4.4$ Hz, 2C2-H), 6.80 (2H, m, ArCH), 6.90 (1H, m, ArCH), 7.70 (1H, m, ArCH); ^{13}C NMR (100 MHz, CDCl_3) δ_{C} 28.3 ($\text{NCO}_2\text{C}(\underline{\text{C}}\text{H}_3)_3$), 42.1 (C-1), 65.6 (C-2), 81.6 ($\text{NCO}_2\text{C}(\underline{\text{C}}\text{H}_3)_3$), 117.0 (ArCH), 120.2 (ArCH), 123.5 (ArCH), 124.4 (ArCH), 145.9 (ArC-Q). The resonances for the C=O group and the aromatic C-N were not observed in ^{13}C NMR spectrum. The spectroscopic properties of this compound were consistent with the data available in the literature [Jangili et al., 2013].

tert-butyl 5-bromo-8-fluoro-2,3-dihydro-4*H*-benzo[*b*][1,4]oxazine-4-carboxylate (**6c**). colourless crystals; $\nu_{\text{max}}/\text{cm}^{-1}$ (film) 2979 (s), 2936 (s), 2890 (m), 1713 (s), 1609 (m), 1582 (m), 1483 (s), 1368 (s), 1161 (s), 1043 (s); ^1H NMR (400 MHz, CDCl_3) δ_{H} 1.41 (9H, s, $\text{NCO}_2\text{C}(\underline{\text{C}}\text{H}_3)_3$), 4.15 (2H, m, 2C1-H), 4.40 (2H, br, 2C2-H), 6.75 (1H, dd, ArCH, $J=10.1, 8.9$ Hz), 6.99 (1H, ddd, ArCH, $J=8.8, 5.0$ Hz); ^{13}C NMR (100 MHz, CDCl_3) δ_{C} 28.0 ($\text{NCO}_2\text{C}(\underline{\text{C}}\text{H}_3)_3$), 66.6 (C-1), 68.1 (C-2), 82.5 ($\text{NCO}_2\text{C}(\underline{\text{C}}\text{H}_3)_3$), 113.6 (d, $J=19.0$ Hz, ArCH), 115.0 (d, $J=3.5$ Hz, ArC), 123.0 (d, $J=7.4$ Hz, ArCH), 150.9 (d, $J=246.0$ Hz, ArCF). The resonances for the C=O group and the quaternary aromatic C-O carbon were not observed in ^{13}C NMR spectrum. The sample did not ionise properly and as such a HRMS could not be obtained.

tert-butyl (*S*)-3-methyl-2,3-dihydro-4*H*-benzo[*b*][1,4]oxazine-4-carboxylate (**6d**). colourless oil; $[\alpha]_{\text{D}}^{20} - 26.6^\circ$ ($c=0.18$, MeOH); $\nu_{\text{max}}/\text{cm}^{-1}$ (film) 2976 (s), 2930 (s), 2876 (m), 1698 (s), 1605 (m), 1585 (m), 1496 (s), 1368 (m), 1171 (m), 1064 (m). ^1H NMR (600 MHz, CDCl_3) δ_{H} 1.34 (3H, d, $J=6.8$ Hz, C1-CH₃), 1.47 (9H, s, $\text{NCO}_2\text{C}(\underline{\text{C}}\text{H}_3)_3$), 4.04 (1H, d, $J=2.0$ Hz, C1-H), 4.60 (2H, m, 2C2-H), 6.81 (2H, m, 2ArCH), 6.89 (1H, m, ArCH), 7.78 (1H, m, ArCH); ^{13}C NMR (100 MHz, CDCl_3) δ_{C} 15.6 (C1-CH₃), 28.4 ($\text{NCO}_2\text{C}(\underline{\text{C}}\text{H}_3)_3$), 46.2 (C-1), 69.0 (C-2), 81.5 ($\text{NCO}_2\text{C}(\underline{\text{C}}\text{H}_3)_3$), 116.7 (ArCH), 120.5 (ArCH), 123.7 (ArCH), 123.9 (ArCH). The

resonances for the C=O and quaternary aromatic C-O and C-N carbons were not observed in ^{13}C NMR spectrum. The ^1H and ^{13}C NMR data were consistent with that available in the literature [Jangili et al., 2013].

tert-butyl (S)-5-bromo-8-fluoro-3-methyl-2,3-dihydro-4*H*-benzo[*b*][1,4]oxazine-4-carboxylate (**6f**). colourless oil; $[\alpha]_{\text{D}}^{20}$ - 25.5° (c =0.2, CHCl_3). $\nu_{\text{max}}/\text{cm}^{-1}$ (film) 2979 (m), 2935 (m), 2889 (m), 1712 (s), 1608 (m), 1585 (m), 1450 (m), 1369 (m), 1171 (m), 1033 (m). ^1H NMR (400 MHz, CDCl_3) δ_{H} 1.10 (3H, d, $J=7.2$ Hz, C1- CH_3), 1.47 (9H, s, $\text{NCO}_2\text{C}(\text{CH}_3)_3$), 4.19 (2H, m, C2- H), 4.78 (1H, br s, C1- H), 6.83 (1H, m, Ar CH), 7.07 (1H, m, Ar CH); ^{13}C NMR (100 MHz, CDCl_3) δ_{C} 15.5 (C1- CH_3), 28.1 ($\text{NCO}_2\text{C}(\text{CH}_3)_3$), 45.9 (C-1), 70.3 (C-2), 82.5 ($\text{NCO}_2\text{C}(\text{CH}_3)_3$), 113.6 (d, $J=18.9$ Hz, Ar CH), 116.3 (s, Ar C), 123.4 (d, $J=7.3$ Hz, Ar CH), 150.6 (d, $J=245.8$ Hz, Ar CF). The resonances for the C=O group and the quaternary aromatic C-O carbon were not observed in ^{13}C NMR spectrum. Elemental Anal Calcd. for $\text{C}_{14}\text{H}_{17}\text{BrFNO}_3$: C, 48.57; H, 4.95, N, 4.05%. Found: C, 48.75; H, 4.68, N, 3.98%. The sample did not ionise properly and as such a HRMS could not be obtained. Thus, **6f** was deprotected to confirm the structure. The ^1H NMR, ^{13}C NMR, ^{19}F NMR and HRMS data is available below.

(S)-5-bromo-8-fluoro-3-methyl-3,4-dihydro-2*H*-benzo[*b*][1,4]oxazine (Boc deprotected **6f**). colourless oil; $[\alpha]_{\text{D}}^{20}$ +13.5° (c=0.2, CHCl_3). ^1H NMR (400 MHz, CDCl_3) δ_{H} 1.28 (3H, d, $J=6.4$ Hz, C1- CH_3), 3.63 (1H, m, C1- H), 3.80 (1H, dd, $J=10.4, 7.8$ Hz, C2- H), 4.26 (1H, brs, NH), 4.29 (1H, m, C2- H), 6.42 (1H, m, Ar CH), 6.95 (1H, m, Ar CH); ^{13}C NMR (150 MHz, CDCl_3) δ_{C} 17.6 (C1- CH_3), 45.3 (C-1), 70.4 (C-2), 102.9 (Ar C , d, 2.2 Hz), 103.7 (d, $J=19.9$ Hz, Ar CH), 123.2 (d, $J=8.6$ Hz, Ar CH), 132.2 (d, $J=14.9$ Hz, Ar C), 133.2 (d, $J=4.4$ Hz, Ar C),

151.0 (d, $J=242.2$ Hz, ArCF). HRMS-ES⁺: m/z [M+H] calcd for C₉H₁₀NOFBr: 245.9930; found: 245.9931.

2.5 References

- Achari, B., Mandal, S.B., Dutta, P.K., Chowdhury, C., Perspectives on 1,4-benzodioxins, 1,4-benzoxazines and their 2,3-dihydro derivatives. *Synlett*, **2004**, 2449-2467.
- Agoes, L., Briand, G.G., Burford, N., Cameron, T.S., Kwiatkowski, W., Robertson, K.N., The structurally flexible bicyclic bis(2-hydroxyethanethiolato)bismuth(III) complex: A model for asymmetric monoanionic chelation of bismuth(III). *Inorganic Chemistry*, **1997**, 36, 2855-2860.
- Atarashi, S., Tsurumi, H., Fujiwara, T., Hayakawa, I., Asymmetric reduction of 7,8-difluoro-3-methyl-2*H*-1,4-benzoxazine - synthesis of a key intermediate of (*S*)-(-)-ofloxacin (DR-3355). *Journal of Heterocyclic Chemistry*, **1991**, 28, 329-331.
- Atarashi, S., Yokohama, S., Yamazaki, K.I., Sakano, K.I., Imamura, M., Hayakawa, I., Synthesis and antibacterial activities of optically-active ofloxacin and its fluoromethyl derivative. *Chemical & Pharmaceutical Bulletin*, **1987**, 35, 1896-1902.
- Balint, J., Egri, G., Fogassy, E., Bocskei, Z., Simon, K., Gajary, A., Friesz, A., Synthesis, absolute configuration and intermediates of 9-fluoro-6,7-dihydro-5-methyl-1-oxo-1*H*,5*H*-benzo [*i,j*]quinolizine-2-carboxylic acid (flumequine). *Tetrahedron: Asymmetry*, **1999**, 10, 1079-1087.
- Bower, J.F., Szeto, P., Gallagher, T., Enantiopure 1,4-benzoxazines via 1,2-cyclic sulfamidates. Synthesis of levofloxacin. *Organic Letters*, **2007**, 9, 3283-3286.
- Bunnett, J.F., Zahler, R.E., Aromatic nucleophilic substitution reactions. *Chemical Reviews*, **1951**, 49, 273-412.
- Coutts, I.G.C., Southcott, M.R., The conversion of phenols to primary and secondary aromatic-amines via a Smiles rearrangement. *Journal of the Chemical Society-Perkin Transactions 1*, **1990**, 767-771.
- Dias, N., Goossens, J.F., Baldeyrou, B., Lansiaux, A., Colson, P., Di Salvo, A., Bernal, J., Turnbull, A., Mincher, D.J., Bailly, C., Oxoazabeno[*de*]anthracenes conjugated to amino acids: Synthesis and evaluation as DNA-binding antitumor agents. *Bioconjugate Chemistry*, **2005**, 16, 949-958.
- Dobson, C.M., Protein folding and misfolding. *Nature*, **2003**, 426, 884-890.
- Ganguly, N.C., Mondal, P., Roy, S., Mitra, P., Ligand-free copper-catalyzed efficient one-pot access of benzo[*b*]pyrido[3,2-*f*][1,4]oxazepinones through *O*-heteroarylation-Smiles rearrangement-cyclization cascade. *RSC Advances*, **2014**, 4, 55640-55648.
- Goodman, L., Gu, H.B., Pophristic, V., Gauche effect in 1,2-difluoroethane. Hyperconjugation, bent bonds, steric repulsion. *Journal of Physical Chemistry A*, **2005**, 109, 1223-1229.

- Ebner, C., Pfaltz, A., Chiral dihydrobenzo-1,4-oxazines as catalysts for the asymmetric transfer-hydrogenation of alpha,beta-unsaturated aldehydes. *Tetrahedron*, **2011**, 67, 10287-10290.
- Farahani, M.D., Honarparvar, B., Albericio, F., Maguire, G.E.M., Govender, T., Arvidsson, P.I., Kruger, H.G., Proline *N*-oxides: Modulators of the 3D conformation of linear peptides through "NO-turns". *Organic & Biomolecular Chemistry*, **2014**, 12, 4479-4490.
- Fang, L., Zuo, H., Li, Z.B., He, X.Y., Wang, L.Y., Tian, X., Zhao, B.X., Miao, J.Y., Shin, D.S., Synthesis of benzo[*b*][1,4]oxazin-3(4*H*)-ones via Smiles rearrangement for antimicrobial activity. *Medicinal Chemistry Research*, **2011**, 20, 670-677.
- Feng, E., Huang, H., Zhou, Y., Ye, D., Jiang, H., Liu, H., Copper(I)-catalyzed one-pot synthesis of 2*H*-1,4-benzoxazin-3-(4*H*)-ones from *O*-halophenols and 2-chloroacetamides. *Journal of Organic Chemistry*, **2009**, 74, 2846-2849.
- Hays, S.J., Caprathe, B.W., Gilmore, J.L., Amin, N., Emmerling, M.R., Michael, W., Nadimpalli, R., Nath, R., Raser, K.J., Stafford, D., Watson, D., Wang, K., Jaen, J.C., 2-Amino-4*H*-3,1-benzoxazin-4-ones as inhibitors of C1r serine protease. *Journal of Medicinal Chemistry*, **1998**, 41, 1060-1067.
- Hurst, T.E., Kitching, M.O., da Frola, L.C.R.M., Guimaraes, K.G., Dalziel, M.E., Snieckus, V., Metal-free synthesis of dibenzoxazepinones via a one-pot SNAr and Smiles rearrangement process: Orthogonality with copper-catalyzed cyclizations. *Synlett*, **2015**, 26, 1455-1460.
- Jana, S., Ashokan, A., Kumar, S., Verma, A., Kumar, S., Copper-catalyzed trifluoromethylation of alkenes: Synthesis of trifluoromethylated benzoxazines. *Organic & Biomolecular Chemistry*, **2015**, 13, 8411-8415.
- Jangili, P., Kashanna, J., Das, B., Synthesis of dihydrobenzo[1,4]oxazines using copper catalyzed intramolecular ring closure reaction. *Tetrahedron Letters*, **2013**, 54, 3453-3456.
- Kang, J., Kam, K.H., Ghate, M., Hua, Z., Kim, T.H., Reddy, C.R., Chandrasekhar, S., Shin, D.S., An efficient synthesis of 2*H*-1,4-benzoxazin-3(4*H*)-ones via Smiles rearrangement. *ARKIVOC*, **2008**, 67-76.
- Kang, S.B., Ahn, E.J., Kim, Y., Kim, Y.H., A facile synthesis of (*S*)-(-)-7,8-difluoro-3,4-dihydro-3-methyl-2*H*-1,4-benzoxazine by zinc chloride assisted Mitsunobu cyclization reaction. *Tetrahedron Letters*, **1996**, 37, 9317-9320.
- Kitching, M.O., Hurst, T.E., Snieckus, V., Copper-catalyzed cross-coupling interrupted by an opportunistic Smiles rearrangement: An efficient domino approach to dibenzoxazepinones. *Angewandte Chemie-International Edition*, **2012**, 51, 2925-2929.
- Komnatnyy, V.V., Chiang, W.-C., Tolker-Nielsen, T., Givskov, M., Nielsen, T.E., Bacteria-triggered release of antimicrobial agents. *Angewandte Chemie-International Edition*, **2014**, 53, 439-441.
- Lei, T., Xia, X., Wang, J.-Y., Liu, C.-J., Pei, J., "Conformation locked" strong electron-deficient poly(*p*-phenylene vinylene) derivatives for ambient-stable *n*-type field-effect transistors: Synthesis, properties, and effects of fluorine substitution position. *Journal of the American Chemical Society*, **2014**, 136, 2135-2141.

- Li, S., Li, Z., Wu, J., Synthesis of benzoindolines via a copper-catalyzed reaction of 1-bromoethynyl-2-(cyclopropylidenemethyl)arenes with *N*-allylsulfonamide. *Advanced Synthesis & Catalysis*, **2012**, 354, 3087-3094.
- Lopez-Iglesias, M., Busto, E., Gotor, V., Gotor-Fernandez, V., Chemoenzymatic asymmetric synthesis of 1,4-benzoxazine derivatives: Application in the synthesis of a levofloxacin precursor. *Journal of Organic Chemistry*, **2015**, 80, 3815-3824.
- Mitscher, L.A., Sharma, P.N., Chu, D.T.W., Shen, L.L., Pernet, A.G., Chiral DNA gyrase inhibitors. 2. Asymmetric-synthesis and biological-activity of the enantiomers of 9-fluoro-3-methyl-10-(4-methyl-1-piperazinyl)-7-oxo-2,3-dihydro-*H*-7-pyrido[1,2,3-*de*]-1,4-benzoxazine-6-carboxylic acid (ofloxacin). *Journal of Medicinal Chemistry*, **1987**, 30, 2283-2286.
- Nishizaka, M., Mori, T., Inoue, Y., Conformation elucidation of tethered donor-acceptor binaphthyls from the anisotropy factor of a charge-transfer band. *Journal of Physical Chemistry Letters*, **2010**, 1, 2402-2405.
- O'Hagan, D., Understanding organofluorine chemistry. An introduction to the C-F bond. *Chemical Society Reviews*, **2008**, 37, 308-319.
- Parai, M.K., Panda, G., A convenient synthesis of chiral amino acid derived 3,4-dihydro-2*H*-benzo[*b*][1,4]thiazines and antibiotic levofloxacin. *Tetrahedron Letters*, **2009**, 50, 4703-4705.
- Purser, S., Moore, P.R., Swallow, S., Gouverneur, V., Fluorine in medicinal chemistry. *Chemical Society Reviews*, **2008**, 37, 320-330.
- Rablen, P.R., Hoffmann, R.W., Hrovat, D.A., Borden, W.T., Is hyperconjugation responsible for the "*gauche* effect" in 1-fluoropropane and other 2-substituted-1-fluoroethanes? *Journal of the Chemical Society-Perkin Transactions 2*, **1999**, 1719-1726.
- Seeman, J.I., Effect of conformational change on reactivity in organic chemistry. Evaluations, applications, and extensions of Curtin-Hammett Winstein-Holness kinetics. *Chemical Reviews*, **1983**, 83, 83-134.
- Ribas, X., Gueell, I., Cu(I)/Cu(III) catalytic cycle involved in Ullmann-type cross-coupling reactions. *Pure and Applied Chemistry*, **2014**, 86, 345-360.
- Sangiorgio, C., Marsden, S.P., Blacker, A.J., McGowan, P.C., Copper catalysed Ullmann type chemistry: From mechanistic aspects to modern development. *Chemical Society Reviews*, **2014**, 43, 3525-3550.
- Sang, P., Yu, M., Tu, H., Zou, J., Zhang, Y., Highly regioselective synthesis of fused seven-membered rings through copper-catalyzed cross-coupling. *Chemical Communications*, **2013**, 49, 701-703.
- Satoh, K., Inenaga, M., Kanai, K., Synthesis of a key intermediate of levofloxacin via enantioselective hydrogenation catalyzed by iridium(I) complexes. *Tetrahedron: Asymmetry*, **1998**, 9, 2657-2662.
- Snape, T.J., A truce on the Smiles rearrangement: Revisiting an old reaction-the Truce-Smiles rearrangement. *Chemical Society Reviews*, **2008**, 37, 2452-2458.

- Sparr, C., Salamanova, E., Schweizer, W.B., Senn, H.M., Gilmour, R., Theoretical and X-ray crystallographic evidence of a fluorine-imine *gauche* effect: An addendum to dunathan's stereoelectronic hypothesis. *Chemistry-A European Journal*, **2011**, 17, 8850-8857.
- Wang, X.-B., Yang, J., Wang, L.-S., Observation of entropic effect on conformation changes of complex systems under well-controlled temperature conditions. *Journal of Physical Chemistry A*, **2008**, 112, 172-175.
- Xia, S., Liu, J.-Q., Wang, X.-H., Tian, Y., Wang, Y., Wang, J.-H., Fang, L., Zuo, H., The synthesis of 4,7-disubstituted-2*H*-benzo[*b*][1,4]oxazin-3(4*H*)-ones using Smiles rearrangement and their *in vitro* evaluation as platelet aggregation inhibitors. *Bioorganic & Medicinal Chemistry Letters*, **2014**, 24, 1479-1483.
- Zhang, P., Terefenko, E.A., Fensome, A., Zhang, Z., Zhu, Y., Cohen, J., Winneker, R., Wrobel, J., Yardley, J., Potent nonsteroidal progesterone receptor agonists: Synthesis and SAR study of 6-aryl benzoxazines. *Bioorganic & Medicinal Chemistry Letters*, **2002**, 12, 787-790.
- Zhao, Y., Wu, Y., Jia, J., Zhang, D., Ma, C., One-pot synthesis of benzo-1,4-thiazin-3(4*H*)-ones and a theoretical study of the S-N type Smiles rearrangement mechanism. *Journal of Organic Chemistry*, **2012**, 77, 8501-8506.
- Zuo, H., Meng, L., Ghate, M., Hwang, K.H., Cho, Y.K., Chandrasekhar, S., Reddy, C.R., Shin, D.S., Microwave-assisted one-pot synthesis of benzo[*b*][1,4]oxazin-3(4*H*)-ones via Smiles rearrangement. *Tetrahedron Letters*, **2008**, 49, 3827-3830.

Chapter 3. How do hydrogen bonds affect the dynamic behaviour of an organic molecule?

Abstract

Two fluorine and bromine **Boc** protected phenoxypropanamine compounds were investigated to determine how hydrogen bonds affect the dynamic behaviour of an organic molecule. Using an SC-XRD (single crystal X-ray diffraction), the presence of a folded backbone for the fluorine-containing compound was established. In addition, the presence of an inter-molecular (conventional and non-conventional) hydrogen bond (HB) was detected by means of the XRD technique. To investigate the conformation preference and available interactions in the solution of these molecules, variable temperature (VT) NMR in two different concentrations, 2D NMR at low temperature and QM (quantum mechanics) study, were performed. These investigations confirmed that the observed interactions in the solid phase were maintained and that competition between inter- and intra- non-conventional HB (originated from fluorine atoms) were present in dilute solutions at high temperatures. It appeared that fluorine assisted the occurrence of inter-molecular cross-coupling at room temperature.

3.1 Introduction

Amide bonds are one of the major functional groups contained in FDA-approved drugs [Albericio and Kruger, 2012]. This bond links the monomers of amino acids together forming proteins and enzymes, essential for cellular function. The chemistry behind this functional group has therefore attracted considerable attention [Pattabiraman and Bode, 2011; Albericio and Kruger, 2012]. The amide group has the potential to act as a hydrogen bond (HB) donor (from the NH site), or as a HB acceptor (from the carbonyl site) [Johansson et al., 1974]. Both inter- and/or intra-molecular HB have been extensively investigated and discussed [Kollman and Allen, 1972; Desiraju, 1996]. It has been shown that the introduction of an amide group into an organic backbone creates a hydrogen bond, affecting the conformation of the chemical backbone and changing the biological activity of the drug [Laursen et al., 2013]. These weak chemical interactions are effective in many biological systems, and can be used to design supramolecular assemblies and scaffolds [Ward and Raithby, 2013]. Among these weak interactions, hydrogen bonds [Desiraju, 1996; Steiner, 2002; Emenike et al., 2013; Nagy, 2013] halogen–bonds [Steiner, 2002; Metrangolo et al., 2005; Fuller et al., 2012], and van der Waals dispersive forces [Hunter, 2004; Mati and Cockroft, 2010; Scharf et al., 2013; Yang et al., 2013] are most important [Chiarucci et al., 2014].

Although the hydrogen bond was discovered early in the 20th century, it still attracts substantial research interest [Steiner, 2002]. Hydrogen bonds are significant because of its application in structure, function, and dynamics of many chemical systems [Steiner, 2002]. The fields in which it plays a role include general inorganic and organic chemistry, biochemistry, pharmacy, medicine, molecular mineralogy, material science, and

supramolecular chemistry [Steiner, 2002]. Parallel developments in these fields further stimulate research into hydrogen bonds [Steiner, 2002].

Hydrogen bonds can either be inter- or intra-molecular, depending on the type of atom associated with them. Inter-molecular hydrogen bonding plays a substantial role in solid and solution phase chemistry. When a covalently bound hydrogen atom bound to elements such as N, O or F forms a second weak bond, to another electronegative atom (N, O or F), this is called a classical hydrogen bond [Taylor, 2016]. The strength of the hydrogen bond is dependent on the solvent used [Eltayar et al., 1993]. Inter- and intra-molecular hydrogen bonding can also be influenced by varying solvent systems and their concentrations. Inter-molecular HB is affected more by varying concentrations, since decreasing the concentration reduces inter-molecular interactions. Crystallographic data has on occasion showed the presence of HB between a hydrogen atom attached to a sp^x ($x=1-3$) hybridized carbon and an electronegative atom. This type of bond is called a non-conventional hydrogen bond (non-conventional HB) [Desiraju, 1996; Alkorta and Elguero, 1998].

The HB donor in a non-conventional HB has to be electron deficient in order to be attracted to an electron-rich atom [Alkorta and Elguero, 1998]. The specific parameters that play a key role in non-conventional HBs are well established. The C(H) neighbours of an electronegative group (through space), or aromatic ring (via the anisotropic effect), have an acidic profile and get involved in non-conventional HB [Alkorta and Elguero, 1998]. The routine hydrogen bond acceptors in organic molecules are N, O and F, as well as other halogen atoms [Alkorta and Elguero, 1998; Jones et al., 2008]. Based on previous research, the ability of halogens to form a hydrogen bond is in the order of $F > Cl > Br > I$ [Kovács and Varga, 2006].

The strength, presence and configuration of intra-molecular HB is difficult to establish by means of direct experimental methods [Preimesberger et al., 2015]. HBs are often modelled using crystallographic structures and theoretical, idealized parameters. Therefore, the detection of HB remains a challenge [Preimesberger et al., 2015]. Additionally, the HB plays a crucial role in mediating dynamic processes, and in stabilizing static structures [Desiraju, 2011]. Thus, although the general principles of H-bonding are rudimentary and taught in general chemistry, HBs have a certain degree of complexity, and therefore continue to be actively studied [Arunan et al., 2011; Desiraju, 2011; Perrin and Burke, 2014].

We recently described the synthesis of fluorinated chiral 1,4-benzoxazines from their corresponding chiral adducts in the presence of a base and copper catalyst [Alapour et al., 2015]. The reported Smiles Rearrangement (SR) coupling reaction, for formation of 1,4-benzoxazines provided different yields, based on the functionality of the corresponding adducts. However, the crystal structures were in solid phase, whereas the synthetic reaction took place in the liquid phase. The presence of an inter-molecular HB was detected in the crystallographic data. However, this type of interaction can change when the organic compound enters solution. To investigate the available inter- and/or intra-molecular interactions in these molecules, and their effect on the conformation of the backbone in solution, a variable temperature (VT)-NMR in two different concentrations, and computational techniques were applied. Finally, the present study explains a simple procedure for determining HB interactions in organic molecules, and their dynamic behaviour (in a solution phase), via NMR and computational techniques.

3.2 Results and discussion

SC-XRD (single crystal X-Ray diffraction) of compounds **1** and **2** showed the presence of an inter-molecular HB (hydrogen bond) in the solid state. This intermolecular HB length in **1** was 2.094 Å, while **2** presented a slightly weaker HB at 2.232 Å (**Figure 3-1**). No intra-molecular HB was detected by SC-XRD in these two molecules. A variable temperature NMR (VT-NMR) experiment, in two different concentrations was applied to further investigate the stability of HBs in the solution phase of the molecules under study.

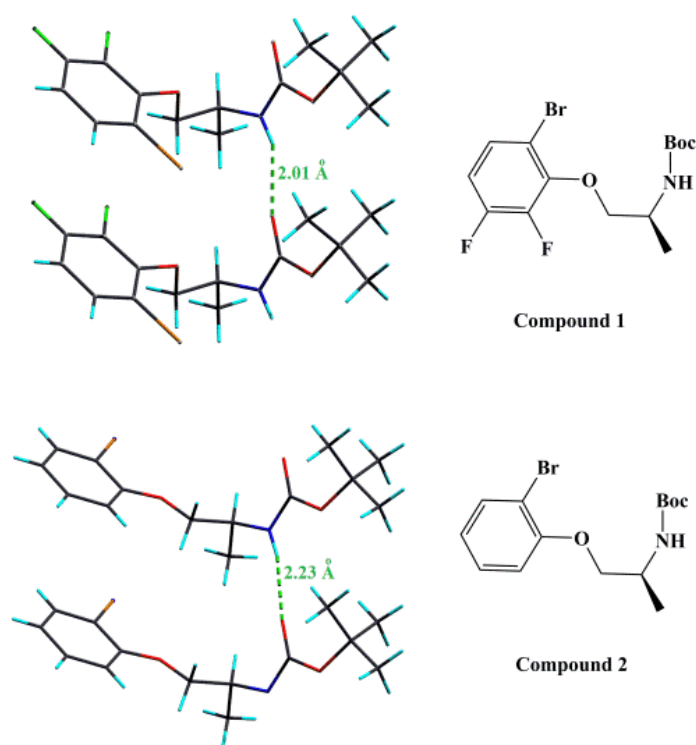


Figure 3-1 Hydrogen bonds detected by means of SC-XRD in compounds **1** and **2**[Alapour et al., 2015]

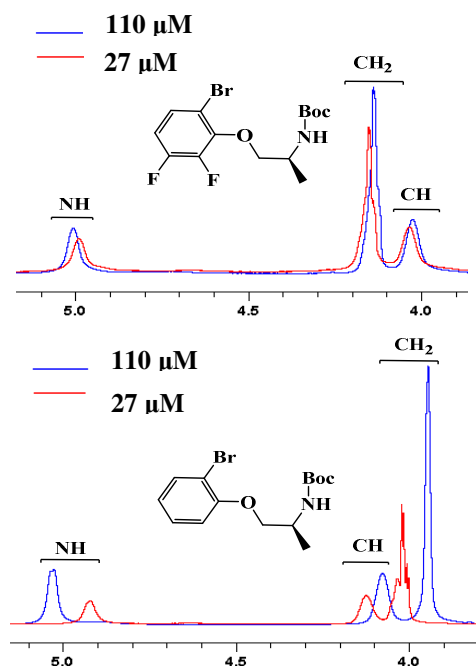
Normally, the strength of the HB in the solution phase can be determined by a δ (chemical shift) variation of a proton in the HB donor (in this case amidic NH, due to the Boc protecting group) [Farahani et al., 2014]. The NH peak in **1** at 27 μ M resonated at δ 5.00, while **2**

resonated at δ 4.92 (**Table 3-1**). The small difference in δ values (0.08) was expected from the crystallographic data since the HB in **1** was stronger than that in **2** and caused the NH peak in **1** to move slightly downfield in comparison to **2**. In the diluted solutions (27 μM), the chance of NH exposure in the molecule to solvent molecules is high (CDCl_3 with medium polarity), however since Cl is not a good hydrogen bond acceptor, this would not affect our calculations (**Table 3-1**) [Desiraju, 2002; Chaudhari et al., 2013].

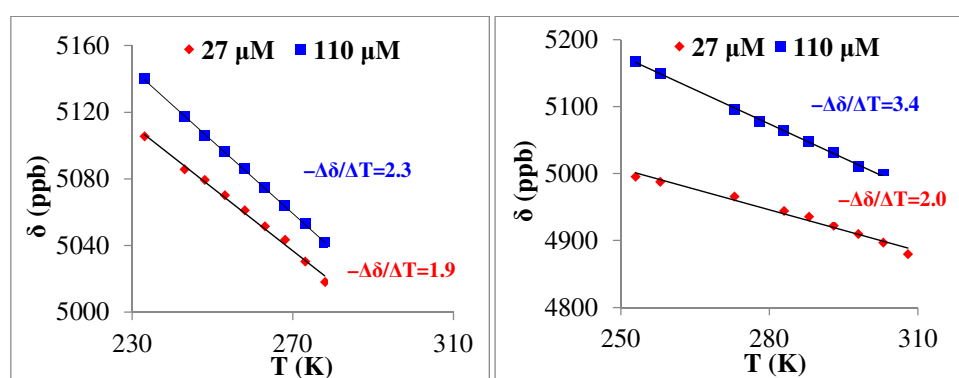
In the concentrated solution the change in $\Delta\delta_{(\text{Comp1-Comp2})}$ was small (-0.02) (**Table 3-1**). However, when the solutions are diluted, and the interaction between molecules is limited, $\Delta\delta_{(\text{Comp1-Comp2})}$ (0.08) is larger. Taking into account each molecule on its own, the change in $\Delta\delta_{(110 \mu\text{M} - 27 \mu\text{M})}$ for **1** was small (0.01), compared to **2** (0.11). These two factors indicate that the HB in **2** is weaker than that in **1**. These NMR studies in solution support the observed crystallographic data in the solid state (**Figure 3-1**).

A further investigation of the HB, by means of VT-NMR, was also performed. Increasing the temperature weakens interactions in organic molecules [Clayden et al., 2012]. Thus, an increase in temperature results in less hydrogen bonding and a decrease of δ , due to a greater degree of shielding. **Table 3-1** shows that inter-molecular HB in compound **1** was less temperature-sensitive than compound **2**, since the $\Delta(\Delta\delta/\Delta T)_{110-27 \mu\text{M}}$ are 0.4 and 1.4 for compounds **1** and **2**, respectively. The large value of $\Delta(\Delta\delta/\Delta T)_{110-27 \mu\text{M}}$ for **2** indicated that the inter-molecular HB was stronger in **1** than in **2** (**Figure 3-2**). Thus, the hydrogen bonding in compounds **1** and **2** was examined using two variables, concentration and temperature leading to the same conclusions.

Table 3-1 Effect of concentration variations on the available inter-molecular HB of compounds **1** and **2**.



	Comp. 1	Comp. 2	$\Delta\delta_{(\text{Comp1-Comp2})}$
$\delta_{\text{NH}} (\text{C} = 27 \mu\text{M})$	5.00	4.92	0.08
$\delta_{\text{NH}} (\text{C} = 110 \mu\text{M})$	5.01	5.03	-0.02
$\Delta\delta_{(110 \mu\text{M}-27 \mu\text{M})}$	0.01	0.11	



Comp. 1 [$-\Delta\Delta\delta/\Delta\Delta T_{(110 \mu\text{M}-27 \mu\text{M})} = 0.3$] **Comp. 2** [$-\Delta\Delta\delta/\Delta\Delta T_{(110 \mu\text{M}-27 \mu\text{M})} = 1.4$]

Figure 3-2 VT-NMR studies of the NH group on dilute and concentrated solutions of compounds **1** and **2**

The resonances of the CH and CH₂ segments were present at δ 4.03 and 4.14 respectively in compound **1**. However, in compound **2**, the CH resonance was more deshielded than the CH₂ resonance (CH₂ at δ 4.01 and CH at δ 4.11). This was mainly due to the electronegativity of a fluorine atom in the *ortho* position of the phenyl ring. The ¹H NMR spectra of the de-protected **Boc** compounds **1** and **2** in literature showed the same order of the resonances as our results [Bower et al., 2007]. The broad peaks observed for both CH and CH₂ in the ¹H NMR spectra of compounds **1** and **2** (**Table 3-1**) was an indication of bond rotation in these molecules.

Determination of the coalescence point, $T_c = 273$ K for compound **1** and $T_c = 303$ K for **2** and chemical shift of two protons in CH₂, in both molecules ($\Delta\nu = \nu_A - \nu_B$), allowed us to calculate the rotational barrier (ΔG^\ddagger), using the Eyring equation as calculated by Chen et al. (2012).

$$\Delta G^\ddagger = 2.303 RT (10.319 + \log T_C - \log k_C)$$

$$\Delta G^\ddagger = 0.0191 \times T_C (9.97 + \log T_C - \log (\nu_A - \nu_B))$$

Accordingly, the rotational barrier, ΔG^\ddagger for **1** and **2** are 57.46 and 63.15 kJ mol⁻¹ is associated with *cis/trans* isomerisation of the amide bond.

CH and CH₂ in compounds **1** and **2** also experienced a significant shift as a result of temperature variation. In compound **1**, the slope, $\Delta(-\delta(\text{ppb})/T(\text{K}))$ for both of these segments in dilute media (27 μM) were positive, -0.25 and -1.33 respectively (**Figure 3-3**). These values increased by a factor of approximately 2 when the concentration increased to 110 μM . The same trend was not followed in compound **2**, since $-\Delta\delta/\Delta T$ were +4.89 and +2.31, for the CH resonances at 27 and 110 μM respectively.

Thus, it could be proposed from the NH, CH and CH₂ chemical shift variations by temperature and concentration that inter-molecular interactions had a direct influence on the conformation of these molecules. However, the irregular trends for the obtained slope of CH and CH₂ required further investigation.

The presence of competition between the inter- and intra-molecular non-conventional HB was detected in **Figure 3-3**. The temperature variation appeared to strongly affect inter-molecular non-conventional HB (especially in the concentrated solutions) in this system. Therefore, the unusual behaviour of CH and CH₂ in compound **1** (δ shifting downfield by increasing the temperature), could be explained by the increase in the number of intra-molecular HB, and breaking of the inter-molecular non-conventional HB during the temperature increase. In compound **2**, this was true only for the CH₂ group and not the CH group, since compound **2** contains hydrogen instead of fluorine. Since F is a better HB acceptor than Br, intramolecular HB is seen for both the CH and CH₂ in compound **1**, but only for the CH₂ in compound **2** (without the fluorine).

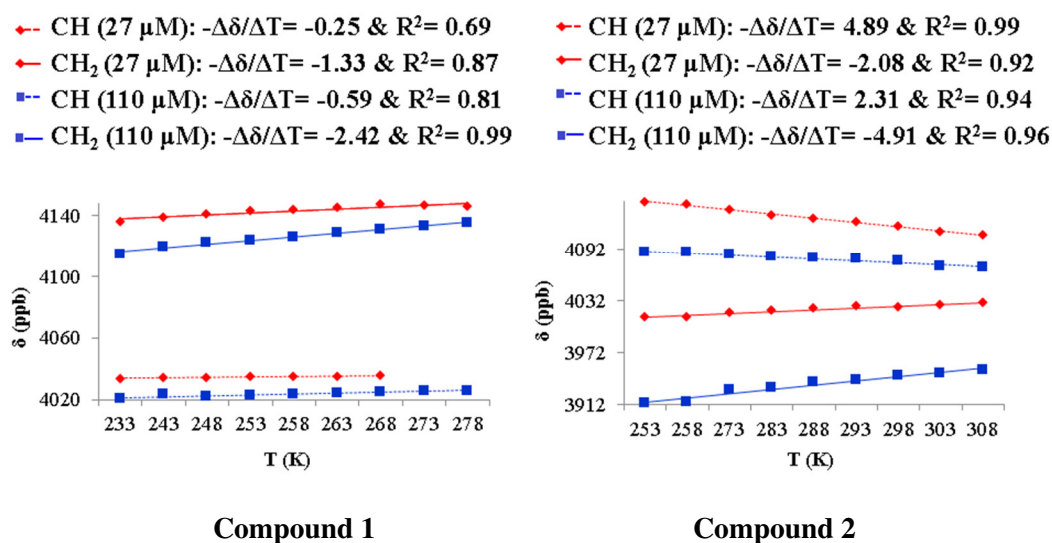


Figure 3-3 VT-NMR studies of the CH and CH₂ groups on dilute and concentrated solutions of compounds **1** and **2**

The SC-XRD data showed the presence of inter-molecular non-conventional HB between F atoms and CH₂ of the other molecule with the same structure in compound **1** (**Figure 3-4**).

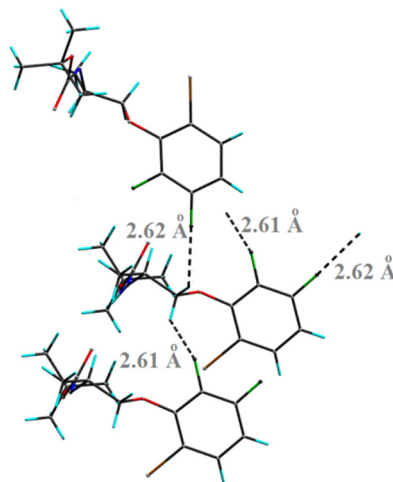


Figure 3-4 The detection of inter-molecular non conventional HB in compound **1** via SC-XRD.

Interestingly, at room temperature, the NH and Boc methyl resonances of **1** was present as a single peak at δ 4.9 and δ 1.47, however, the ¹H NMR spectrum of the same compound at -40 °C showed two distinct peaks 0.31-0.32 ppm apart for the NH resonance in compounds **1** and **2**, indicative of both *cis* and *trans* isomers (**Figure 3-5**). We have assigned the more downfield resonance to the more stable *trans* isomer, since this was present in a greater amount. It is quite evident that the *trans* isomer is more stable at lower temperatures from the integration of the peaks. Our results indicate that the *cis* and *trans* isomers occur in the ratio of approximately 1:9. Further to this, it was also noted that the chemical shift of the NH resonance in the *cis* isomer is more shielded than that in the *trans* isomer. This indicates that there is a greater degree of intermolecular hydrogen bonding in the *trans* isomer.

The appearance of a single NH and *t*-butyl resonance at room temperature was the result of rapid interconversion of *cis*- and *trans*-isomers around the amide bond. At room temperature a rotational barrier of 100 kJ mol⁻¹ is needed for *cis/trans* isomerisation [Clayden et al., 2012]. As mentioned earlier, the rotational energy barrier (ΔG^\ddagger) was 57.46, and 63.15 kJ mol⁻¹ for compounds **1** and **2**, respectively indicating that *cis/trans* isomerism would occur at room temperature.

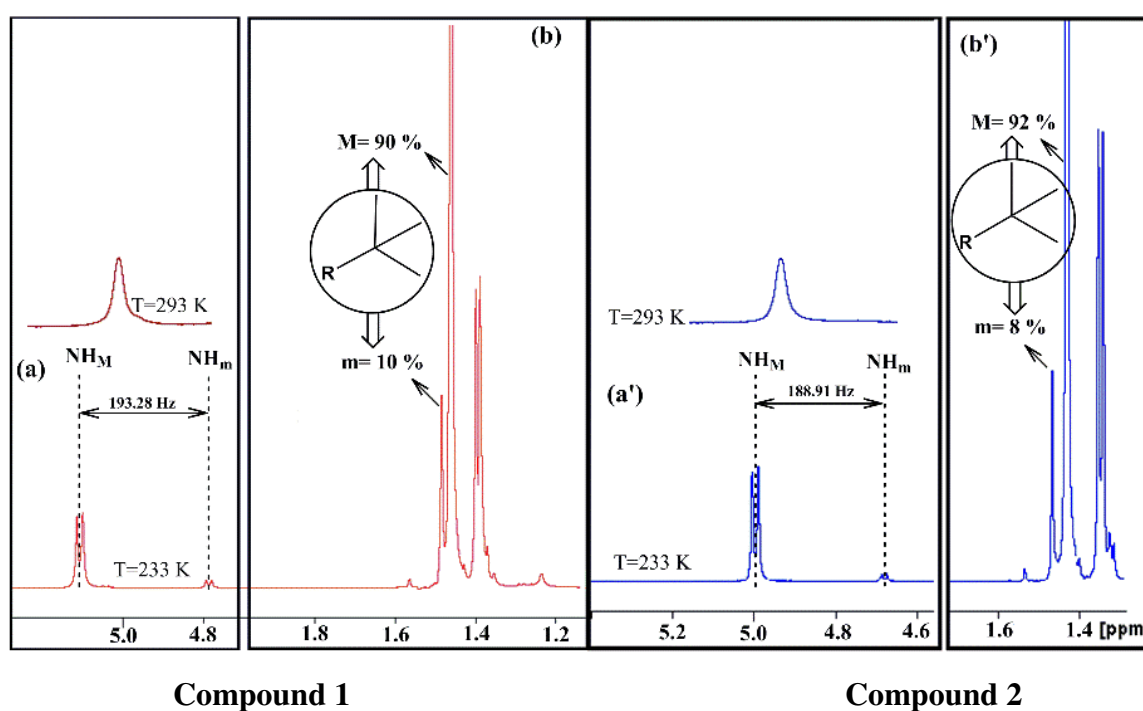


Figure 3-5 Major and minor NH and methyl *t*-butyl resonances in the ¹H NMR spectra of **1** and **2** at -40 °C (CDCl₃, 27 μM)

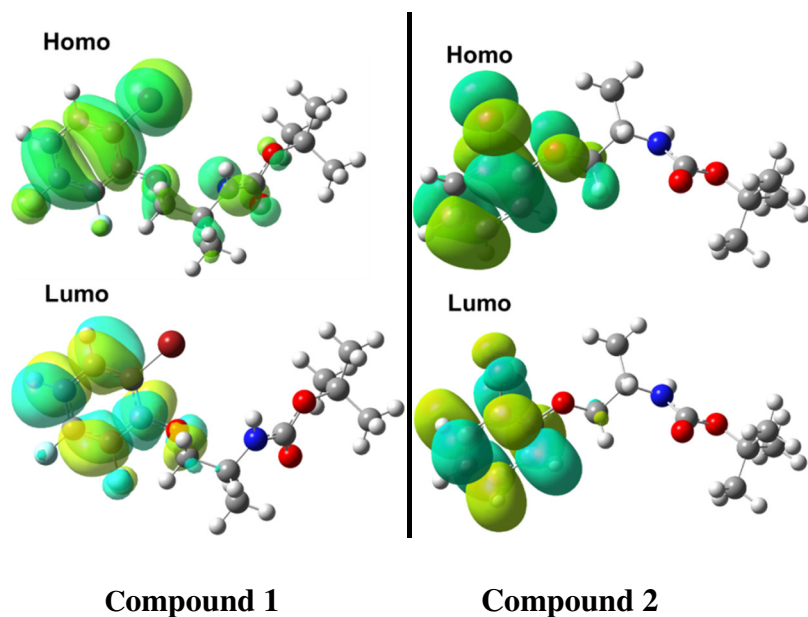


Figure 3-6 HOMO and LUMO plots by QM calculations

According to **Figure 3-6**, there was a greater degree of electron delocalization over the Ar-CH₂-CH-NH-C(O) moiety in the HOMO of compound **1** compared to **2**. This indicated that the NH of **1** would be a greater HB donor than that of **2**. This is evident in the crystal structure of the two molecules (**Figure 3-1**), where **1** had an intermolecular HB interaction of 2.01 Å, stronger than that of **2** with the same interaction being 2.23 Å.

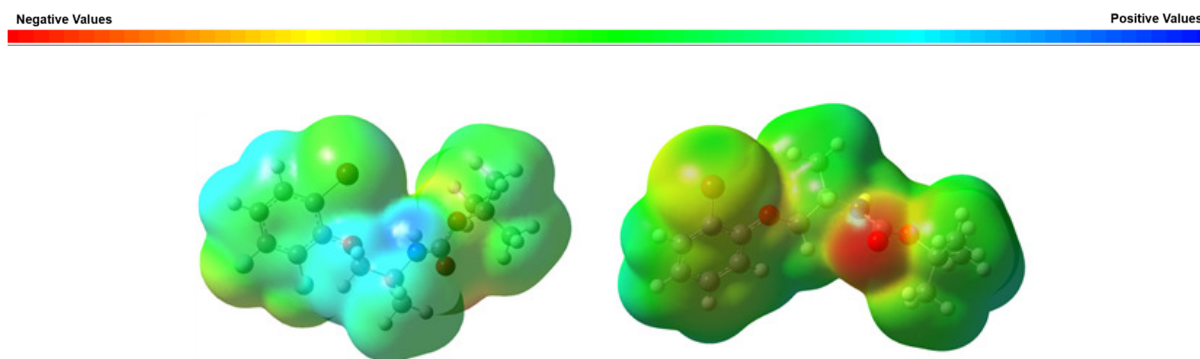


Figure 3-7 MEP plots for compounds **1** and **2** according to experimental and QM results

In addition, the Molecular Electrostatic Potential plot (MEP) (**Figure 3-7**), indicated that the presence of F atoms in structure **1** induced a different electron distribution to that of **2** within the molecule. The region close to the NH in compound **1** was electron deficient, suggesting that the NH proton is acidic and a good HB donor. On the other hand, an electron rich region around the oxygen of the C=O group in structure **2** showed increased electron density at the oxygen of the C=O group, suggesting a good environment for HB.

3.3 Conclusion

It was shown that the addition of fluorine atoms to the aromatic moiety affected the inter- and intra-molecular hydrogen bonding (HB) of the molecule. The NH group of compound **1** was shown to be a stronger HB donor than that in compound **2**. In addition, investigation of the CH₂ and CH groups around the amide group revealed competition between inter- and intra-molecular non-conventional HB. There is evidence that the molecule containing fluorine atoms, compound **1**, in the *ortho*- and *meta*- positions, has non-conventional HB with CH₂ and CH, while an intra-molecular non-conventional HB is only found between CH₂ and Br in compound **2**, when F atoms are absent. It was seen in this study that at certain concentrations and temperatures, the hydrogen bonding changed from intermolecular non-conventional HB to intramolecular non-conventional HB, causing the conformation of the molecule to be folded. This effect was more evident in the fluorinated compound **1** than when the fluorine was absent (compound **2**).

3.4 Material and methods

Compounds **1** and **2** were synthesised according to our recently published procedure [Alapour et al., 2015].

NMR data evaluation:

^1H and ^{13}C NMR spectra were recorded in CDCl_3 using Bruker 400 and 600 MHz NMR instruments respectively. Dynamic NMR spectroscopy was carried out on a 600 MHz NMR instrument. The WM-250 magnet pole gap was modified to allow safe operation (no magnet O-ring freezing) down to 93 K. The NMR sample temperature was varied using a Bruker BCU-Xtreme temperature control unit with a Bruker BVT-3000 digital temperature control unit. Between 233 and 343 K, the error in temperature measurement can be as high as 2 K. NMR samples were prepared in precision 5-mm NMR tubes. Samples were allowed to equilibrate for a minimum of 10 min at each temperature before the spectrum was recorded. Samples were prepared by dissolving enough compounds in 0.5 mL of the solvent to achieve 27 and 110 μM in a 5 mm diameter NMR tube. Chemical shifts are reported in parts per million (ppm) on the δ scale.

Experimental calculations

Determination of the coalescence point ($T_c = 303$ K) for compound **1** and ($T_c = 273$ K) for **2** as well as the difference in chemical shift of the two protons in CH_2 of both molecules ($\Delta\nu = \nu_A - \nu_B$) allowed us to calculate the Gibbs free activation energy (ΔG^\ddagger) using the Eyring equation [Chen et al., 2012]:

$$\Delta G^\ddagger = 2.303 RT (10.319 + \log T_c - \log k_c)$$

$$\Delta G^\ddagger = 0.0191 \times T_c (9.97 + \log T_c - \log (\nu_A - \nu_B))$$

Theoretical calculations

The hybrid B3LYP level of theory (DFT with 6-31++G(d,p) basis set) was applied in order to obtain stable structures for the ground state of fluorophenoxypropanamine (FPP) and to

compute its structural properties. All calculations were performed using Gaussian 09 software [Frisch, 2004]. The optimized structural parameters were used in the vibrational frequency and calculations of molecular orbitals. The CHCl₃ solvent effect was described using the PCM approach as implemented by Gaussian 09 software.

The following three calculations were carried out: (i) the highest occupied molecular orbital (HOMO); (ii) the lowest unoccupied molecular orbital (LUMO); and (iii) molecular electrostatic potential (MEP).

3.5 References

- Alapour, S., Ramjugernath, D., Koorbanally, N.A., Copper-catalysed cross-coupling affected by the Smiles rearrangement: A new chapter on diversifying the synthesis of chiral fluorinated 1,4-benzoxazine derivatives. *RSC Advances*, **2015**, 5, 83576-83580.
- Albericio, F., Kruger, H.G., Therapeutic peptides. *Future Medicinal Chemistry*, **2012**, 4, 1527-1531.
- Alkorta, I., Elguero, J., Non-conventional hydrogen bonds. *Chemical Society Reviews*, **1998**, 27, 163-170.
- Arunan, E., Desiraju, G.R., Klein, R.A., Sadlej, J., Scheiner, S., Alkorta, I., Clary, D.C., Crabtree, R.H., Dannenberg, J.J., Hobza, P., Kjaergaard, H.G., Legon, A.C., Mennucci, B., Nesbitt, D.J., Definition of the hydrogen bond (IUPAC recommendations 2011). *Pure and Applied Chemistry*, **2011**, 83, 1637-1641.
- Bower, J.F., Szeto, P., Gallagher, T., Enantiopure 1,4-benzoxazines via 1,2-cyclic sulfamidates. Synthesis of levofloxacin. *Organic Letters*, **2007**, 9, 3283-3286.
- Chaudhari, S.R., Mogurampelly, S., Suryaprakash, N., Engagement of CF₃ group in N-H...F-C hydrogen bond in the solution state: NMR spectroscopy and md simulation studies. *Journal of Physical Chemistry B*, **2013**, 117, 1123-1129.
- Chen, W., Twum, E.B., Li, L., Wright, B.D., Rinaldi, P.L., Pang, Y., Rotational energy barrier of 2-(2',6'-dihydroxyphenyl)benzoxazole: A case study by NMR. *Journal of Organic Chemistry*, **2012**, 77, 285-290.
- Chiarucci, M., Ciogli, A., Mancinelli, M., Ranieri, S., Mazzanti, A., The experimental observation of the intramolecular NO₂/CO interaction in solution. *Angewandte Chemie, International Edition*, **2014**, 53, 5405-5409.
- Clayden, J., Greeves, N., Warren, S., *Organic chemistry*, 2nd Ed. OUP Oxford, New York, **2012**.
- Desiraju, G.R., A bond by any other name. *Angewandte Chemie, International Edition*, **2011**, 50, 52-59.

- Desiraju, G.R., Hydrogen bridges in crystal engineering: Interactions without borders. *Accounts of Chemical Research*, **2002**, 35, 565-573.
- Desiraju, G.R., The C-H...O hydrogen bond: Structural implications and supramolecular design. *Accounts of Chemical Research*, **1996**, 29, 441-449.
- Eltayar, N., Mark, A.E., Vallat, P., Brunne, R.M., Testa, B., Vangunsteren, W.F., Solvent-dependent conformation and hydrogen-bonding capacity of cyclosporine A: Evidence from partition-coefficients and molecular-dynamics simulations. *Journal of Medicinal Chemistry*, **1993**, 36, 3757-3764.
- Emenike, B.U., Carroll, W.R., Roberts, J.D., Conformational preferences of *cis*-1,3-cyclopentanedicarboxylic acid and its salts by ¹H NMR spectroscopy: Energetics of intramolecular hydrogen bonds in DMSO. *Journal of Organic Chemistry*, **2013**, 78, 2005-2011.
- Farahani, M.D., Honarparvar, B., Albericio, F., Maguire, G.E.M., Govender, T., Arvidsson, P.I., Kruger, H.G., Proline *N*-oxides: Modulators of the 3D conformation of linear peptides through "NO-turns". *Organic & Biomolecular Chemistry*, **2014**, 12, 4479-4490.
- Fuller, R.O., Griffith, C.S., Koutsantonis, G.A., Lapere, K.M., Skelton, B.W., Spackman, M.A., White, A.H., Wild, D.A., Supramolecular interactions between hexabromoethane and cyclopentadienyl Ruthenium bromides: Halogen bonding or electrostatic organisation? *CrystEngComm*, **2012**, 14, 804-811.
- Hunter, C.A., Quantifying intermolecular interactions: Guidelines for the molecular recognition toolbox. *Angewandte Chemie, International Edition*, **2004**, 43, 5310-5324.
- Johansson, A., Kollman, P., Rothenberg, S., McKelvey, J., Hydrogen bonding ability of the amide group. *Journal of the American Chemical Society*, **1974**, 96, 3794-3800.
- Jones, C.R., Qureshi, M.K.N., Truscott, F.R., Hsu, S.-T.D., Morrison, A.J., Smith, M.D., A nonpeptidic reverse turn that promotes parallel sheet structure stabilized by C-H...O hydrogen bonds in a cyclopropane γ -peptide. *Angewandte Chemie, International Edition*, **2008**, 47, 7099-7102.
- Kollman, P.A., Allen, L.C., Theory of the hydrogen bond. *Chemical Reviews*, **1972**, 72, 283-303.
- Kovács, A., Varga, Z., Halogen acceptors in hydrogen bonding. *Coordination Chemistry Reviews*, **2006**, 250, 710-727.
- Laursen, J.S., Engel-Andreasen, J., Fristrup, P., Harris, P., Olsen, C.A., *Cis-trans* amide bond rotamers in β -peptoids and peptoids: Evaluation of stereoelectronic effects in backbone and side chains. *Journal of the American Chemical Society*, **2013**, 135, 2835-2844.
- Mati, I.K., Cockroft, S.L., Molecular balances for quantifying non-covalent interactions. *Chemical Society Reviews*, **2010**, 39, 4195-4205.
- Metrangolo, P., Neukirch, H., Pilati, T., Resnati, G., Halogen bonding based recognition processes: A world parallel to hydrogen bonding. *Accounts of Chemical Research*, **2005**, 38, 386-395.
- Nagy, P.I., Are the intramolecular O-H...F and O-H...Cl hydrogen bonds maintained in solution? A theoretical study. *Journal of Physical Chemistry A*, **2013**, 117, 2812-2826.

- Pattabiraman, V.R., Bode, J.W., Rethinking amide bond synthesis. *Nature*, **2011**, 480, 471-479.
- Perrin, C.L., Burke, K.D., Variable-temperature study of hydrogen-bond symmetry in cyclohexene-1,2-dicarboxylate monoanion in chloroform-*d*. *Journal of the American Chemical Society*, **2014**, 136, 4355-4362.
- Preimesberger, M.R., Majumdar, A., Aksel, T., Sforza, K., Lectka, T., Barrick, D., Lecomte, J.T.J., Direct NMR detection of bifurcated hydrogen bonding in the alpha-helix *N*-caps of ankyrin repeat proteins. *Journal of the American Chemical Society*, **2015**, 137, 1008-1011.
- Scharf, D.H., Chankhamjon, P., Scherlach, K., Heinekamp, T., Willing, K., Brakhage, A.A., Hertweck, C., Epidithiodiketopiperazine biosynthesis: A four-enzyme cascade converts glutathione conjugates into transannular disulfide bridges. *Angewandte Chemie, International Edition*, **2013**, 52, 11092-11095.
- Steiner, T., The hydrogen bond in the solid state. *Angewandte Chemie, International Edition*, **2002**, 41, 49-76.
- Taylor, R., It isn't, it is: The C-H...X (X = O, N, F, Cl) interaction really is significant in crystal packing. *Crystal Growth & Design*, **2016**, 16, 4165-4168.
- Ward, M.D., Raithby, P.R., Functional behaviour from controlled self-assembly: Challenges and prospects. *Chemical Society Reviews*, **2013**, 42, 1619-1636.
- Yang, L., Adam, C., Nichol, G.S., Cockroft, S.L., How much do van der Waals dispersion forces contribute to molecular recognition in solution? *Nature Chemistry*, **2013**, 5, 1006-1010.

Chapter 4. Copper-free Sonogashira coupling of 2-trifluoromethyl-4-chloroquinoline with alkynyl acetylene in the formation of fluorinated 4-(alkynyl)-quinolines using Pd(II) and xantphos

Abstract

Quinolines are well known scaffolds in many pharmaceutical drugs used to treat amongst others, malaria, cancer and bacterial infections. In this work, 19 novel derivatives of quinoline were synthesised using the Sonogashira coupling reaction. The reaction conditions were optimized to obtain the highest possible yield. The structures of the synthesised compounds were elucidated using NMR spectroscopy along with mass spectrometry and single crystal XRD. It was found that the presence of different groups at C-8 on the quinoline ring can change the charge distribution of the molecules and subsequently alter the final yield of the product. The crystal data also revealed the presence of π - π stacking between the quinoline derivatives. These novel compounds can be used as a core scaffold for the synthesis of many biologically active compounds due to the presence of the alkyne functionality.

4.1 Introduction

Quinoline (also known as 1-aza-naphthalene or benzo[*b*]pyridine) is a nitrogen containing heterocyclic aromatic compound, which has attracted the attention of medicinal and synthetic chemists for decades due to its various pharmaceutical applications. They are used as antimalarials (quinine, quinidine, chloroquine, mefloquine, amodiaquine and primaquine), antivirals (saquinavir), antibacterials (fluoroquinolones such as ciprofloxacin, ofloxacin, sparfloxacin, gatifloxacin), as antiglaucoma compounds (cartiolol), cardiotonics (vesnarinone), anthelmintics (oxamniquine), local anaesthetics (dibucaine), antipsychotics (aripiprazole, brexpiprazole), antiasthmatics (montelukast), anticancer drugs (camptothecin, irinotecan, topotecan) and antifungal and antiprotozoal drugs (clioquinol) [Kumar et al., 2009; Bawa et al., 2010; Afzal et al., 2015]. Bedaquiline is another example of a fluorinated quinoline marketed as an antibiotic [Hayakawa et al., 1986]. In particular, the mefloquine core contains a 2,8-bis(trifluoromethyl)quinoline moiety with a CF₃ group on the quinoline scaffold [Biot et al., 2000]. The ability to efficiently functionalize haloquinolines into substituted derivatives via metal-catalyzed cross-coupling reactions is highly desirable in synthetic organic chemistry as this could lead to novel molecules with enhanced bioactivity.

Fluorinated compounds are widespread in the pharmaceutical industry with almost 15–20% of all new drugs licenced annually, containing fluorine in their core structure [Hagmann, 2008]. Fluorine has shown increased solubility, lipophilicity, metabolic stability and binding selectivity when incorporated into drugs, contributing to enhanced biological properties. Understanding the chemistry of fluorinated organic compounds still remains a challenging area in chemical research. The trifluoromethyl group, known to enhance the lipophilicity of organic molecules, has its own interesting chemistry, having an electron-withdrawing effect

[O'Hagan, 2010]. Hence, there is considerable interest in developing methods for the controlled introduction of trifluoromethyl groups into small molecules [Liang et al., 2013].

Aryl, alkynyl or alkenyl moieties in quinoline derivatives have shown widespread potential pharmacological activity [Angibaud et al., 2002; Godel et al., 2002; Reddy et al., 2009]. Alkynes, for example are potential building blocks for unsaturated molecular scaffolds due to their structural stability and ability to form conjugated π systems [Tykwinski, 2003]. C-C coupling reactions catalyzed by Pd with various ligands are frequently used for the synthesis of organic compounds [Miyaura and Suzuki, 1995; Sonogashira, 2002; Kawanami et al., 2007]. The Sonogashira coupling reaction, which involves Pd-catalysts, provides a direct and easy method for the synthesis of acetylenic compounds [Yi et al., 2007]. It can be used in the synthesis of a variety of compounds including heterocycles, several natural products and pharmaceuticals [Grissom et al., 1996; Tykwinski, 2003; Yi et al., 2007]. The Sonogashira cross-coupling reaction employs a catalytic system comprising a combination of Pd, phosphines and CuI, which are reacted with the substrates. However, the presence of CuI can result in the formation of some Cu-(I) acetylides *in-situ* that lead to oxidative homocoupling reactions of alkynes [Siemsen et al., 2000; Li et al., 2005].

The reaction discovered by Sonogashira [Sonogashira et al., 1975, Sonogashira, 2002] has been modified over the years to include different ligands, Pd compounds, solvents and bases [Sonogashira, 2002; Bakherad et al., 2010; Feng et al., 2010]. The amount of catalyst used in the reaction has also been investigated as well as the use of microwave synthesis in order to promote C-C bond formation [Kabalka et al., 2000]. The most important modification is the elimination of copper salts, hence eliminating oxidative homocoupling of acetylenes (Glaser-

type reaction), which cannot be avoided in copper-mediated reactions [Siemsen et al., 2000; Das et al., 2015; Dewan et al., 2016; Mandegani et al., 2016].

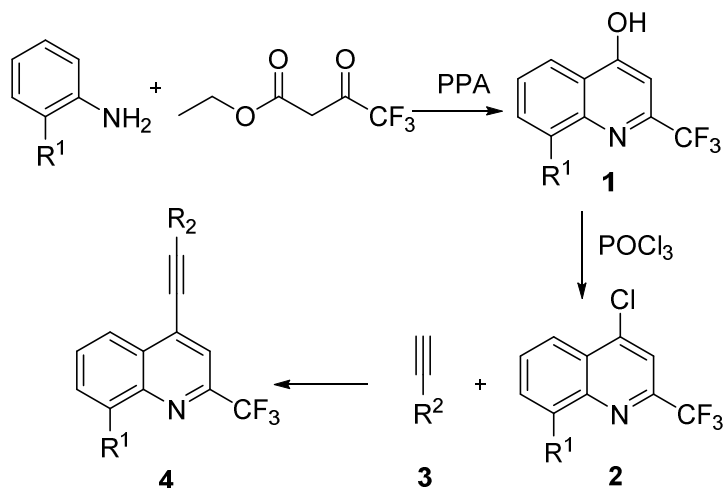
We herein report the synthesis of fluorinated 4-alkynylquinolines (potential pharmaceuticals) via the Sonogashira coupling reaction. In addition we have included CF₃ groups at C-2 and C-8 of the quinoline ring to further study the role of fluorine in the chemistry of these molecules. To the best of our knowledge this is the first report of a synthetic procedure to produce fluorinated 4-alkynyl-2-arylquinolines via the Sonogashira coupling reaction.

4.2 Results and discussion

In the reaction sequence of the titled reaction (**Scheme 4-1**), 2-substituted anilines were cyclized to 2,8-bis(substituted)quinolin-4-ol (**1**) using heat with ethyl 4,4,4-trifluoro-3-oxobutanoate in the presence of polyphosphoric acid (PPA) at 150 °C. The quinolin-4-ol (**1**) was subsequently refluxed with fresh phosphorus oxychloride (POCl₃) yielding the corresponding 4-chloro-2-quinoline derivatives **2**, after which the chlorine was substituted for an alkynyl group resulting in the formation of the target compounds **4a-x**. This last step was carried out at 70 °C in degassed THF:water (9:1) using Pd(OAc)₂, xantphos as a catalyst and triethylamine (TEA) as a base.

Optimization of the reaction conditions for the final step was carried out using 4-chloroquinoline (**2**) and acetylene (**3**) as a model reaction. The effect of two different Pd catalysts, four different solvent systems, five different bases and three different co-catalysts was examined for the Sonogashira coupling step. All reactions were carried out for 12 hours as an increase in the reaction time did not improve the final yield of product. The best reaction conditions identified occurred with Pd(OAc)₂ as the catalyst without a co-catalyst,

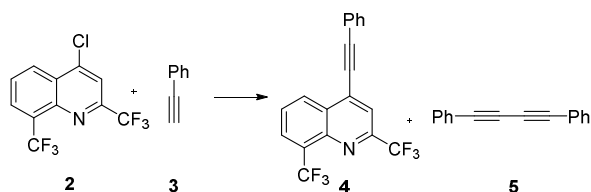
xantphos as the ligand, a 9:1 mixture of THF:water as solvent and TEA as base (**Entry 3** in **Table 4-1**).



Scheme 4-1 Synthesis of 4-alkynyl quinolines **4**.

The addition of co-catalysts resulted in increased yields of the alkynyl dimer (**5**) and decreased yields of the product (**4**) (**Entry 11, 12**). If the acetylene precursors were not added slowly in the reaction, an increase in the yields of the dimer (**5**) was also observed. These side products are brought about by homocoupling of the alkynes or Glaser type coupling and are produced *in-situ* by the generation of copper acetylides (upon exposure to oxidative agents or air).²⁹ The presence of a copper co-catalyst was previously reported to reduce the yields of Sonogashira cross-coupling reactions, which corroborates our findings.²⁴ The presence of these side products in the reaction is undesirable as they make it difficult to purify the desired product.

Table 4-1 Optimization of conditions for the final step in the synthesis of 4-alkynyl quinolines **4**



Entry	Catalyst	Ligand	Solvent	Base	Co-catalyst	Yield ^{a, b} 4	Yield ^{a, b} 5
1	PdCl₂	xantphos	THF:Water	TEA	None	58	5
2	Pd(OAc) ₂	P(Ph)₃	THF:Water	TEA	None	52	10
3	Pd(OAc)₂	xantphos	THF:Water	TEA	None	80	7
4	Pd(OAc) ₂	xantphos	DMSO	TEA	None	15	7
5	Pd(OAc) ₂	xantphos	DMF	TEA	None	27	6
6	Pd(OAc) ₂	xantphos	THF	TEA	None	31	8
7	Pd(OAc) ₂	xantphos	THF:Water	Pyrrolidine	None	56	10
8	Pd(OAc) ₂	xantphos	THF:Water	Piperidine	None	62	28
9	Pd(OAc) ₂	xantphos	THF:Water	NH(iPr)₂	None	21	9
10	Pd(OAc) ₂	xantphos	THF:Water	None	None	NR	NR
11	Pd(OAc) ₂	xantphos	THF:Water	TEA	CuI	12	80
12	Pd(OAc) ₂	xantphos	THF:Water	TEA	Cu(OAc)₂	10	70
13	Pd(OAc) ₂	xantphos	THF:Water	TEA	TBAB^c	18	20

^a Reaction conditions: **2** (1 mmol), **3** (1.5 mmol), base (2 equiv), Pd(OAc)₂ (2.5 mol %), ligand (10 mol %) and solvent (10 mL) at 70 °C for 12 hrs.

^b Isolated yield

^c TBAB : Tetra-*N*-butylammonium bromide

A proposed mechanism of the copper-free reaction is shown in **Scheme 4-2**. Phosphonates, amines and ethers (used as ligands or solvents) can reduce Pd(II) to Pd(0)L₂, typically via a σ -complexation-dehydropalladation-reduction elimination [Chinchilla and Najera, 2007]. The catalytically active Pd(0)L₂ species **I** is also stabilized by ligands present. The catalytic cycle begins with the oxidative addition of 4-chloroquinoline to palladium (0) resulting in intermediate **II**, known to be the rate-determining step for the Sonogashira reaction. This is followed by π co-ordination of the alkyne to Pd, resulting in an alkyne-Pd(II) complex **III** [Chinchilla and Najera, 2007]. Removal of the acetylenic proton with triethylamine results in

co-ordination of the acid carbon in acetylene to the metal **IV**. In a further step the product **4** is released by a reductive elimination reaction regenerating the Pd catalyst in the process.

After optimizing the reaction conditions on **4a**, various 4-alkynylquinolines (**Figure 4-1**) were prepared via coupling of 4-chloroquinolines using optimized conditions. In general, the yield of aliphatic alkynes (**4p-4s**) was lower than aromatic alkynes (**Figure 4-1**). It was also found that the introduction of the electron withdrawing trifluoromethyl group at C-8 increased the yield (compounds **4h-4o**) while electron donating methyl groups in the same position decreased the yield (compounds **4d-g**).

It was also observed that between the compounds **4k** and **4l** (with the trifluoromethyl group on the alkyne portion of the molecule being in the *para* and *ortho* positions respectively) the yield for the *ortho* derivative **4l** was lower. It was also observed that the yields of the *para* and *ortho* fluoro derivatives (**4m** and **4o**) were lower than in the unsubstituted alkyne derivative (**4h**), while that of the difluoro derivative (**4n**) did not change. This could possibly be due to resonance effects of the *ortho* and *para* substituted derivatives. Electron donating *t*-butyl groups on the acetylenic aromatic ring was also shown to increase yields (**4c**, **4f** and **4j**).

The chemistry of phenylacetylene can only influence the last two steps of the proposed mechanism in scheme **2**. This is when phenylacetylene is co-ordinated to the metal through π bonds. The presence of the electron donating *t*-butyl group could stabilise this co-ordinated intermediate by increasing the electron density of the acetylenic bond, resulting in higher yields for the *t*-butyl derivatives.

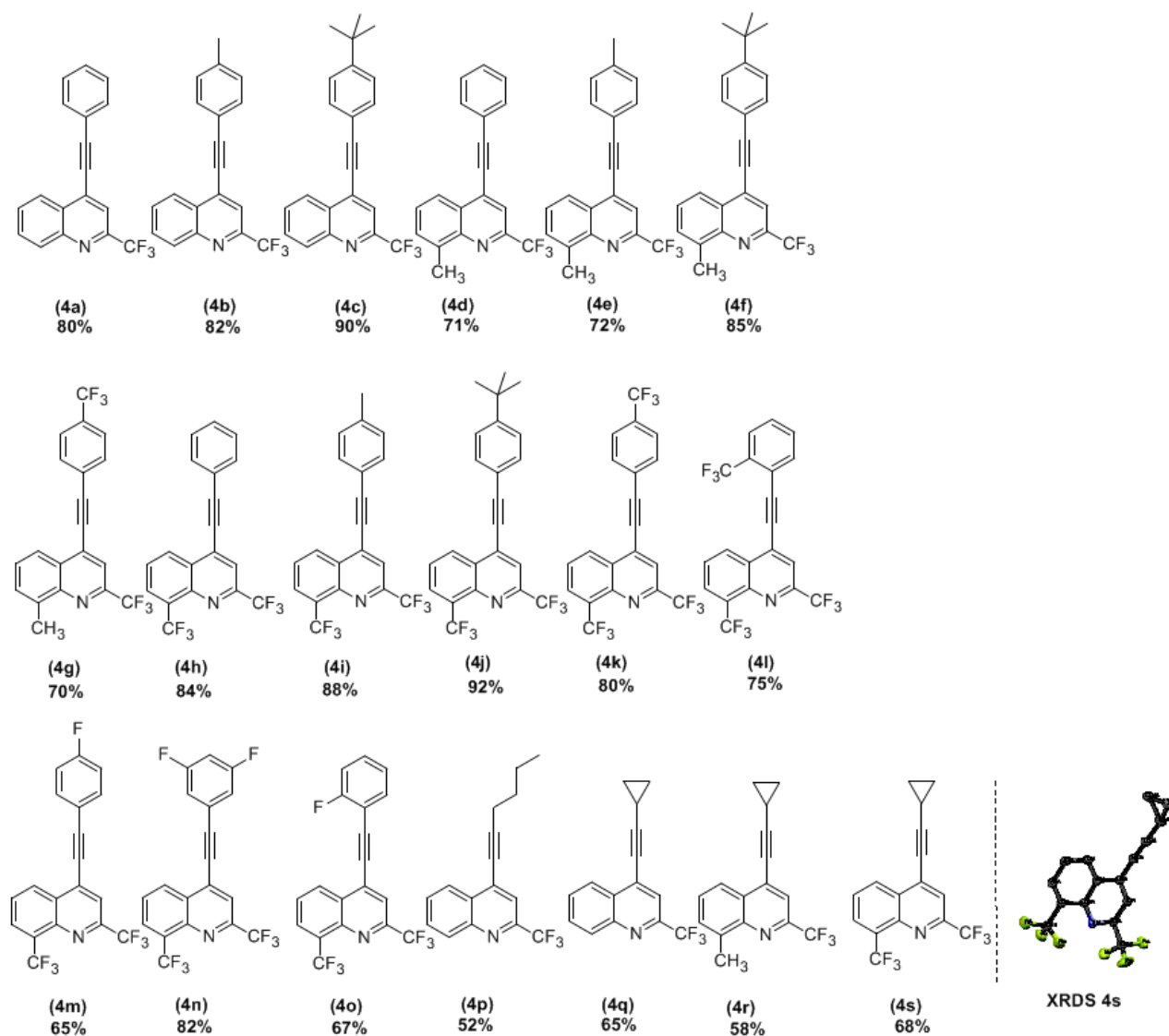
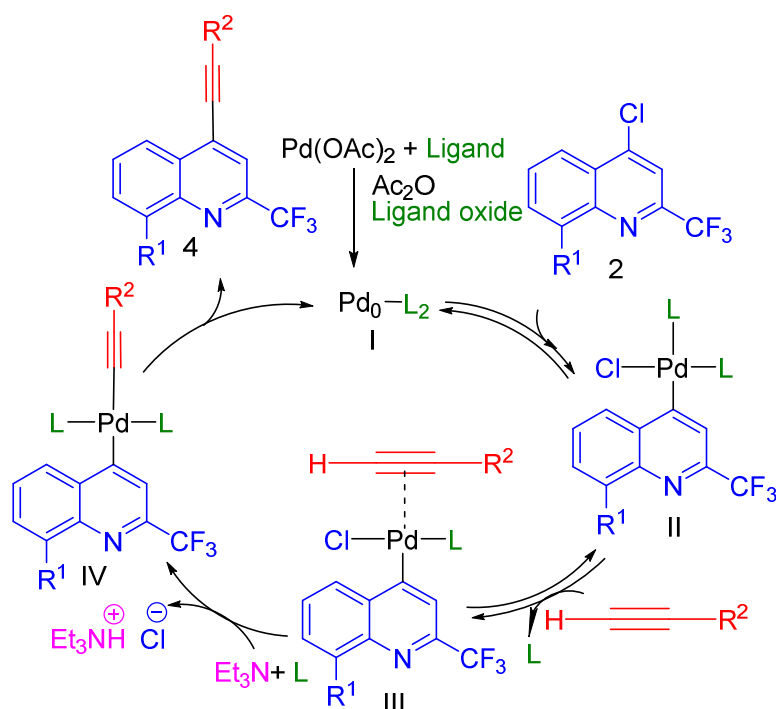


Figure 4-1 Novel derivatives of quinoline by application of the Sonogashira coupling reaction under optimised conditions

All the isolated products were characterized by NMR and Mass spectrometry. The acetylenic carbon resonances are characteristic for these molecules at δ 80-100 in the ¹³C NMR spectrum. In addition a HMBC correlation between H-3 and the more shielded acetylenic carbon resonance occurred, as well as between the aromatic protons of the acetylenic derived moiety with the more deshielded acetylenic carbon resonance, which allowed the assignment of the two acetylene carbon resonances to be made.



Scheme 4-2 Plausible mechanism for formation of 4-alkynyl-2-quinolines through a Sonogashira copper-free coupling reaction.

The structure and conformation of one of the molecules **4s** was confirmed by single crystal X-ray diffraction. Essentially, the molecule is planar with the two bulky trifluoromethyl groups adding bulk around the C-2 and C-8 carbon atoms. In addition to this interaction, the cyclopropyl group situated at the *para*-position with respect to the quinoline nitrogen atoms are situated at two different configurations folding out of the planar ring in both directions. Additionally, π - π stacking interactions between the quinoline rings in an off centred parallel type occurred and can be seen in **Figure 4-2** [Chernov'yants et al., 2015]. The rings in the π -stacked compound are parallel with dihedral angles between the planes being 1.72° in an offset arrangement [Chernov'yants et al., 2015]. The perpendicular distance between the rings was about 3.81-3.93 Å. The packing diagram of the π -stacked compound **4s** is depicted in **Figure 4-2**.

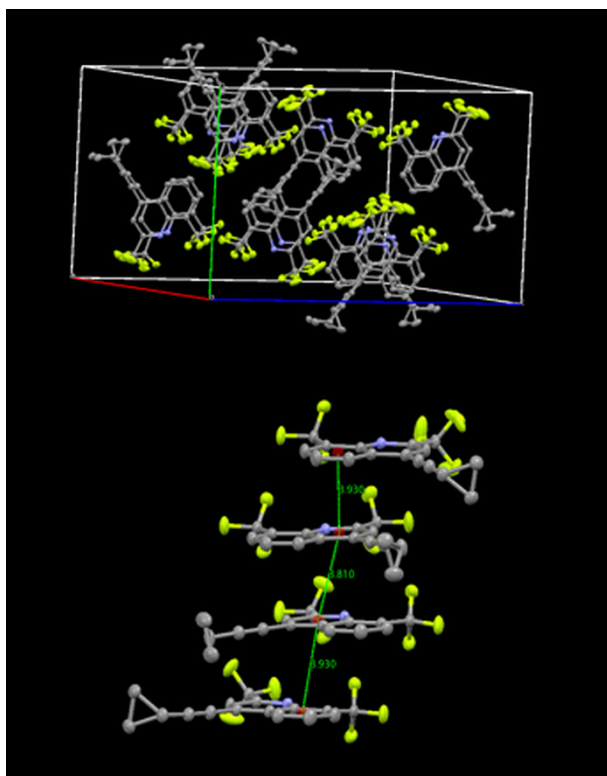


Figure 4-2 Packing diagram of π -stacked compound **4s**

4.3 Conclusion

Our method presents a direct route for $sp-sp^2$ bond formation and eliminates oxidative dimerization of the alkyne in the Sonogashira coupling reaction, which occurs as a side reaction when a copper co-catalyst is used. The availability of the catalyst, high catalytic activity and water as the co-solvent make the present reaction an attractive method for the synthesis of these substituted quinolines, which have the possibility of possessing an extensive range of biological activities.

4.4 Experimental section

General methods and materials

Reagents and solvents were purchased from Sigma Aldrich and used as received. Commercially available Merck Kieselgel 60 F254 aluminium backed plates were used for TLC analysis. Visualisation of TLC plates was achieved by UV fluorescence and iodine vapour. Compounds were purified by column chromatography packed with 60-200 mesh Silica gel.

All NMR spectra were recorded on Bruker AVANCE III 400 or 600 MHz instruments. Chemical shifts are quoted in parts per million (ppm) downfield from TMS as the internal standard and the coupling constants are reported in Hertz. Multiplicities of the NMR resonances are abbreviated as s (singlet), d (doublet), t (triplet), q (quartet), m (multiplet) and br (broad). Assignments of ^1H NMR, ^{13}C NMR and ^{19}F NMR resonances were made with the aid of COSY, NOESY, HMBC and HSQC experiments. A Waters Synapt G2 quadrupole time-of-flight mass spectrometer fitted with a Waters Ultra pressure liquid chromatograph was used for HRMS analysis. The instrument was operated with an electrospray ionization probe in the positive mode and data was acquired in MS scan mode from m/z 100-2000. Infra-red spectra were recorded in the range 4000-600 cm^{-1} on a Perkin Elmer Spectrophotometer as neat films onto a NaCl window. Abbreviations used in the description of IR spectra are: w (weak), m (medium), s (strong) and br (broad).

Synthetic procedure

Compounds **1** and **2** were prepared according to standard procedures reported in the literature [Eswaran et al., 2010].

Preparation of 4-alkyne quinoline (**4**):

A mixture of 4-chloroquinoline, **2** (0.5 mmol), acetylenes, **3** (1 mmol), xantphos (10 mmol %), triethylamine (2.0 equiv.), water (0.5 mL) and tetrahydrofuran (5.0 mL) was degassed twice using argon gas. Pd(OAc)₂ (2.5 mmol %) was then added, and the mixture degassed twice again and heated at 70 °C in a sealed tube under Ar for 12 hours. After completion of the reaction, the resulting solution was filtered off using celite (to remove the catalyst) and the filtrate concentrated *in vacuo*. The crude products were subjected to silica-gel column chromatography using hexane/ethyl acetate (9:1) to afford the pure products.

4-(phenylethynyl)-2-(trifluoromethyl)quinoline (**4a**). $\nu_{\max}/\text{cm}^{-1}$ (film) 3054 (m), 2922 (m), 2224 (s), 1606 (m), 1549 (m), 1374 (m), 1250 (m), 1147 (s). ¹H NMR (400 MHz, CDCl₃) δ_{H} 7.42 (4H, m), 7.69 (2H, m), 7.83 (1H, t, $J=7.6$ Hz), 7.90 (1H, s), 8.13 (1H, d, $J=8.4$ Hz), 8.24 (1H, d, $J=8.5$ Hz); ¹³C NMR (100 MHz, CDCl₃) δ_{C} 88.4, 91.5, 121.4, 121.8, 123.9, 124.5, 128.5, 128.7, 129.6, 130.2, 130.8, 132.3, 134.4, 134.7, 143.0, 149.0. The signal for an aromatic quaternary carbon was not observed in the ¹³C NMR spectrum. HRMS–ES⁺: m/z [M+H] calcd. for C₁₈H₁₁F₃N: 298.0838, found: 298.0840.

4-(*p*-tolylethynyl)-2-(trifluoromethyl)quinoline (**4b**). $\nu_{\max}/\text{cm}^{-1}$ (film) 3059 (m), 2922 (m), 2213 (s), 2197 (m), 1580 (m), 1514 (m), 1394 (m), 1280 (m), 1173 (s), 1143 (s), 1097 (m). ¹H NMR (400 MHz, CDCl₃) δ_{H} 2.42 (3H, s), 7.24 (2H, d, $J=7.8$ Hz), 7.57 (2H, d, $J=8.0$ Hz), 7.74 (1H, t, $J=7.6$ Hz), 7.84 (1H, t, $J=7.3$ Hz), 7.88 (1H, s), 8.24 (1H, d, $J=8.4$ Hz), 8.42 (1H, d, $J=8.3$ Hz); ¹³C NMR (100 MHz, CDCl₃) δ_{C} 21.7, 84.0, 100.9, 118.6, 119.1, 126.0, 128.4, 129.0, 129.5, 130.5, 131.1, 132.0, 132.3, 140.3, 147.2. The signals for the two aromatic quaternary carbons were not observed in the ¹³C NMR spectrum. HRMS–ES⁺: m/z [M+H] calcd. for C₁₉H₁₃F₃N: 312.0995, found: 312.0994.

4-((4-(*tert*-butyl)phenyl)ethynyl)-2-(trifluoromethyl)quinoline (**4c**). ν_{\max} / cm^{-1} (film) 2960 (m), 2221 (s), 1603 (m), 1592 (m), 1310 (s), 1280 (m), 1149 (s). ^1H NMR (400 MHz, CDCl_3) δ_{H} 1.33 (9H, s), 7.42 (2H, d, $J=8.4$ Hz), 7.63 (3H, m), 7.80 (1H, m), 7.88 (1H, s), 8.10 (1H, d, $J=8.6$ Hz), 8.22 (1H, d, $J=8.4$ Hz); ^{13}C NMR (100 MHz, CDCl_3) δ_{C} 31.1, 88.1, 92.0, 118.5, 121.6, 123.8, 124.5, 125.5, 127.3, 128.6, 130.2, 130.7, 132.2, 134.5 (q, $J=32.2$ Hz), 143.3, 149.0, 153.2. The signal for an aromatic quaternary carbon was not observed in the ^{13}C NMR spectrum. HRMS–ES⁺: m/z [M+H] calcd. for $\text{C}_{22}\text{H}_{19}\text{F}_3\text{N}$: 354.1464, found: 354.1463.

8-methyl-4-(phenylethynyl)-2-(trifluoromethyl)quinoline (**4d**). ν_{\max} / cm^{-1} (film) 3055 (m), 2921 (m), 2222 (m), 1608 (m), 1559 (m), 1363 (s), 1267 (s), 1150 (s). ^1H NMR (400 MHz, CDCl_3) δ_{H} 2.87 (s, 3H), 7.41 (3H, m), 7.56 (1H, m), 7.68 (3H, m), 7.68 (1H, m), 7.89 (1H, s), 7.96 (1H, d, $J=8.5$ Hz); ^{13}C NMR (100 MHz, CDCl_3) δ_{C} 18.6, 89.1, 90.8, 121.5 (q, $J=5.3$ Hz), 121.7 (q, $J=2.1$ Hz), 128.5, 129.4, 130.8, 132.3, 138.4, 142.0, 148.4. The signals for the four aromatic quaternary carbons were not observed in the ^{13}C NMR spectrum. HRMS–ES⁺: m/z [M+H] calcd. for $\text{C}_{19}\text{H}_{13}\text{F}_3\text{N}$: 312.0995, found: 312.0992.

8-methyl-4-(*p*-tolylethynyl)-2-(trifluoromethyl)quinoline (**4e**). ν_{\max} / cm^{-1} (film) 2925 (m), 2200 (m), 2217 (m), 1588 (m), 1514 (m), 1281 (s), 1104 (s). ^1H NMR (400 MHz, CDCl_3) δ_{H} 2.41 (3H, s), 2.84 (3H, s), 7.24 (2H, d, $J=8.1$ Hz), 7.56 (2H, d, $J=8.1$ Hz), 7.64 (2H, m), 7.86 (1H, s), 8.26 (1H, d, $J=8.2$ Hz); ^{13}C NMR (100 MHz, CDCl_3) δ_{C} 17.8, 21.7, 84.4, 100.1, 118.8 (q, $J=5.2$ Hz), 123.8, 128.4, 128.7, 129.4, 131.0, 132.0, 132.1, 139.0, 140.1, 146.0, 146.4. The signals of two aromatic quaternary carbons were not observed in the ^{13}C NMR spectrum. HRMS–ES⁺: m/z [M+H] calcd. for $\text{C}_{20}\text{H}_{15}\text{F}_3\text{N}$: 326.1151, found: 326.1148.

4-((4-(*tert*-butyl)phenyl)ethynyl)-8-methyl-2-(trifluoromethyl)quinoline (**4f**). ν_{\max} /cm⁻¹ (film) 2965 (m), 2201 (m), 1589 (m), 1392 (m), 1311 (m), 1281 (s), 1190 (s), 1129 (s), 1067 (s). ¹H NMR (400 MHz, CDCl₃) δ_{H} 1.35 (9H, s), 2.84 (3H, s), 7.45 (2H, m), 7.60 (3H, m), 7.66 (1H, d, $J=6.9$ Hz), 7.86 (1H, s), 8.25 (1H, d, $J=8.0$ Hz); ¹³C NMR (100 MHz, CDCl₃) δ_{C} 17.8, 31.1, 35.0, 84.4, 100.1, 118.9 (q, $J=2.0$ Hz), 123.8, 125.4, 125.6, 128.4, 128.7, 130.9, 131.8, 132.1, 132.3, 138.9, 146.4, 146.4, 153.2. HRMS–ES⁺: m/z [M+H] calcd. for C₂₃H₂₁F₃N: 368.1621, found: 368.1619.

8-methyl-2-(trifluoromethyl)-4-((4-(trifluoromethyl)phenyl)ethynyl)quinoline (**4g**). ν_{\max} /cm⁻¹ (film) 2927 (m), 2222 (w), 1613 (m), 1392 (m), 1319 (s), 1159 (m), 1103 (s), 1063 (s). ¹H NMR (400 MHz, CDCl₃) δ_{H} 2.85 (3H, s), 7.63 (1H, t, $J=7.5$ Hz), 7.70 (3H, m), 7.77 (2H, d, $J=8.2$ Hz), 7.90 (1H, s), 8.23 (1H, d, $J=8.0$ Hz); ¹³C NMR (100 MHz, CDCl₃) δ_{C} 17.8, 86.8, 97.6, 119.3 (q, $J=2.0$ Hz), 123.5, 125.6 (q, $J=3.8$ Hz), 128.3, 129.1, 131.0, 131.2, 131.5, 132.3, 135.7, 139.1, 146.1, 146.4. The signals for the two aromatic quaternary carbons were not observed in the ¹³C NMR spectrum. HRMS–ES⁺: m/z [M+H] calcd. for C₂₀H₁₂F₆N: 380.0868, found: 380.0868.

4-(phenylethynyl)-2,8-bis(trifluoromethyl)quinoline (**4h**). ν_{\max} /cm⁻¹ (film) 3062 (w), 2220 (m), 1601 (m), 1591 (m), 1309 (s), 1130 (s), 1143 (s). ¹H NMR (400 MHz, CDCl₃) δ_{H} 7.45 (3H, m), 7.68 (2H, m), 7.78 (1H, t, $J=7.6$ Hz), 7.96 (1H, s), 8.19 (1H, d, $J=7.3$ Hz), 8.62 (1H, d, $J=8.3$ Hz); ¹³C NMR (100 MHz, CDCl₃) δ_{C} 83.9, 101.3, 120.0, 121.3, 122.1, 124.8, 127.7, 128.7, 128.8, 129.0, 129.5 (q, $J=5.3$ Hz), 130.1, 130.3, 132.2, 132.5, 143.7, 148.0 (q, $J=36.5$ Hz). HRMS–ES⁺: m/z [M+H] calcd. for C₁₉H₁₀F₆N: 366.0712, found: 366.0722.

4-(*p*-tolylethynyl)-2,8-bis(trifluoromethyl)quinoline (**4i**). ν_{\max} / cm^{-1} (film) 2927 (w), 2198 (m), 1590 (s), 1309 (s), 1132 (s). ^1H NMR (400 MHz, CDCl_3) δ_{H} 2.40 (3H, s), 7.22 (2H, d, $J=8.1$ Hz), 7.52 (2H, d, $J=8.1$ Hz), 7.74 (1H, t, $J=7.8$ Hz), 7.91 (1H, s), 8.15 (1H, d, $J=7.2$ Hz), 8.57 (1H, d, $J=8.4$ Hz); ^{13}C NMR (100 MHz, CDCl_3) δ_{C} 21.6, 83.5, 101.9, 117.0, 118.2, 119.8, 122.2, 122.5, 124.9, 127.6, 128.7, 129.4 (q, $J=5.4$ Hz), 130.3, 132.1, 132.7, 141.0, 143.7, 148.3 (q, $J=35.5$ Hz). HRMS–ES⁺: m/z [M+H] calcd. for $\text{C}_{20}\text{H}_{12}\text{F}_6\text{N}$: 380.0868, found: 380.0873.

4-((4-(*tert*-butyl)phenyl)ethynyl)-2,8-bis(trifluoromethyl) quinoline (**4j**). ν_{\max} / cm^{-1} (film) 2963 (m), 2213 (m), 1590 (s), 1517 (w), 1312 (s), 1136 (s), 922 (m), 321 (m), 771 (m), 560 (m). ^1H NMR (400 MHz, CDCl_3) δ_{H} 1.36 (9H, s), 7.47 (2H, d, $J=8.4$ Hz), 7.61 (2H, d, $J=8.4$ Hz), 7.76 (1H, t, $J=7.8$ Hz), 7.94 (1H, s), 8.17 (1H, d, $J=7.2$ Hz), 8.60 (1H, d, $J=8.2$ Hz); ^{13}C NMR (100 MHz, CDCl_3) δ_{C} 29.7, 35.1, 83.5, 101.8, 118.3, 119.9 (q, $J=5.3$ Hz), 122.1, 122.4, 124.9, 125.8, 127.6, 129.5, 130.4, 131.9, 132.8, 143.7, 148.2 (q, $J=35.2$ Hz), 153.8. The signal of an aromatic quaternary carbon was not observed in the ^{13}C NMR spectrum. HRMS–ES⁺: m/z [M+H] calcd. for $\text{C}_{23}\text{H}_{18}\text{F}_6\text{N}$: 422.1338, found: 422.1335.

2,8-bis(trifluoromethyl)-4-((4-(trifluoromethyl)phenyl) ethynyl) quinoline (**4k**). ν_{\max} / cm^{-1} (film) 3118 (w), 2220 (m), 1593 (m), 1310 (s), 1066 (s). ^1H NMR (400 MHz, CDCl_3) δ_{H} 7.72 (2H, d, $J=8.3$ Hz), 7.82 (3H, m), 8.01 (1H, m), 8.20 (1H, d, $J=8.2$ Hz), 8.60 (1H, d, $J=8.3$ Hz); ^{13}C NMR (100 MHz, CDCl_3) δ_{C} 85.8, 99.1, 120.4, 122.0, 122.5, 125.7 (q, $J=3.6$ Hz), 126.8, 128.0, 128.5, 129.7 (q, $J=5.5$ Hz), 130.1, 131.7, 132.4. The signals for the five aromatic quaternary carbons were not observed in the ^{13}C NMR spectrum. HRMS–ES⁺: m/z [M+H] calcd. for $\text{C}_{20}\text{H}_9\text{F}_9\text{N}$: 434.0586, found: 434.0580.

2,8-bis(trifluoromethyl)-4-((2-(trifluoromethyl)phenyl)ethynyl) quinoline (**4l**). ν_{\max} / cm^{-1} (film) 2965 (w), 2218 (w), 1589 (m), 1310 (m), 1127 (s). ^1H NMR (400 MHz, CDCl_3) δ_{H} 7.59 (2H, m), 7.79 (3H, m), 7.97 (1H, s), 8.20 (1H, d, $J=7.2$ Hz), 8.61 (1H, d, $J=8.3$ Hz); ^{13}C NMR (100 MHz, CDCl_3) δ_{C} 88.9, 96.3, 119.4 (q, $J=10.3$ Hz), 120.4, 122.0, 122.3, 124.8, 126.3 (q, $J=5.1$ Hz), 128.0, 129.6 (q, $J=5.3$ Hz), 129.8, 130.2, 131.8, 132.1, 134.5, 143.7, 148.0, 148.3. The signals for two aromatic quaternary carbons were not observed in the ^{13}C NMR spectrum. HRMS–ES⁺: m/z [M+H] calcd. for $\text{C}_{20}\text{H}_9\text{F}_9\text{N}$: 434.0586, found: 434.0585.

4-((4-fluorophenyl)ethynyl)-2,8-bis(trifluoromethyl)quinoline (**4m**). ν_{\max} / cm^{-1} (film) 2953 (w), 2222 (m), 1589 (s), 1505 (s), 1307 (s), 1103 (s). ^1H NMR (400 MHz, CDCl_3) δ_{H} 7.16 (2H, m), 7.67 (2H, m), 7.79 (1H, t, $J=7.9$ Hz), 7.96 (1H, s), 8.20 (1H, d, $J=7.2$ Hz), 8.60 (1H, d, $J=8.2$ Hz); ^{13}C NMR (100 MHz, CDCl_3); δ_{C} 83.7, 100.1, 116.2 (d, $^2J_{\text{C-F}}=22.6$ Hz), 117.5 (q, $J=3.6$ Hz), 120.1, 123.5 (d, $^1J_{\text{C-F}}=273.2$ Hz), 127.7, 128.6, 129.6 (q, $J=5.3$ Hz), 130.2, 132.3, 134.2 (d, $^3J_{\text{C-F}}=8.7$ Hz), 162.3, 164.8. The signals for three aromatic quaternary carbons were not observed in the ^{13}C NMR spectrum. HRMS–ES⁺: m/z [M+H] calcd. for $\text{C}_{19}\text{H}_9\text{F}_7\text{N}$: 384.0623, found: 384.0612.

4-((3,5-difluorophenyl)ethynyl)-2,8-bis(trifluoromethyl) quinoline (**4n**). ν_{\max} / cm^{-1} (film) 3087 (w), 2954 (m), 1616 (m), 1590 (s), 1320 (m), 1303 (m), 1136 (s). ^1H NMR (400 MHz, CDCl_3) δ_{H} 6.95 (1H, m), 7.20 (2H, m), 7.82 (1H, t, $J=8.0$ Hz), 7.99 (1H, s), 8.23 (1H, d, $J=7.3$ Hz), 8.56 (1H, d, $J=8.5$ Hz); ^{13}C NMR (100 MHz, CDCl_3) δ_{C} 85.3, 98.1, 106.3 (t, $^2J_{\text{C-F}}=25.4$ Hz), 115.1 (d, $^2J_{\text{C-F}}=27.3$ Hz), 120.5, 122.0, 123.8, 124.8, 125.9, 128.1, 129.8 (d, $^3J_{\text{C-F}}=5.3$ Hz), 130.0, 131.4, 139.0, 148.2, 161.7, 164.2. HRMS–ES⁺: m/z [M+H] calcd. for $\text{C}_{19}\text{H}_7\text{F}_8\text{N}$: 402.0524, found: 402.0540.

4-((4-(*tert*-butyl)phenyl)ethynyl)-2-(trifluoromethyl)quinoline (**4o**). ν_{\max} / cm^{-1} (film) 3085 (w), 2926 (m), 2219 (w), 1591 (s), 1312 (m), 1138 (s). ^1H NMR (400 MHz, CDCl_3) δ_{H} 7.20 (2H, m), 7.45 (1H, m), 7.62 (1H, td, $J=7.4, 1.7$ Hz), 7.78 (1H, t, $J=7.8$ Hz), 7.96 (1H, s), 8.18 (1H, d, $J=7.2$ Hz), 8.62 (1H, d, $J=7.9$ Hz); ^{13}C NMR (100 MHz, CDCl_3) δ_{C} 88.8 (d, $J=3.4$ Hz), 94.5, 110.2 (d, $^2J_{\text{C-F}}=15.5$ Hz), 115.9 (d, $^2J_{\text{C-F}}=20.5$ Hz), 119.9, 122.1, 124.4 (d, $^4J_{\text{C-F}}=3.7$ Hz), 128.0, 129.6 (q, $J=5.3$ Hz), 130.3, 132.0, 134.5 (d, $^3J_{\text{C-F}}=8.2$ Hz), 133.6, 143.7, 148.2 (m), 163.2 (d, $^1J_{\text{C-F}}=253.2$ Hz). The signals for three aromatic quaternary carbons were not observed in the ^{13}C NMR spectrum. HRMS-ES⁺: m/z [M+H] calcd. for $\text{C}_{19}\text{H}_9\text{F}_7\text{N}$: 384.0618, found: 384.0609.

4-(hex-1-yn-1-yl)-2-(trifluoromethyl)quinoline (**4p**). ν_{\max} / cm^{-1} (film) 3015 (w), 2225 (m), 1583 (m), 1387 (m), 1175 (s), 1096 (s). ^1H NMR (400 MHz, CDCl_3) δ_{H} 1.00 (3H, t, $J=7.3$ Hz), 1.56 (2H, m), 1.71 (2H, m), 2.60 (2H, t, $J=7.1$ Hz), 7.68 (1H, td, $J=7.7, 1.0$ Hz), 7.75 (1H, s), 7.80 (1H, td, $J=7.7, 1.4$ Hz), 7.19 (1H, d, $J=8.5$ Hz), 8.30 (1H, d, $J=8.3$ Hz), ^{13}C NMR (100 MHz, CDCl_3) δ_{C} 13.6, 19.5, 22.1, 30.4, 76.2, 102.9, 119.3, 120.1, 122.8, 125.6, 129.6, 131.6, 133.0, 147.2 (q, $J=34.2$ Hz), 148.0. The signal for an aromatic quaternary carbon was not observed in the ^{13}C NMR spectrum. HRMS-ES⁺: m/z [M+H] calcd. for $\text{C}_{16}\text{H}_{15}\text{F}_3\text{N}$: 278.1151, found: 278.1151.

4-(cyclopropylethynyl)-2-(trifluoromethyl)quinoline (**4q**). ν_{\max} / cm^{-1} (film) 3090 (w), 3018 (w), 2927 (w), 2221 (m), 1584 (m), 1997 (m), 1198 (s), 1104 (s). ^1H NMR (400 MHz, CDCl_3) δ_{H} 1.02 (4H, m), 1.64 (1H, m), 7.68 (1H, t, $J=7.5$ Hz), 7.80 (1H, td, $J=7.2, 1.2$ Hz), 8.18 (1H, d, $J=8.5$ Hz), 7.88 (1H, d, $J=8.3$ Hz), 8.26 (1H, d, $J=8.4$ Hz), ^{13}C NMR (100 MHz, CDCl_3) δ_{C} 0.6, 9.4, 71.5, 106.3, 119.2, 126.0, 126.5, 127.4 (q, $J=5.3$ Hz), 128.8, 130.4, 130.9,

133.0, 138.7. The signal for an aromatic quaternary carbon was not observed in the ^{13}C NMR spectrum. HRMS–ES $^+$: m/z [M+H] calcd. for $\text{C}_{15}\text{H}_{11}\text{F}_3\text{N}$: 262.0838, found: 262.0841.

4-(cyclopropylethynyl)-8-methyl-2-(trifluoromethyl)quinoline (**4r**). ν_{max} / cm^{-1} (film) 3022 (w), 2226 (m), 1592 (m), 1421 (m), 1309 (m), 1174 (m), 1126 (s), 1055 (s). ^1H NMR (400 MHz, CDCl_3) δ_{H} 1.00 (m, 4H), 1.62 (1H, m), 2.80 (3H, s), 7.53 (1H, t, $J=8.0$ Hz), 7.61 (1H, d, $J=7.0$ Hz), 7.70 (1H, s), 8.09 (1H, d, $J=8.2$ Hz); ^{13}C NMR (100 MHz, CDCl_3) δ_{C} 0.0, 8.8, 17.2, 71.3, 104.8, 118.4, 119.6, 122.4, 123.2, 127.9, 128.3, 130.2, 132.2, 138.1, 145.6 (q, $J=34.8$ Hz). HRMS–ES $^+$: m/z [M+H] calcd. for $\text{C}_{16}\text{H}_{13}\text{F}_3\text{N}$: 276.0995, found: 276.0991.

4-(cyclopropylethynyl)-2,8-bis(trifluoromethyl)quinolone (**4s**). ν_{max} / cm^{-1} (film) 3025 (w), 2226 (m), 1585 (m), 1424 (m), 1308 (m), 1160 (m), 1122 (s), 1055 (s). ^1H NMR (400 MHz, CDCl_3) δ_{H} 0.99 (m, 2H), 1.06 (m, 2H), 1.63 (1H, m), 7.66 (1H, t, $J=7.8$ Hz), 7.76 (1H, s), 8.10 (1H, d, $J=7.4$ Hz), 8.40 (1H, d, $J=8.0$ Hz); ^{13}C NMR (100 MHz, CDCl_3) δ_{C} 0.0, 8.9, 70.5, 107.0, 118.9, 119.4, 121.6, 121.9, 124.4, 126.7, 128.7 (q, $J=5.3$ Hz), 129.8, 132.9, 143.0, 147.5 (q, $J=35.1$ Hz). HRMS–ES $^+$: m/z [M+H] calcd. for $\text{C}_{16}\text{H}_{10}\text{F}_6\text{N}$: 330.0712, found: 330.0715.

Crystallographic data (excluding structure factors) for the structure in this chapter has been deposited with the Cambridge Crystallographic Data Centre as supplementary publication no. CCDC 1486561. A copy of the data can be obtained, free of charge, on application to CCDC, 12 Union Road, Cambridge CB2 1EZ, UK, (fax: +44-(0)1223-336033 or e-mail: deposit@ccdc.cam.ac.uk).

4.5 References

- Afzal, O., Kumar, S., Haider, M.R., Ali, M.R., Kumar, R., Jaggi, M., Bawa, S., A review on anticancer potential of bioactive heterocycle quinoline. *European Journal of Medicinal Chemistry*, **2015**, 97, 871-910.
- Angibaud, P.R., Venet, M.G., Pilatte, I.N.C., Preparation of quinoline and quinazoline derivatives as farnesyl transferase inhibitors for treatment of tumors and proliferative diseases. **2002**, WO Patent 2002024682A1.
- Bakherad, M., Amin, A.H., Keivanloo, A., Bahramian, B., Raeissi, M., Copper- and phosphine-free Sonogashira coupling reactions of aryl iodides catalyzed by an *N,N*-bis(naphthylideneimino)diethylenetriamine-functionalized polystyrene resin supported Pd(II) complex under aerobic conditions. *Tetrahedron Letters*, **2010**, 51, 5653-5656.
- Bawa, S., Kumar, S., Drabu, S., Kumar, R., Structural modifications of quinoline-based antimalarial agents: Recent developments. *Journal of Pharmacy and Bioallied Sciences*, **2010**, 2, 64-71.
- Biot, C., Delhaes, L., Maciejewski, L.A., Mortuaire, M., Camus, D., Dive, D., Brocard, J.S., Synthetic ferrocenic mefloquine and quinine analogues as potential antimalarial agents. *European Journal of Medicinal Chemistry*, **2000**, 35, 707-714.
- Chernov'yants, M.S., Starikova, Z.A., Kolesnikova, T.S., Karginova, A.O., Lyanguzov, N.V., Synthesis and structure of interaction products of quinoline-2(1*H*)-thione with molecular iodine. *Spectrochimica Acta Part A-Molecular and Biomolecular Spectroscopy*, **2015**, 139, 533-538.
- Chinchilla, R., Najera, C., The Sonogashira reaction: A booming methodology in synthetic organic chemistry. *Chemical Reviews*, **2007**, 107, 874-922.
- Das, S., Samanta, S., Ray, S., Biswas, P., 3,6-Di(pyridin-2-yl)-1,2,4,5-tetrazine capped Pd(0) nanoparticles: A catalyst for copper-free Sonogashira coupling of aryl halides in aqueous medium. *RSC Advances*, **2015**, 5, 75263-75267.
- Dewan, A., Sarmah, M., Bora, U., Thakur, A.J., A green protocol for ligand, copper and base free Sonogashira cross-coupling reaction. *Tetrahedron Letters*, **2016**, 57, 3760-3763.
- Eswaran, S., Adhikari, A.V., Chowdhury, I.H., Pal, N.K., Thomas, K.D., New quinoline derivatives: Synthesis and investigation of antibacterial and antituberculosis properties. *European Journal of Medicinal Chemistry*, **2010**, 45, 3374-3383.
- Feng, Y.-S., Li, Y.-Y., Tang, L., Wu, W., Xu, H.-J., Efficient ligand-free copper-catalyzed C-S cross-coupling of thiols with aryl iodides using KF/Al₂O₃ as base. *Tetrahedron Letters*, **2010**, 51, 2489-2492.
- Godel, T., Hoffmann, T., Schnider, P., Stadler, H., Preparation of 4-phenylpyridines as neurokinin-1 receptor antagonists. **2002**, WO Patent 2002016324A1.
- Grissom, J.W., Gunawardena, G.U., Klingberg, D., Huang, D., The chemistry of enediynes, enyne allenes and related compounds. *Tetrahedron*, **1996**, 52, 6453-6518.

- Hagmann, W.K., The many roles for fluorine in medicinal chemistry. *Journal of Medicinal Chemistry*, **2008**, 51, 4359-4369.
- Hayakawa, I., Atarashi, S., Yokohama, S., Imamura, M., Sakano, K., Furukawa, M., Synthesis and antibacterial activities of optically active ofloxacin. *Antimicrobial Agents and Chemotherapy*, **1986**, 29, 163-164.
- Kabalka, G.W., Wang, L., Namboodiri, V., Pagni, R.M., Rapid microwave-enhanced, solventless sonogashira coupling reaction on alumina. *Tetrahedron Letters*, **2000**, 41, 5151-5154.
- Kawanami, H., Matsushima, K., Sato, M., Ikushima, Y., Rapid and highly selective copper-free Sonogashira coupling in high-pressure, high-temperature water in a microfluidic system. *Angewandte Chemie, International Edition*, **2007**, 46, 5129-5132.
- Kumar, S., Bawa, S., Gupta, H., Biological activities of quinoline derivatives. *Mini-Reviews in Medicinal Chemistry*, **2009**, 9, 1648-1654.
- Li, J.-H., Liang, Y., Xie, Y.-X., Efficient palladium-catalyzed homocoupling reaction and Sonogashira cross-coupling reaction of terminal alkynes under aerobic conditions. *Journal of Organic Chemistry*, **2005**, 70, 4393-4396.
- Liang, T., Neumann, C.N., Ritter, T., Introduction of fluorine and fluorine-containing functional groups. *Angewandte Chemie, International Edition*, **2013**, 52, 8214-8264.
- Mandegani, Z., Asadi, M., Asadi, Z., Nano tetraamine Pd(0) complex as an efficient catalyst for phosphine-free Suzuki reaction in water and copper-free Sonogashira reaction under aerobic conditions. *Applied Organometallic Chemistry*, **2016**, 30, 657-663.
- Miyaura, N., Suzuki, A., Palladium-catalyzed cross-coupling reactions of organoboron compounds. *Chemical Reviews*, **1995**, 95, 2457-2483.
- O'Hagan, D., Fluorine in health care: Organofluorine containing blockbuster drugs. *Journal of Fluorine Chemistry*, **2010**, 131, 1071-1081.
- Reddy, E.A., Islam, A., Mukkanti, K., Bandameedi, V., Bhowmik, D.R., Pal, M., Regioselective alkylation followed by Suzuki coupling of 2,4-dichloroquinoline: Synthesis of 2-alkynyl-4-arylquinolines. *Beilstein Journal of Organic Chemistry*, **2009**, 5, 1-8.
- Siemsen, P., Livingston, R.C., Diederich, F., Acetylenic coupling: A powerful tool in molecular construction. *Angewandte Chemie, International Edition*, **2000**, 39, 2632-2657.
- Sonogashira, K., Development of Pd-Cu catalyzed cross-coupling of terminal acetylenes with sp²-carbon halides. *Journal of Organometallic Chemistry*, **2002**, 653, 46-49.
- Sonogashira, K., Tohda, Y., Hagihara, N., Convenient synthesis of acetylenes. Catalytic substitutions of acetylenic hydrogen with bromo alkenes, iodo arenes, and bromopyridines. *Tetrahedron Letters*, **1975**, 4467-4470.
- Tykwinski, R.R., Evolution in the palladium-catalyzed cross-coupling of sp- and sp²-hybridized carbon atoms. *Angewandte Chemie, International Edition*, **2003**, 42, 1566-1568.

Yi, W.-B., Cai, C., Wang, X., A palladium/perfluoroalkylated pyridine catalyst for Sonogashira reaction of aryl bromides and chlorides in a fluorous biphasic system. *European Journal of Organic Chemistry*, **2007**, 3445-3448.

Chapter 5. Conclusion

We have successfully shown that fluorinated precursors behave differently from other substituted or unsubstituted precursors with regard to metal catalysed cross coupling reactions and have shown them to play a substantial role in these reactions.

It was shown that the copper catalysed ring closing coupling reaction of 2,3-difluorinated Boc-protected phenoxypropanamine to benzoxazine occurred with a yield of 90% at room temperature and took place via a Smiles rearrangement. In contrast, the non-fluorinated Boc-protected phenoxypropanamine reacted only at 90°C and no product was observed at room temperature. Fluorine or trifluoromethane substituents substituted at the *para* position of the phenoxypropanamine precursor was shown to hinder the reaction as conversion to benzoxazine did not occur, even at 90 °C. Based on our proposed mechanism, the conformation of precursors have a direct effect on the SR by shortening or increasing the distance between nucleophile and electrophile in order for nucleophilic substitution to take place. The 2,3-difluorinated phenoxypropanamine has a desirable conformation, allowing the Smiles rearrangement to occur at room temperature, while F or CF₃ in the *para* position has an undesirable conformation for nucleophilic substitution to take place. A crystal structure of the 2,3-difluorinated phenoxypropanamine showed that a folded structure existed, which would facilitate chelation with the catalyst, resulting in higher yield.

In a second metal catalyzed cross coupling reaction (Pd catalyzed Sonogashira coupling), it was shown that a CF₃ group substituted at C-8 on a quinoline nucleus, resulted in better yields of alkynyl substitution at C-4 as compared to a methyl group and hydrogen at the same position (C-8). In these reactions, the yields were greatest with a tertiary butyl group at the *para* position of the phenyl alkynyl group and introduction of fluorine or CF₃ on the aromatic

ring reduced yields. This is thought to be due to the step where phenylacetylene is coordinated to the metal through π bonds, which is stabilised more by electron donating *t*-butyl groups compared to F and CF₃, resulting in higher yields for the *t*-butyl derivatives.

In general, we have shown that the presence of F or fluorinated groups (CF₃ in particular) at different positions of precursors have a substantial effect on reactivity of metal catalyzed cross coupling reactions, brought about by changes in conformation of the precursors.

Future work can involve varying the substituents and position on the quinoline ring and observing the effect it has on the Sonogashira coupling of acetylenes. With regard to the Smiles rearrangement, the reaction can be investigated on the following precursors, 2-bromo-6-fluorophenoxyalkyl, 2-chloro-6-fluorophenoxyalkyl and 2-iodo-6-fluorophenoxyalkyl as well as the 2,3-difluoro-6-chloro and 2,3-difluoro-6-iodo precursors. Conformational studies of these precursors will also shed light on whether or not our premises hold for other systems as well.

Supporting information

Chapter 2

Copper-Catalysed Cross-coupling affected by the Smiles rearrangement: A new chapter on diversifying the synthesis of chiral fluorinated 1,4-benzoxazine derivatives

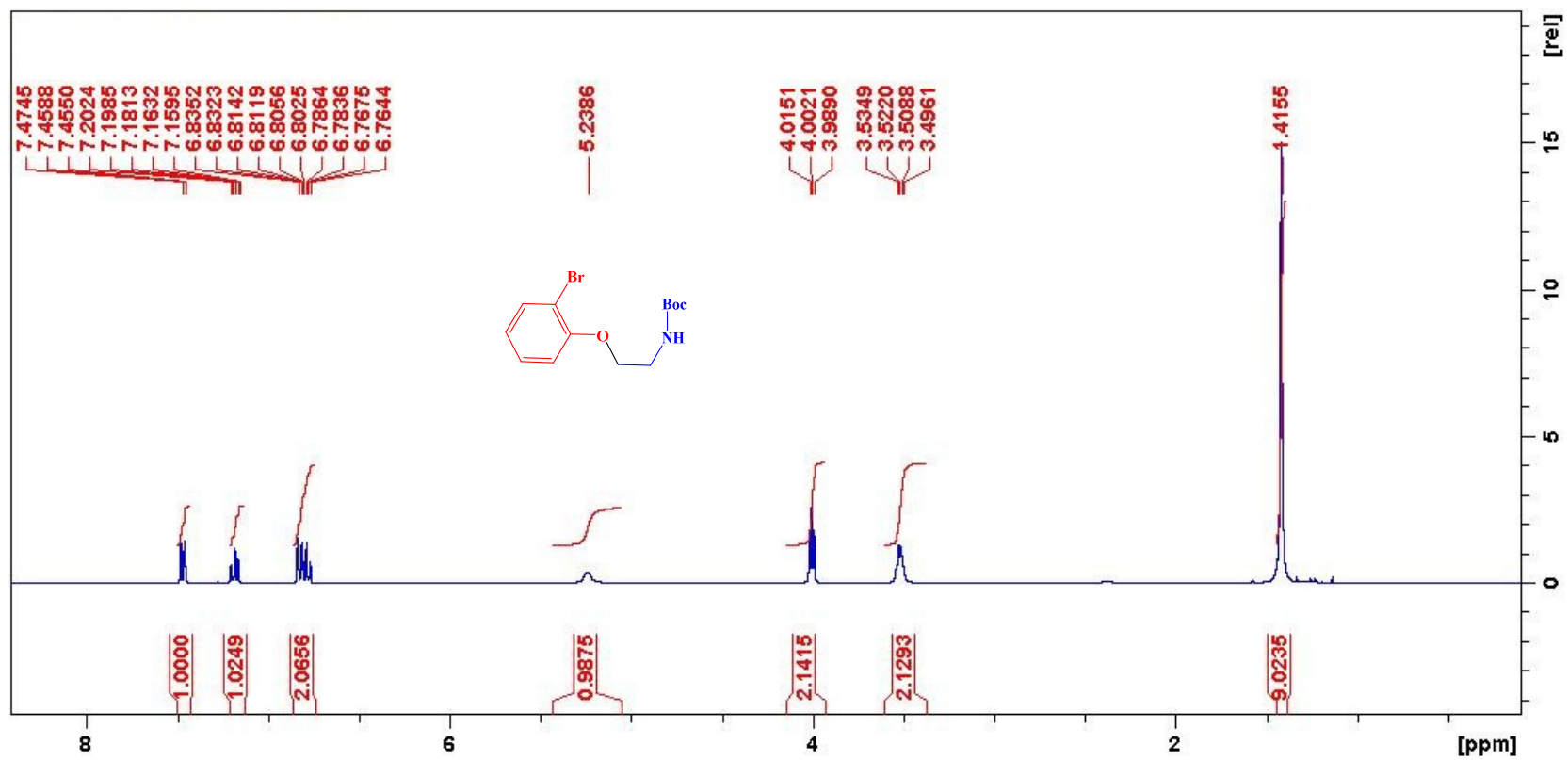
General experimental procedures

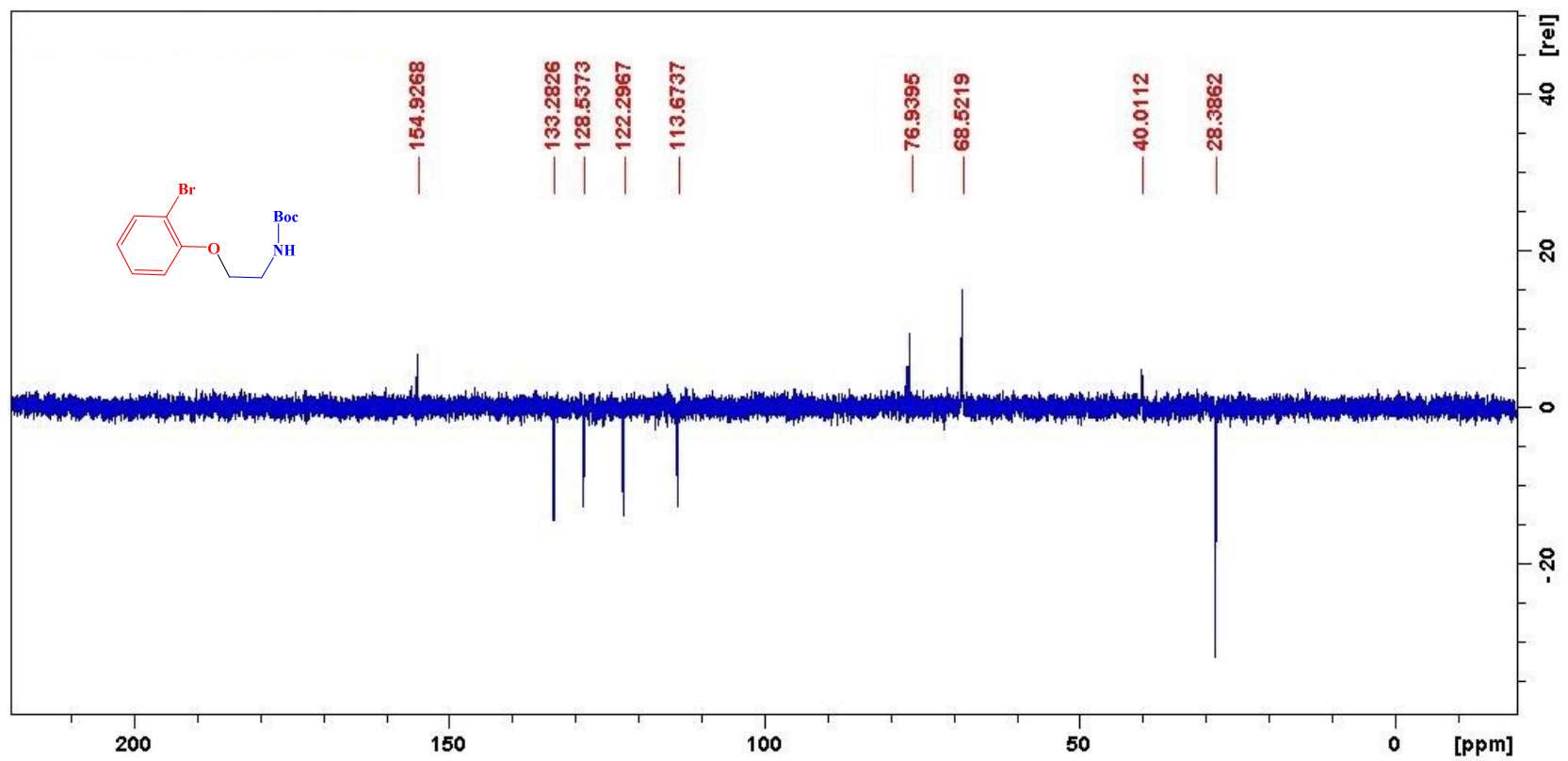
Reagents and solvents were purchased from Sigma Aldrich and used as received. Commercially available Merck Kieselgel 60 F₂₅₄ aluminium backed plates were used for TLC analysis. Visualisation of TLC plates was achieved by UV fluorescence and iodine vapour. Compounds were purified by column chromatography packed with 60-200 mesh Silica gel.

All NMR spectra were recorded on Bruker AVANCE III 400 or 600 MHz instruments. Chemical shifts are quoted in parts per million (ppm) downfield from TMS as the internal standard and the coupling constants are reported in Hertz. Multiplicities of the NMR resonances are abbreviated as s (singlet), d (doublet), t (triplet), q (quartet), m (multiplet) and br (broad). Assignments of ¹H NMR, ¹³C NMR and ¹⁹F NMR resonances were made with the aid of COSY, NOESY, HMBC and HSQC experiments. High resolution spectrometric data were obtained using a Waters micromass LCT premier TOF-MS instrument. Infra-red spectra were recorded in the range 4000-600 cm⁻¹ on a Perkin Elmer Spectrum as neat films onto a NaCl window. Elemental analysis was carried out on a Thermo Scientific Flash 2000. Melting points were obtained on a Stuart Melting Point apparatus SMP11 and are uncorrected. Abbreviations used are: w (weak), m (medium), s (strong) and br (broad). Optical rotations were measured using a Perkin-Elmer 341 polarimeter.

NMR spectra

^1H NMR spectra of **5a**



^{13}C NMR spectra of **5a**

HRMS of **5a**

Elemental Composition Report

Page 1

Single Mass Analysis

Tolerance = 5.0 PPM / DBE: min = -1.5, max = 100.0

Element prediction: Off

Number of isotope peaks used for i-FIT = 3

Monoisotopic Mass, Even Electron Ions

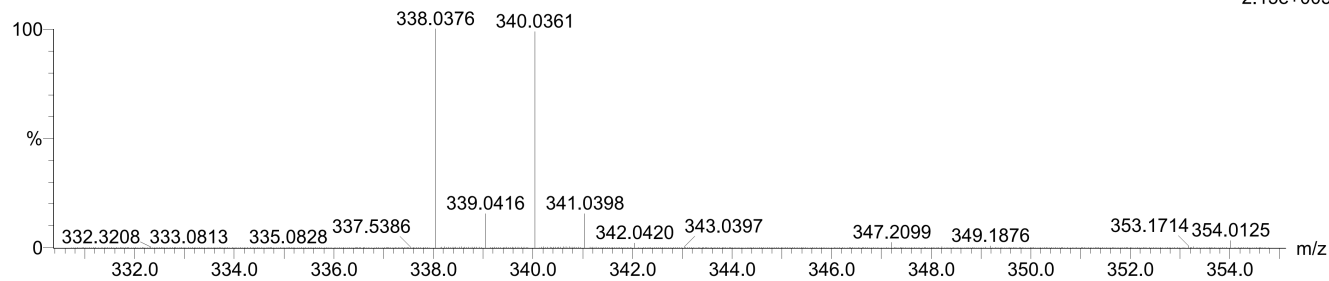
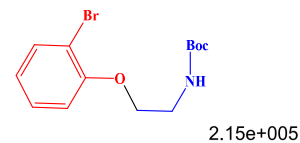
36 formula(e) evaluated with 1 results within limits (up to 20 closest results for each mass)

Elements Used:

C: 10-15 H: 15-20 N: 0-5 O: 0-5 Na: 1-1 Br: 0-1

SZBr 56 (1.856) Cm (1:61)

TOF MS ES+



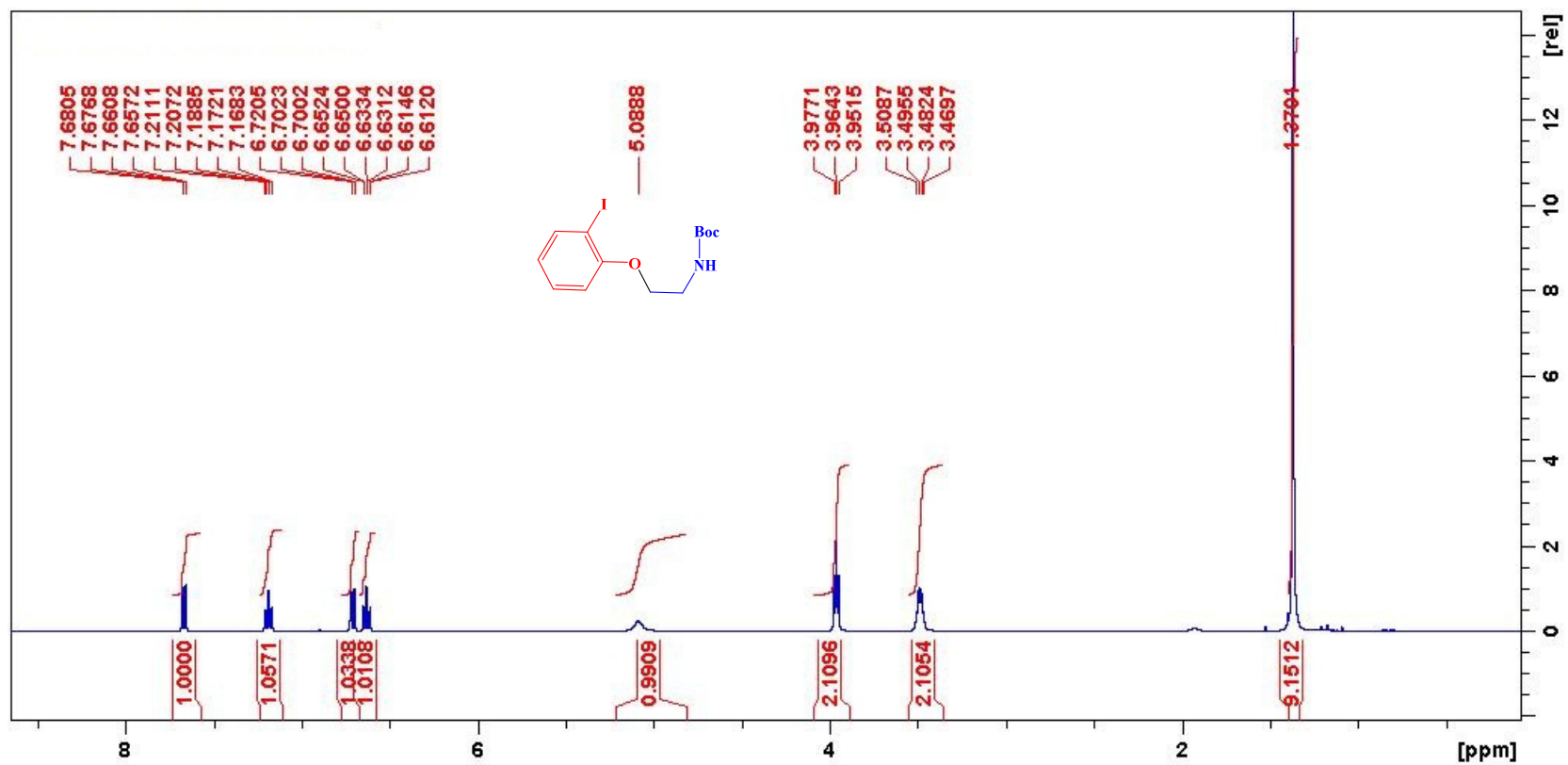
Minimum:

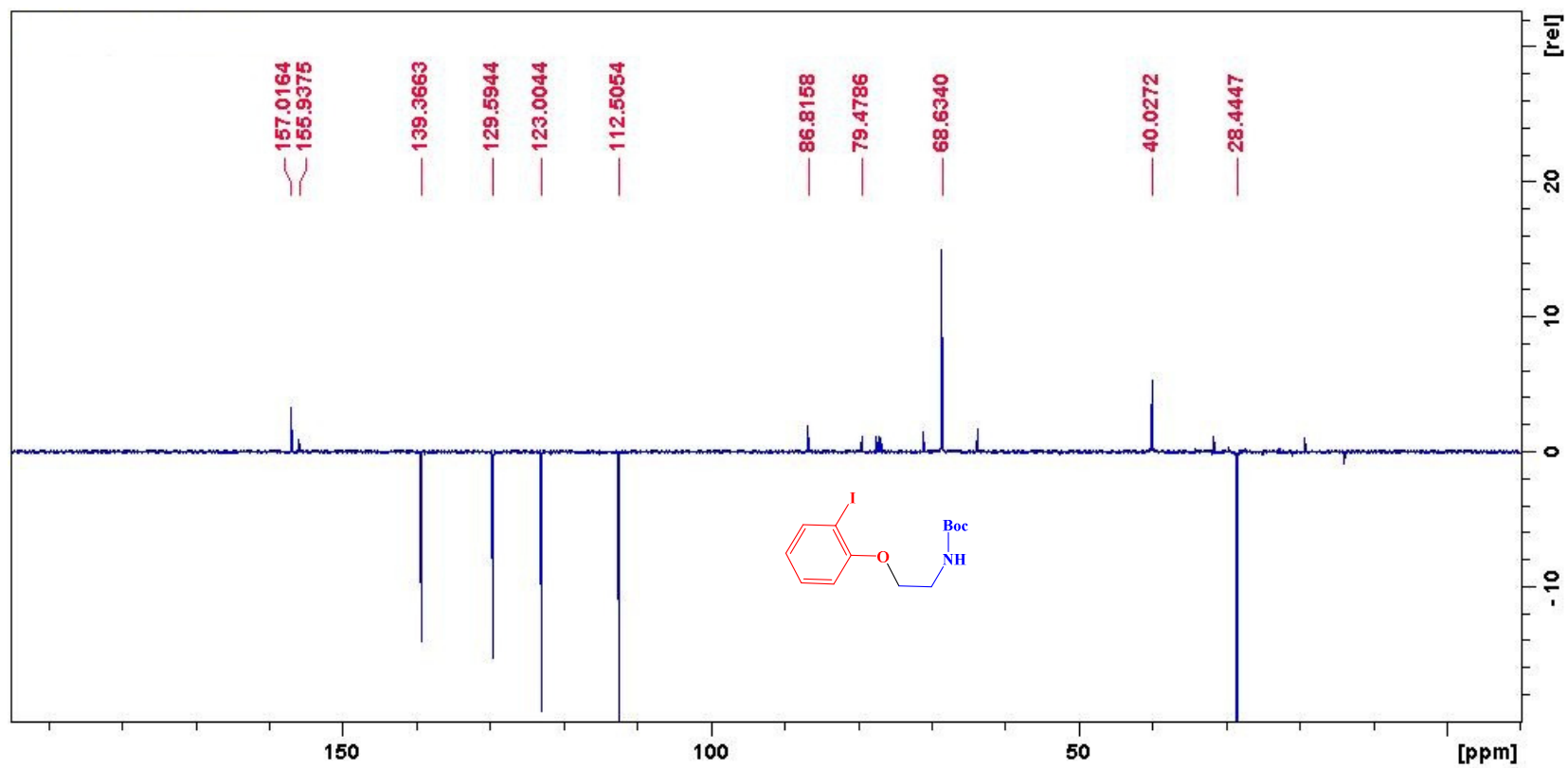
Maximum:

5.0 5.0 -1.5
 100.0

Mass	Calc. Mass	mDa	PPM	DBE	i-FIT	i-FIT (Norm)	Formula
------	------------	-----	-----	-----	-------	--------------	---------

338.0376	338.0368	0.8	2.4	4.5	612.6	0.0	C13 H18 N O3 Na Br
----------	----------	-----	-----	-----	-------	-----	--------------------

¹H NMR spectra of **5b**

^{13}C NMR spectra of **5b**

HRMS of **5b**

Elemental Composition Report

Page 1

Single Mass Analysis

Tolerance = 5.0 PPM / DBE: min = -1.5, max = 100.0

Element prediction: Off

Number of isotope peaks used for i-FIT = 3

Monoisotopic Mass, Even Electron Ions

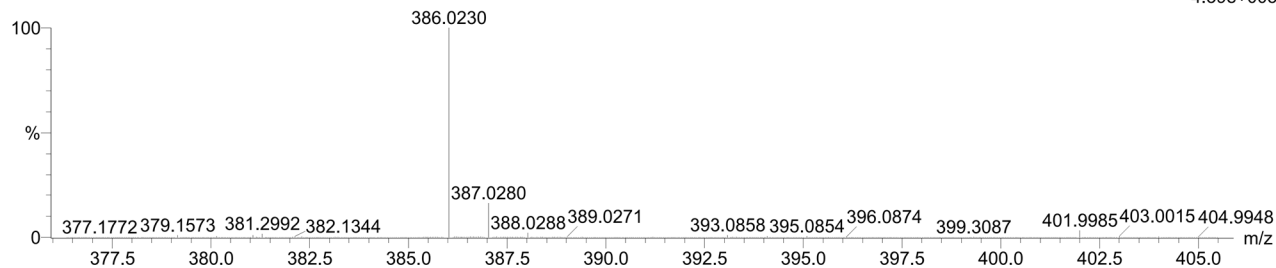
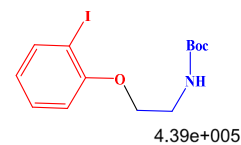
46 formula(e) evaluated with 1 results within limits (up to 20 closest results for each mass)

Elements Used:

C: 10-15 H: 15-20 N: 0-5 O: 0-5 Na: 1-1 I: 0-1

SZI 8 (0.236) Cm (1:61)

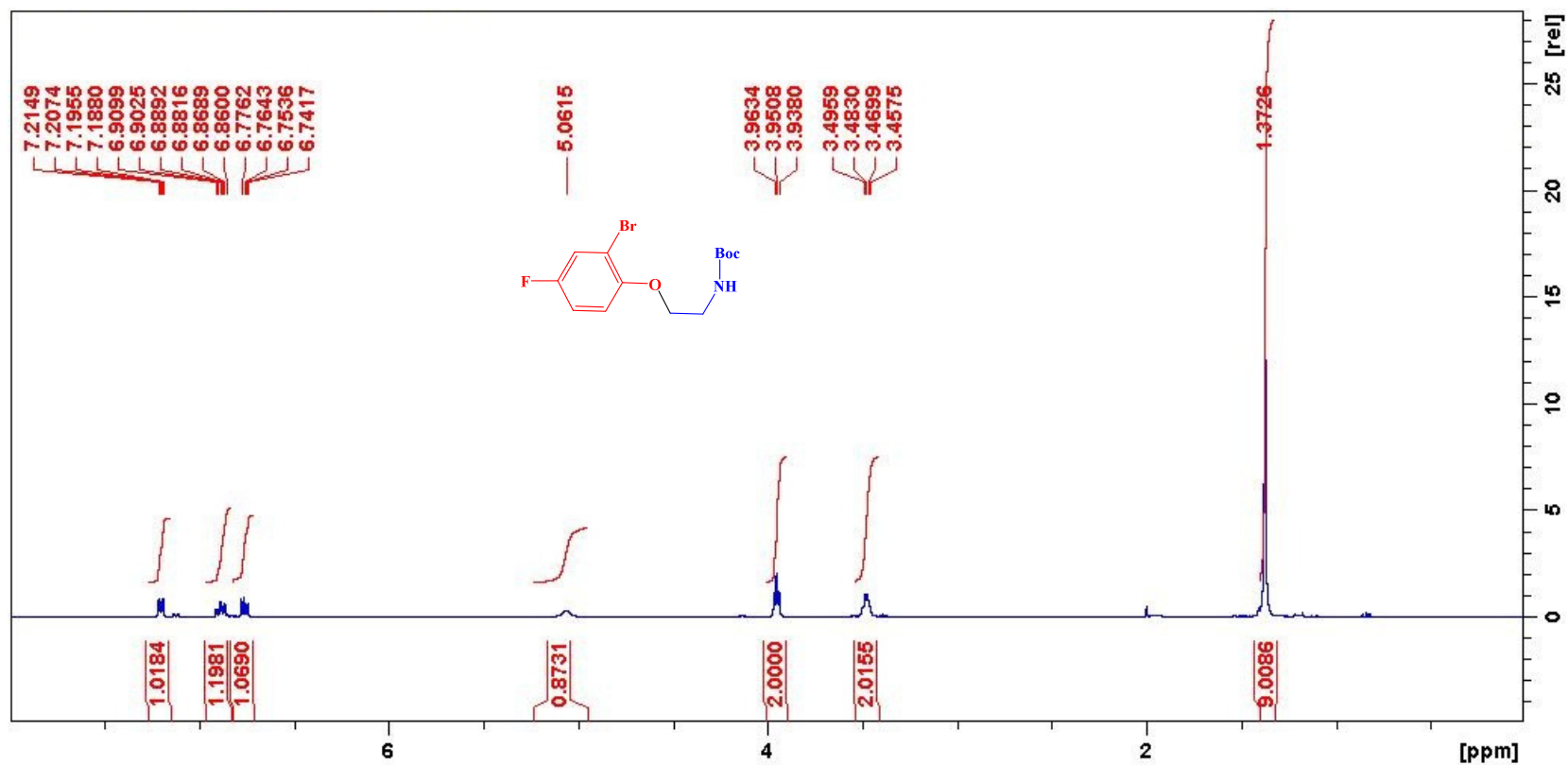
TOF MS ES+

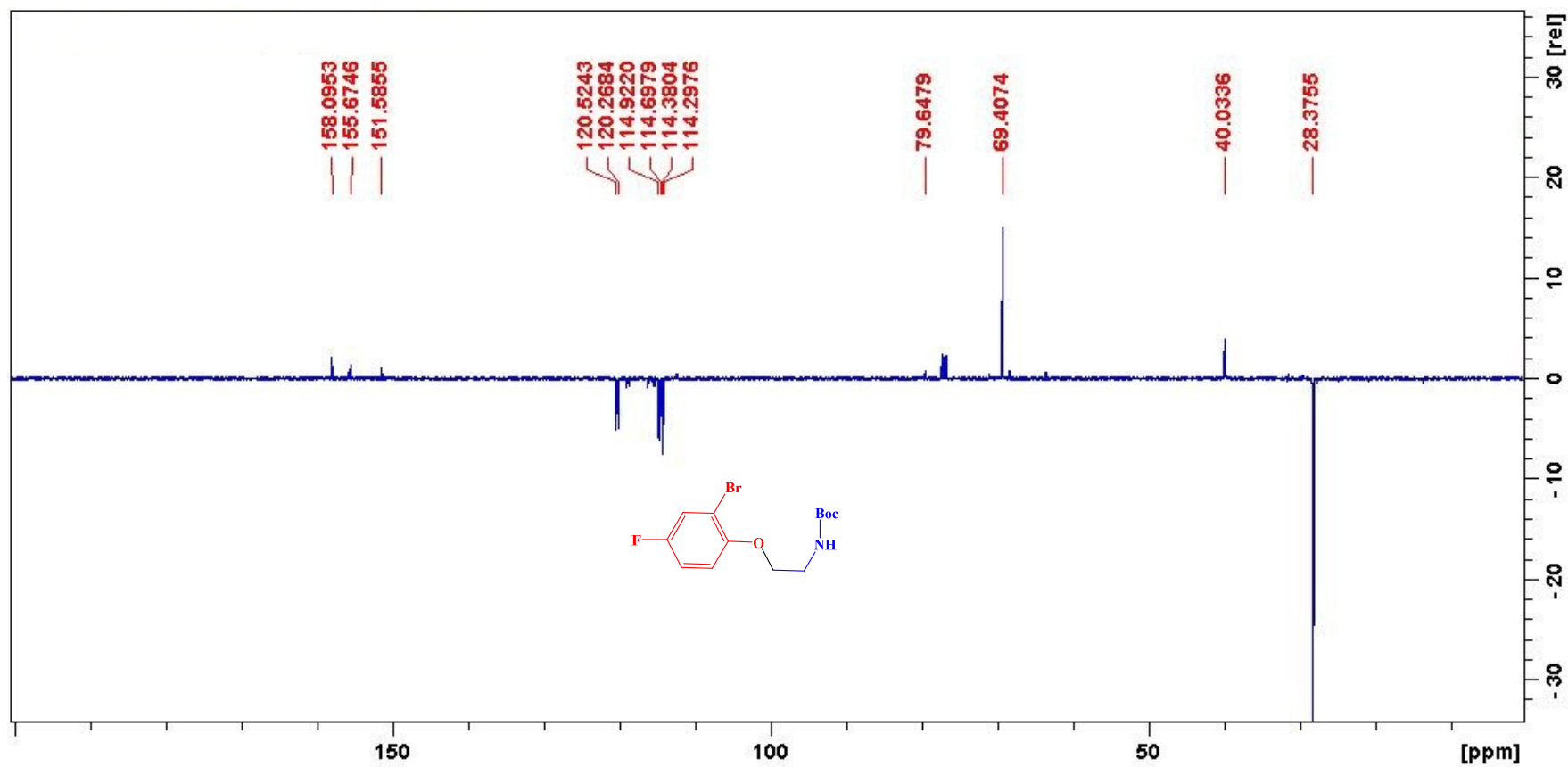


Minimum:

Maximum: 5.0 5.0 -1.5 100.0

Mass	Calc. Mass	mDa	PPM	DBE	i-FIT	i-FIT (Norm)	Formula
386.0230	386.0229	0.1	0.3	4.5	640.5	0.0	C13 H18 N O3 Na I

^1H NMR spectra of **5c**

^{13}C NMR spectra of **5c**

HRMS of **5c**

Elemental Composition Report

Page 1

Single Mass Analysis

Tolerance = 5.0 PPM / DBE: min = -1.5, max = 100.0

Element prediction: Off

Number of isotope peaks used for i-FIT = 3

Monoisotopic Mass, Even Electron Ions

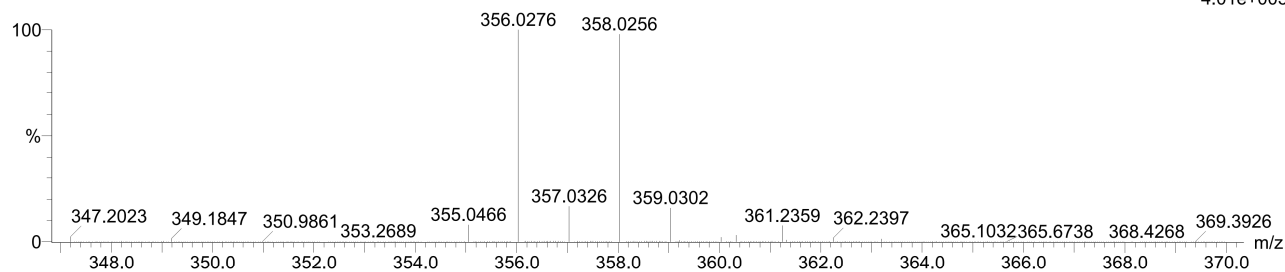
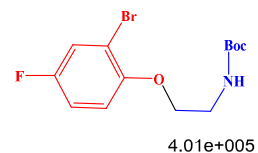
82 formula(e) evaluated with 1 results within limits (up to 20 closest results for each mass)

Elements Used:

C: 10-15 H: 15-20 N: 0-5 O: 0-5 F: 0-1 Na: 1-1 Br: 0-1

SZ1F 58 (1.923) Cm (1:61)

TOF MS ES+



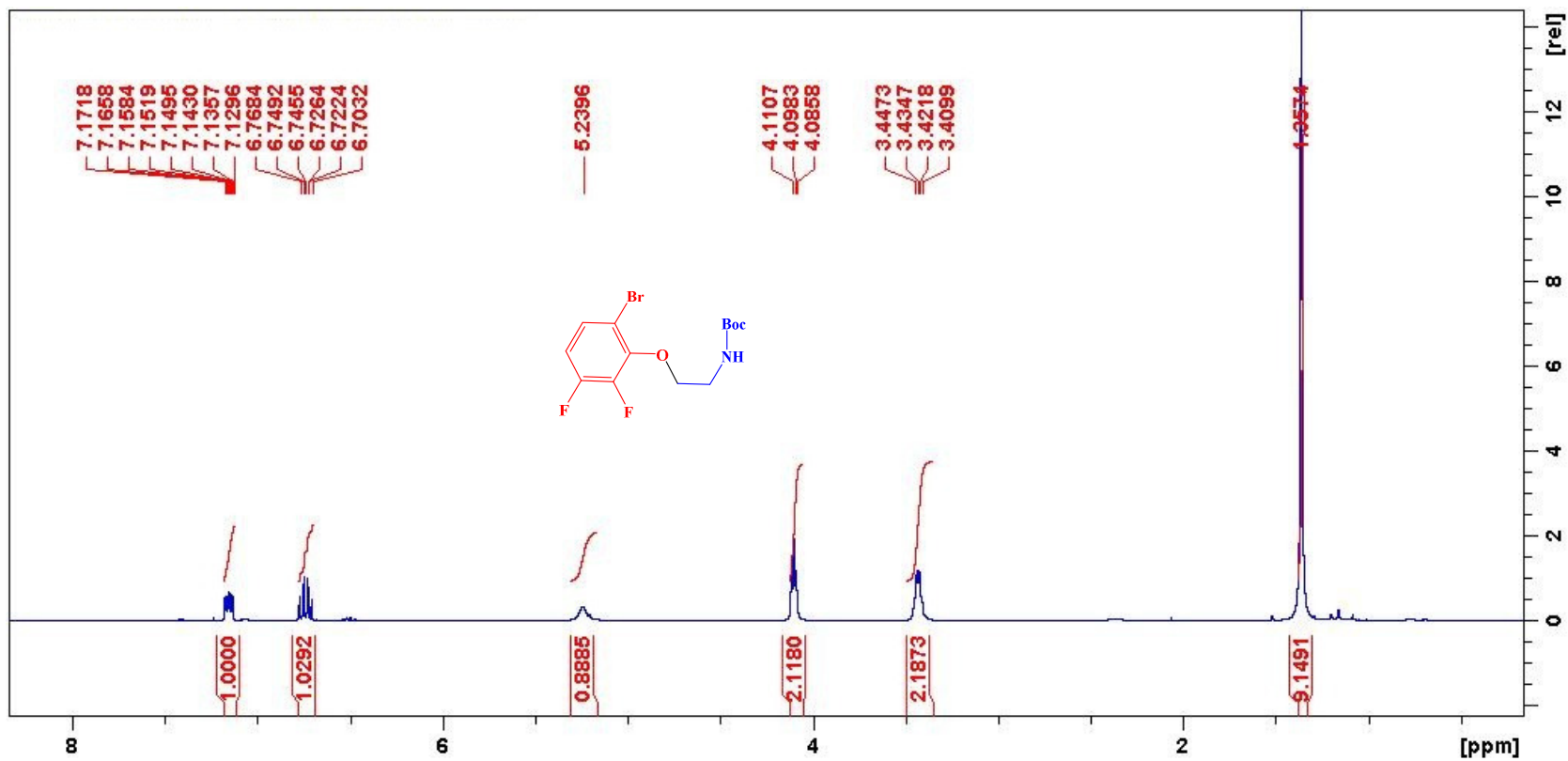
Minimum:

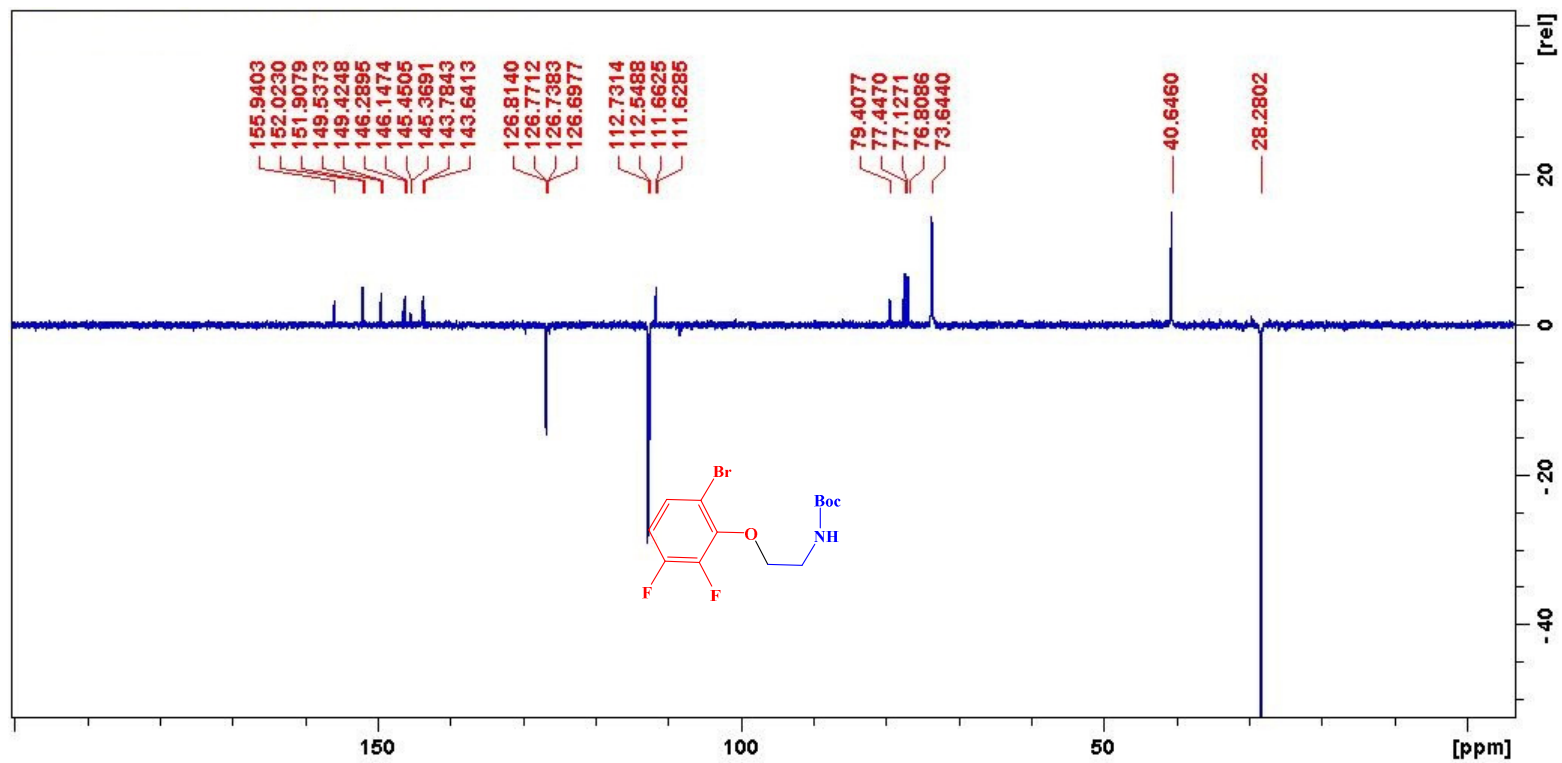
Maximum:

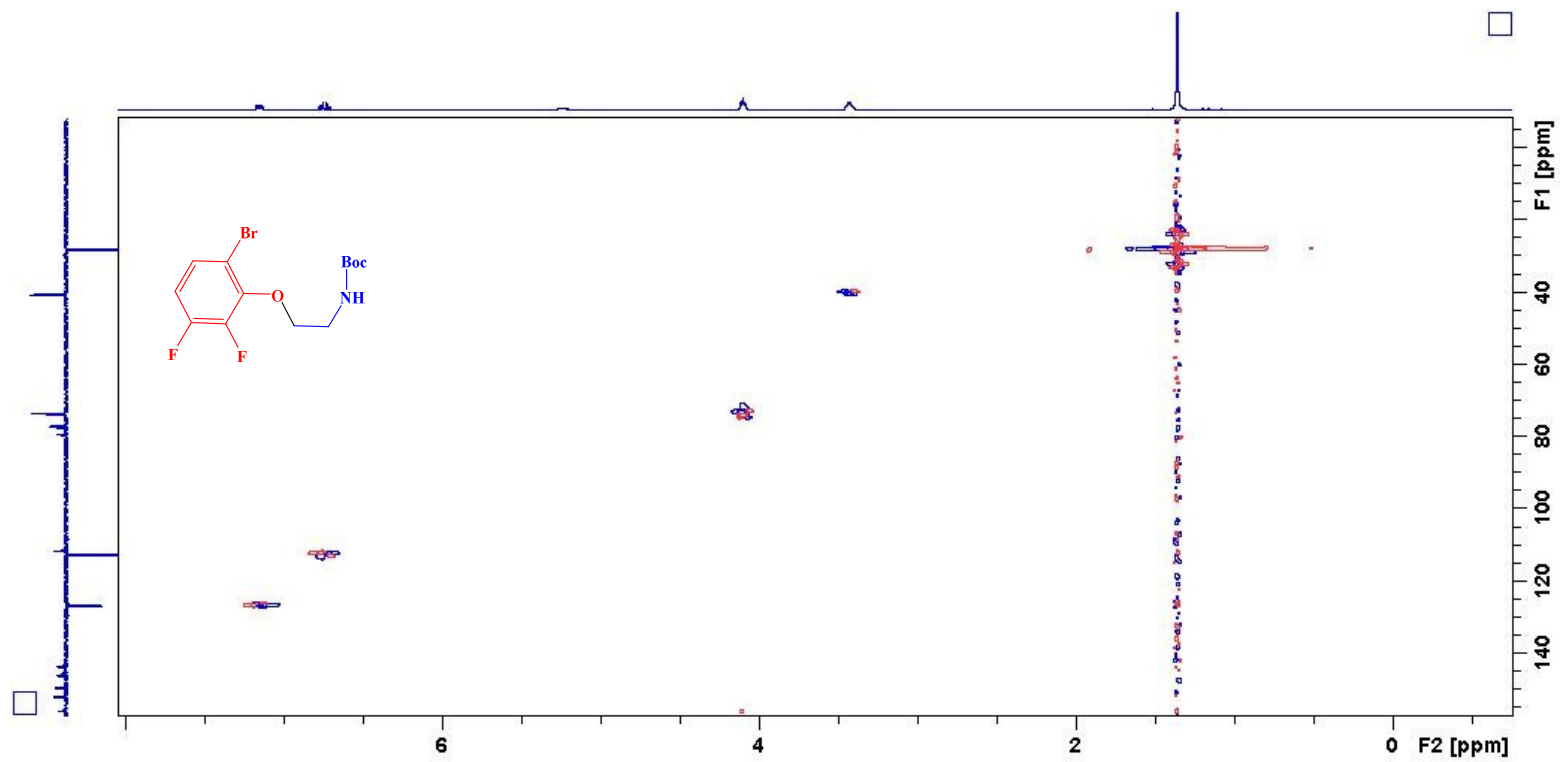
-1.5

100.0

Mass	Calc. Mass	mDa	PPM	DBE	i-FIT	i-FIT (Norm)	Formula
356.0276	356.0274	0.2	0.6	4.5	643.4	0.0	C13 H17 N O3 F Na Br

^1H NMR spectra of **5d**

^{13}C NMR spectra of **5d**

HSQC spectra of **5d**

HRMS of **5d**

Elemental Composition Report

Page 1

Single Mass Analysis

Tolerance = 5.0 PPM / DBE: min = -1.5, max = 100.0

Element prediction: Off

Number of isotope peaks used for i-FIT = 3

Monoisotopic Mass, Even Electron Ions

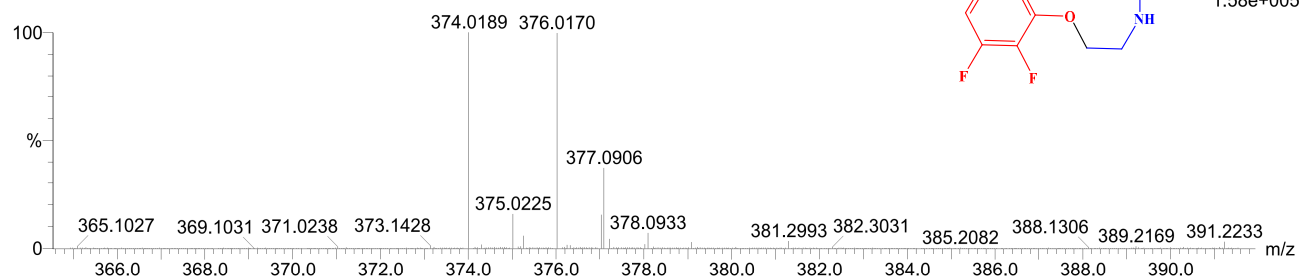
129 formula(e) evaluated with 1 results within limits (up to 20 closest results for each mass)

Elements Used:

C: 10-15 H: 15-20 N: 0-5 O: 0-5 F: 0-2 Na: 1-1 Br: 0-1

SZLV 10 (0.304) Cm (1.61)

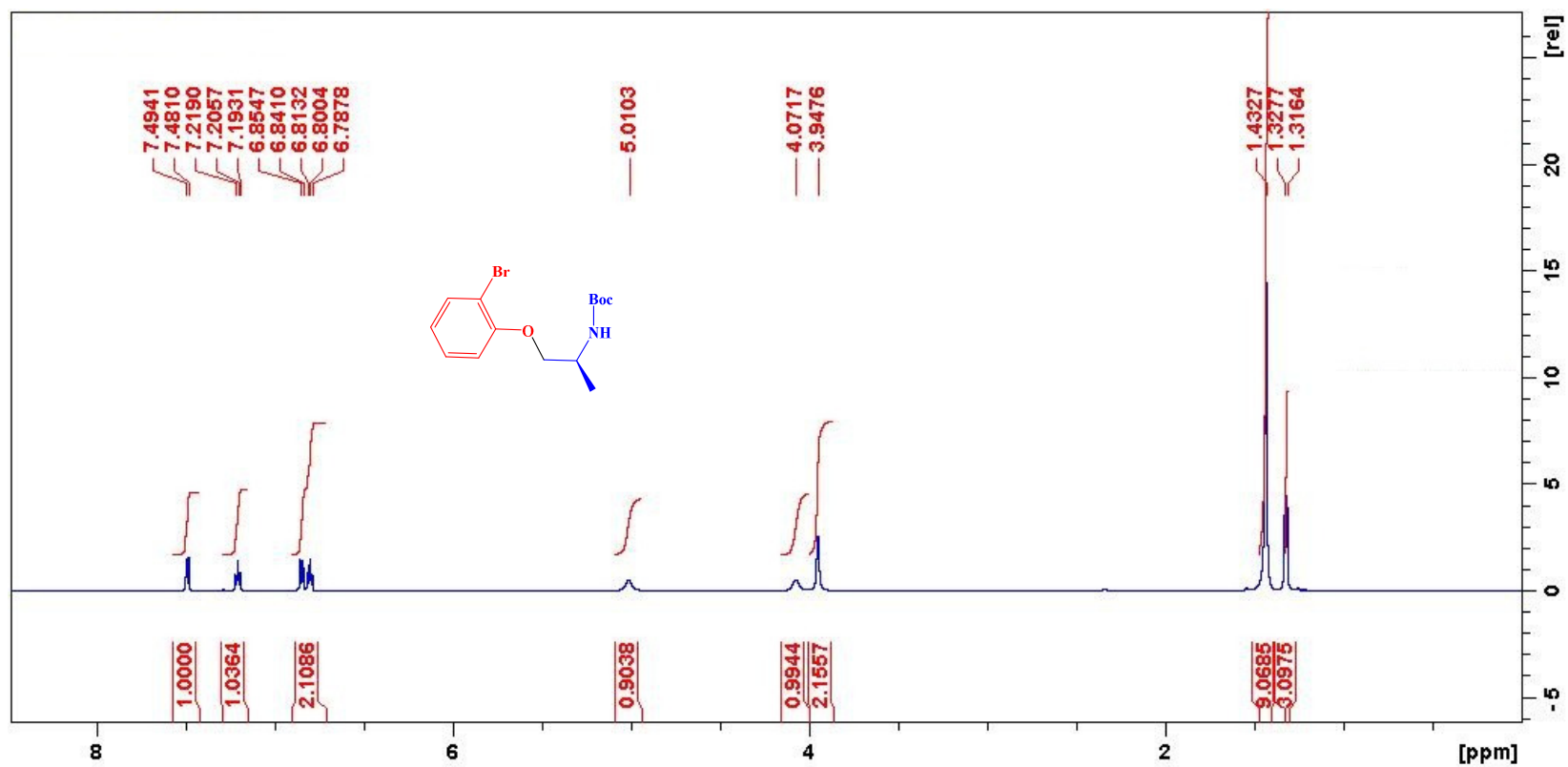
TOF MS ES+

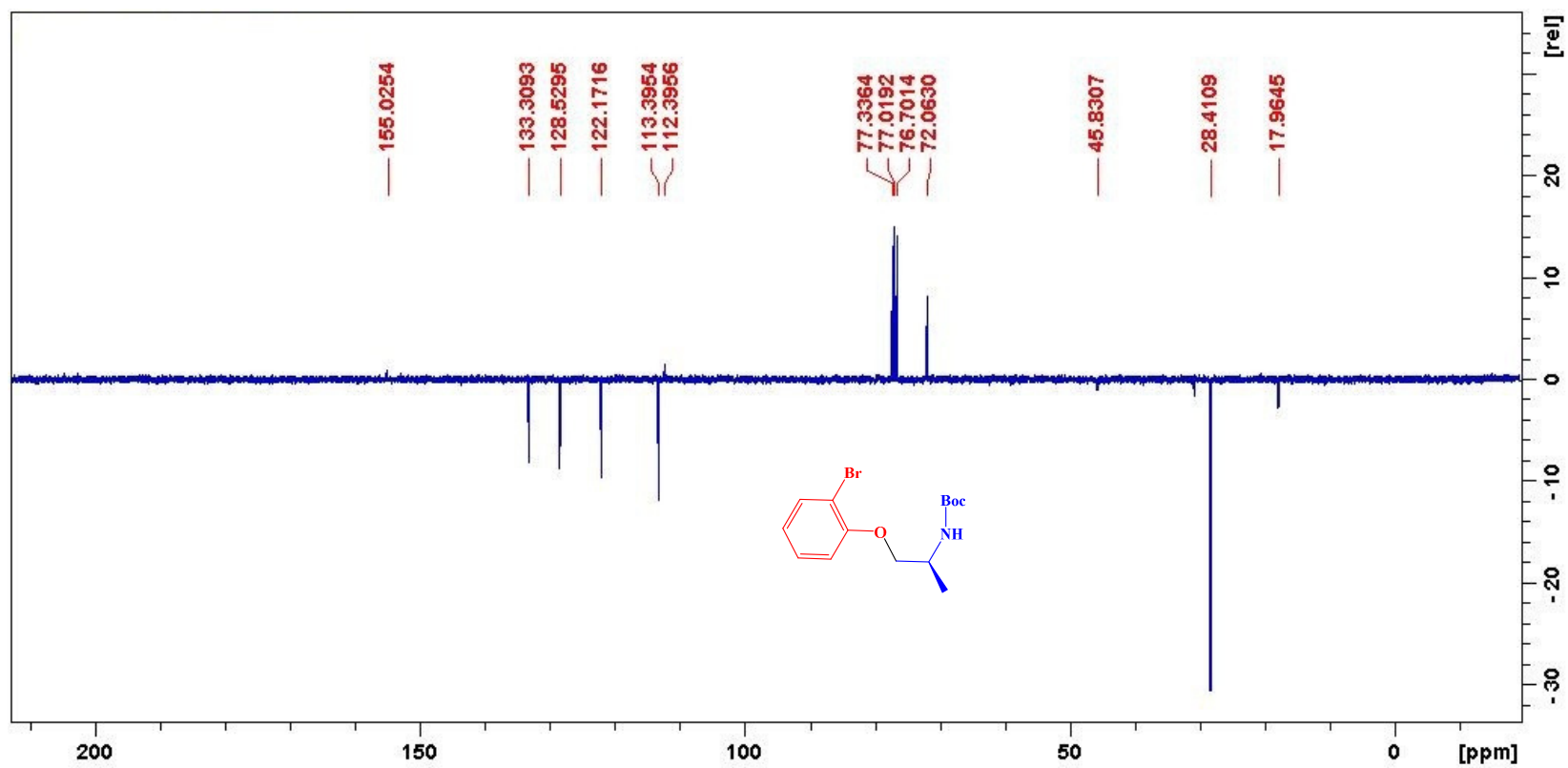


Minimum:

Maximum: 5.0 5.0 -1.5 100.0

Mass	Calc. Mass	mDa	PPM	DBE	i-FIT	i-FIT (Norm)	Formula
374.0189	374.0179	1.0	2.7	4.5	586.2	0.0	C13 H16 N O3 F2 Na Br

^1H NMR spectra of **5e**

^{13}C NMR spectra of **5e**

HRMS of 5e

Elemental Composition Report

Page 1

Single Mass Analysis

Tolerance = 5.0 PPM / DBE: min = -1.5, max = 100.0

Element prediction: Off

Number of isotope peaks used for i-FIT = 3

Monoisotopic Mass, Even Electron Ions

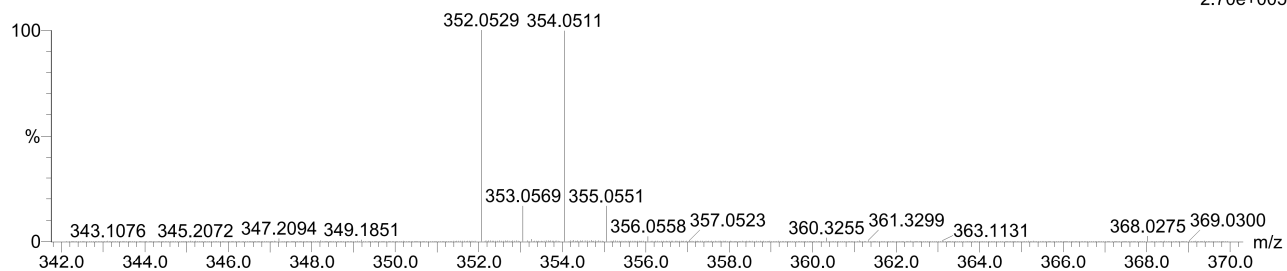
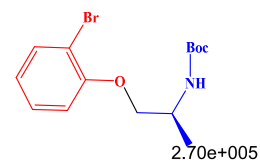
87 formula(e) evaluated with 1 results within limits (up to 20 closest results for each mass)

Elements Used:

C: 10-15 H: 20-25 N: 0-5 O: 0-5 Br: 0-1 Na: 0-1

SZBrMe 2 (0.034) Cm (1:61)

TOF MS ES+



Minimum:

Maximum:

5.0

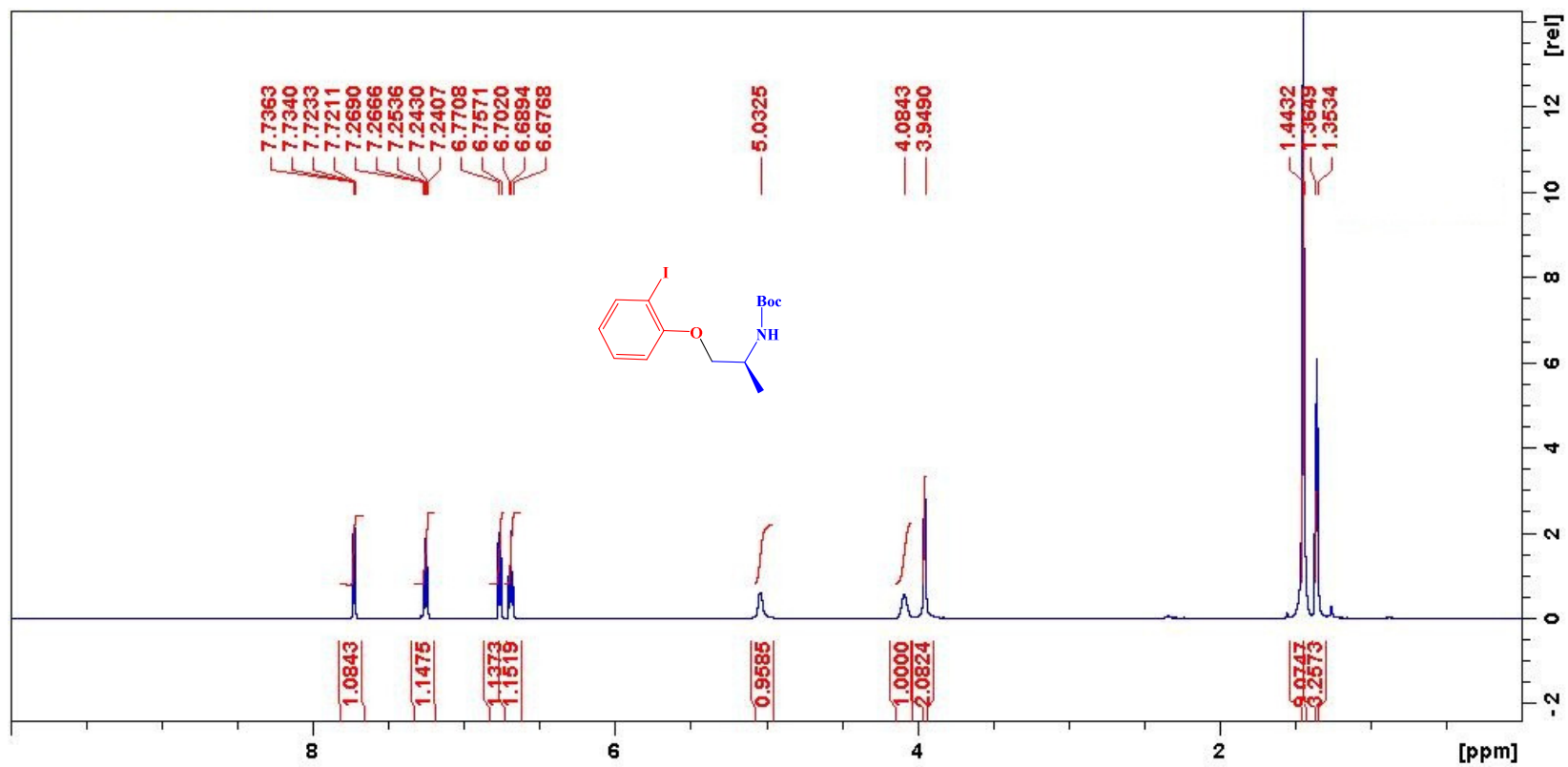
5.0

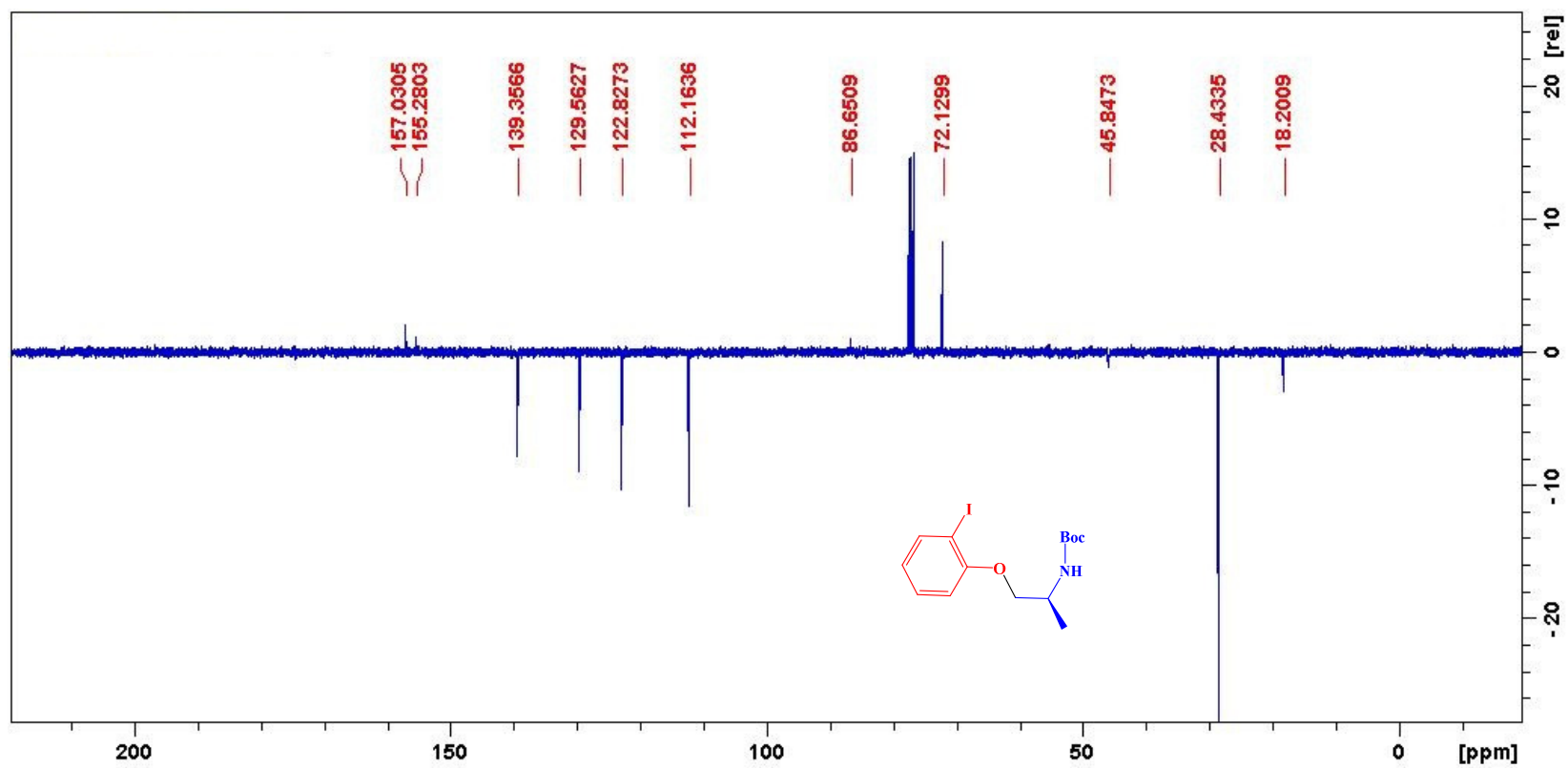
-1.5

100.0

Mass	Calc. Mass	mDa	PPM	DBE	i-FIT	i-FIT (Norm)	Formula
------	------------	-----	-----	-----	-------	--------------	---------

352.0529	352.0524	0.5	1.4	4.5	639.4	0.0	C14 H20 N O3 Br Na
----------	----------	-----	-----	-----	-------	-----	--------------------

¹H NMR spectra of **5f**

^{13}C NMR spectra of **5f**

HRMS of **5f**

Elemental Composition Report

Page 1

Single Mass Analysis

Tolerance = 5.0 PPM / DBE: min = -1.5, max = 100.0

Element prediction: Off

Number of isotope peaks used for i-FIT = 3

Monoisotopic Mass, Even Electron Ions

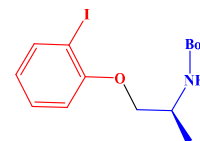
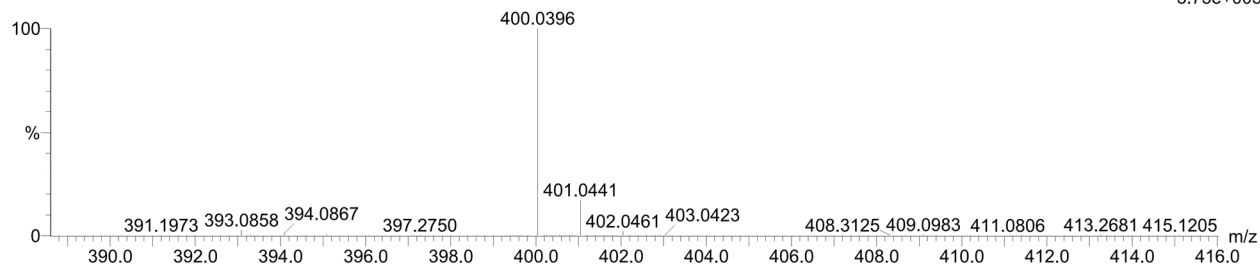
48 formula(e) evaluated with 1 results within limits (up to 20 closest results for each mass)

Elements Used:

C: 10-15 H: 15-20 N: 0-5 O: 0-5 I: 0-1 Na: 1-1

SZIMe 57 (1.890) Cm (1:61)

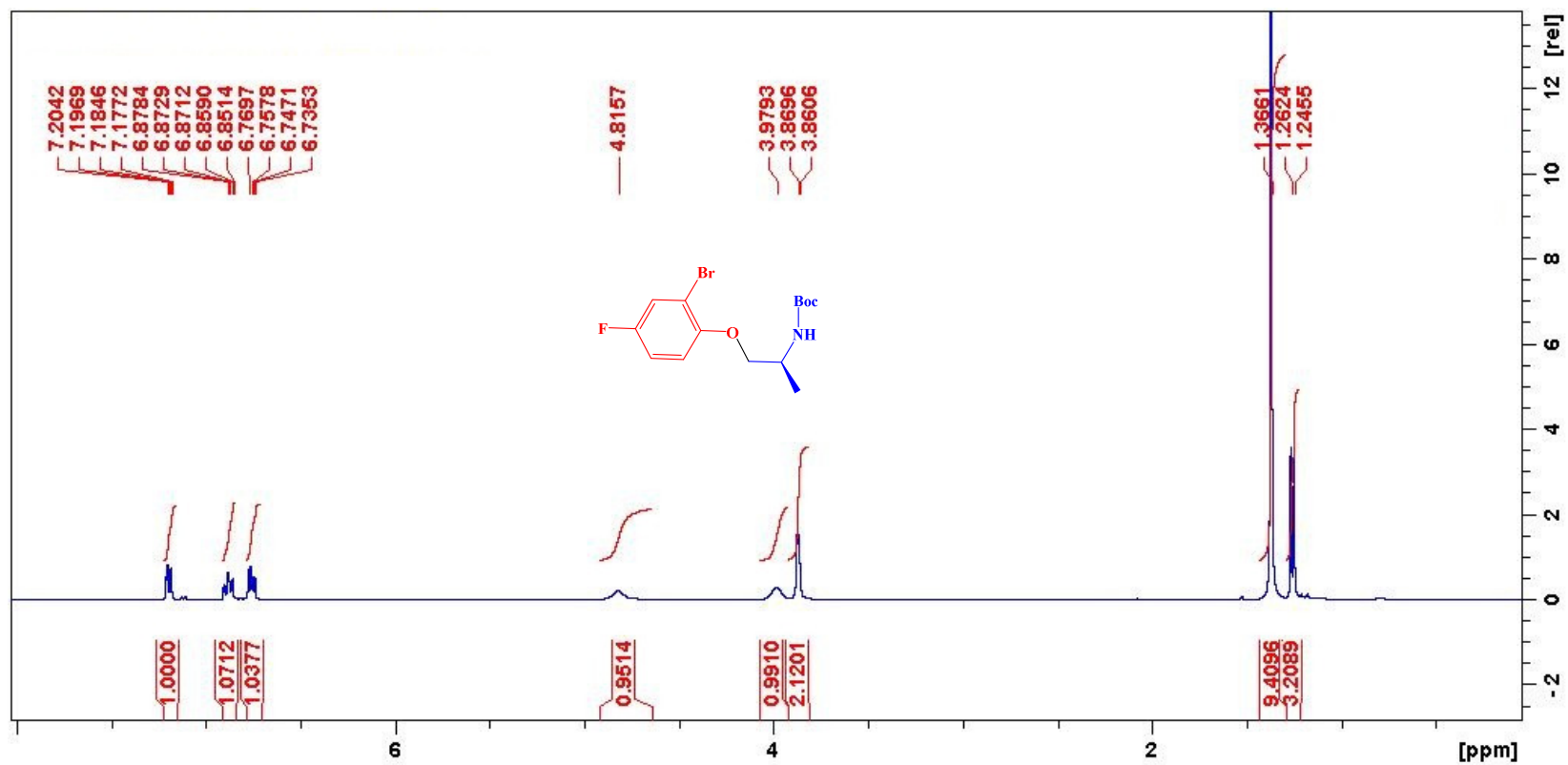
TOF MS ES+

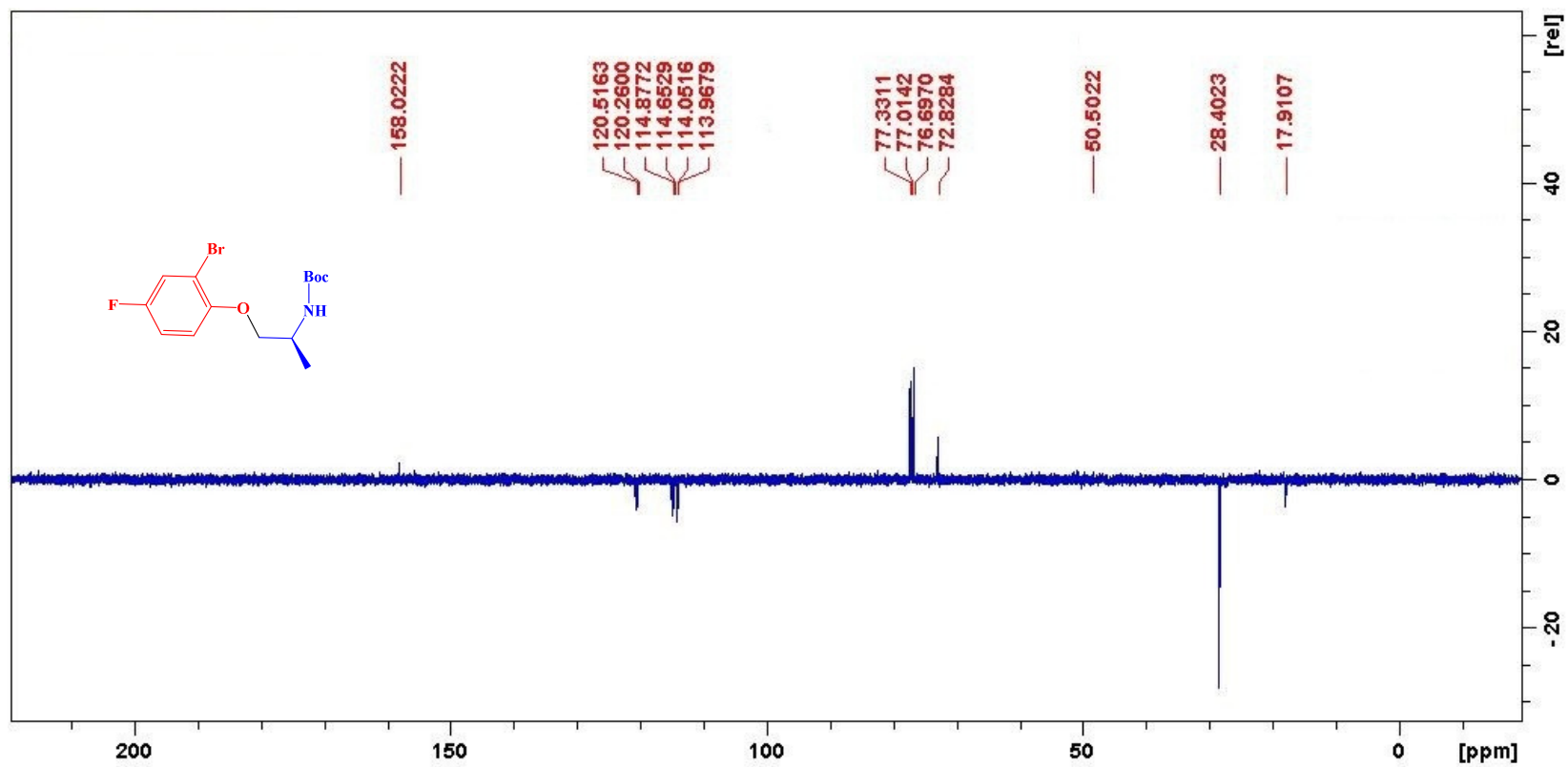


Minimum:

Maximum: 5.0 5.0 -1.5 100.0

Mass	Calc. Mass	mDa	PPM	DBE	i-FIT	i-FIT (Norm)	Formula
400.0396	400.0386	1.0	2.5	4.5	642.4	0.0	C14 H20 N O3 I Na

^1H NMR spectra of **5g**

^{13}C NMR spectra of **5g**

HRMS of 5g

Elemental Composition Report

Page 1

Single Mass Analysis

Tolerance = 5.0 PPM / DBE: min = -1.5, max = 100.0

Element prediction: Off

Number of isotope peaks used for i-FIT = 3

Monoisotopic Mass, Even Electron Ions

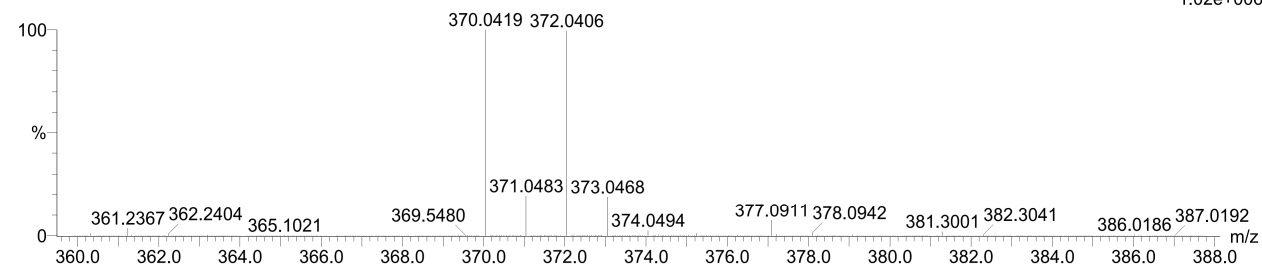
87 formula(e) evaluated with 1 results within limits (up to 20 closest results for each mass)

Elements Used:

C: 10-15 H: 15-20 N: 0-5 O: 0-5 F: 0-1 Na: 1-1 Br: 0-1

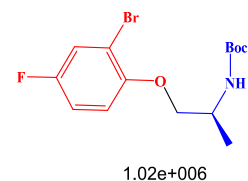
SZ1FMe 8 (0.236) Cm (1:61)

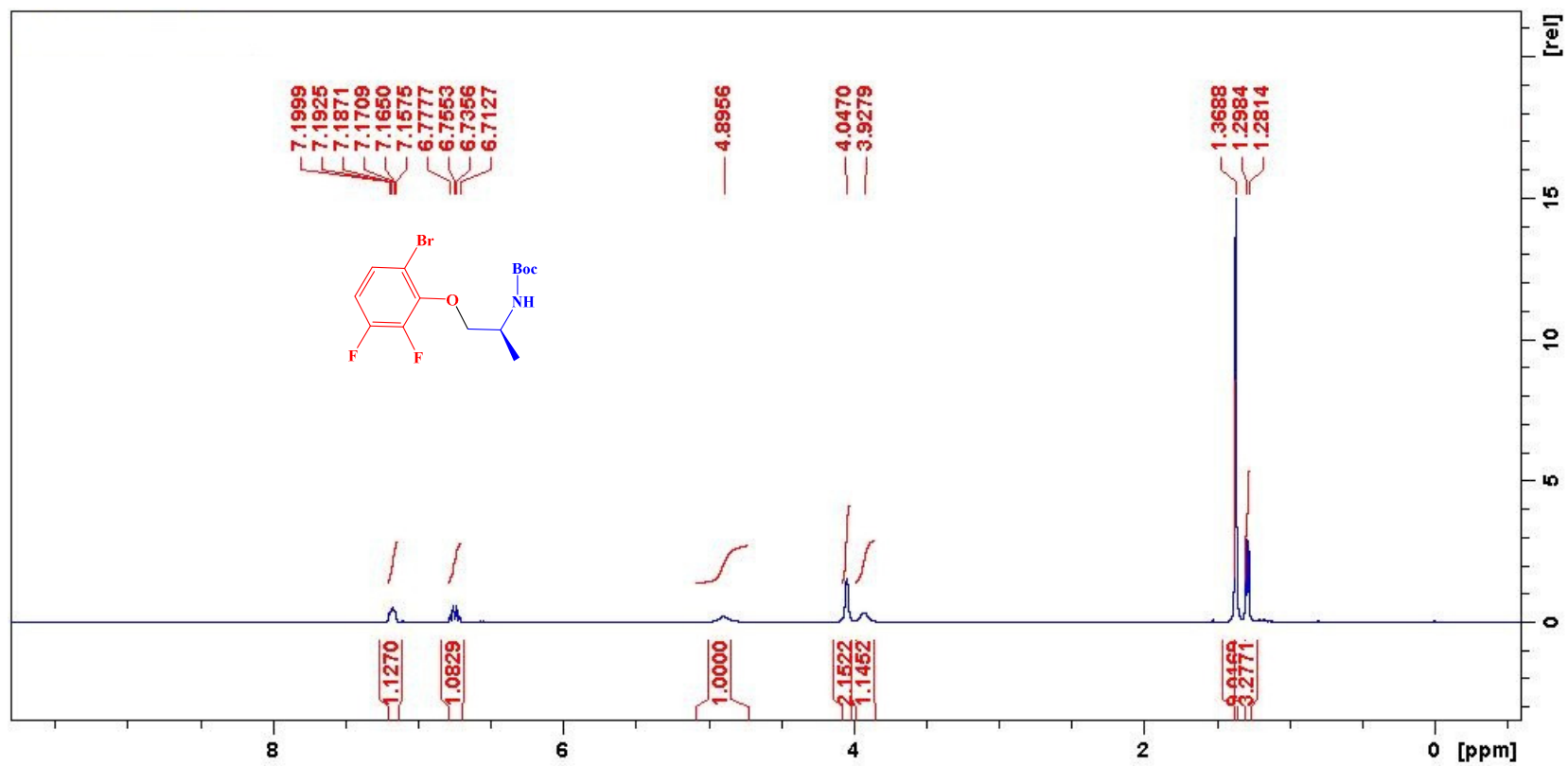
TOF MS ES+

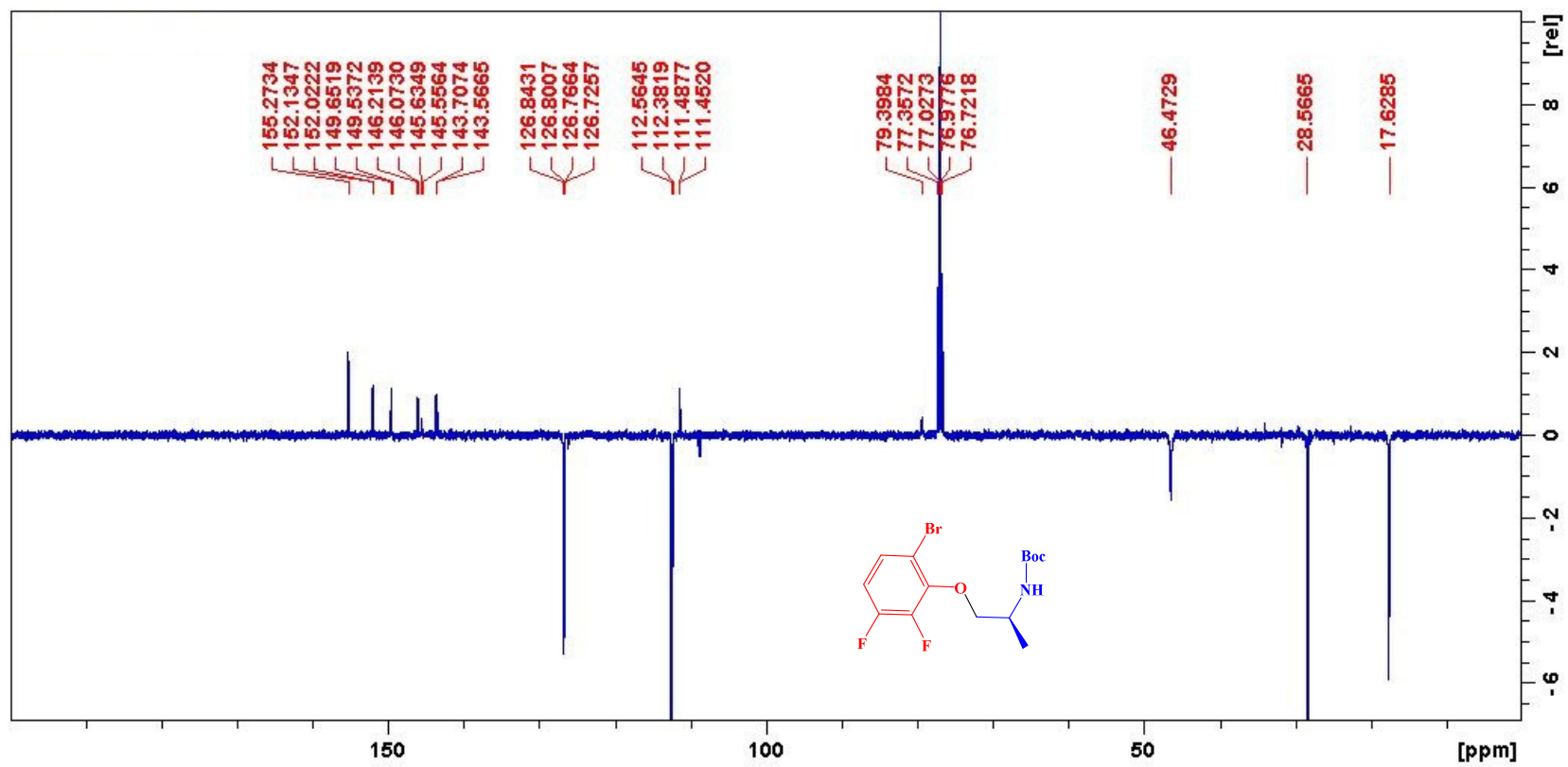


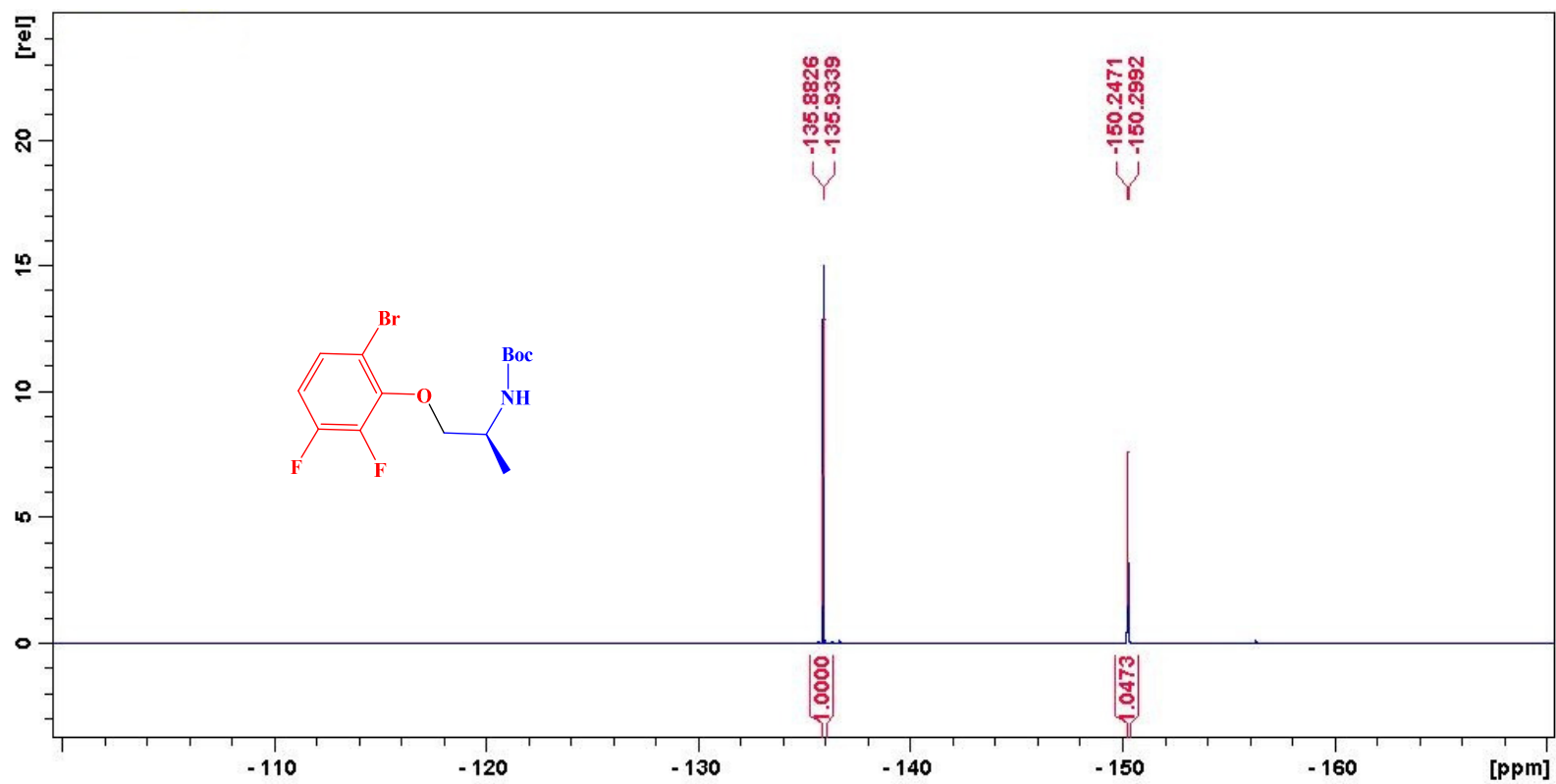
Minimum: -1.5
 Maximum: 5.0 5.0 100.0

Mass	Calc. Mass	mDa	PPM	DBE	i-FIT	i-FIT (Norm)	Formula
370.0419	370.0430	-1.1	-3.0	4.5	680.6	0.0	C14 H19 N O3 F Na Br



¹H NMR spectra of **5h**

^{13}C NMR spectra of **5h**

^{19}F NMR spectra of **5h**

HRMS of 5h

Elemental Composition Report

Page 1

Single Mass Analysis

Tolerance = 5.0 PPM / DBE: min = -1.5, max = 100.0

Element prediction: Off

Number of isotope peaks used for i-FIT = 3

Monoisotopic Mass, Even Electron Ions

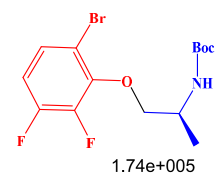
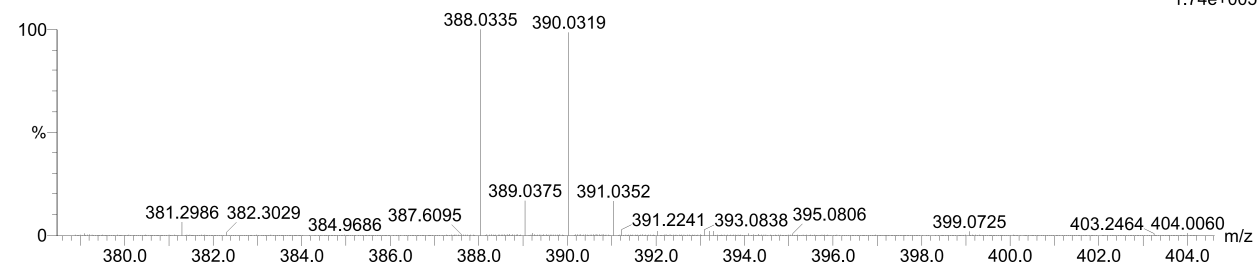
138 formula(e) evaluated with 1 results within limits (up to 20 closest results for each mass)

Elements Used:

C: 10-15 H: 15-20 N: 0-5 O: 0-5 F: 0-2 Na: 1-1 Br: 0-1

SZLVMe 1 (0.034) Cm (1:60)

TOF MS ES+



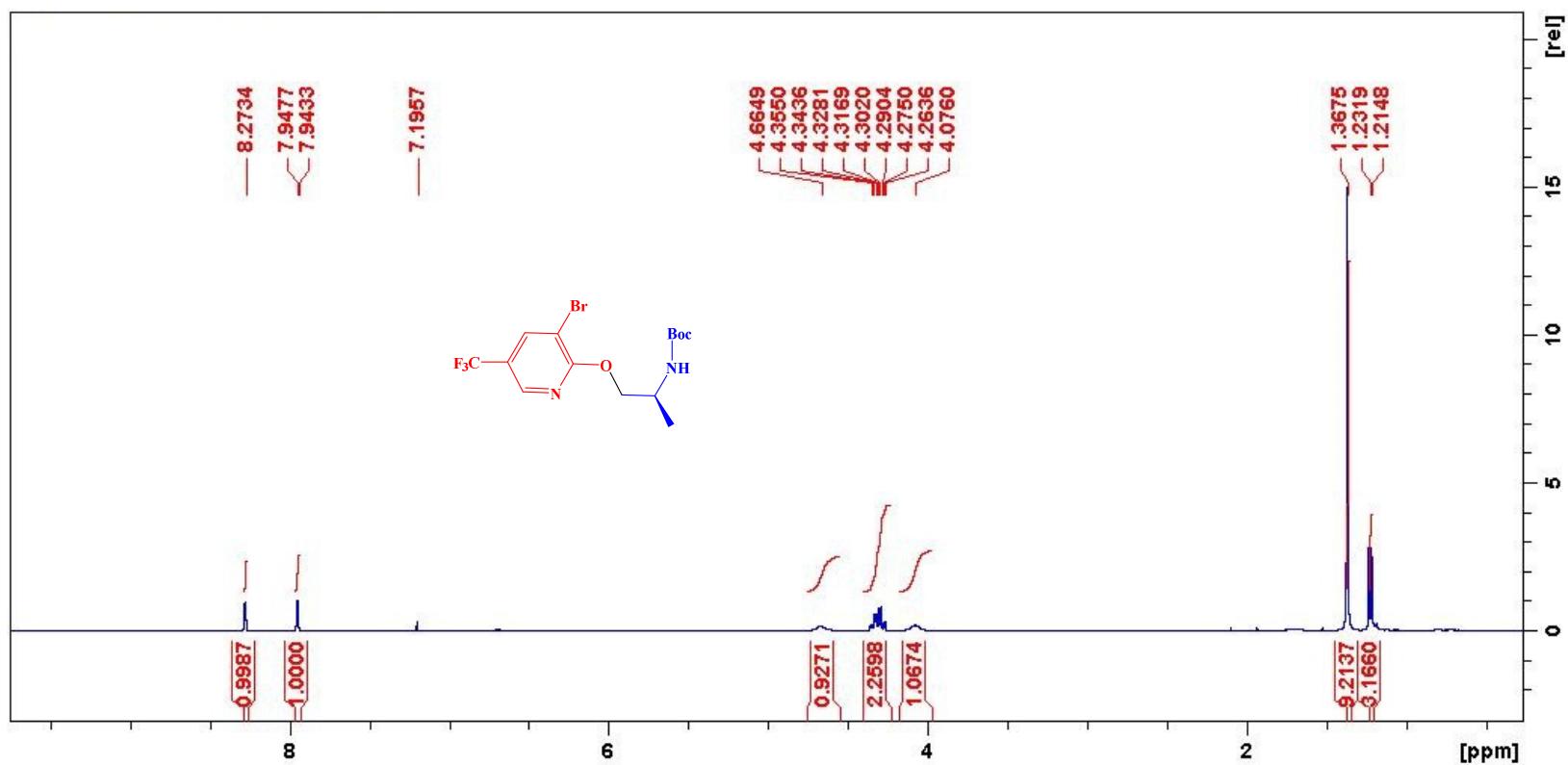
Minimum:

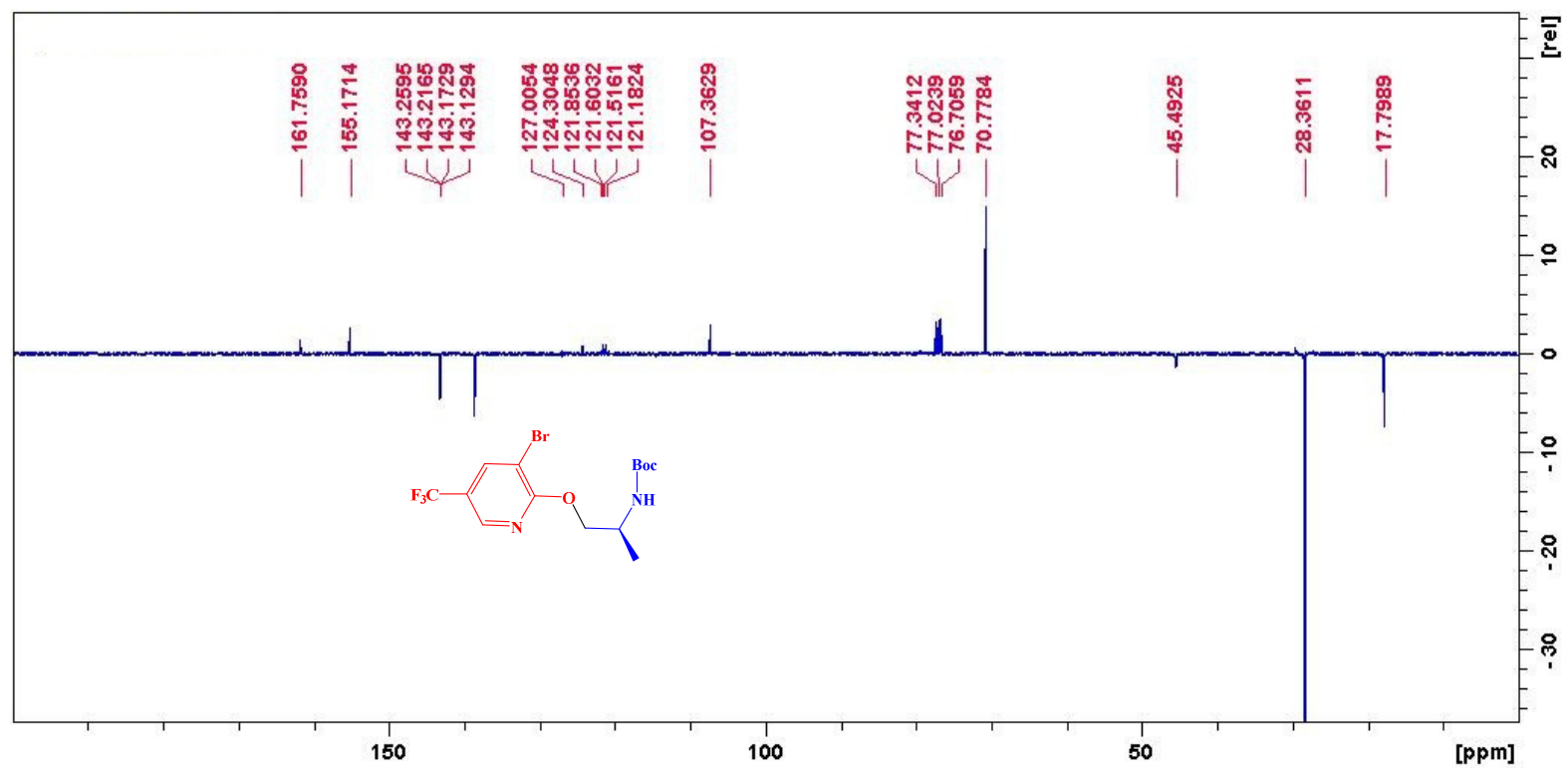
Maximum:

5.0 5.0 -1.5 100.0

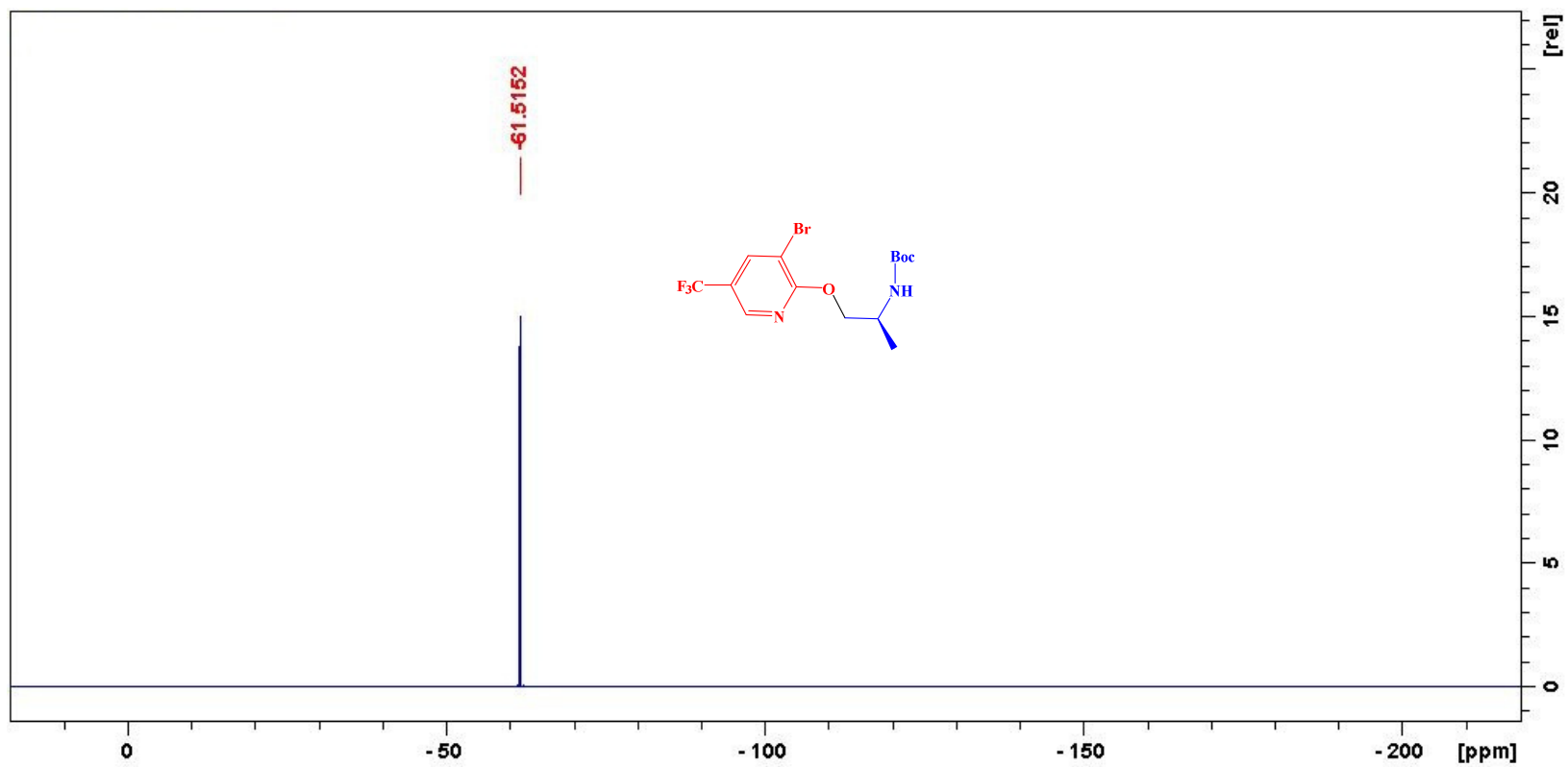
Mass	Calc. Mass	mDa	PPM	DBE	i-FIT	i-FIT (Norm)	Formula
------	------------	-----	-----	-----	-------	--------------	---------

388.0335	388.0336	-0.1	-0.3	4.5	603.8	0.0	C14 H18 N O3 F2 Na Br
----------	----------	------	------	-----	-------	-----	-----------------------

¹H NMR spectra of **5i**

^{13}C NMR spectra of **5i**

^{19}F NMR spectra of **5i**



HRMS of 5i

Elemental Composition Report

Page 1

Single Mass Analysis

Tolerance = 5.0 PPM / DBE: min = -1.5, max = 100.0

Element prediction: Off

Number of isotope peaks used for i-FIT = 3

Monoisotopic Mass, Even Electron Ions

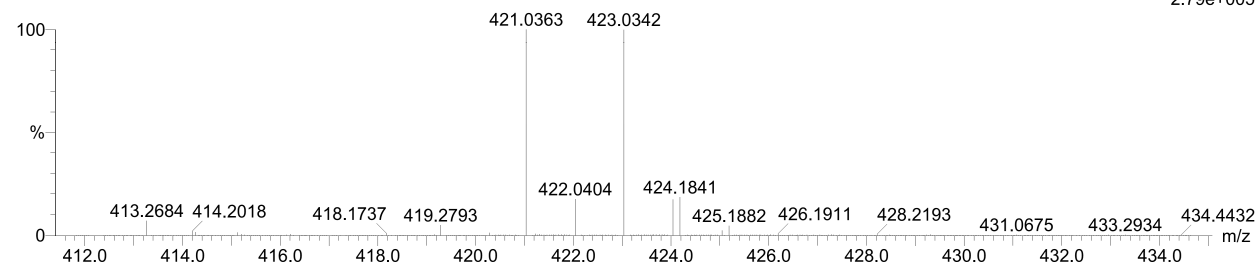
212 formula(e) evaluated with 1 results within limits (up to 20 closest results for each mass)

Elements Used:

C: 10-15 H: 15-20 N: 0-5 O: 0-5 F: 0-3 Br: 0-1 Na: 1-1

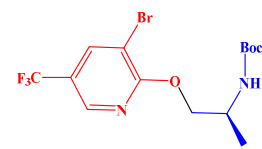
SZCF3NMe 52 (1.720) Cm (1.61)

TOF MS ES+

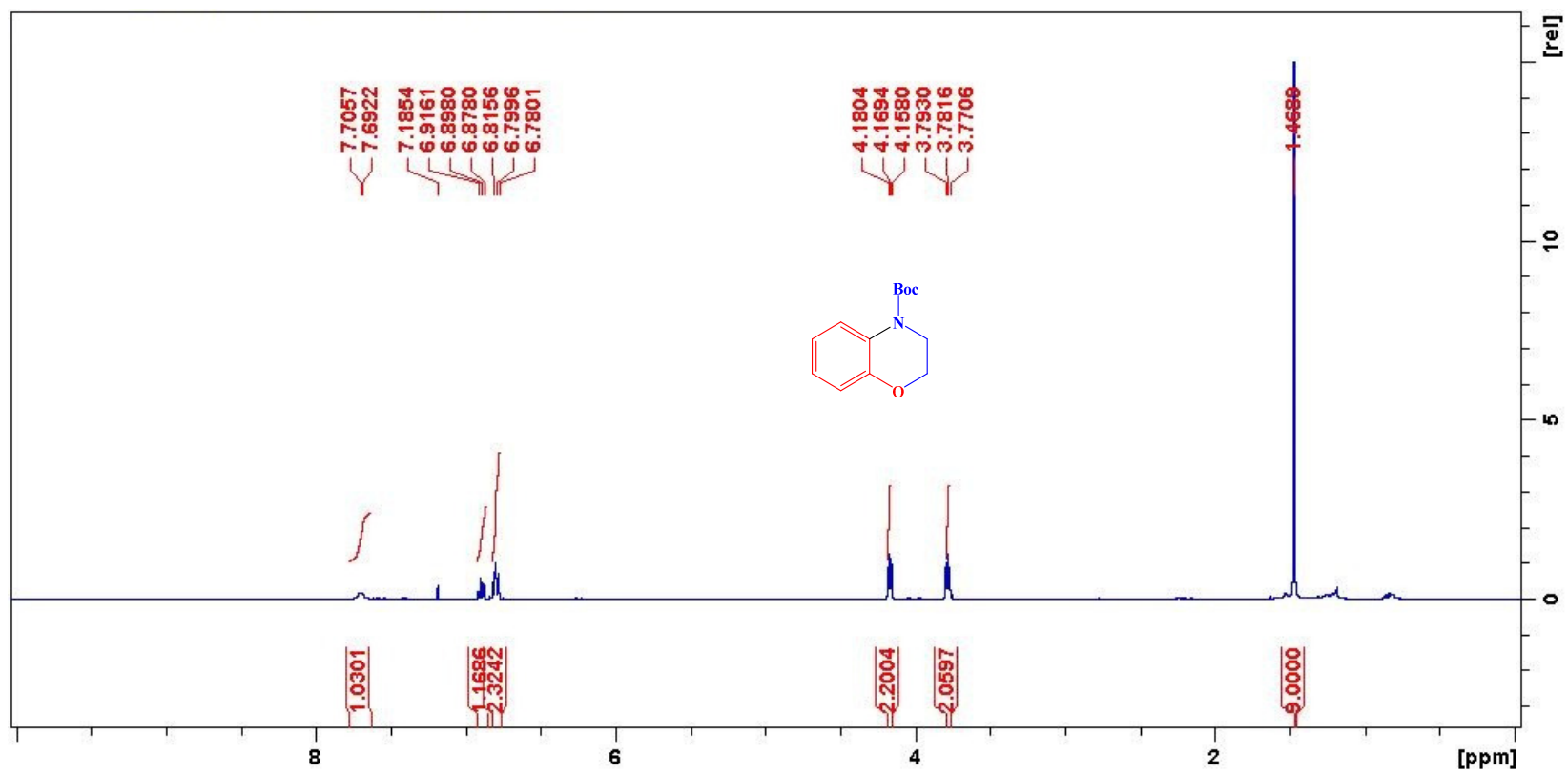


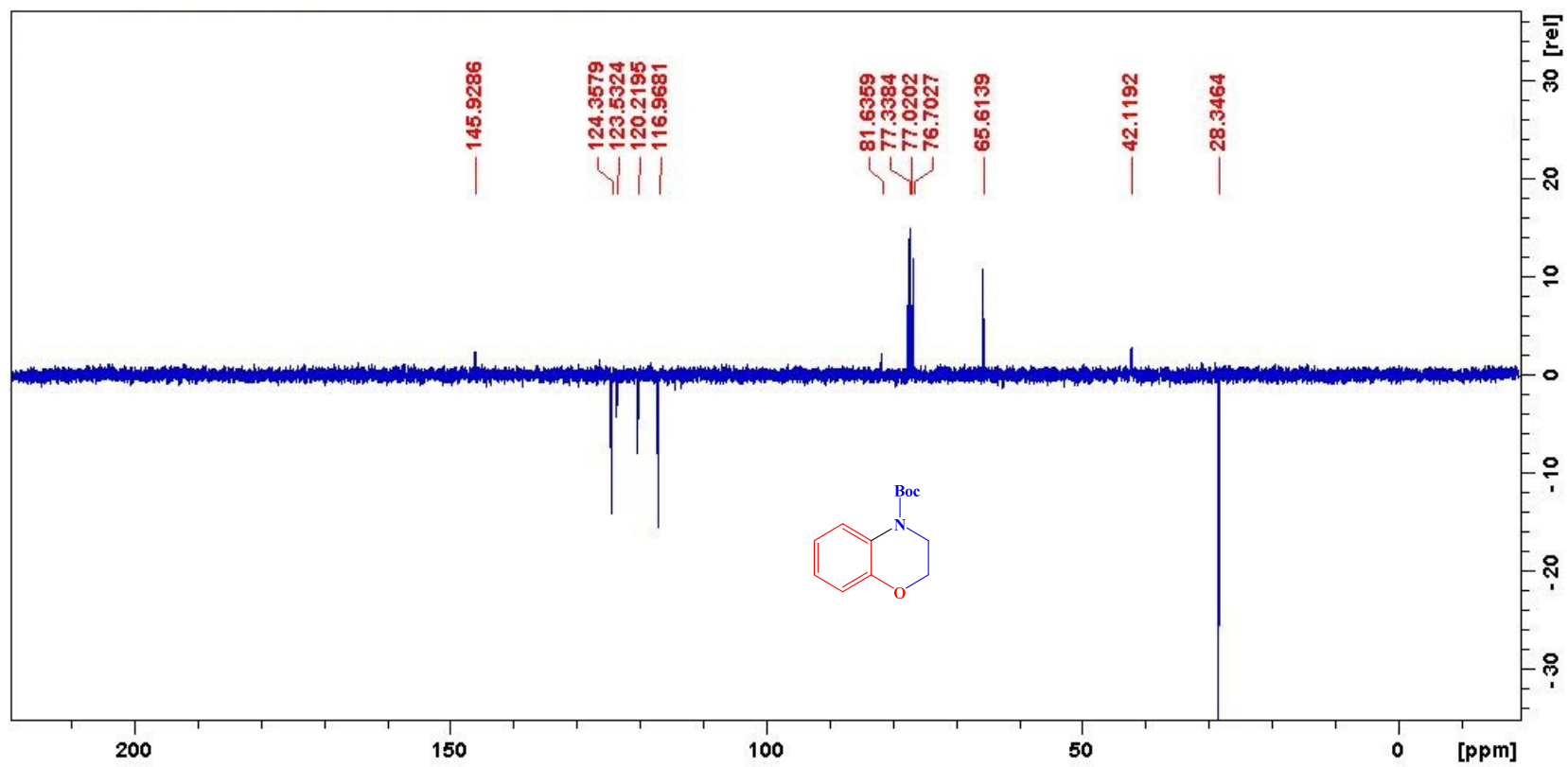
Minimum: -1.5
 Maximum: 5.0 5.0 100.0

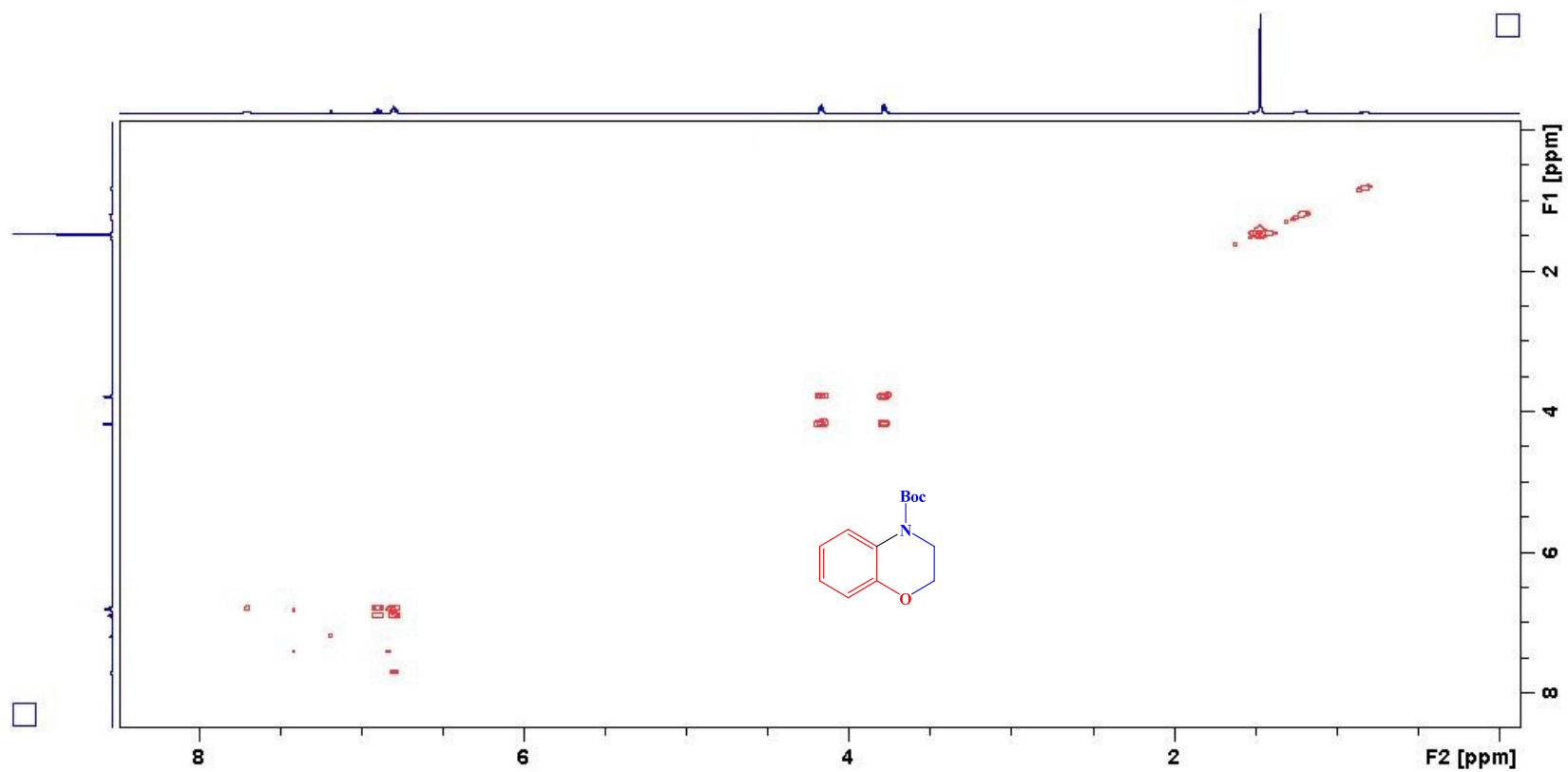
Mass	Calc. Mass	mDa	PPM	DBE	i-FIT	i-FIT (Norm)	Formula
421.0363	421.0351	1.2	2.9	4.5	602.5	0.0	C14 H18 N2 O3 F3 Br Na

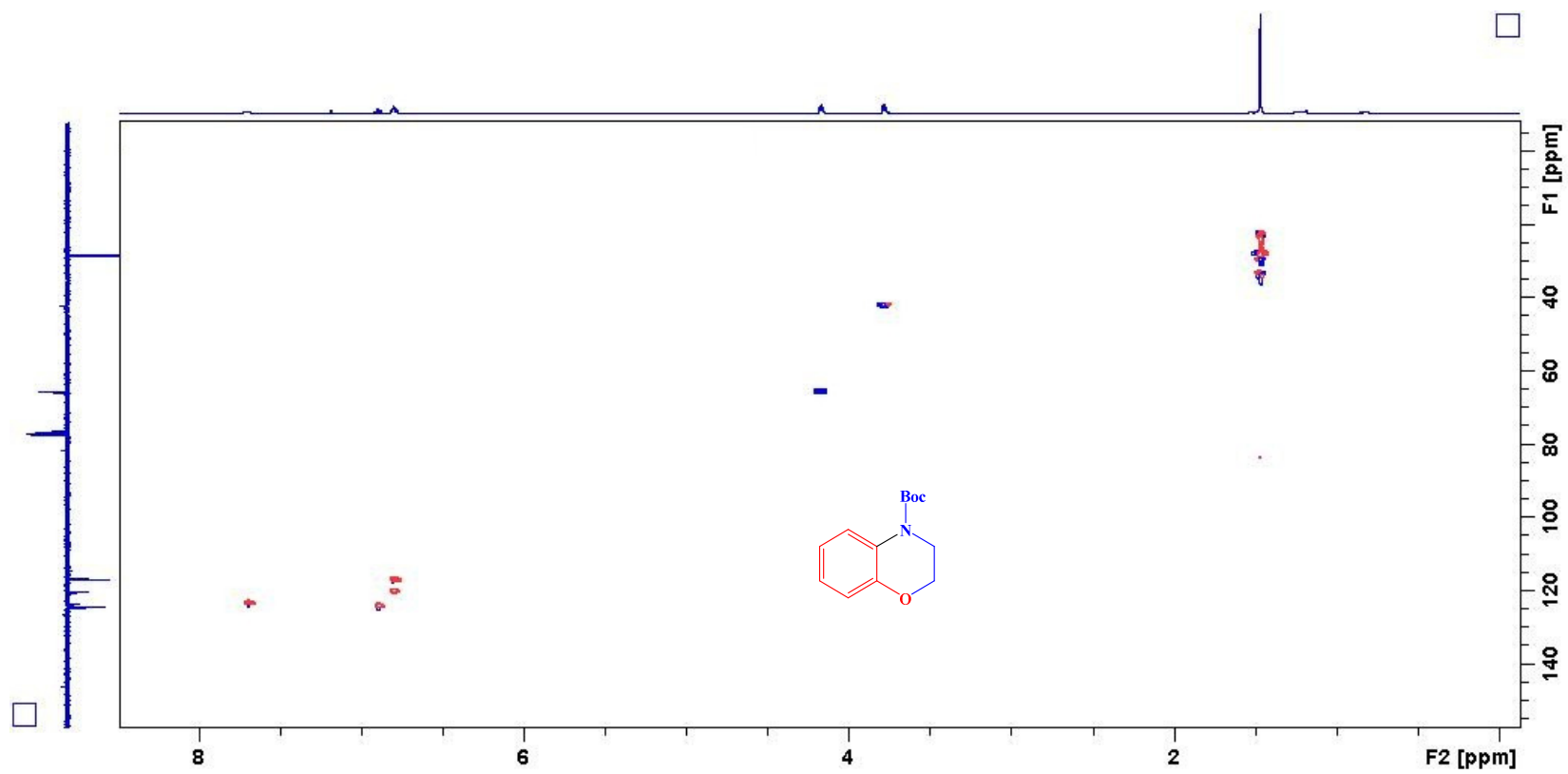


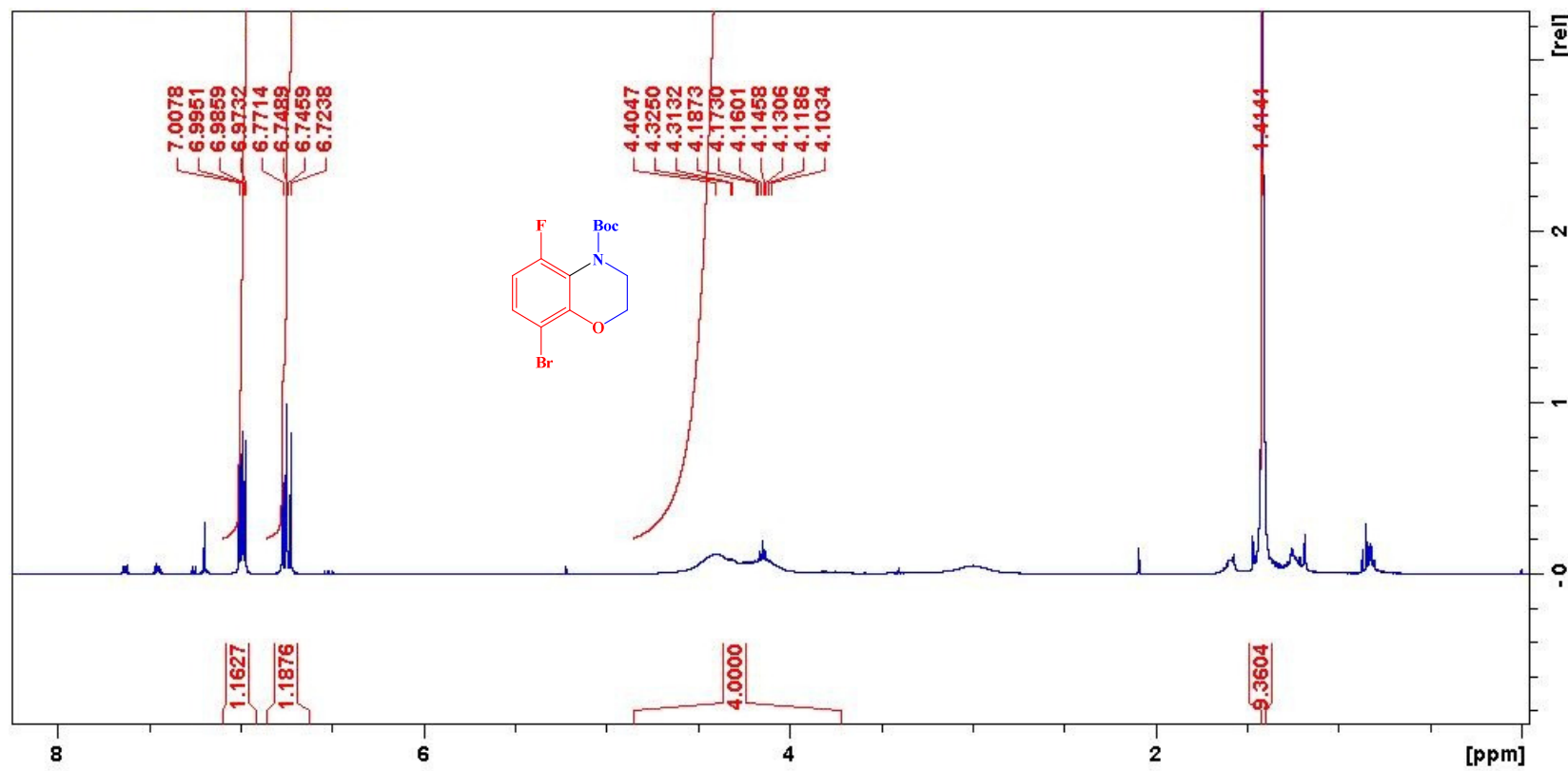
2.79e+005

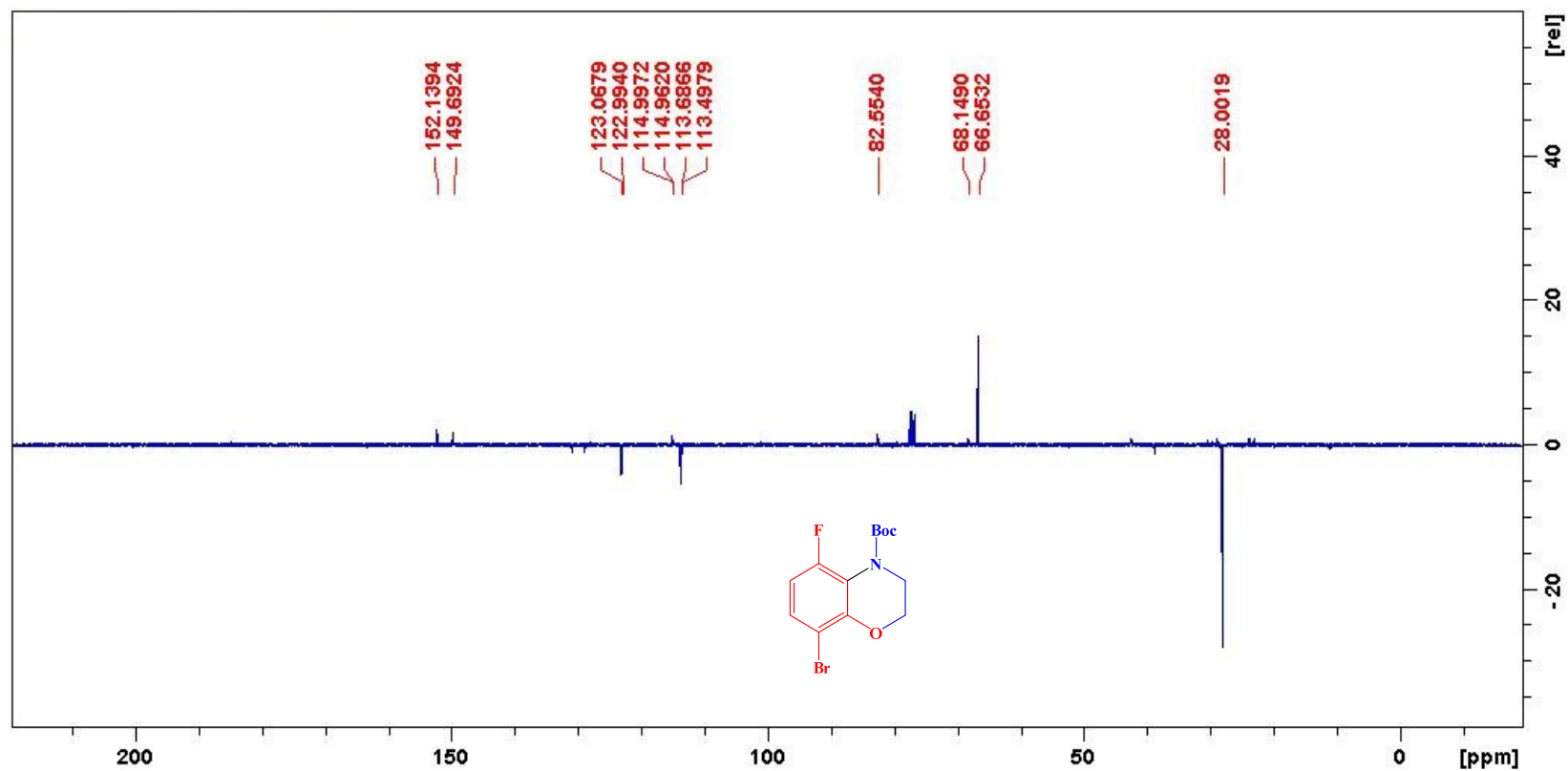
¹H NMR spectra of **6a**

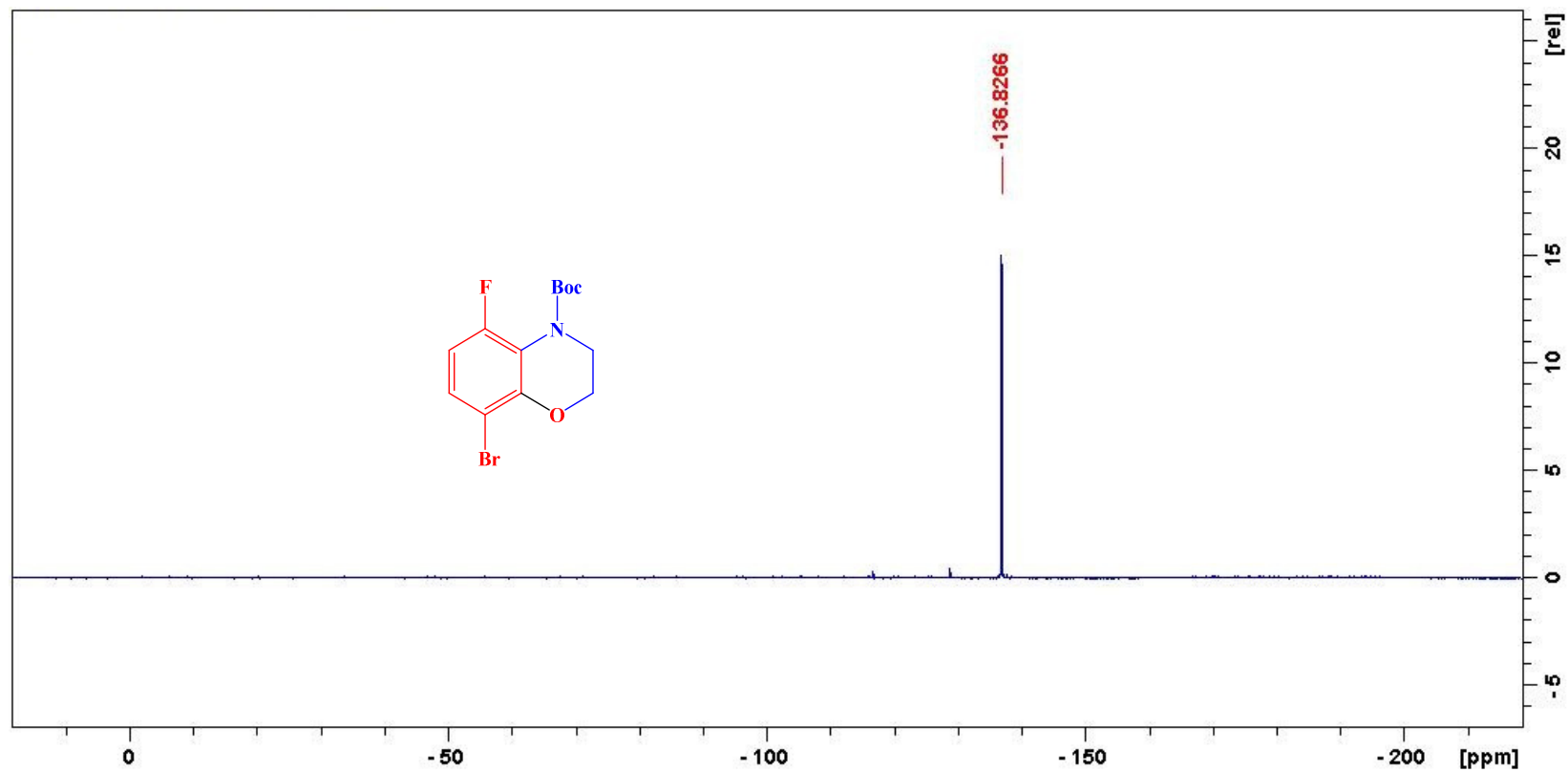
^{13}C NMR spectra of **6a**

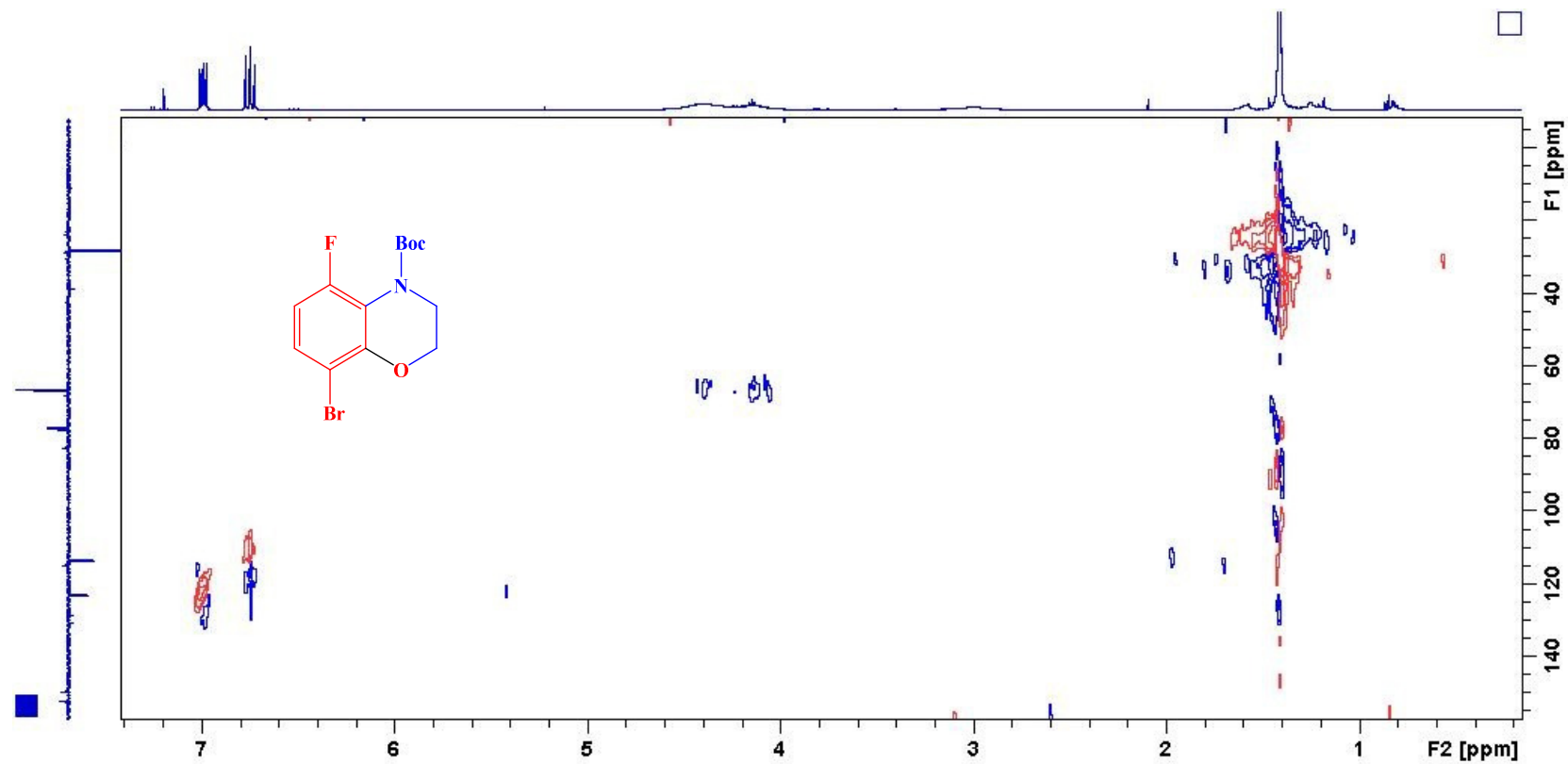
COSY spectra of **6a**

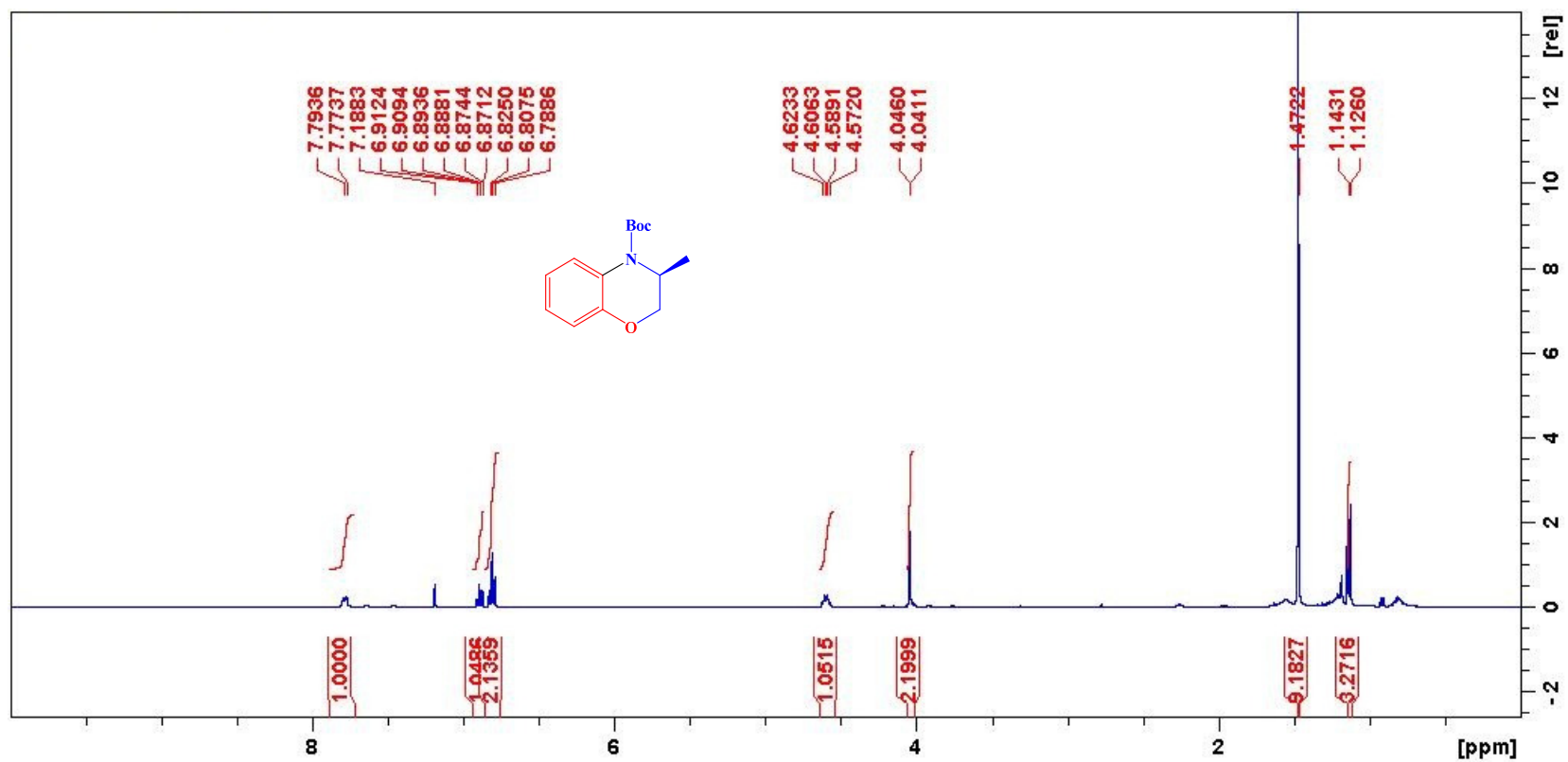
HSQC spectra of **6a**

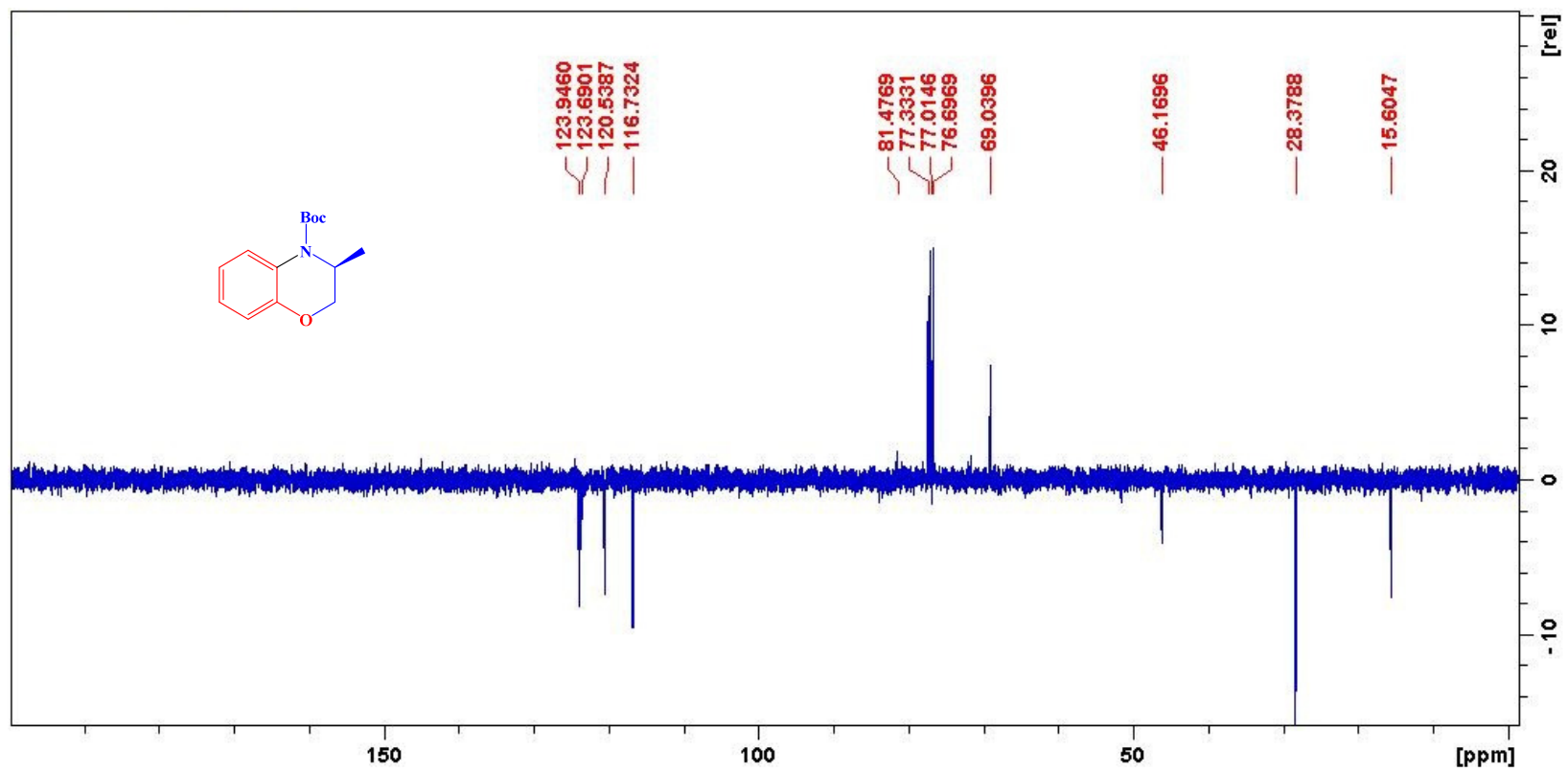
^1H NMR spectra of **6c**

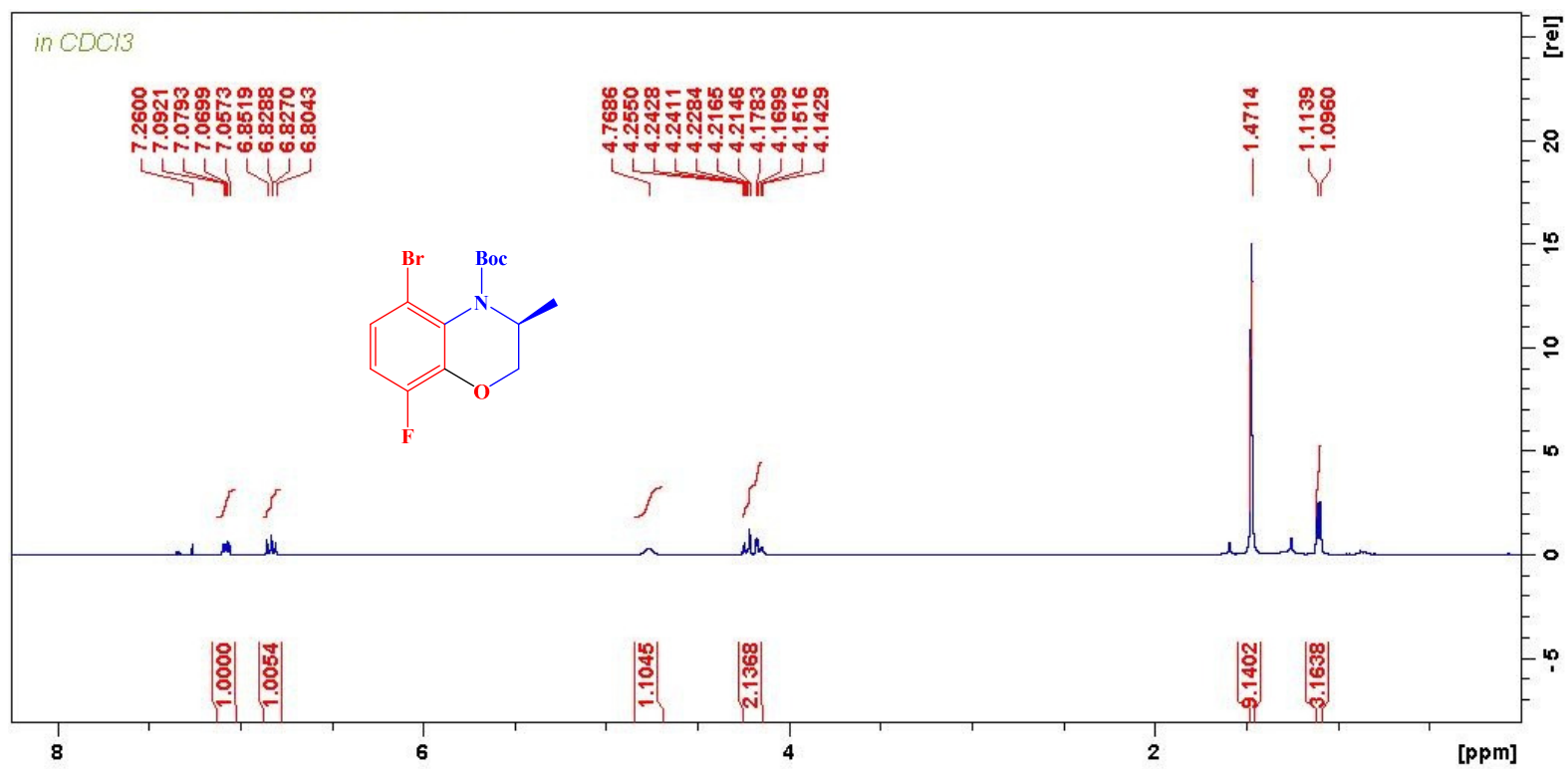
^{13}C NMR spectra of **6c**

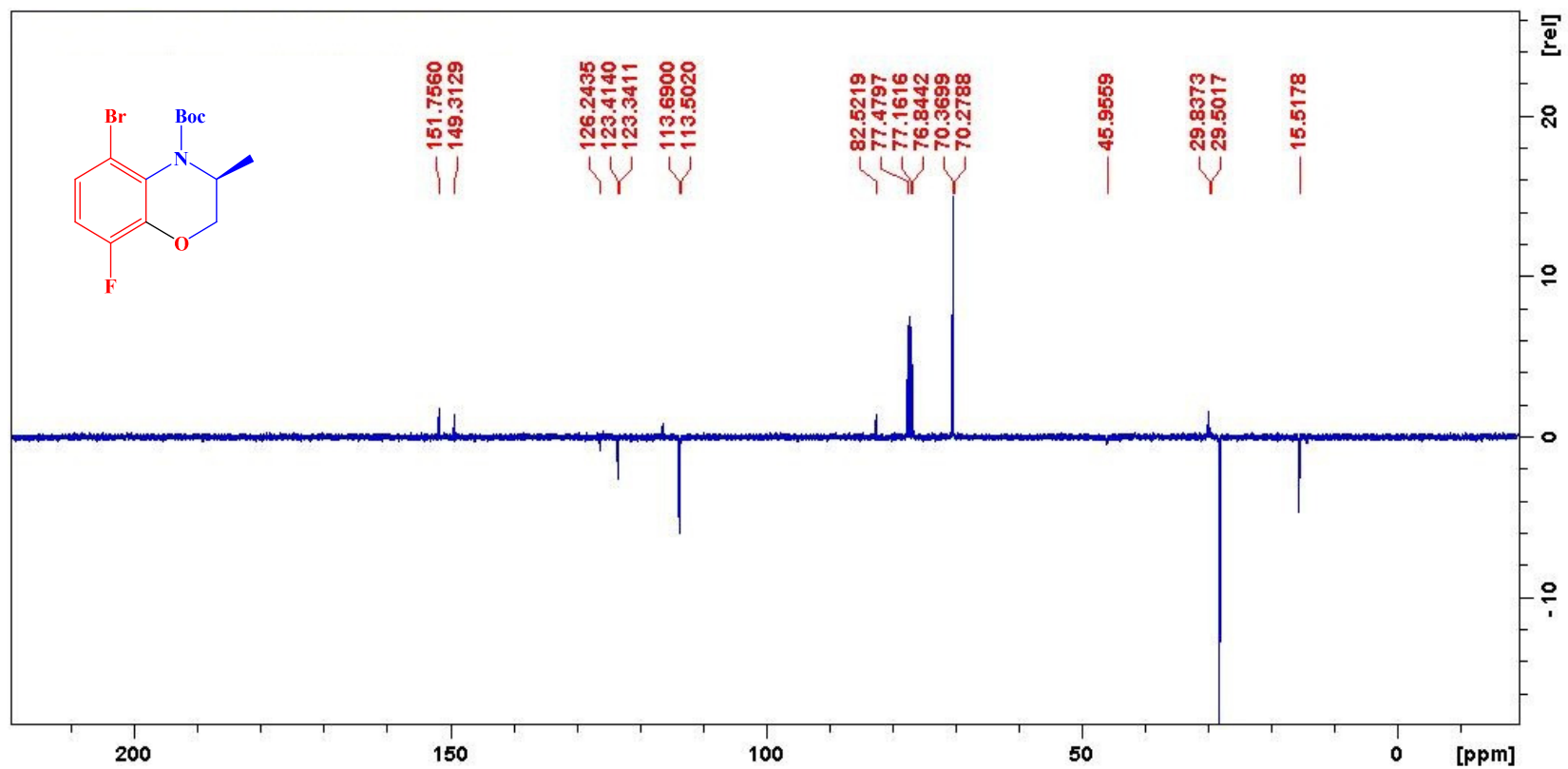
^{19}F NMR spectra of **6c**

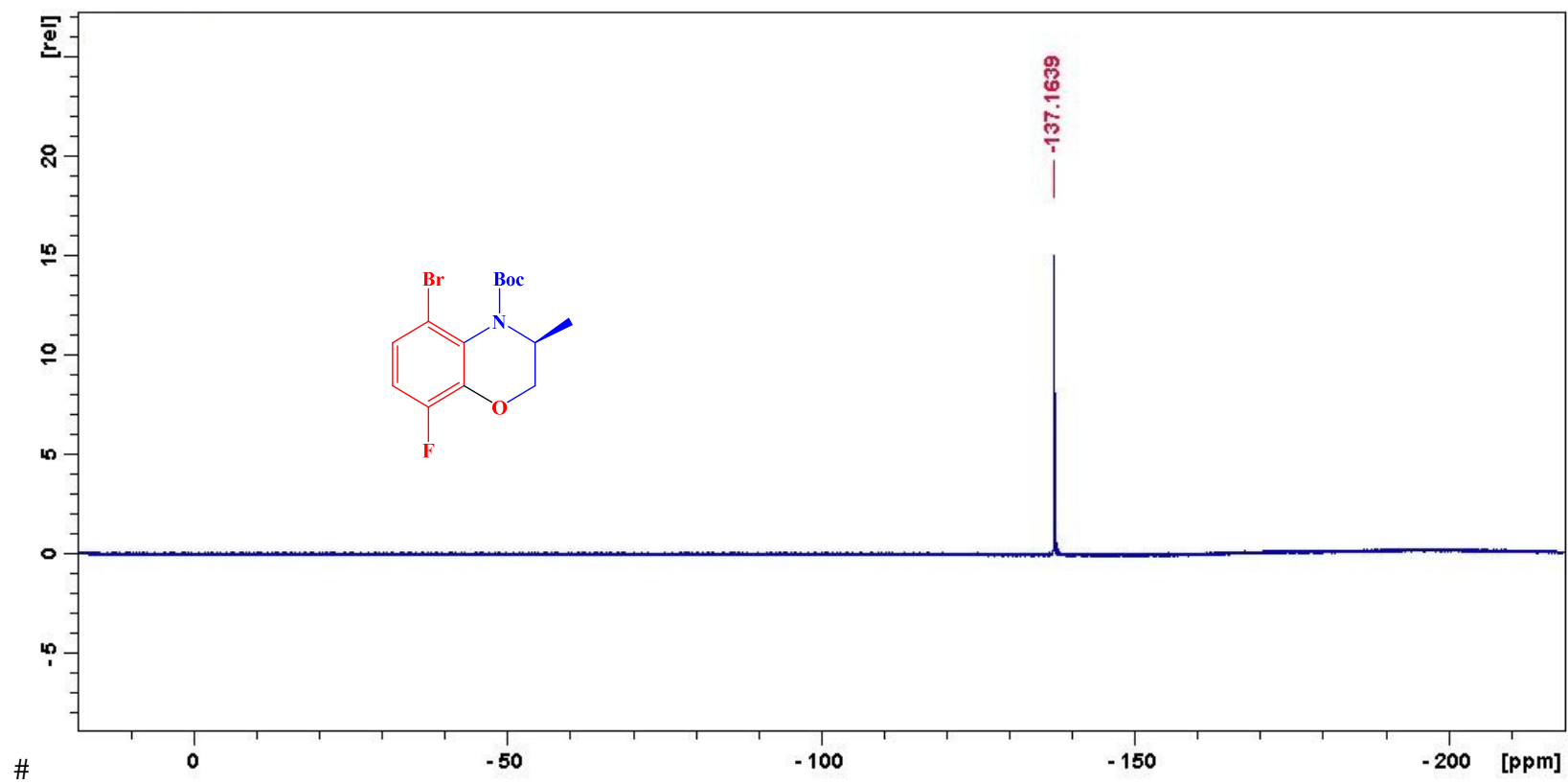
HSQC spectra of **6c**

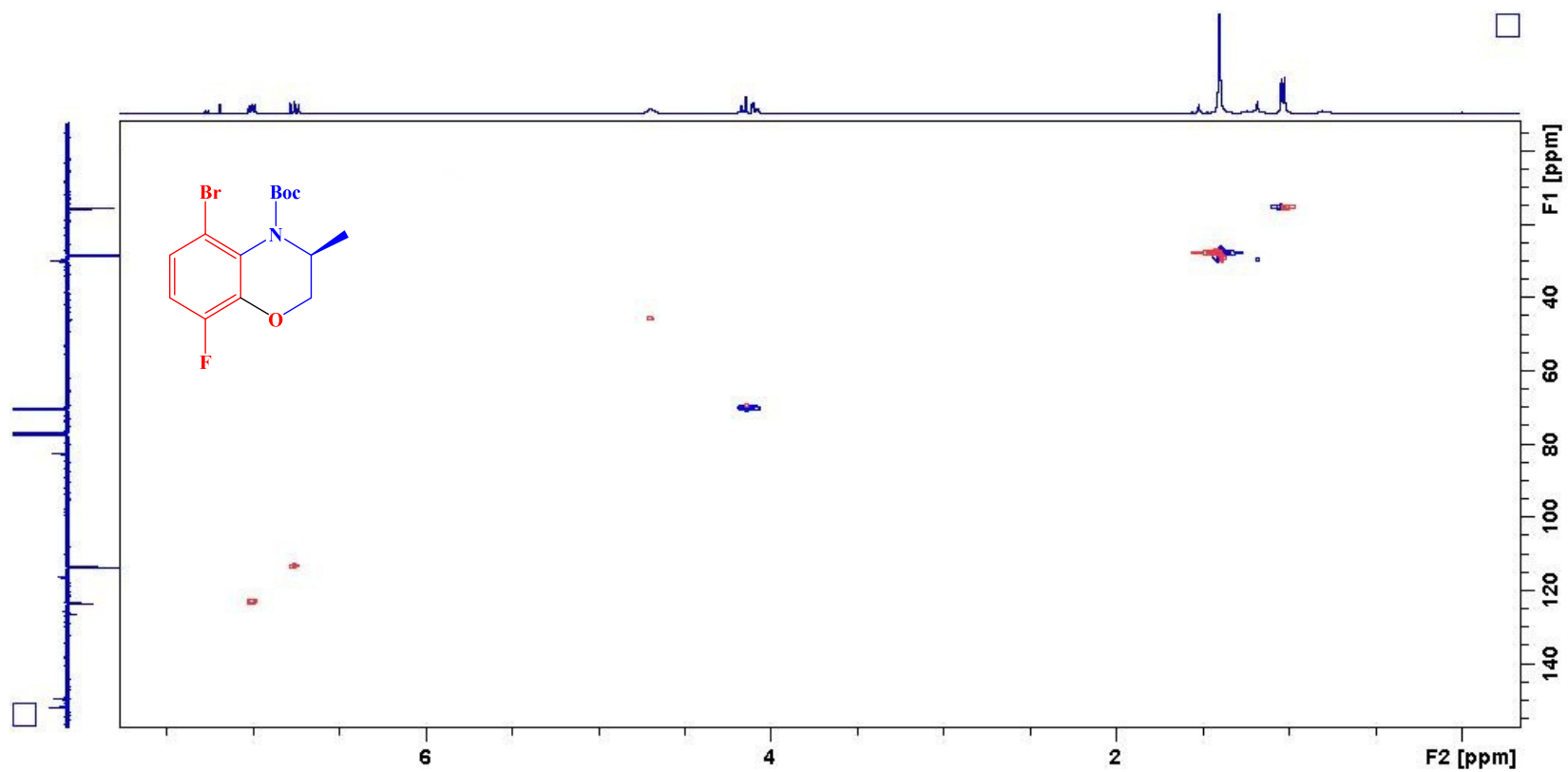
¹H NMR spectra of **6d**

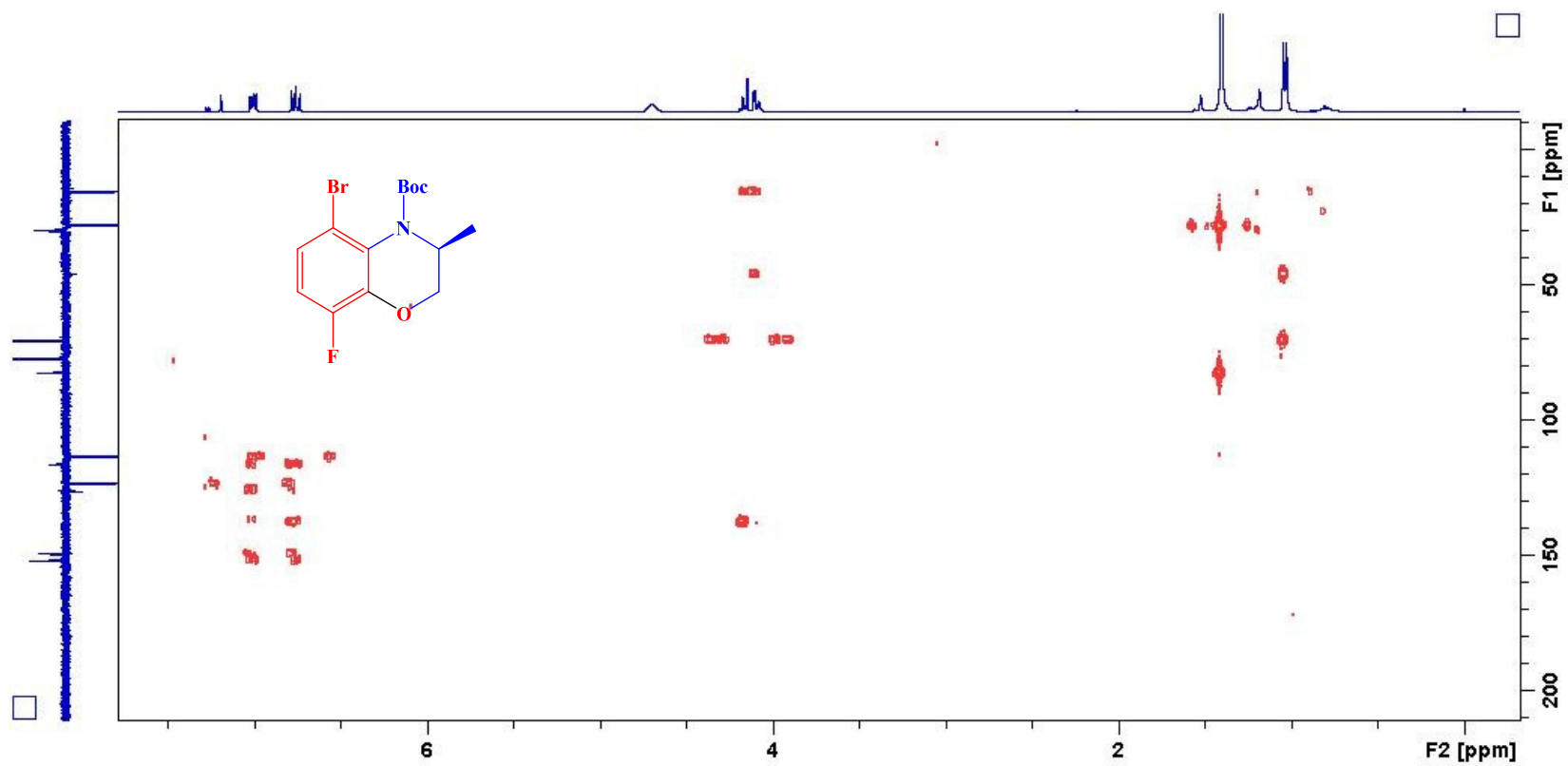
^{13}C NMR spectra of **6d**

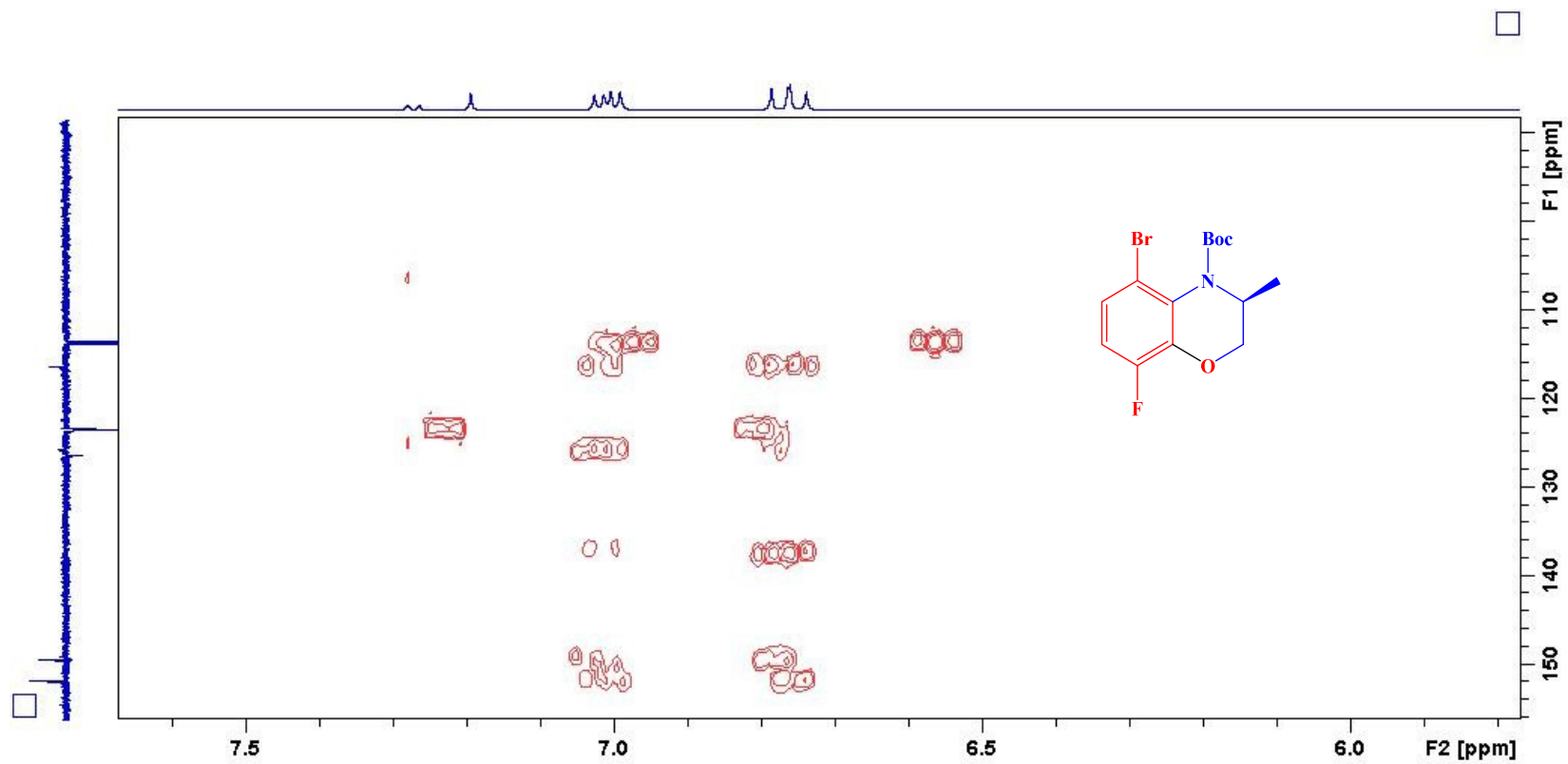
^1H NMR of **6f**

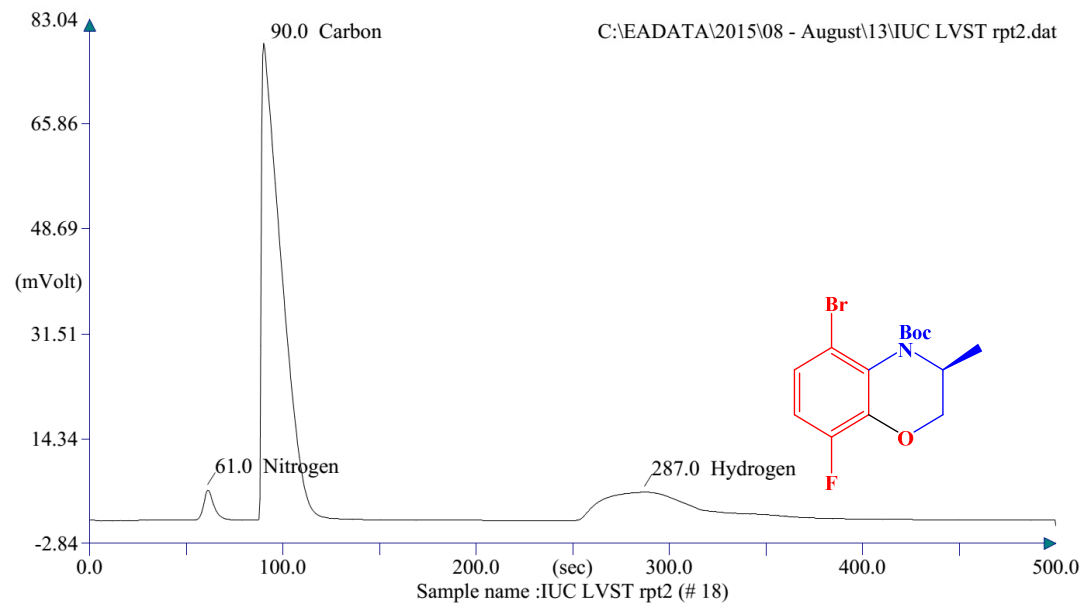
^{13}C NMR of **6f**

^{19}F NMR of **6f**

HSQC spectra of **6f**

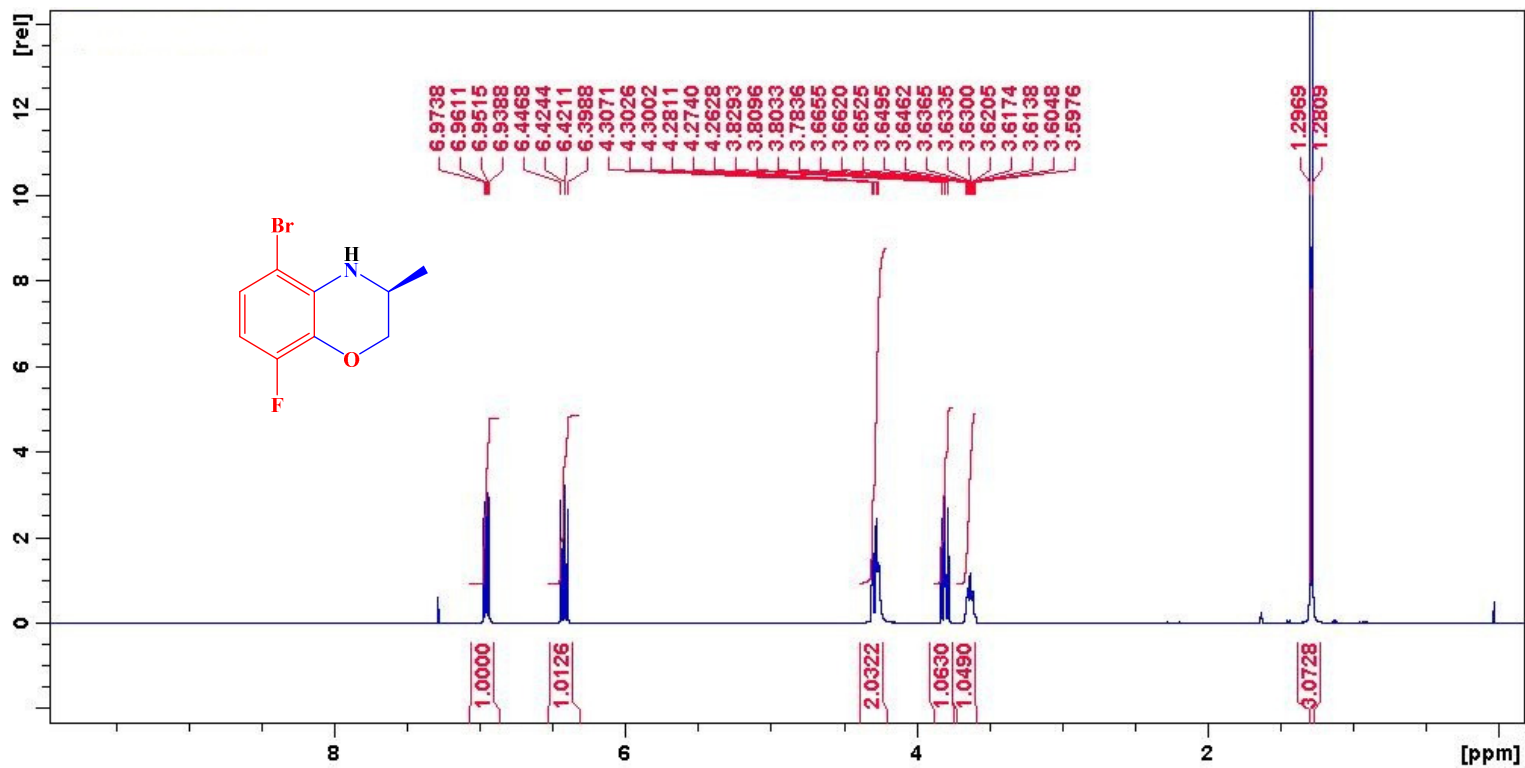
HMBC spectra of **6f**

Expansion of HMBC spectra of **6f**

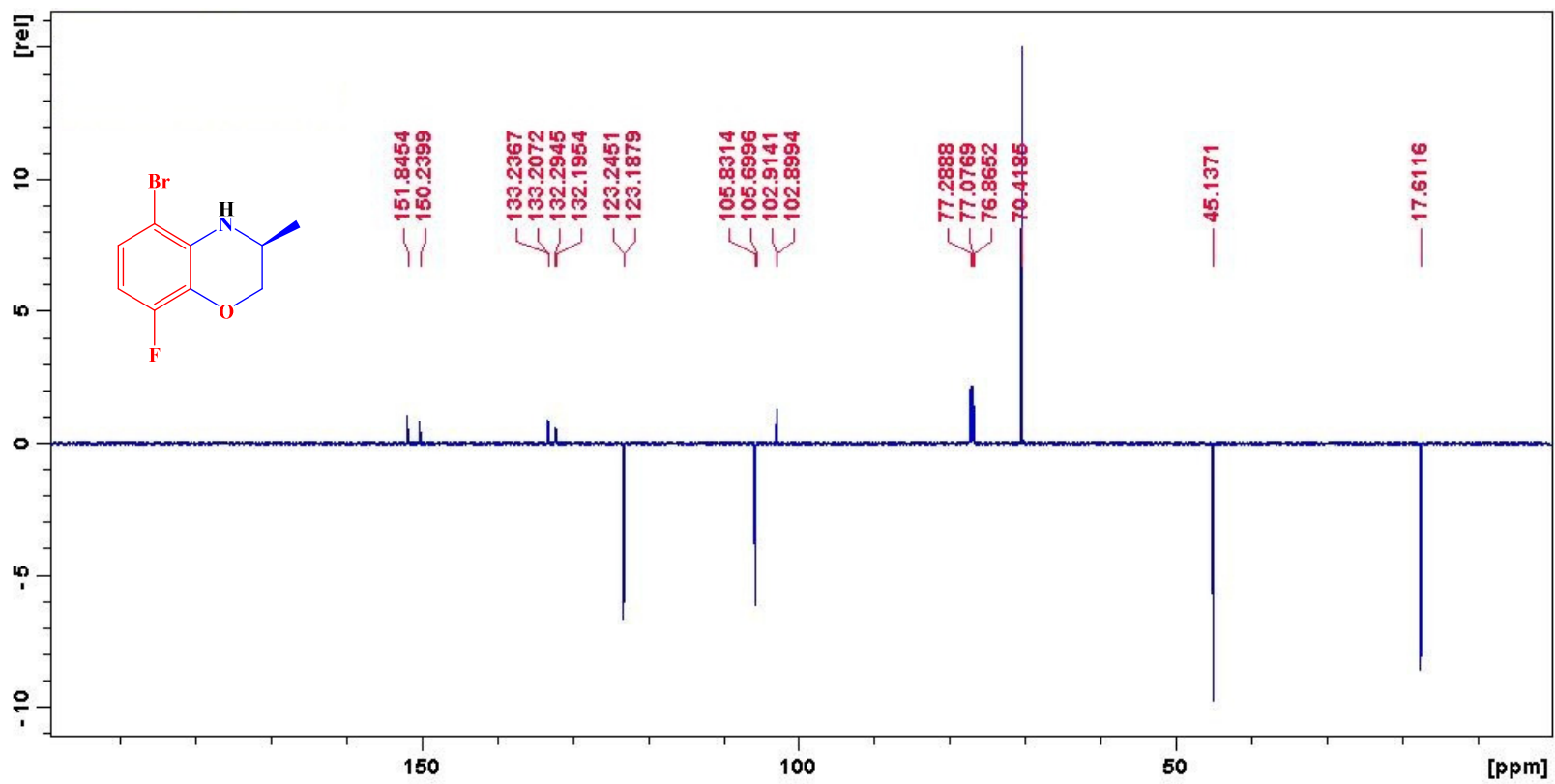
Elemental Analysis
CHNSElemental analysis for **6f**:

Retention Time (min)	Element Name	Element %
1.017	Nitrogen	3.981
1.500	Carbon	48.752
4.783	Hydrogen	4.684
		57.418

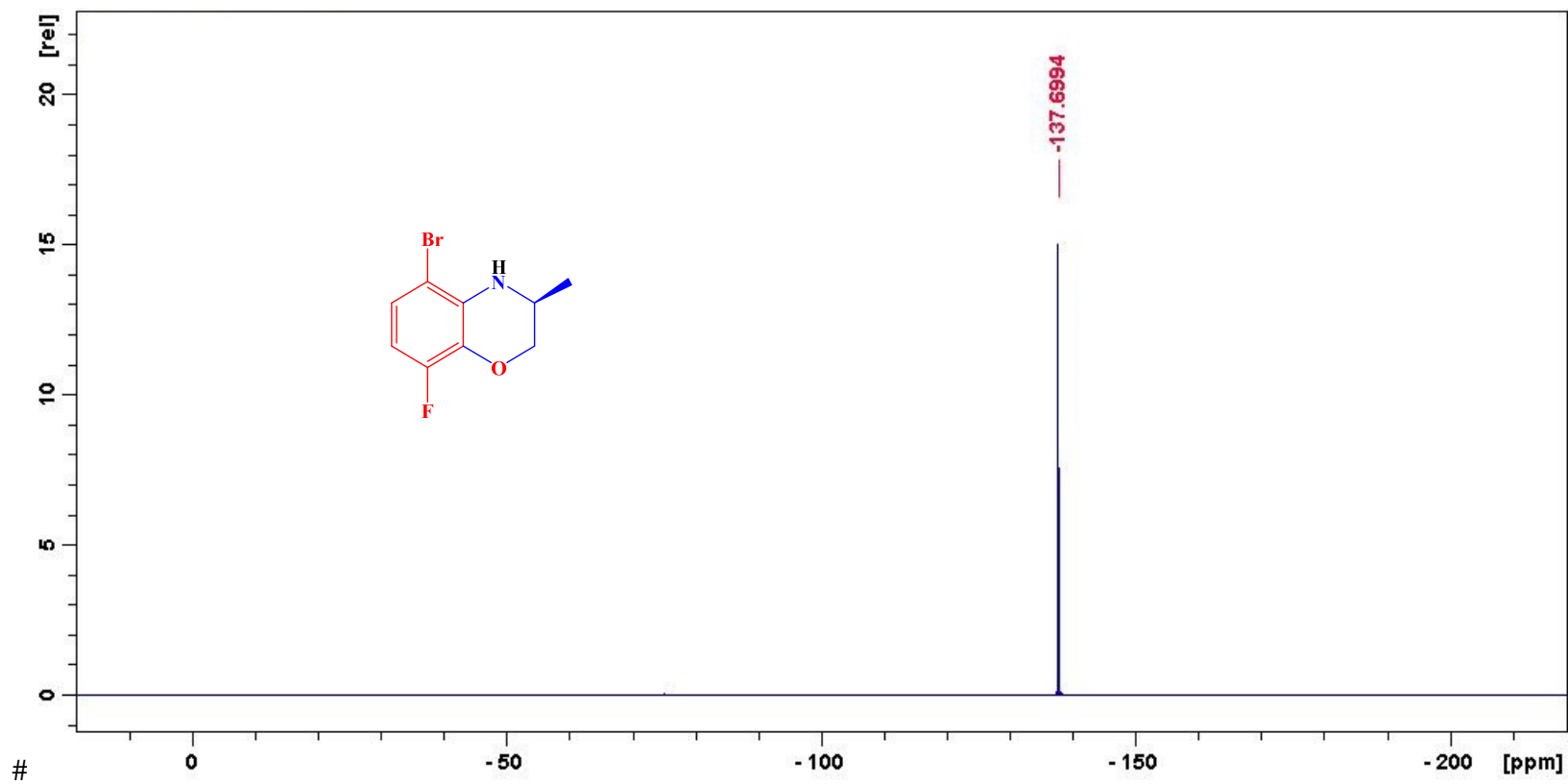
^1H NMR of (*S*)-5-bromo-8-fluoro-3-methyl-3,4-dihydro-2*H*-benzo[*b*][1,4]oxazine (Boc deprotected **6f**):



^{13}C NMR of (*S*)-5-bromo-8-fluoro-3-methyl-3,4-dihydro-2*H*-benzo[*b*][1,4]oxazine (Boc deprotected **6f**):



^{19}F NMR of (*S*)-5-bromo-8-fluoro-3-methyl-3,4-dihydro-2*H*-benzo[*b*][1,4]oxazine (Boc deprotected **6f**):



(S)-5-bromo-8-fluoro-3-methyl-3,4-dihydro-2H-benzo[b][1,4]oxazine (Boc deprotected **6f):****Elemental Composition Report**

Page 1

Single Mass Analysis

Tolerance = 5.0 PPM / DBE: min = -1.5, max = 100.0

Element prediction: Off

Number of isotope peaks used for i-FIT = 3

Monoisotopic Mass, Odd and Even Electron Ions

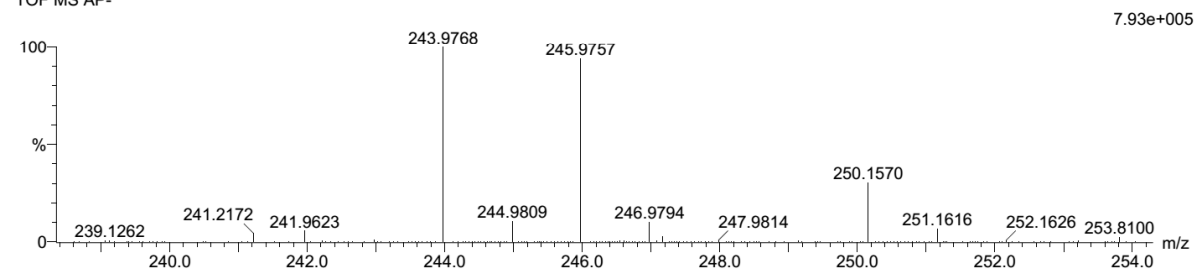
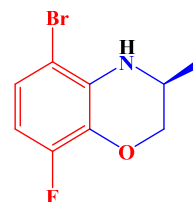
66 formula(e) evaluated with 1 results within limits (up to 20 closest results for each mass)

Elements Used:

C: 5-10 H: 5-10 N: 0-5 O: 1-5 Br: 0-1 F: 0-1

DepLVST AP- 53 (1.754) Cm (1:61)

TOF MS AP-



Minimum:

Maximum:

Mass	Calc. Mass	mDa	PPM	DBE	i-FIT	i-FIT (Norm)	Formula
243.9768	243.9773	-0.5	-2.0	5.5	744.9	0.0	C9 H8 N O Br F

(*S*)-5-bromo-8-fluoro-3-methyl-3,4-dihydro-2*H*-benzo[*b*][1,4]oxazine (Boc deprotected **6f**):

Elemental Composition Report

Page 1

Single Mass Analysis

Tolerance = 5.0 PPM / DBE: min = -1.5, max = 100.0

Element prediction: Off

Number of isotope peaks used for i-FIT = 3

Monoisotopic Mass, Even Electron Ions

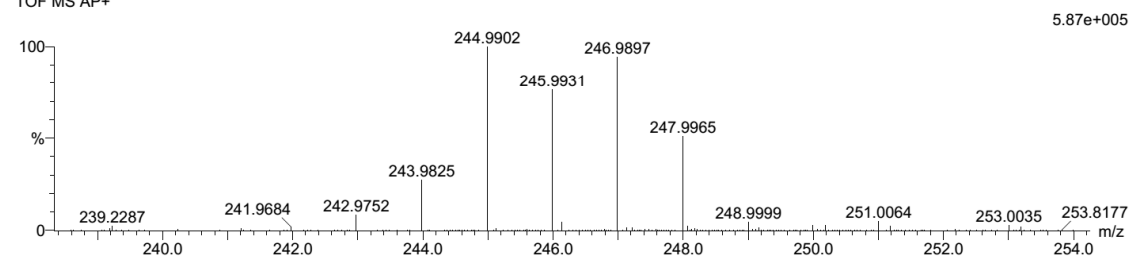
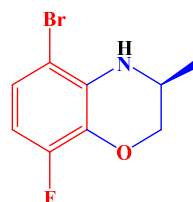
66 formula(e) evaluated with 1 results within limits (up to 20 closest results for each mass)

Elements Used:

C: 5-10 H: 5-10 N: 0-5 O: 1-5 F: 0-1 Br: 0-1

DepLVST AP+ 45 (1.484) Cm (1:61)

TOF MS AP+



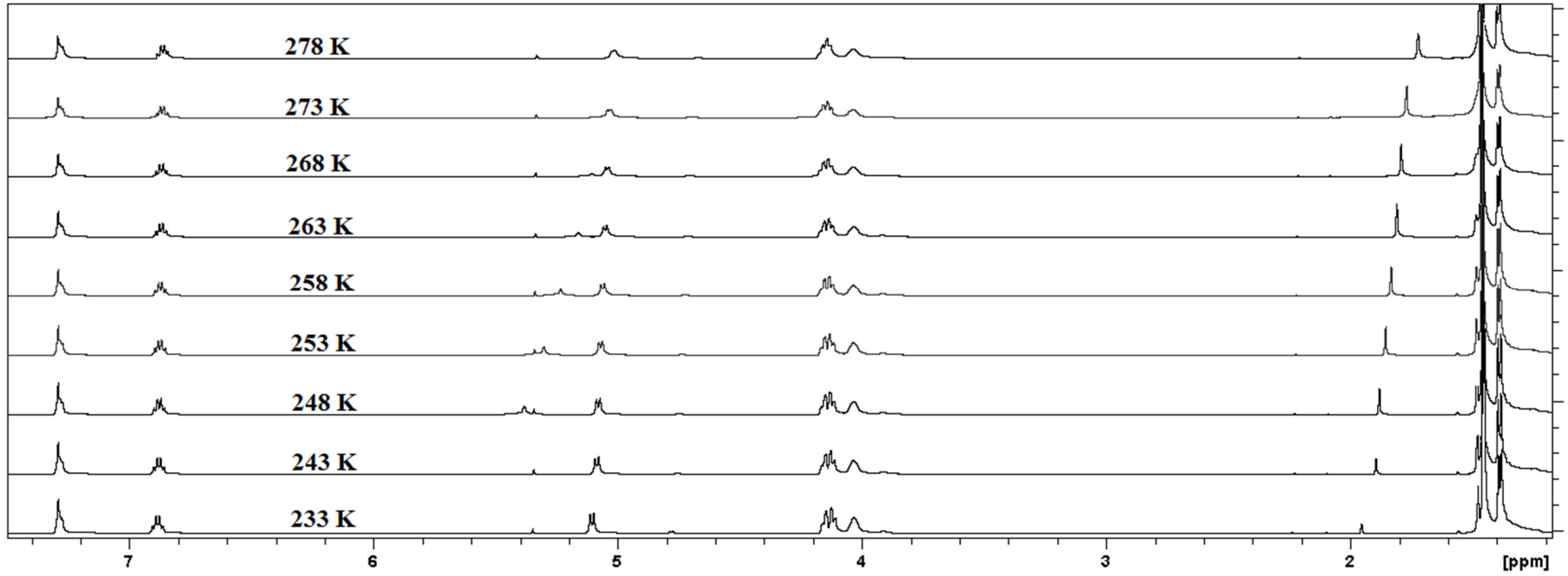
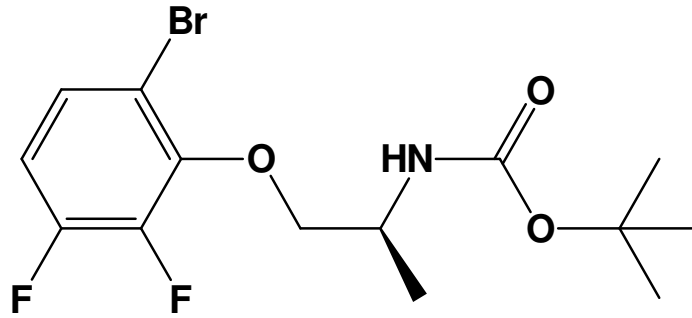
Minimum: -1.5
Maximum: 5.0 5.0 100.0

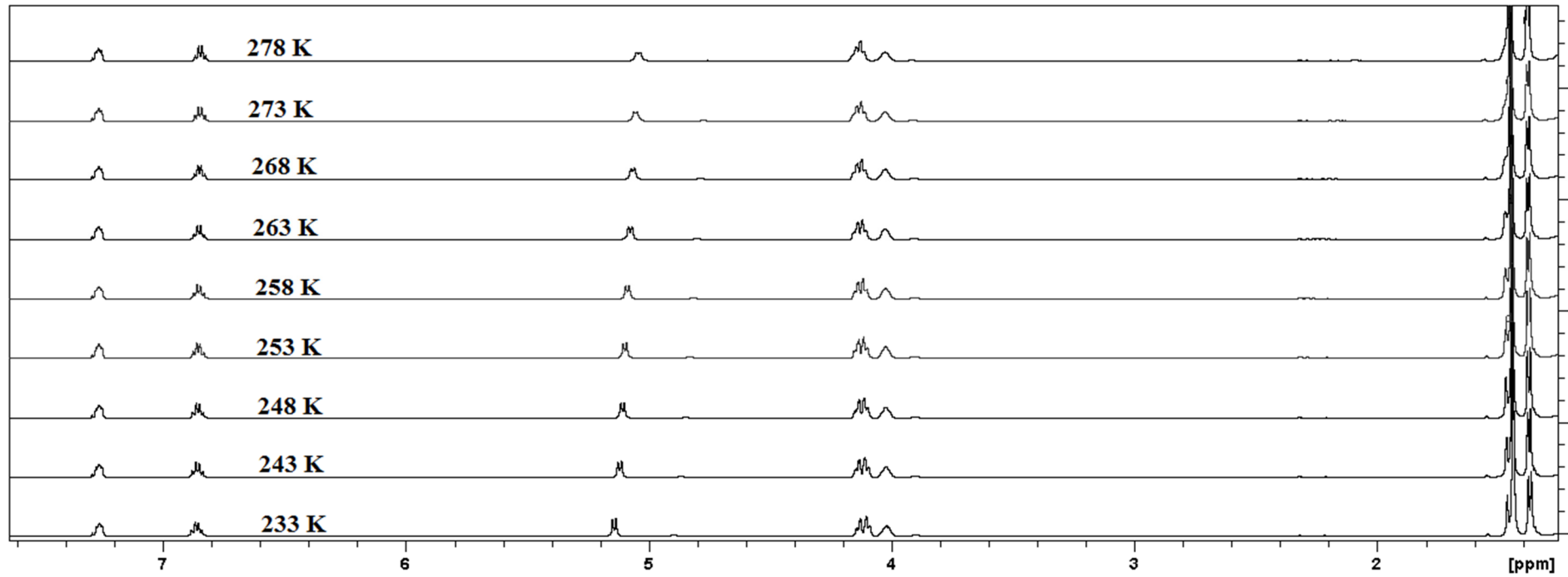
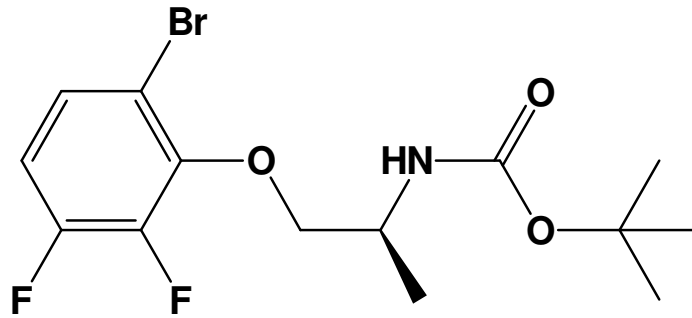
Mass	Calc. Mass	mDa	PPM	DBE	i-FIT	i-FIT (Norm)	Formula
245.9931	245.9930	0.1	0.4	4.5	796.6	0.0	C9 H10 N O F Br

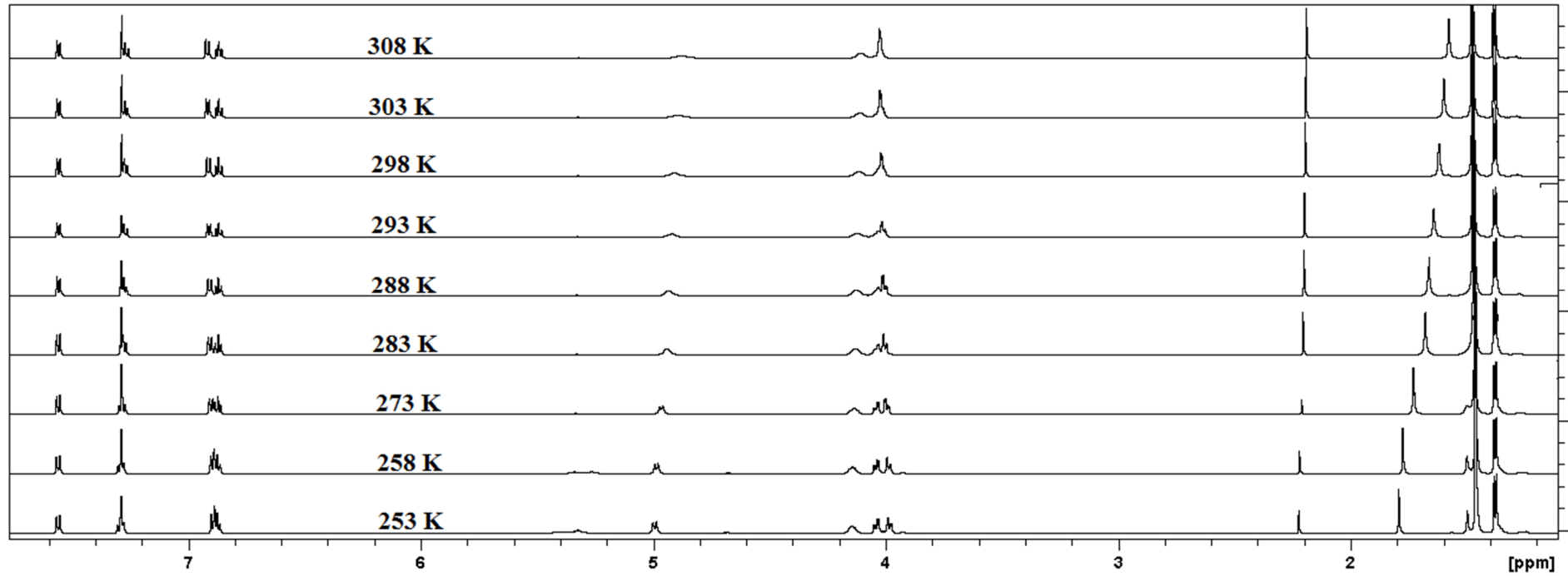
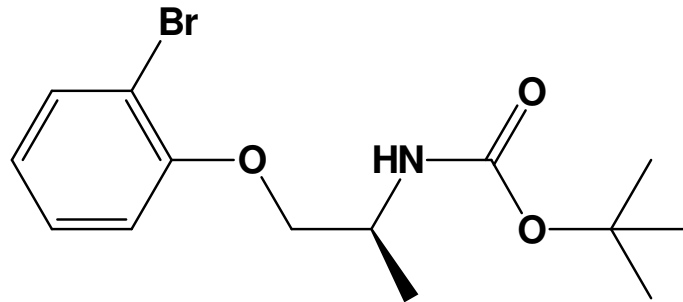
Supporting Information

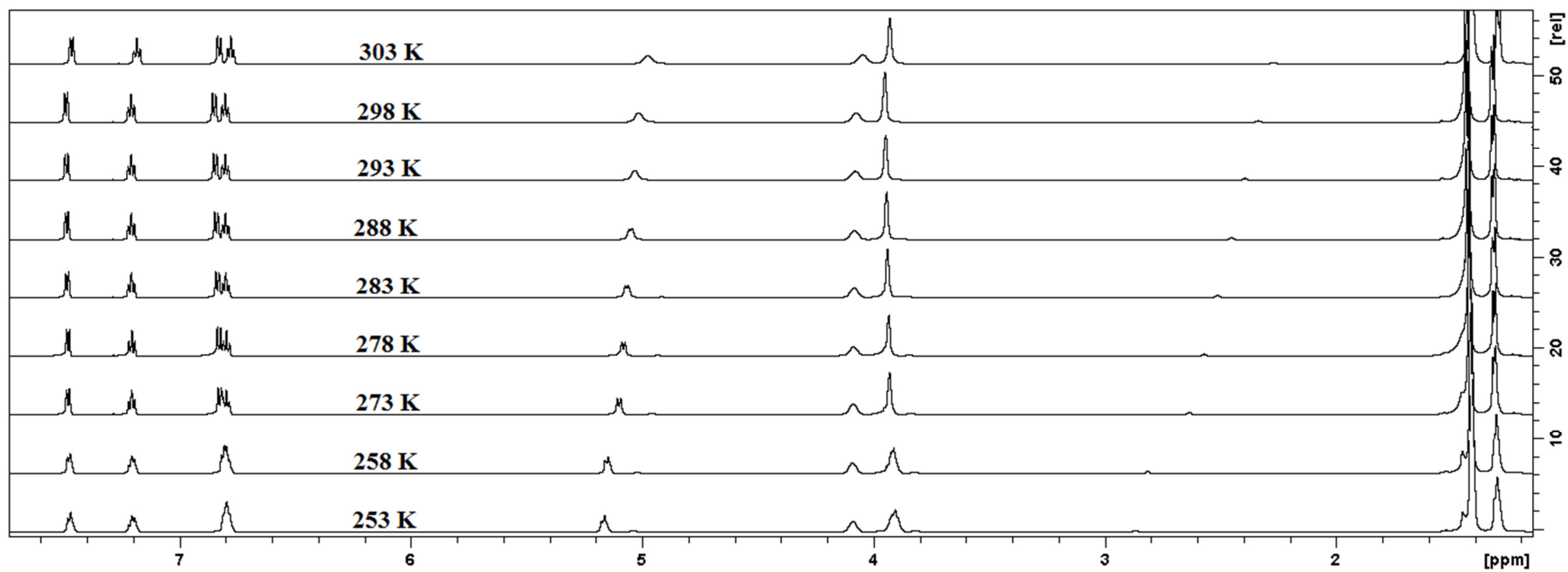
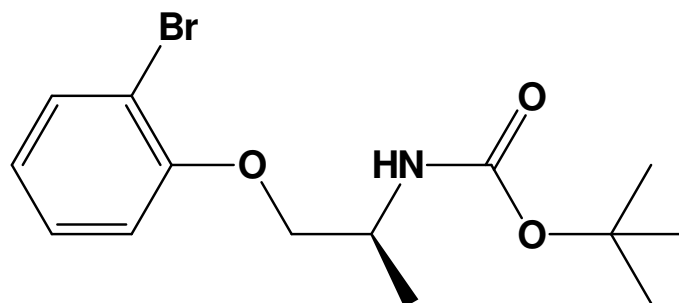
Chapter 3

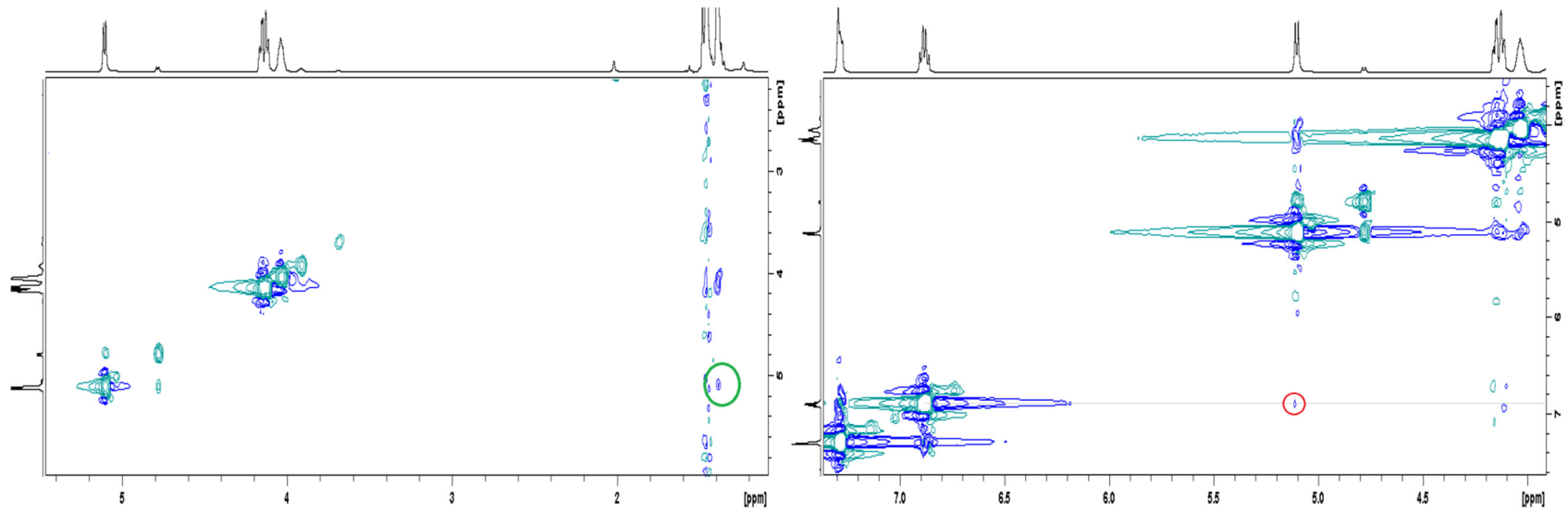
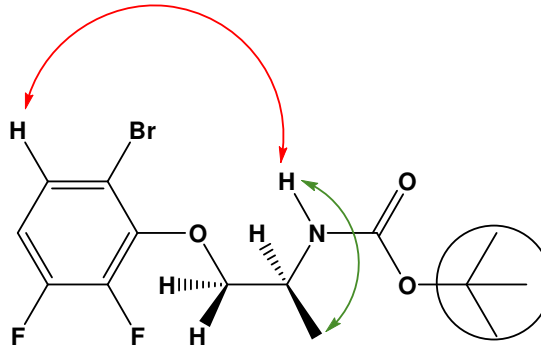
How do hydrogen bonds affect the dynamic behaviour of an organic molecule?

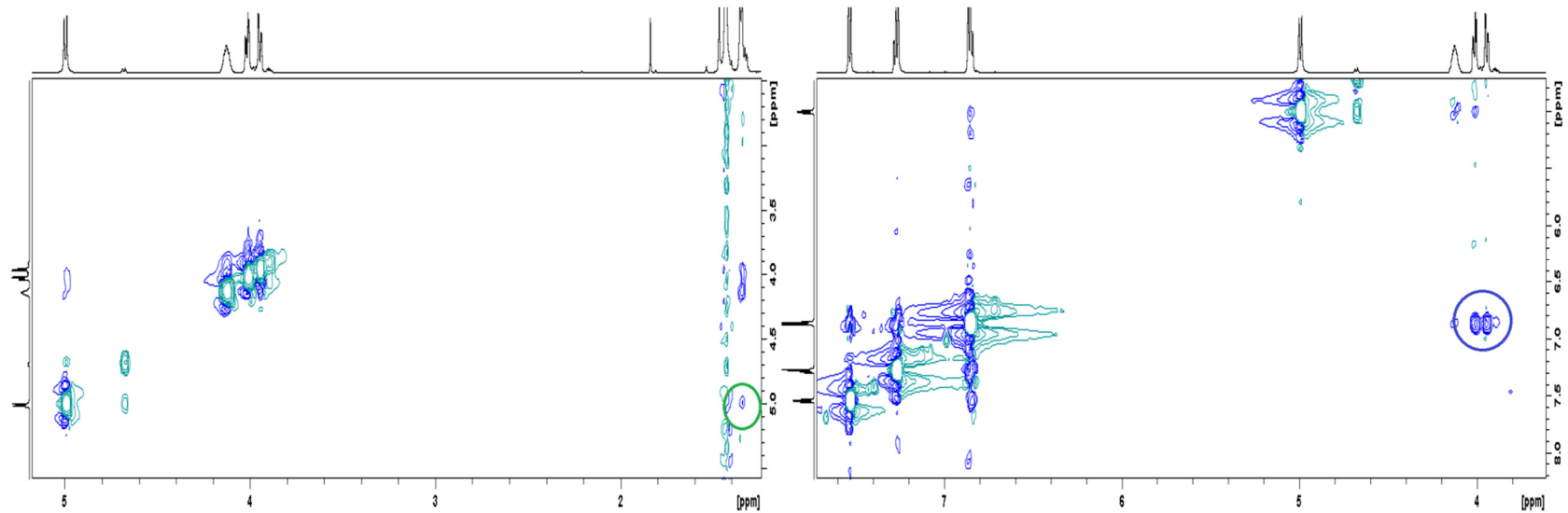
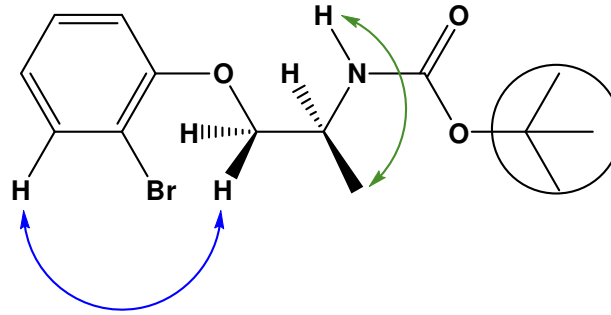
VT-NMR of compound 1 (27 μ M)

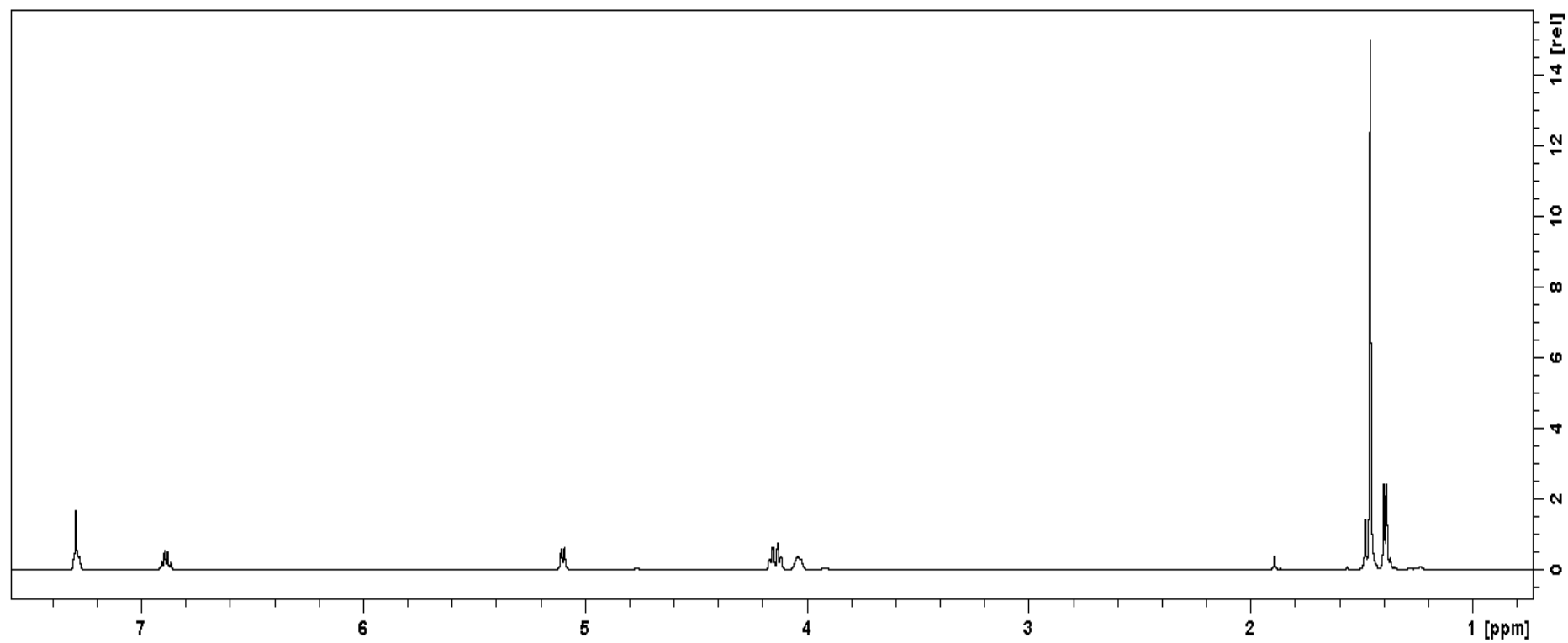
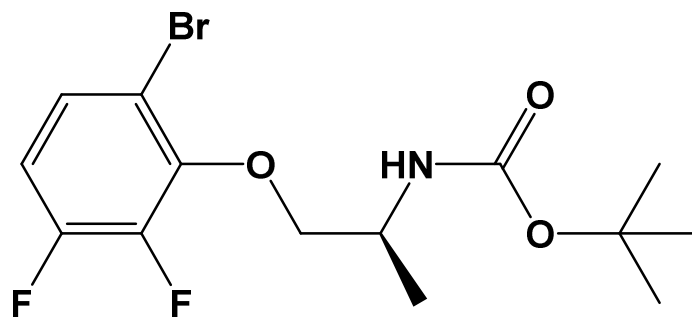
VT-NMR of compound 1 (110 μM)

VT-NMR of compound 2 (27 μ M)

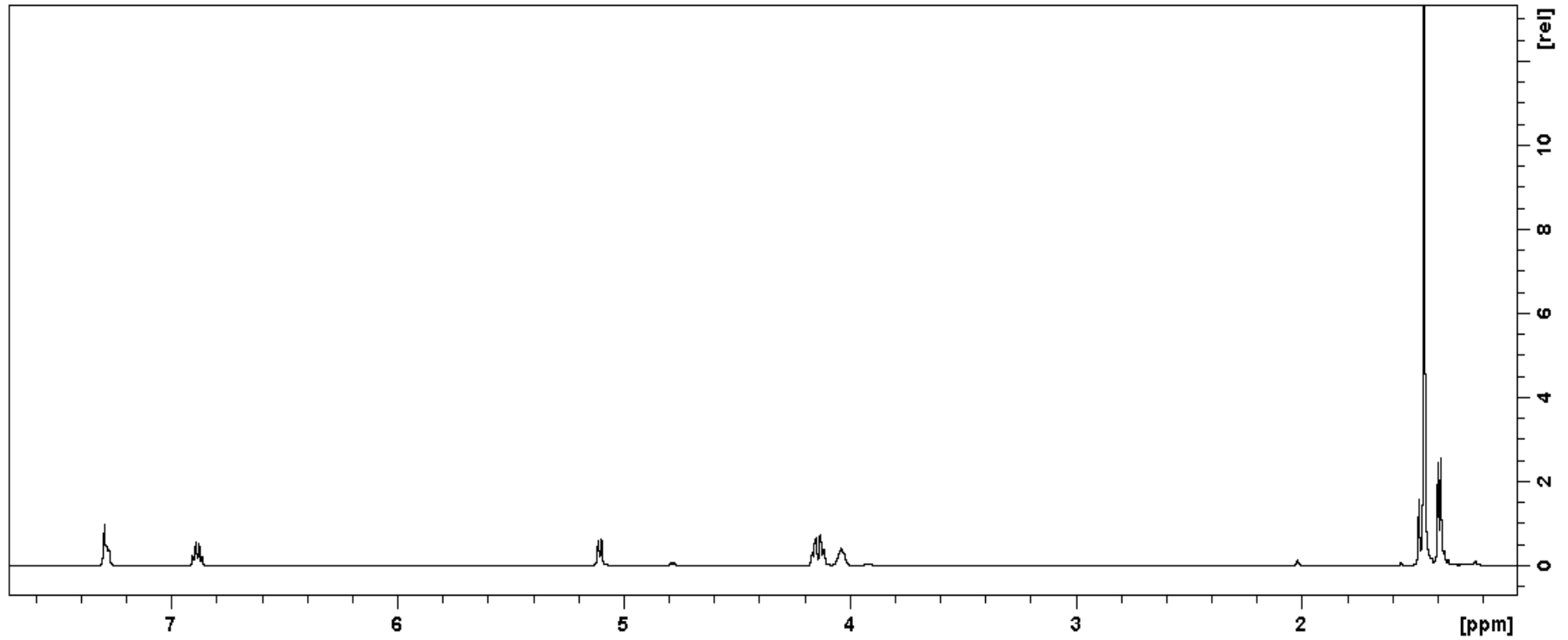
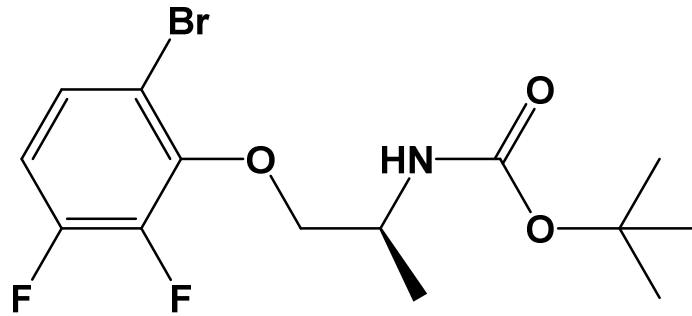
VT-NMR of compound 2 (110 μM)

NOESY spectrum of compound 1 (110 μM) at $-40\text{ }^\circ\text{C}$ 

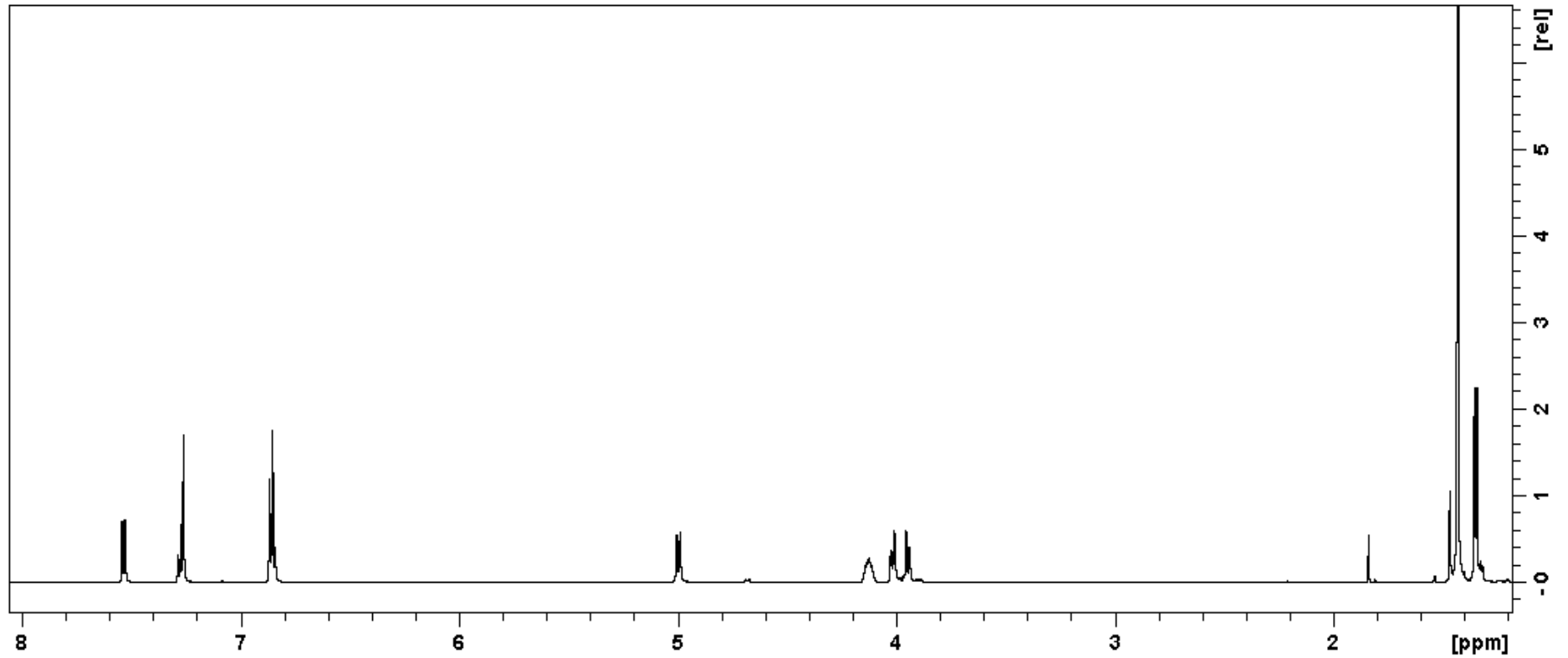
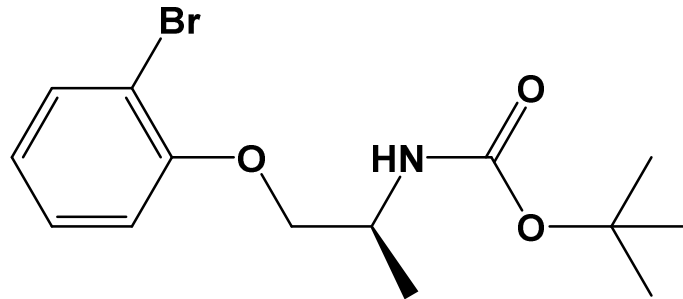
NOESY spectrum of compound 2 (110 μM) at $-40\text{ }^\circ\text{C}$ 

^1H NMR spectrum of compound 1 (27 μM) at $-40\text{ }^\circ\text{C}$ 

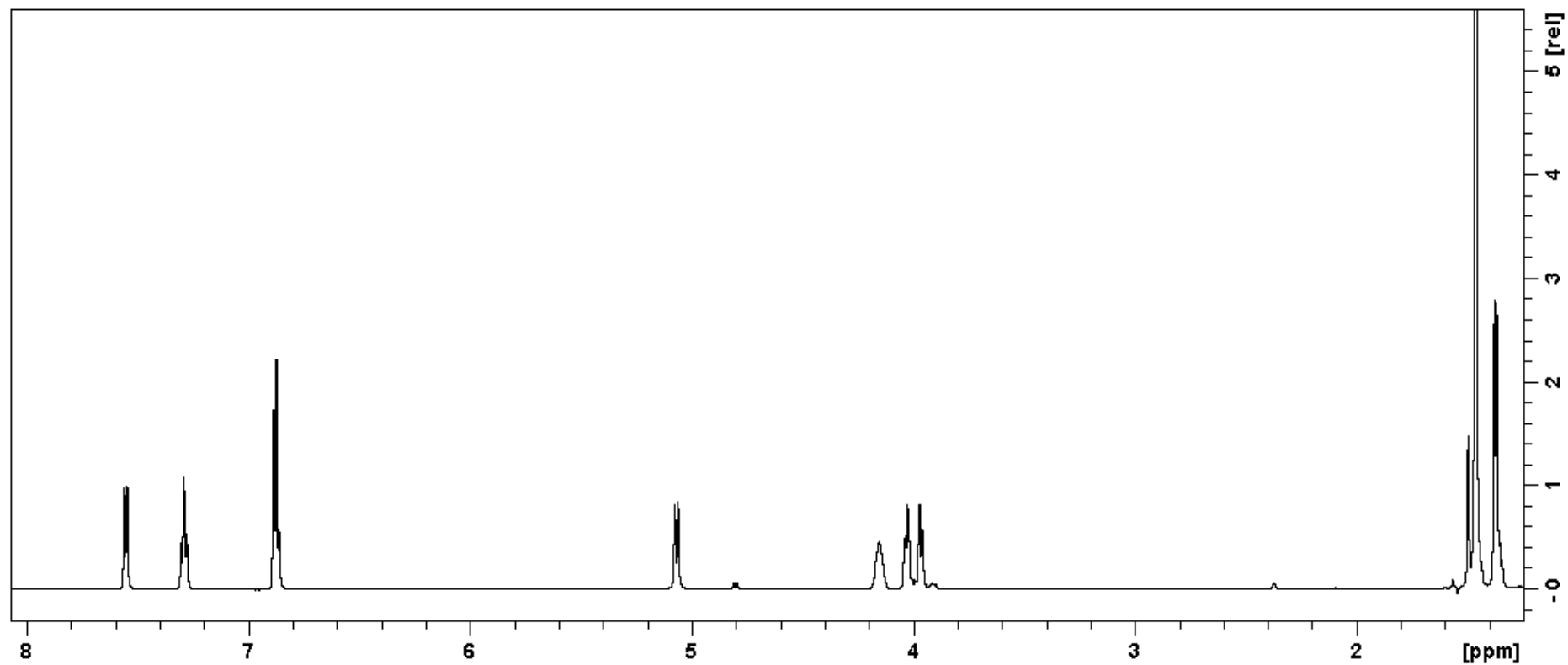
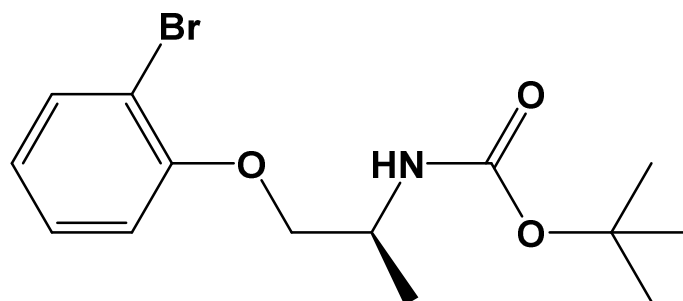
^1H NMR spectrum of compound 1 (110 μM) at $-40\text{ }^\circ\text{C}$



^1H NMR spectrum of compound 2 (27 μM) at -40°C



^1H NMR spectrum of compound 2 (110 μM) at $-40\text{ }^\circ\text{C}$

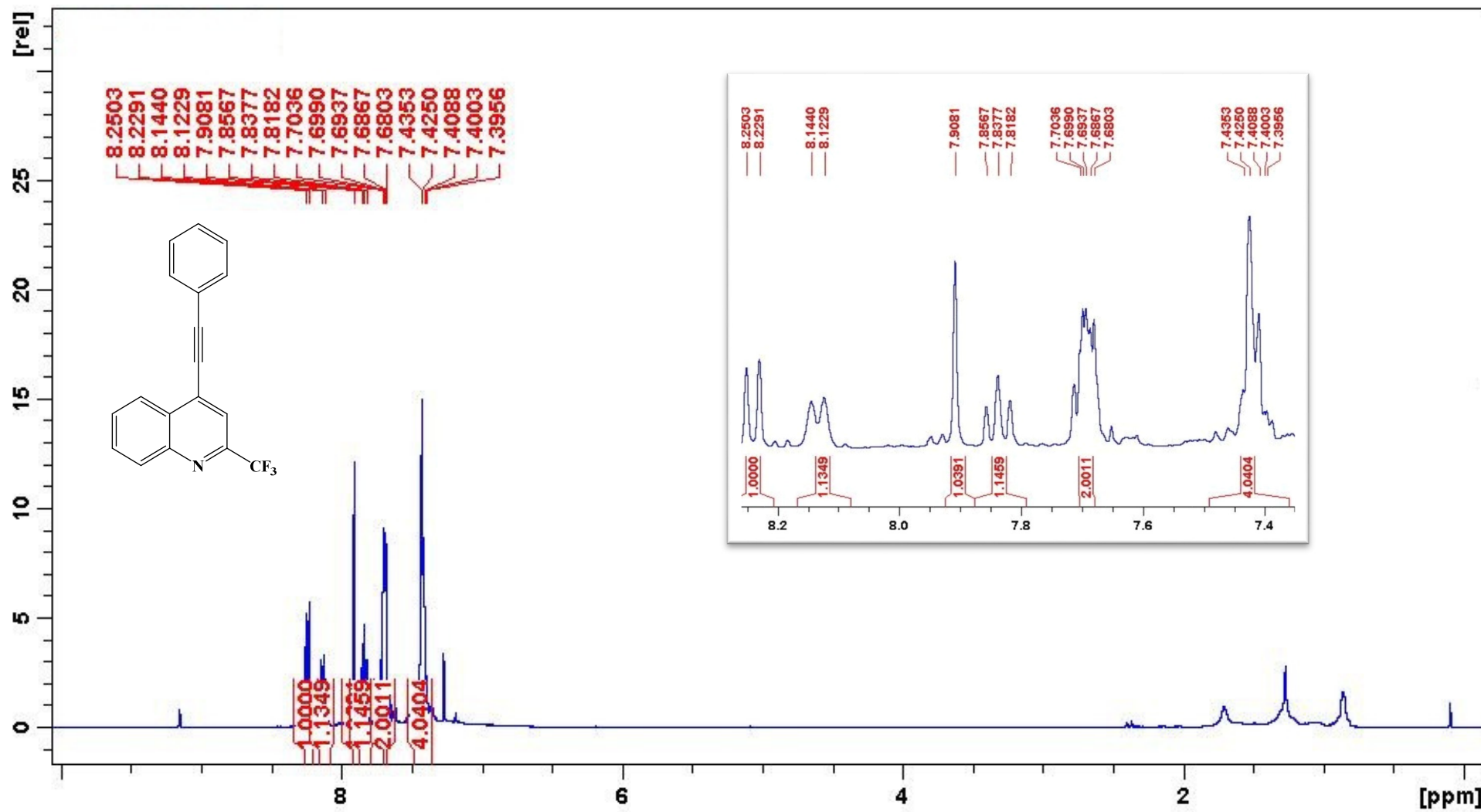


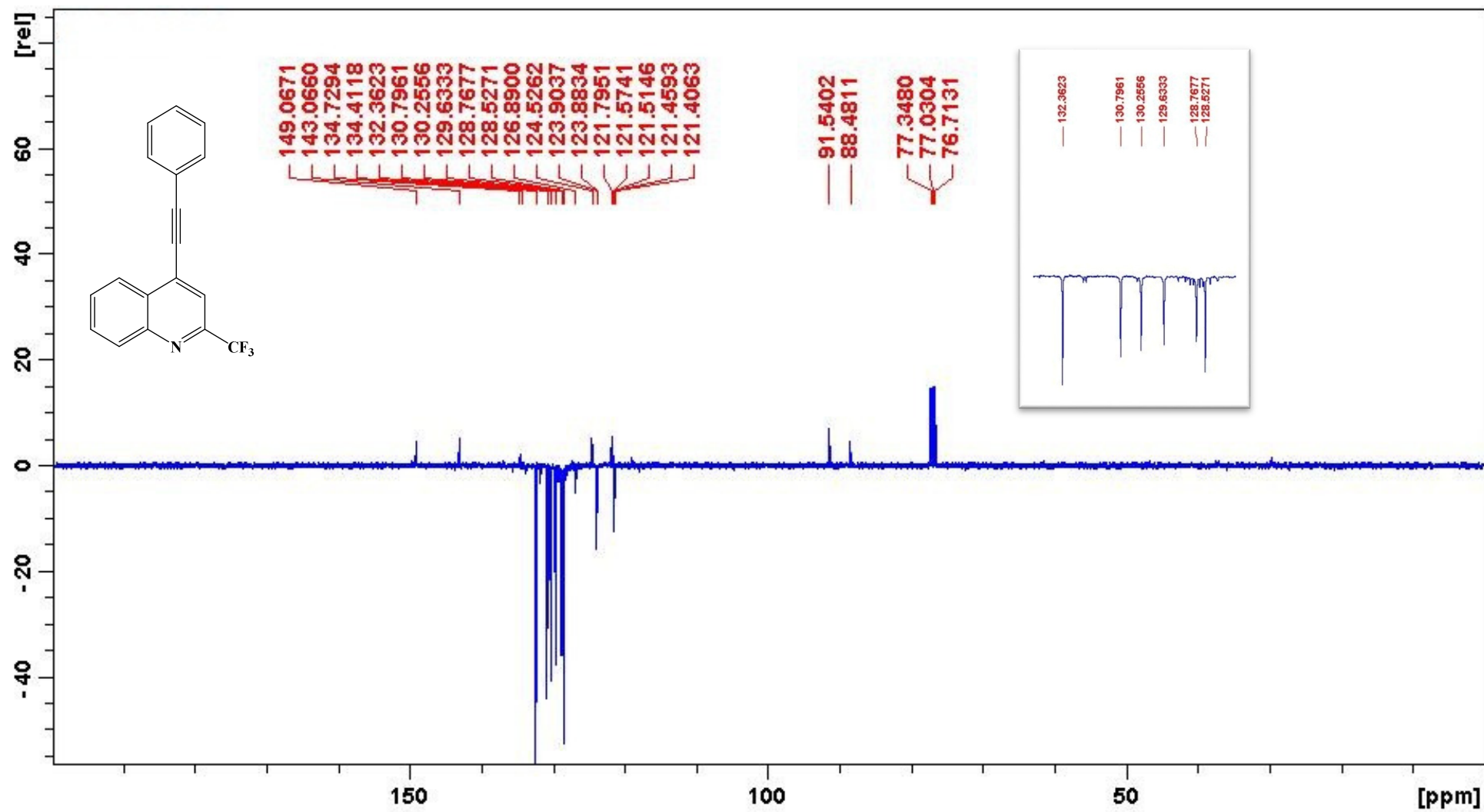
Supporting Information

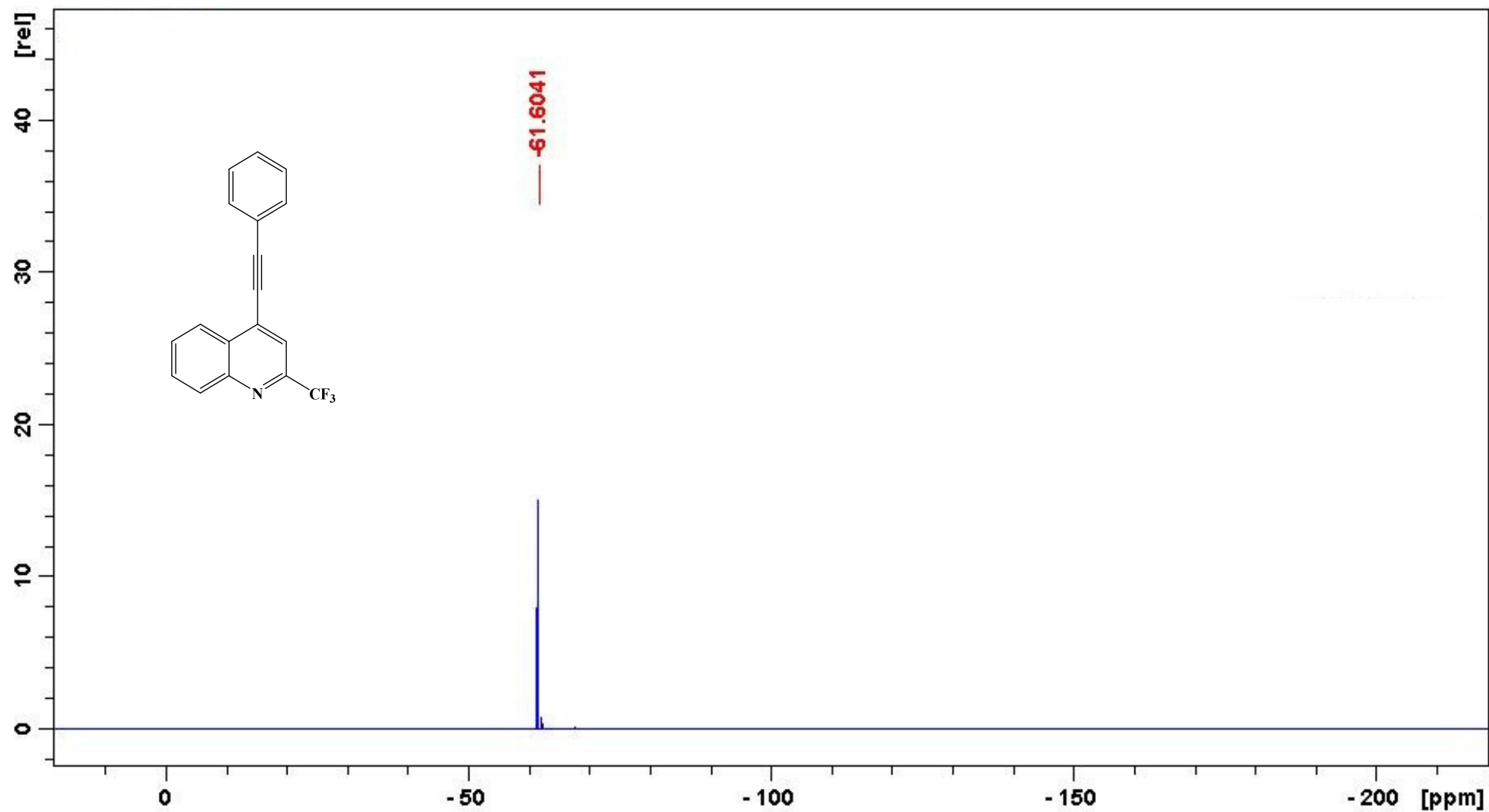
Chapter 4

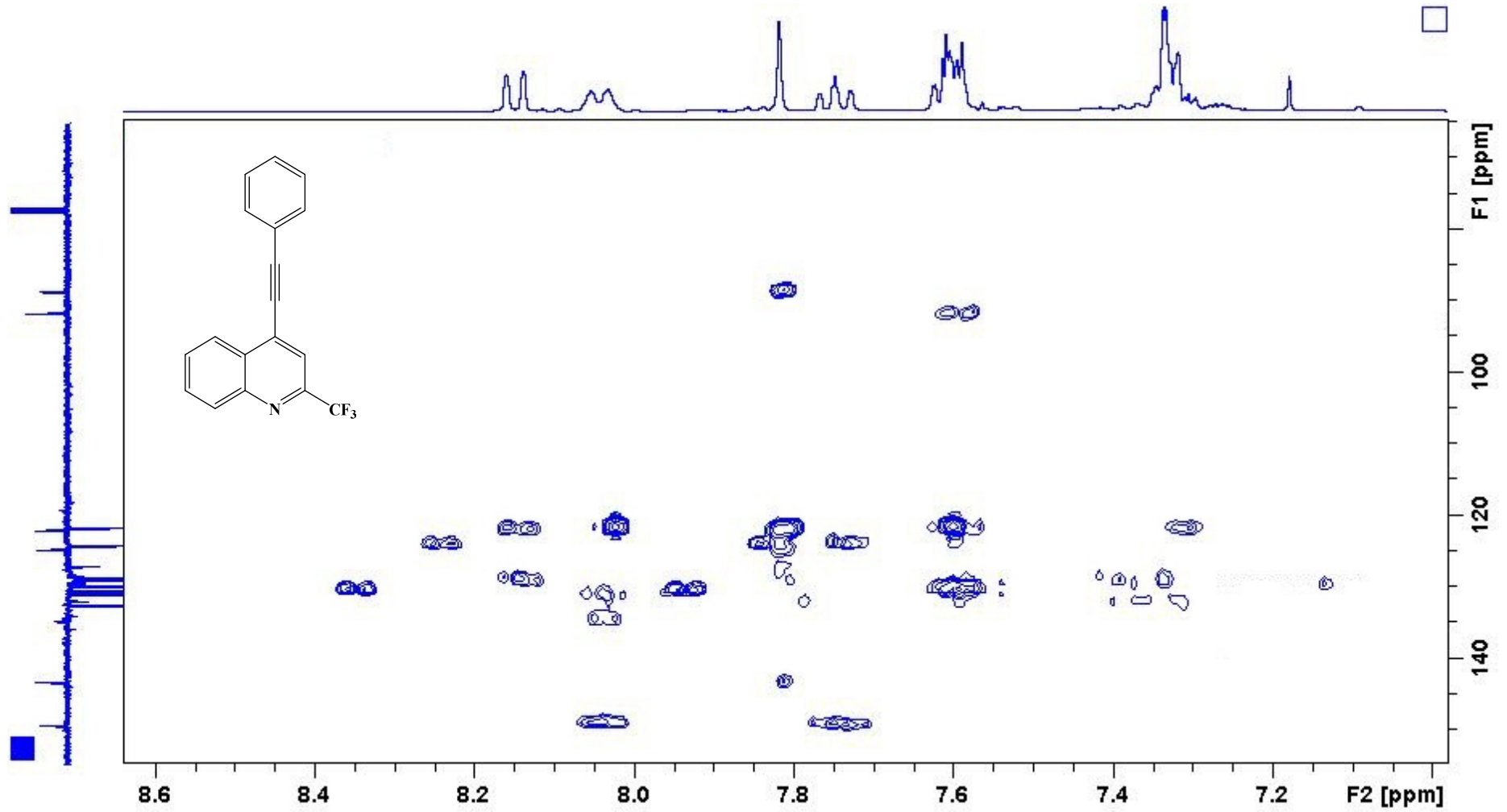
Copper-free Sonogashira coupling of 2-trifluoromethyl-4-chloroquinoline with alkynyl acetylene in the formation of fluorinated 4-(alkynyl)-quinolines using Pd(II) and xantphos

NMR spectra

¹H NMR spectrum of **4a**

^{13}C NMR spectrum of **4a**

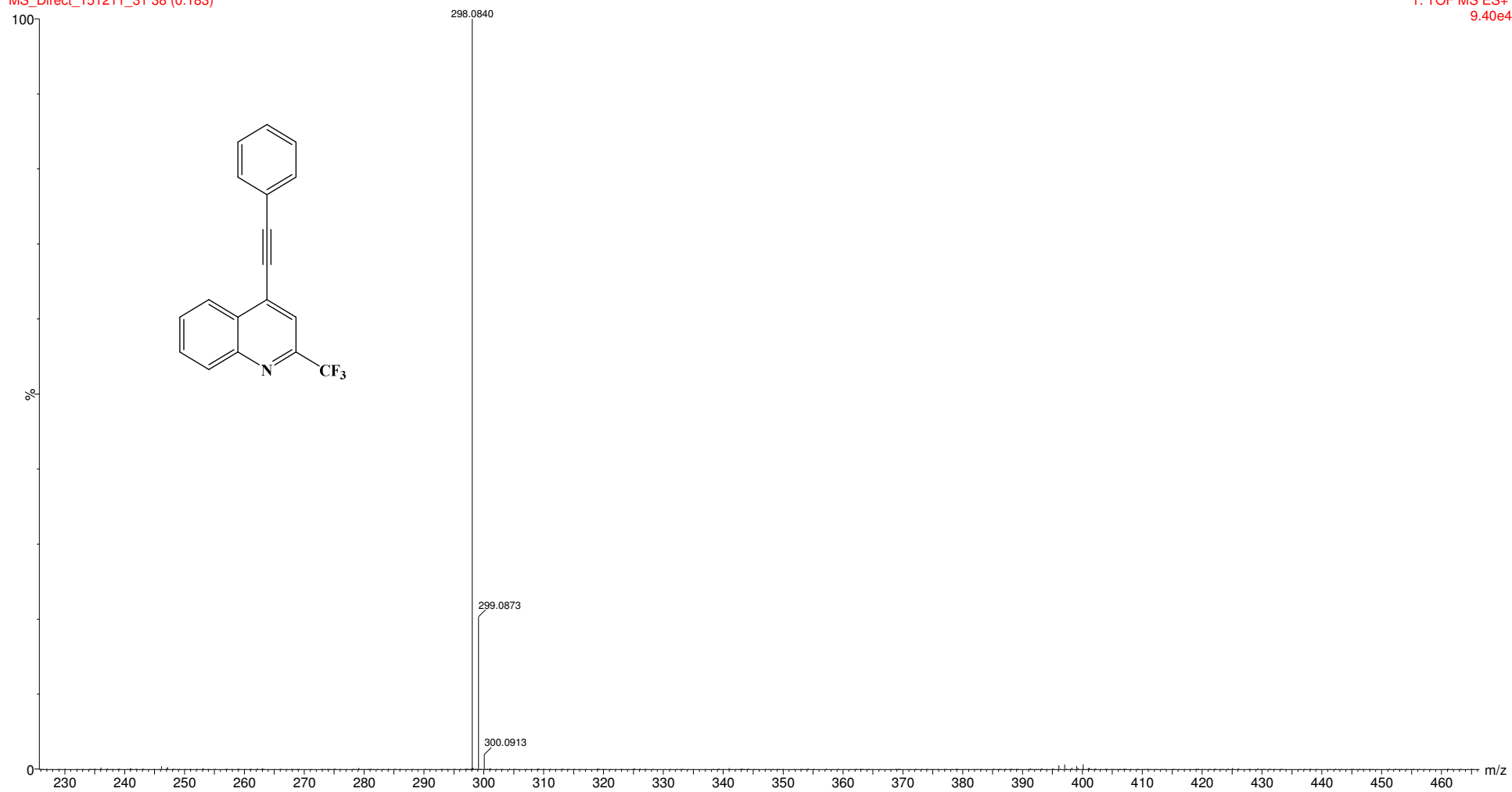
¹⁹F NMR spectrum of **4a**

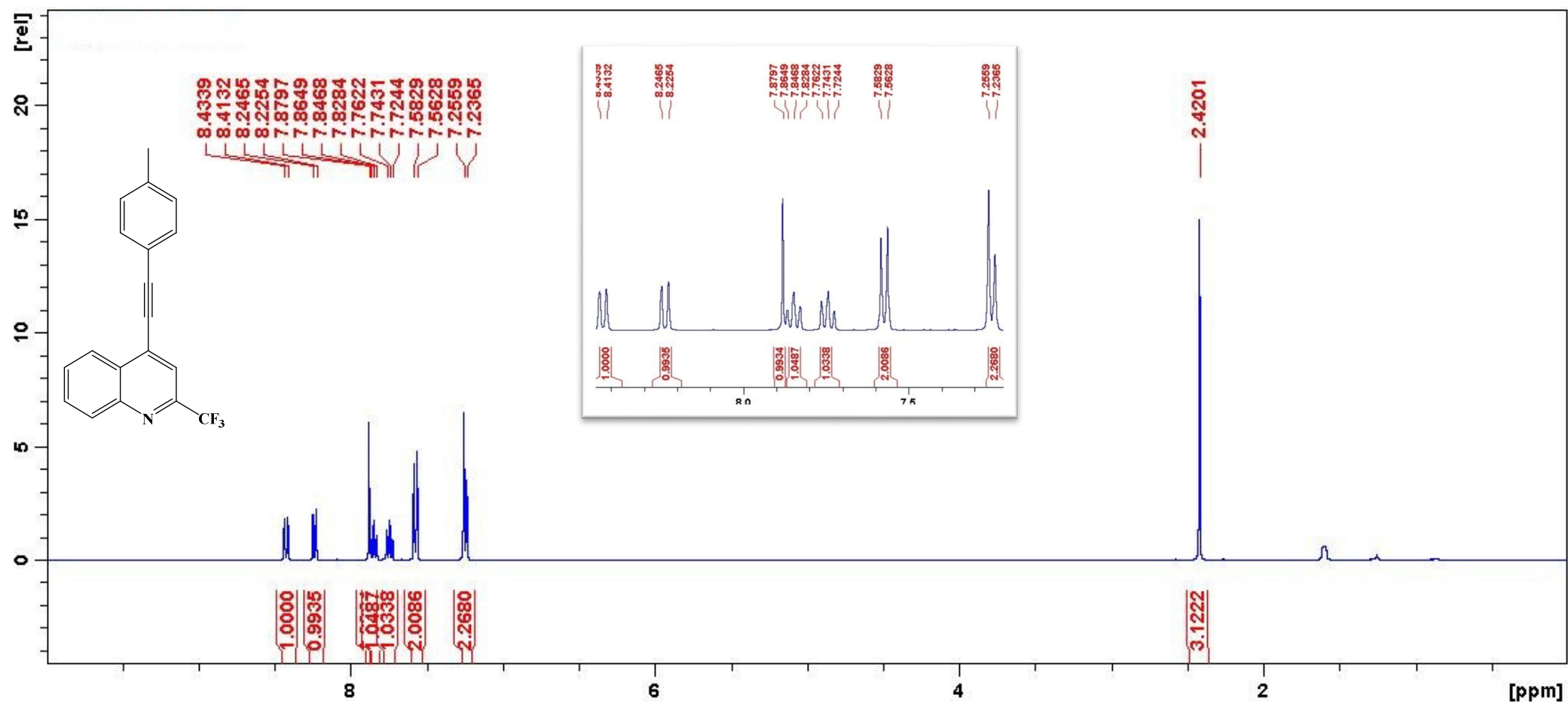
HMBC spectrum of **4a**

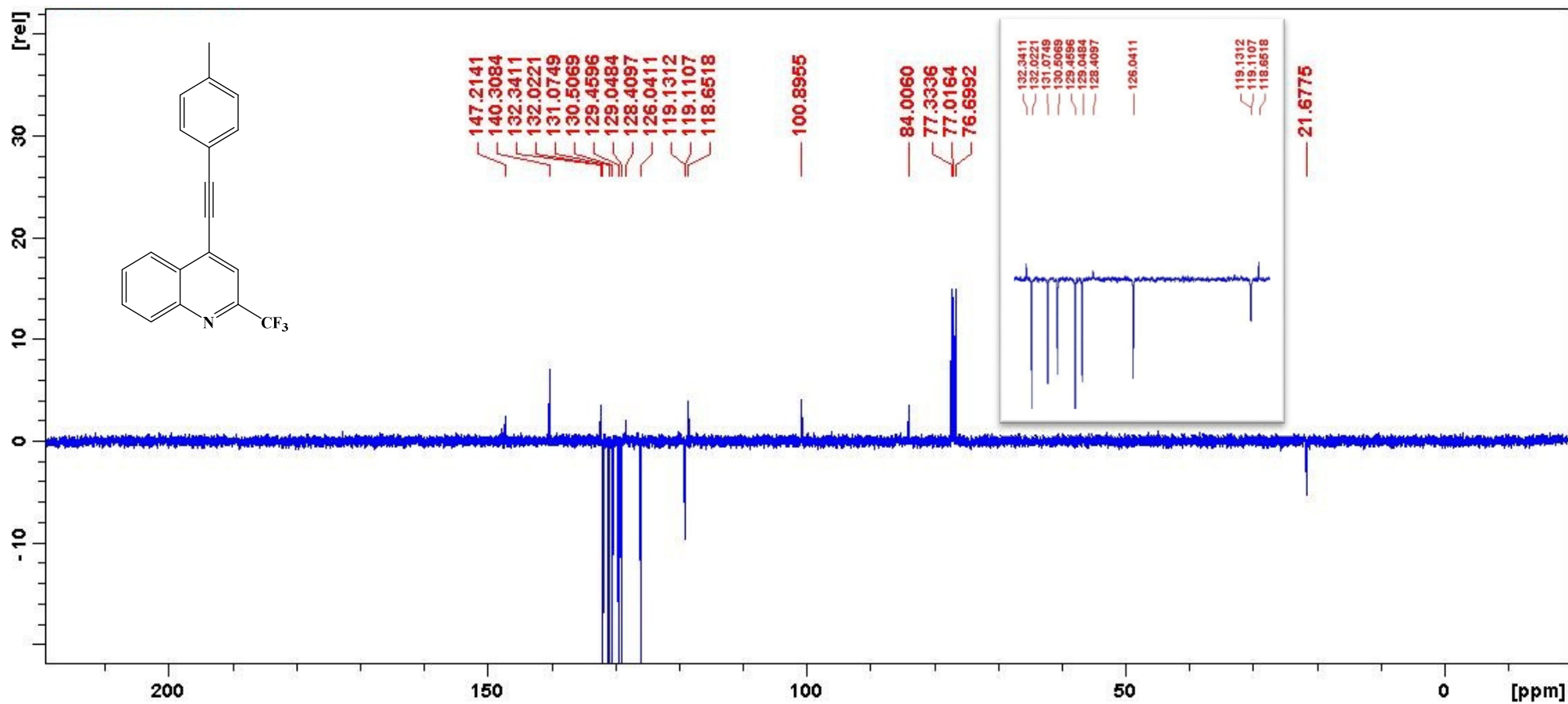
HRMS of **4a**

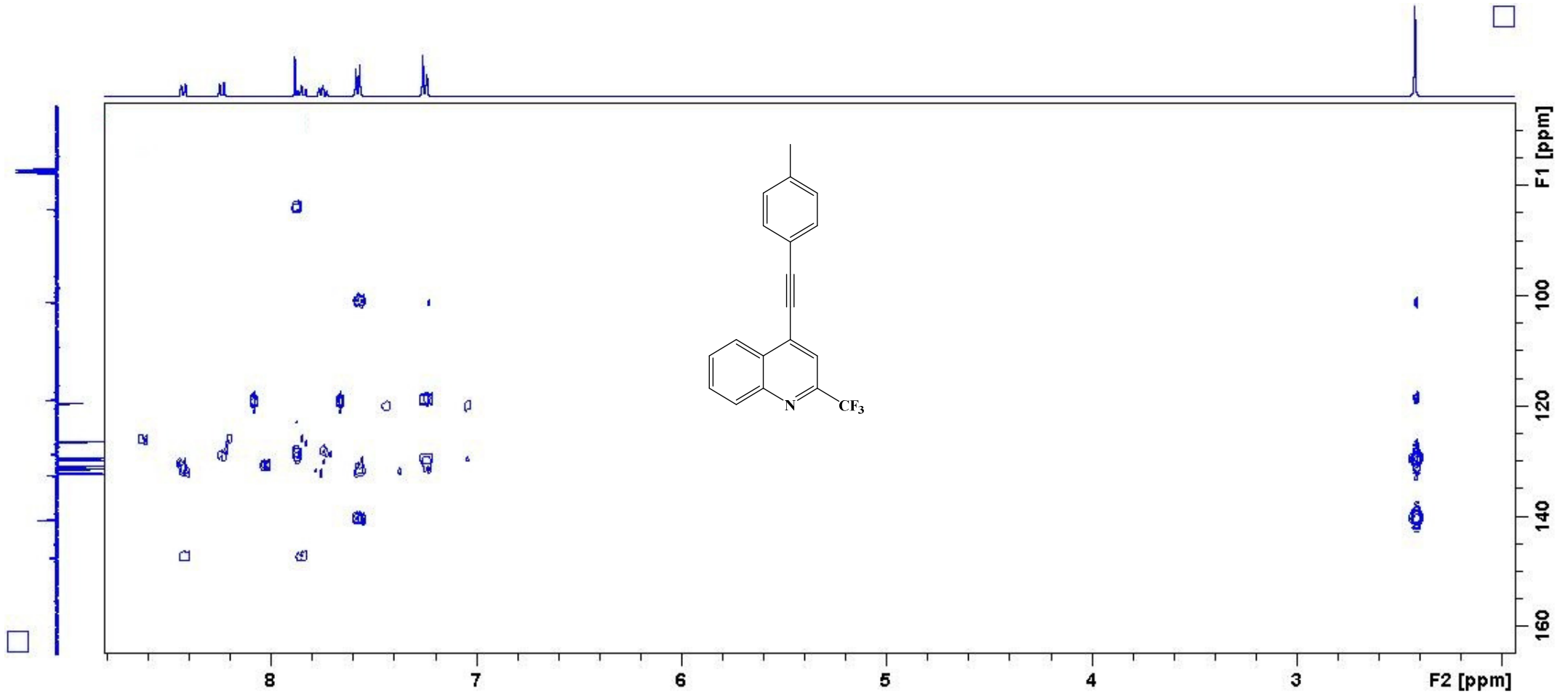
SA1

MS_Direct_151211_31 38 (0.183)

1: TOF MS ES+
9.40e4

¹H NMR spectrum of **4b**

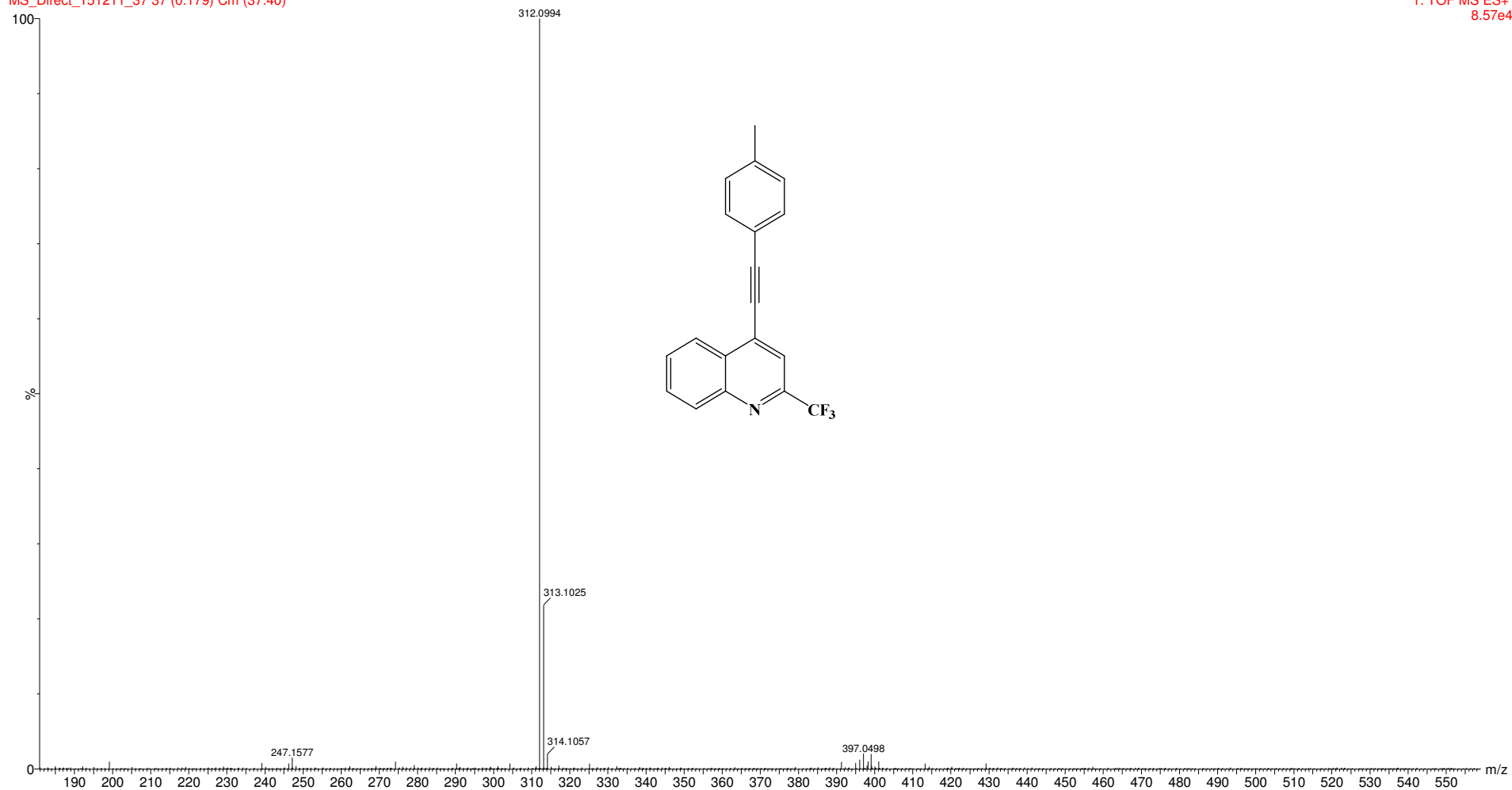
¹³C NMR spectrum of **4b**

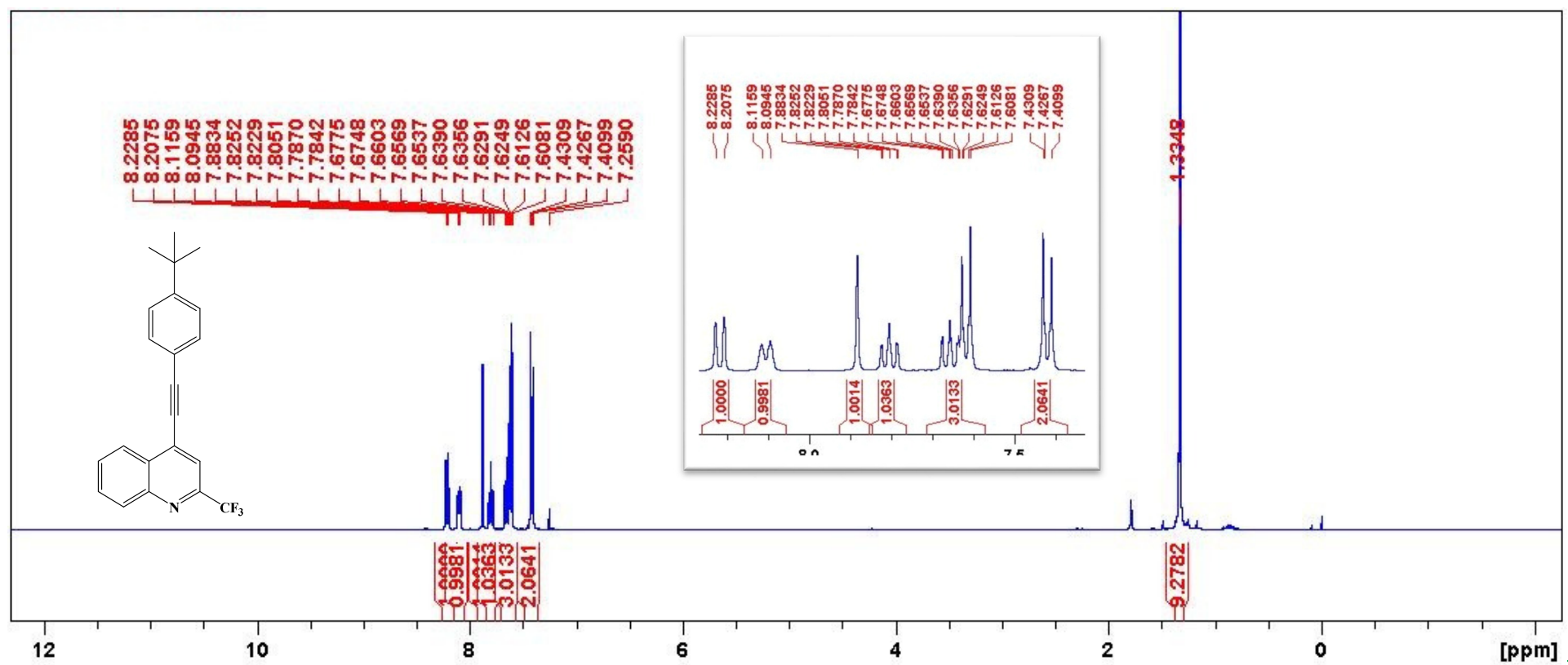
HMBC spectrum of **4b**

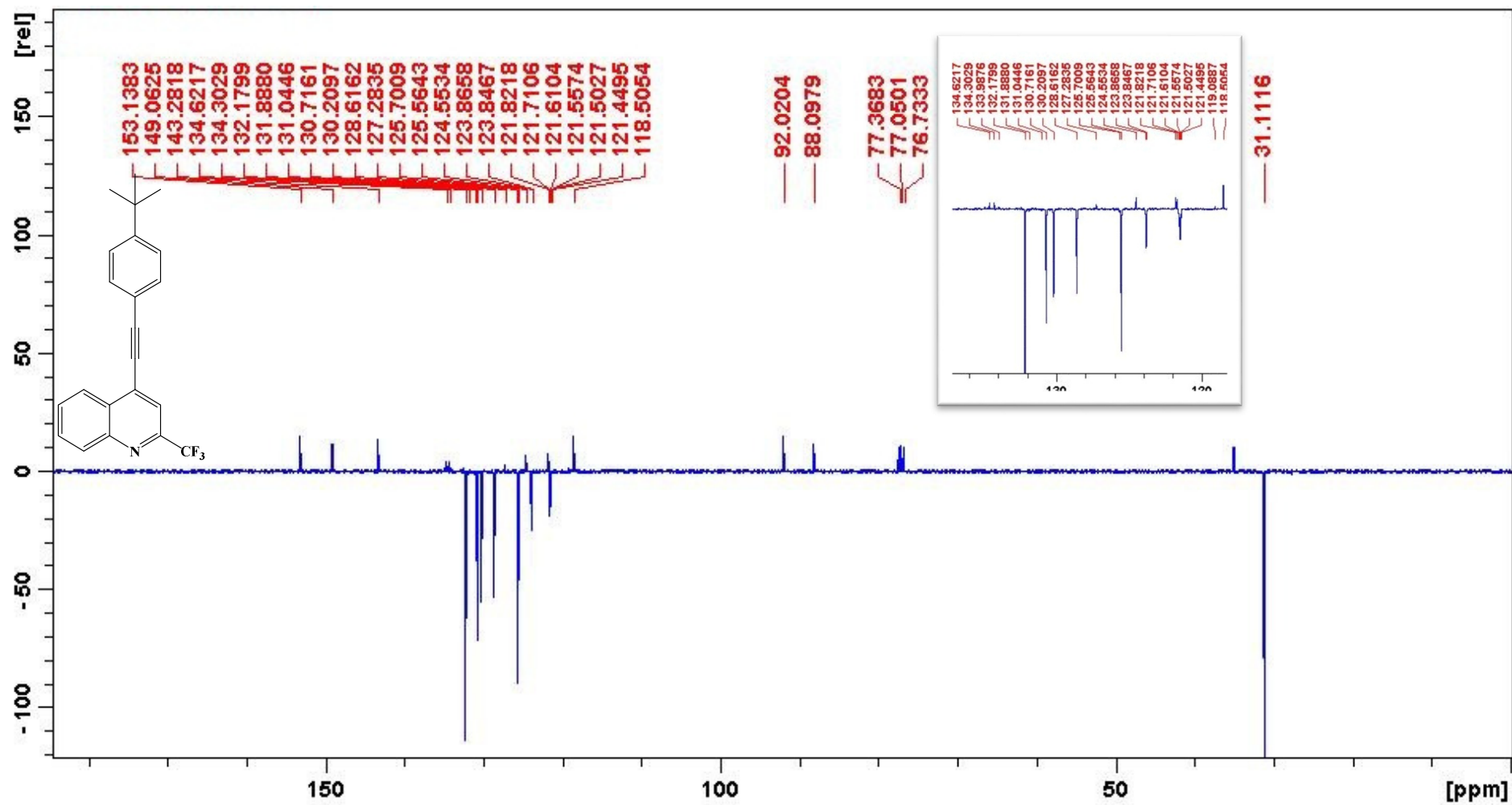
HRMS of **4b**

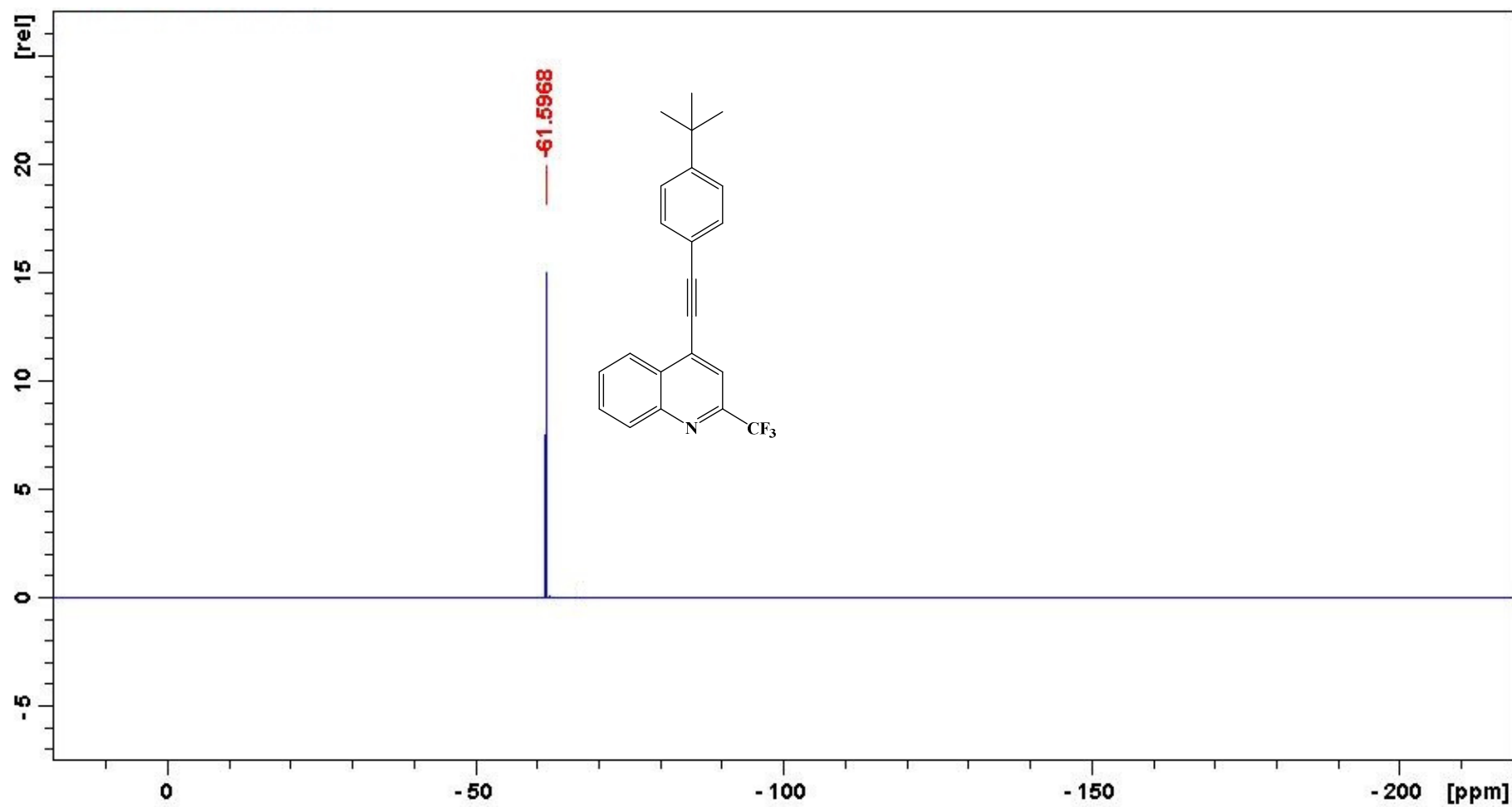
SA7

MS_Direct_151211_37 37 (0.179) Cm (37:40)

1: TOF MS ES+
8.57e4

¹H NMR spectrum of **4c**

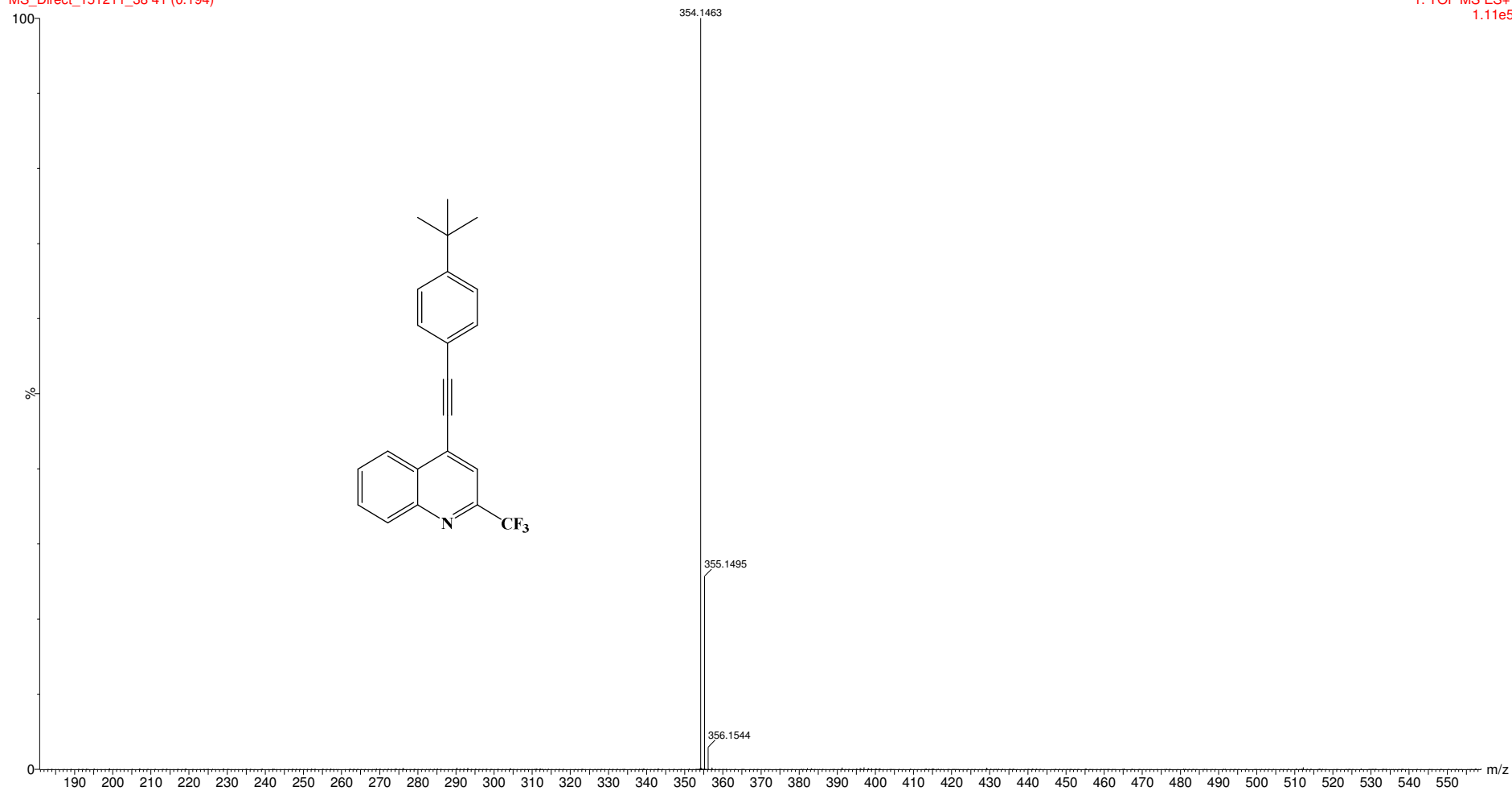
¹³C NMR spectrum of **4c**

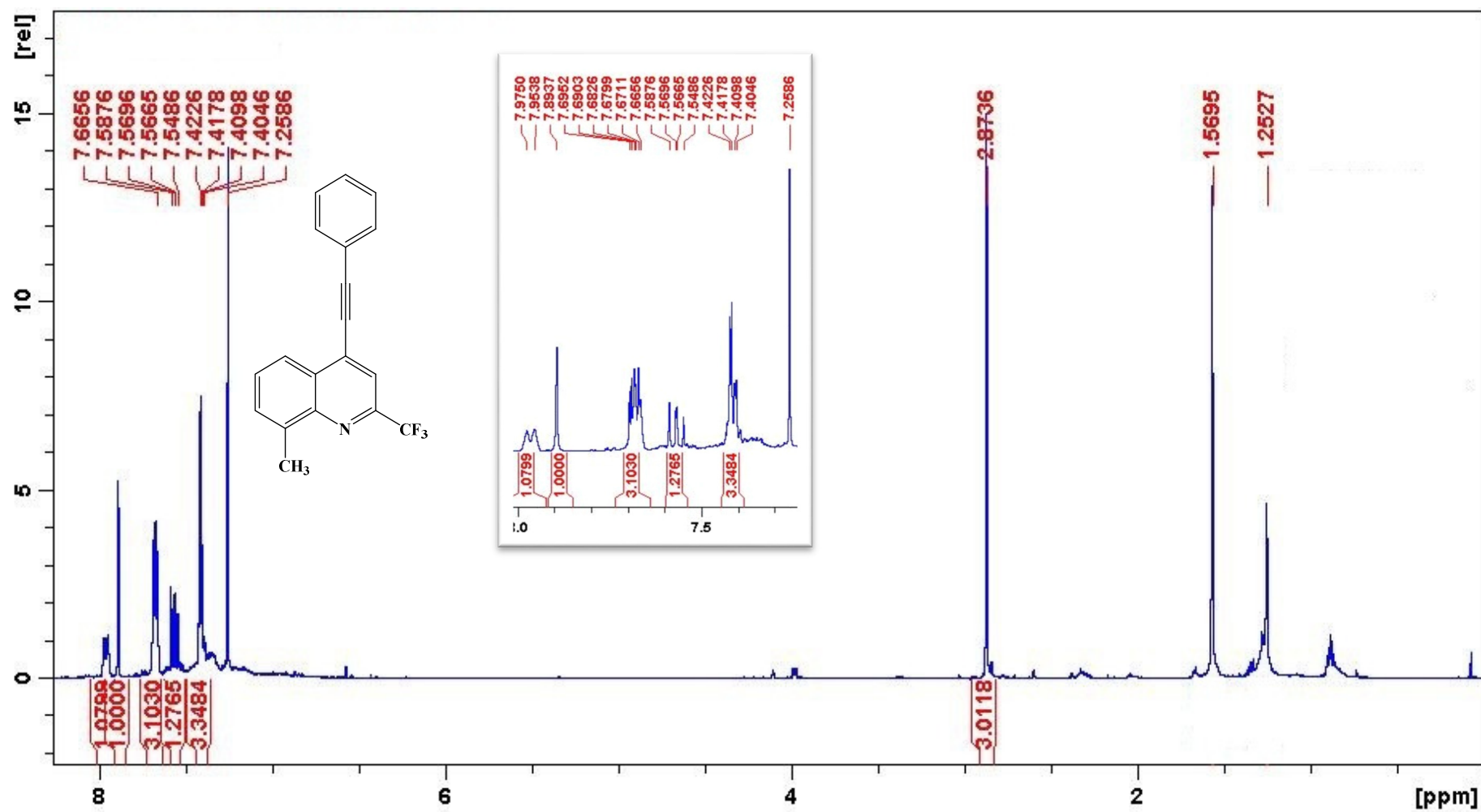
^{19}F NMR spectrum of **4c**

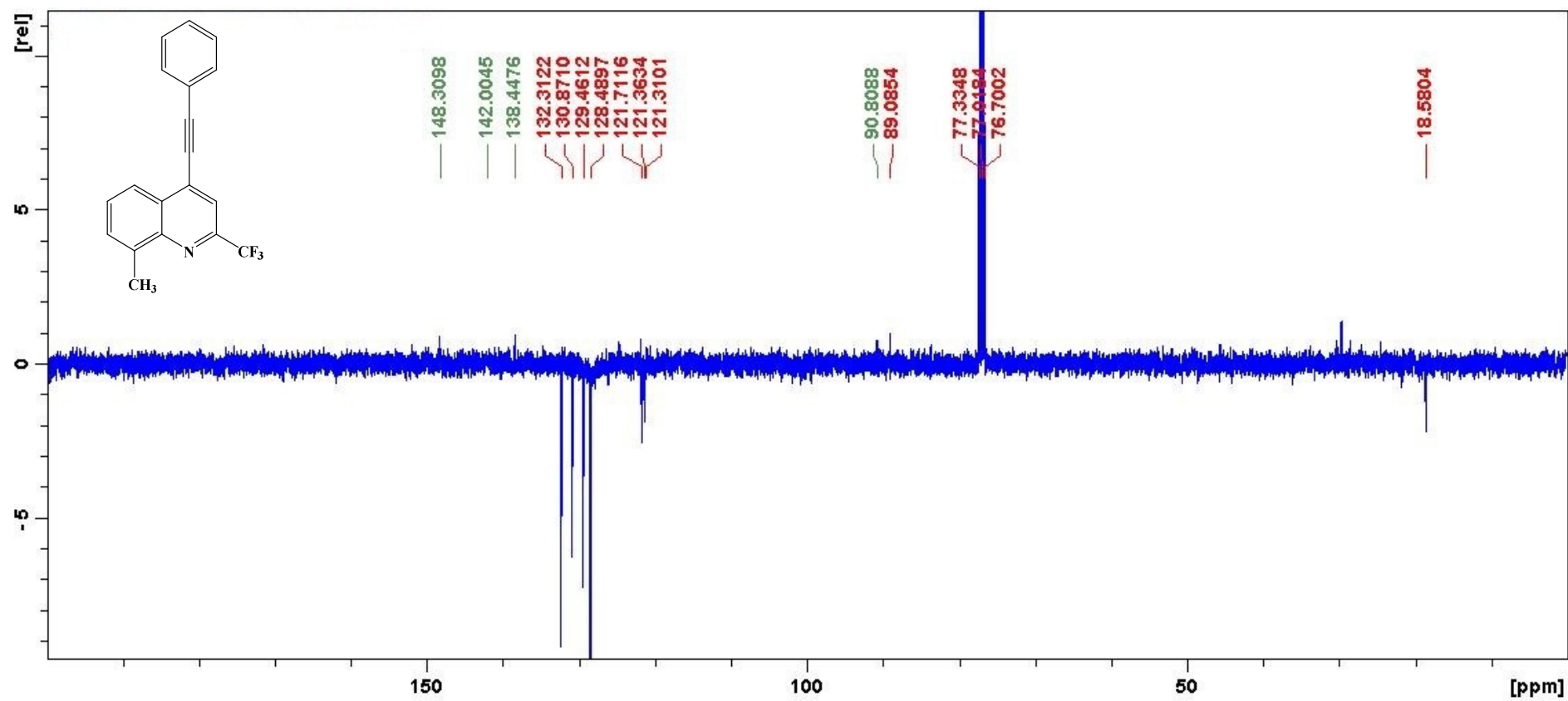
HRMS of **4c**

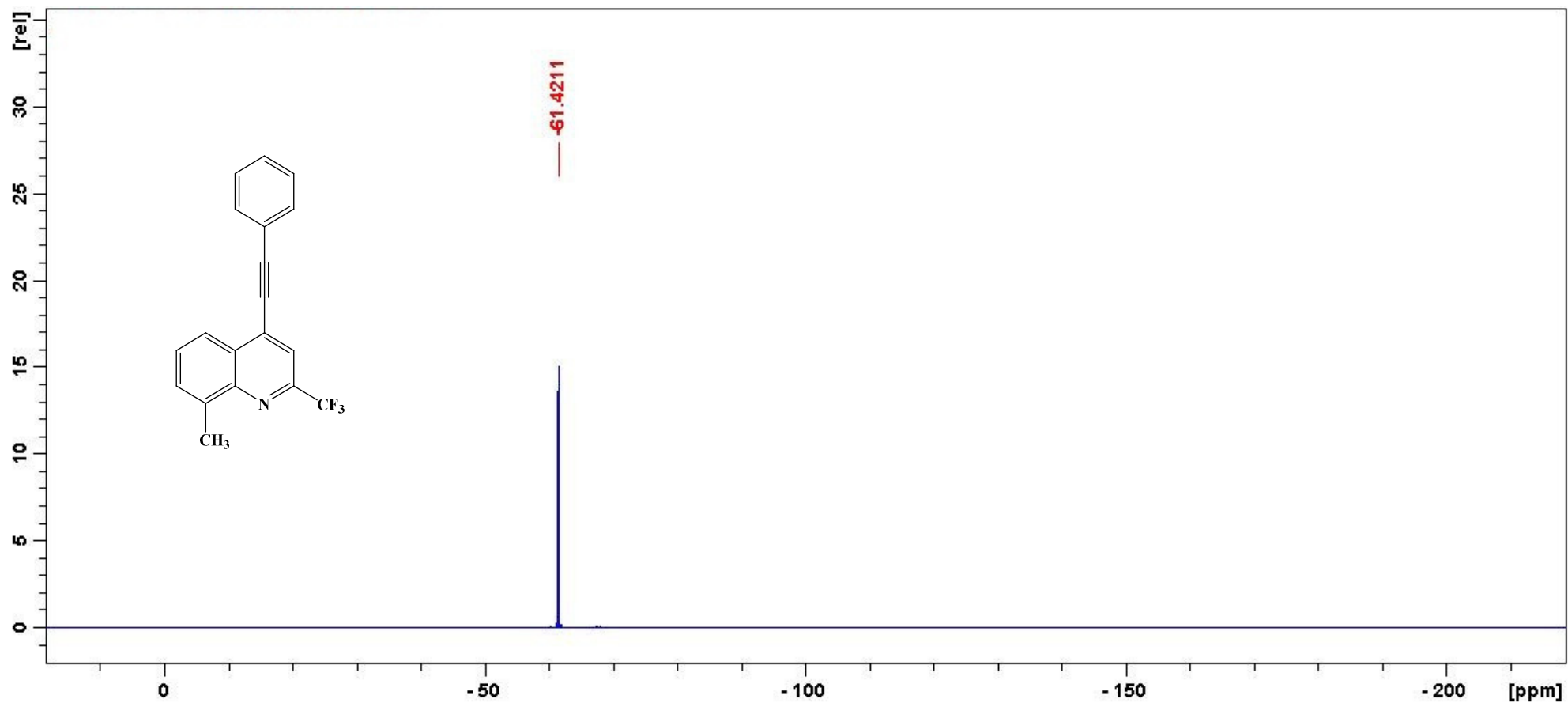
SA8

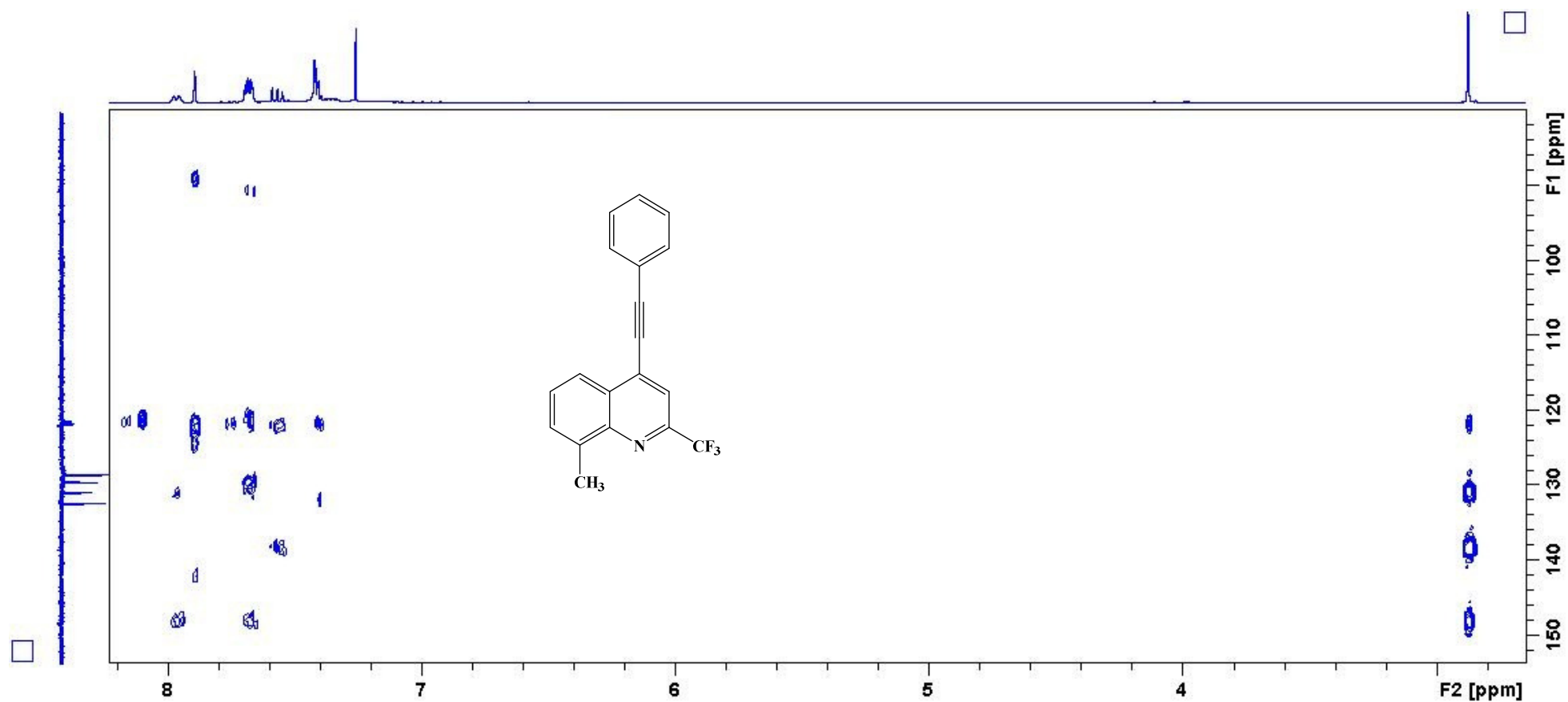
MS_Direct_151211_38.41 (0.194)

1: TOF MS ES+
1.11e5

¹H NMR spectrum of **4d**

^{13}C NMR spectrum of **4d**

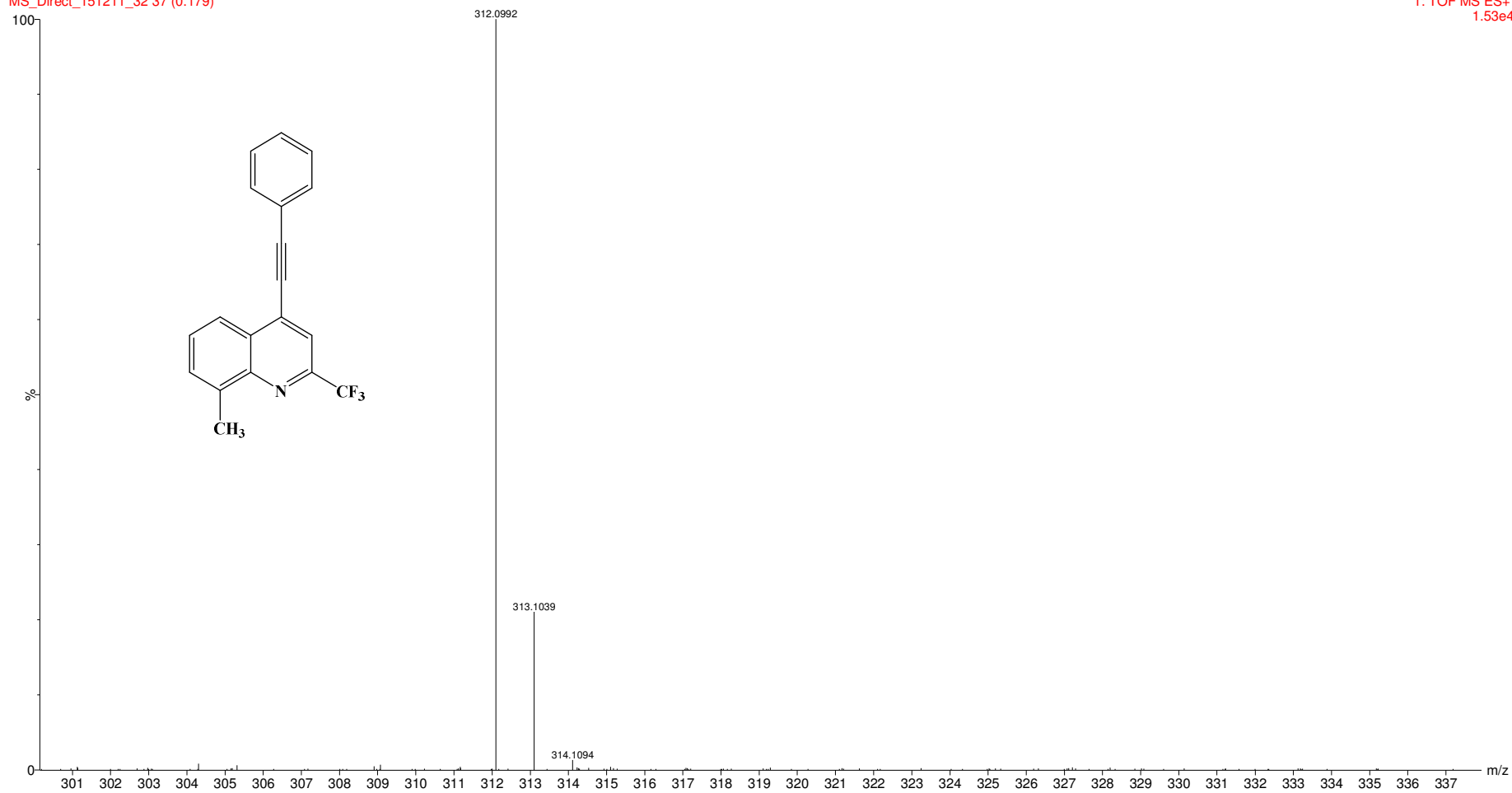
¹⁹F NMR spectrum of **4d**

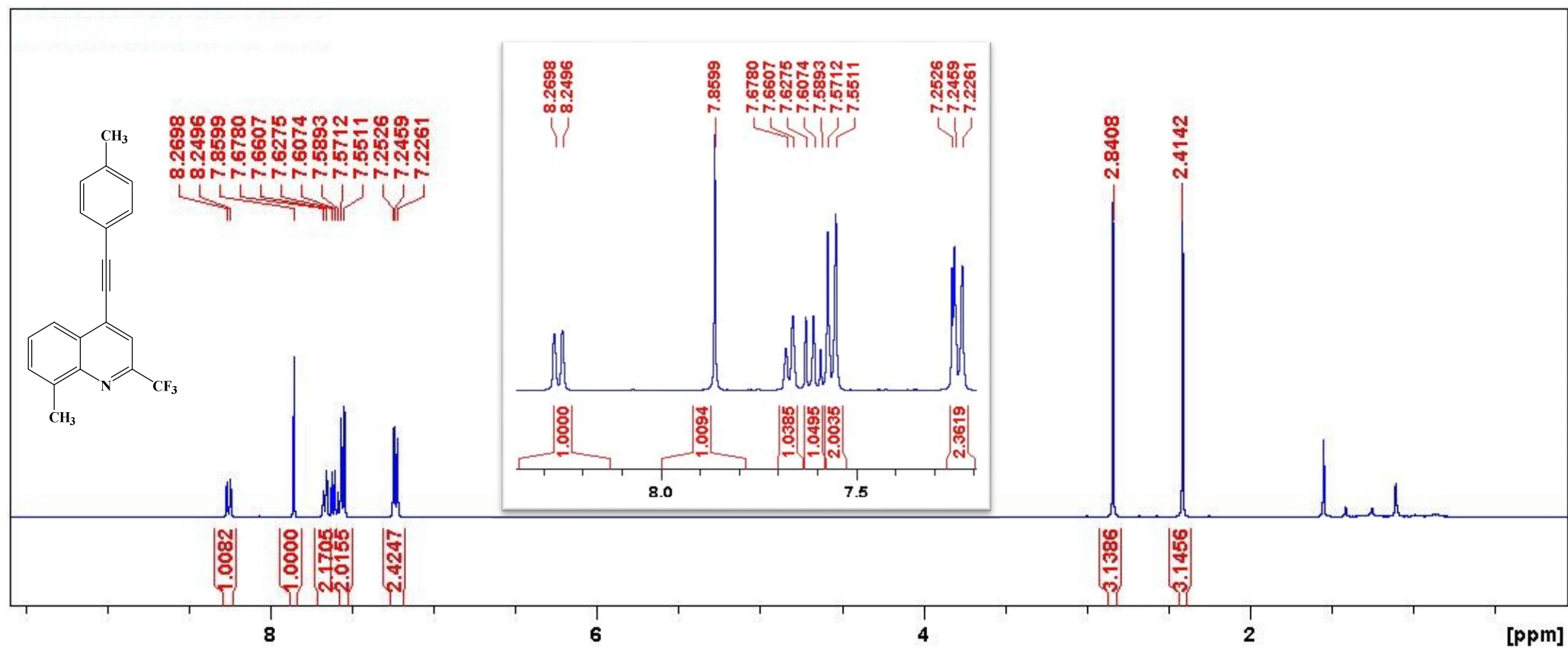
HMBC spectrum of **4d**

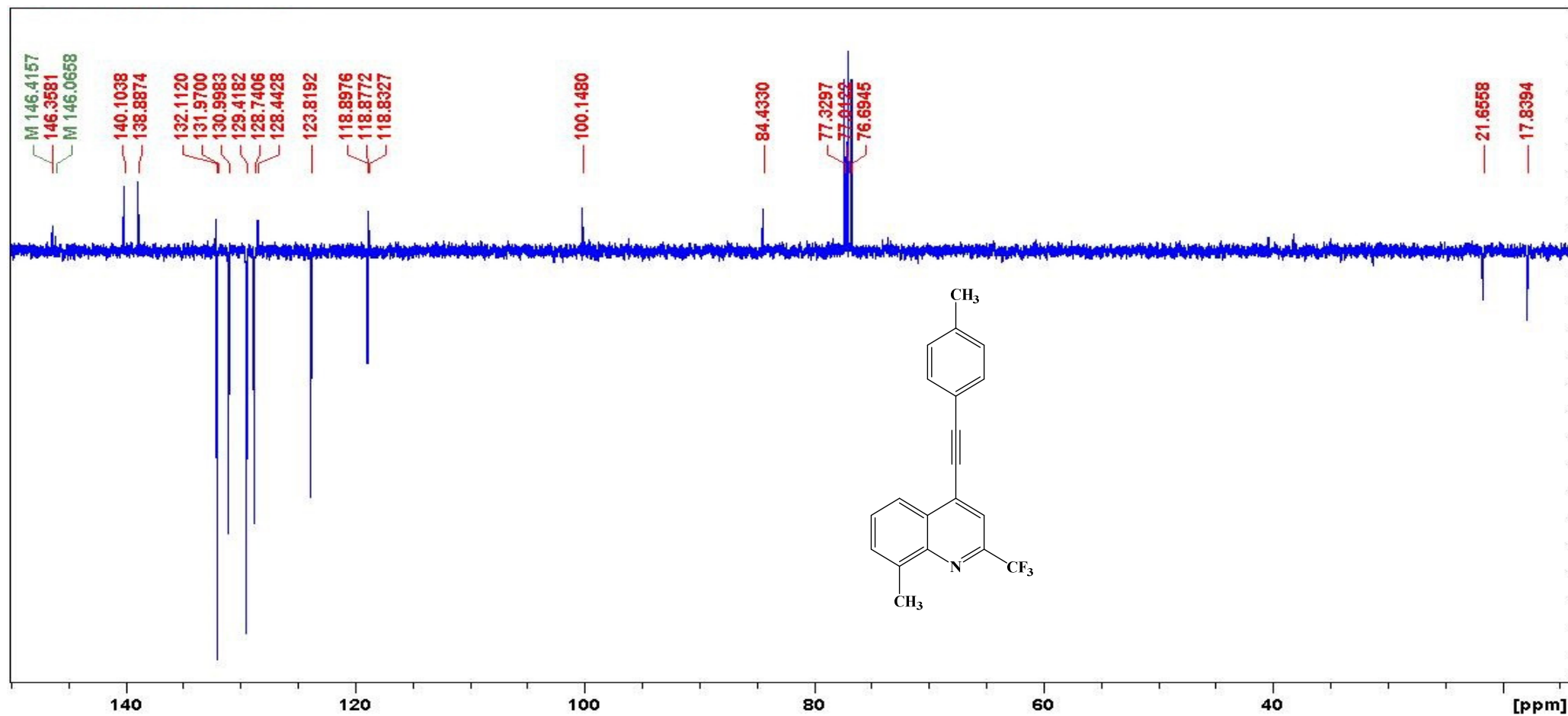
HRMS of **4d**

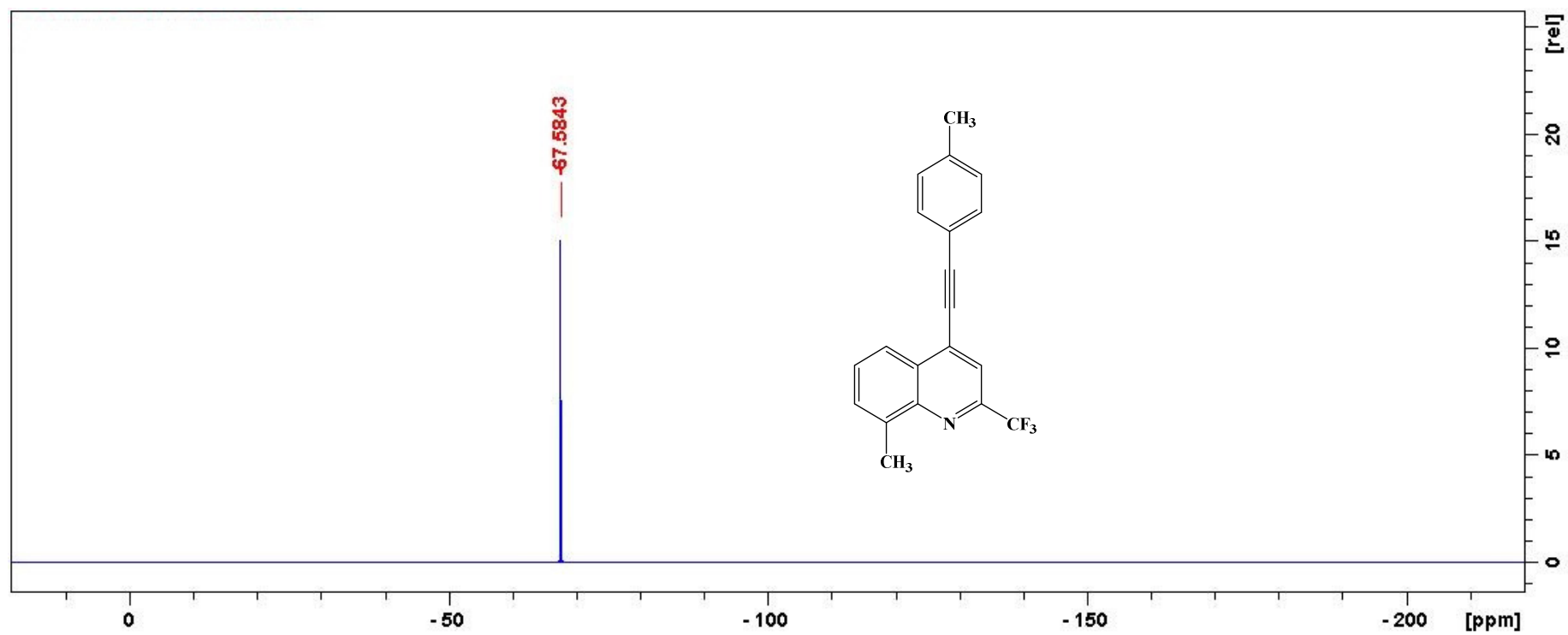
SA2

MS_Direct_151211_32 37 (0.179)

1: TOF MS ES+
1.53e4

¹H NMR spectrum of 4e

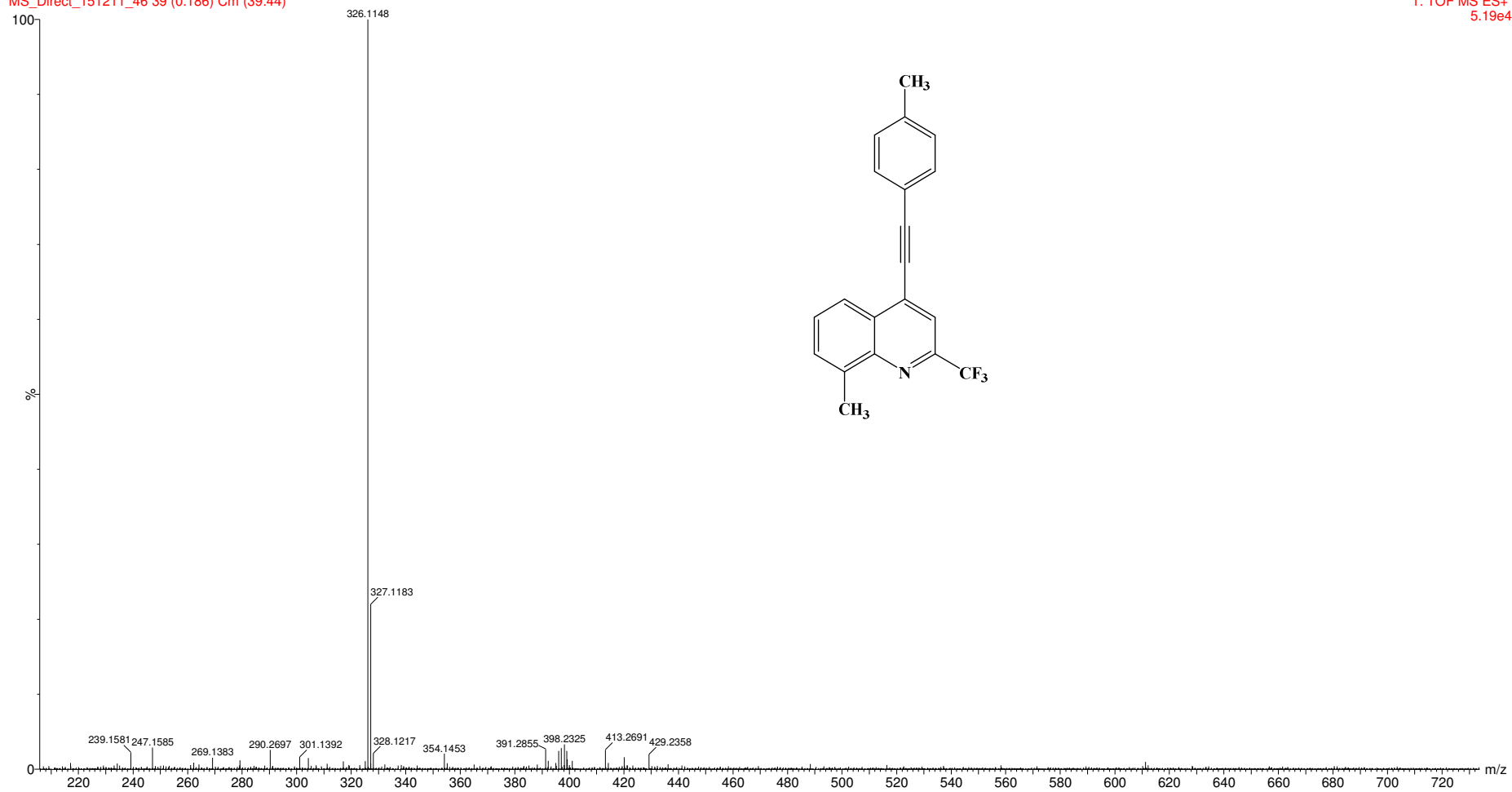
^{13}C NMR spectrum of **4e**

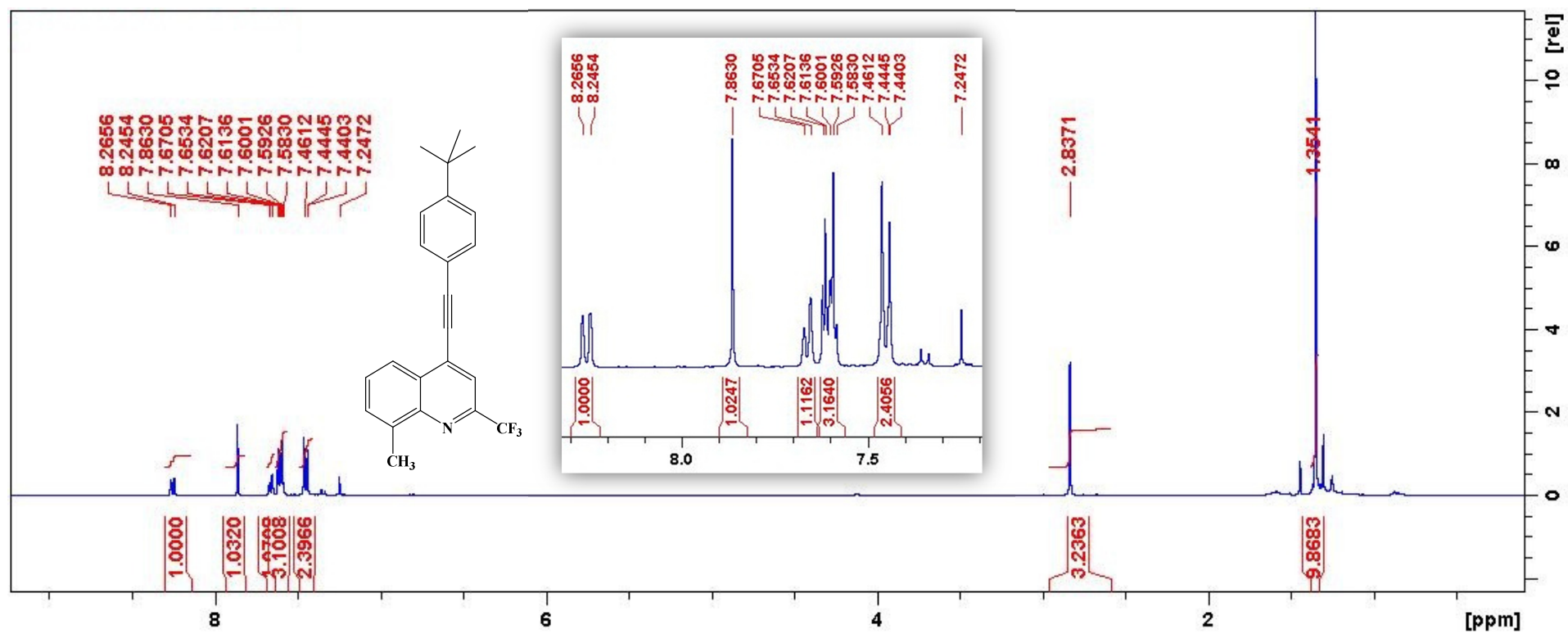
¹⁹F NMR spectrum of **4e**

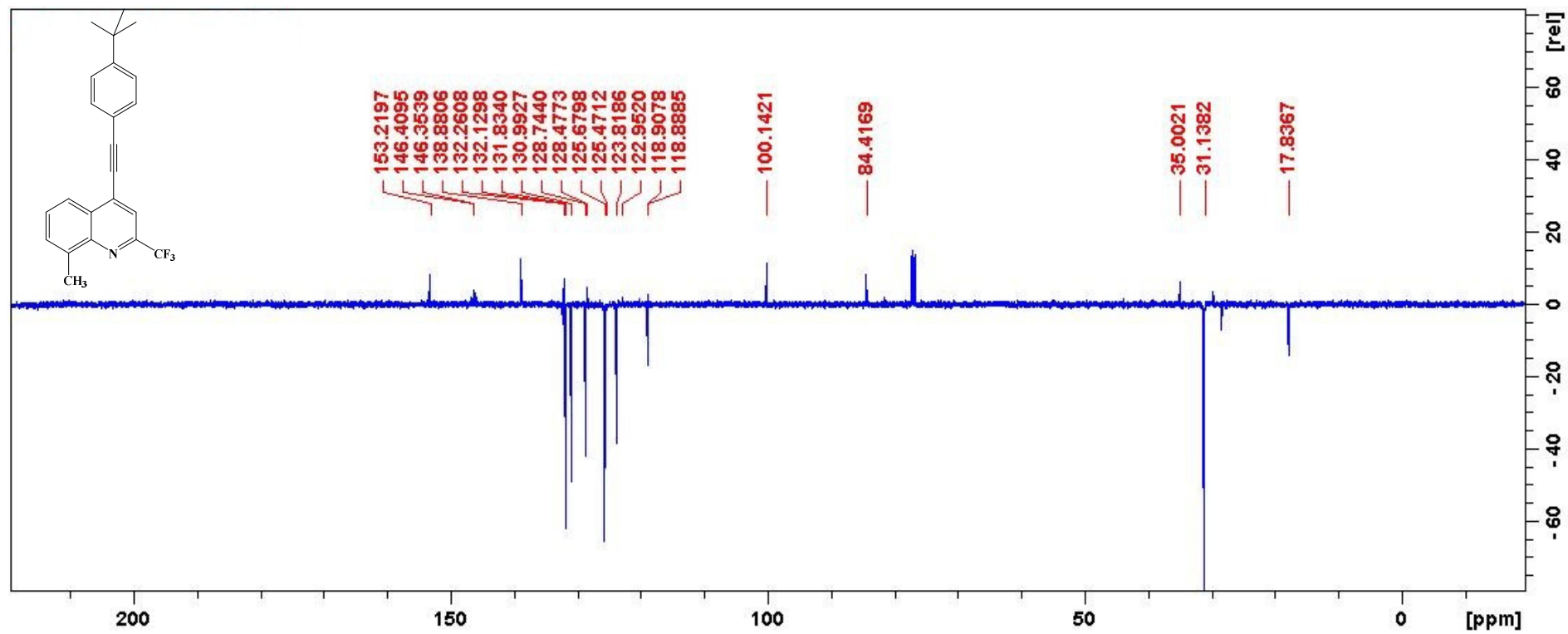
HRMS of 4e

SA25

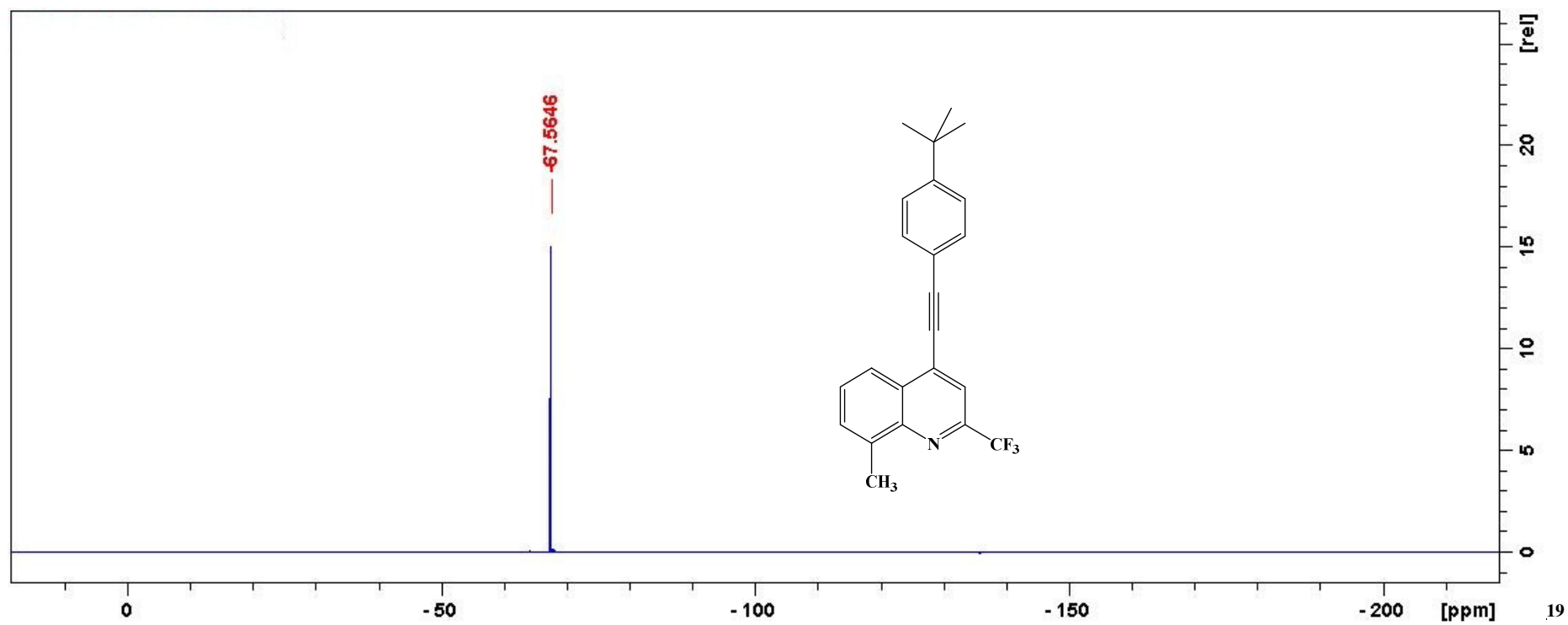
MS_Direct_151211_46 39 (0.186) Cm (39:44)

1: TOF MS ES+
5.19e4

¹H NMR spectrum of 4f

^{13}C NMR spectrum of **4f**

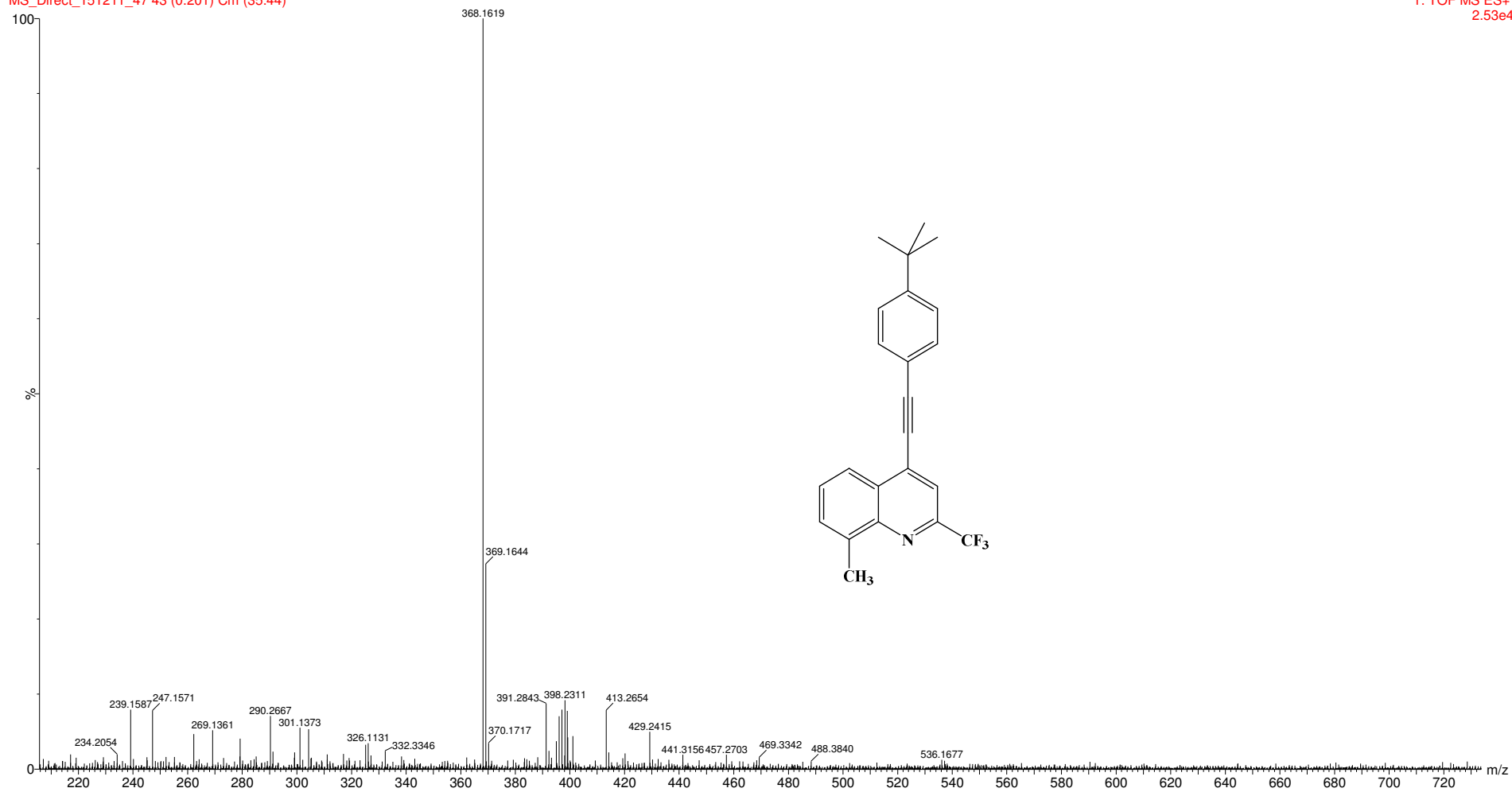
^{19}F NMR spectrum of **4f**

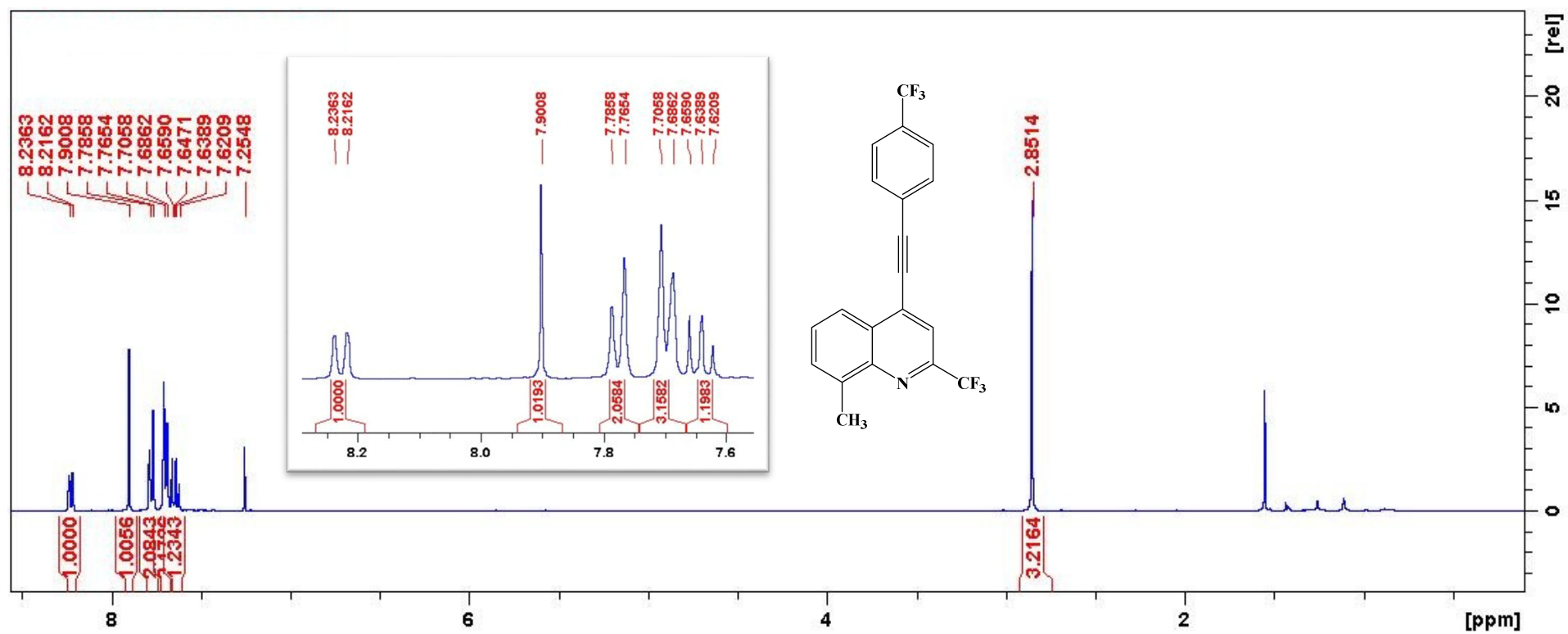


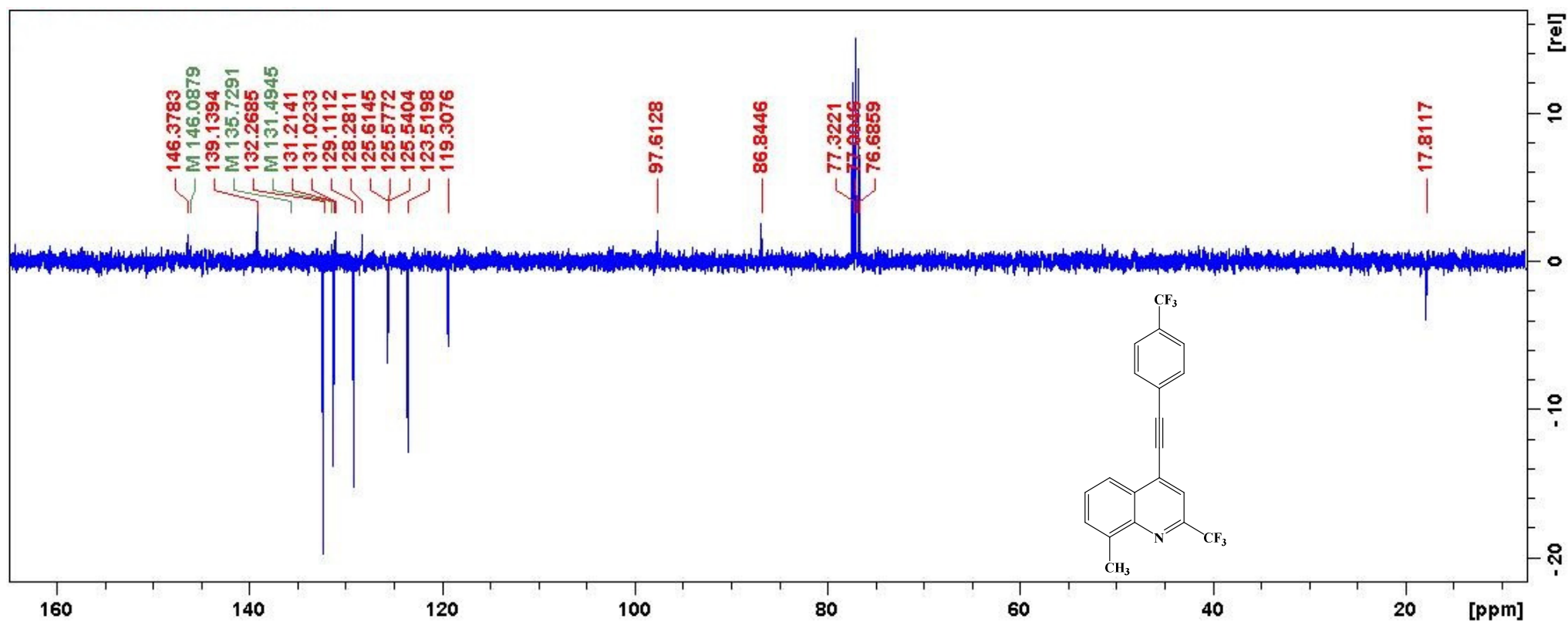
HRMS of 4f

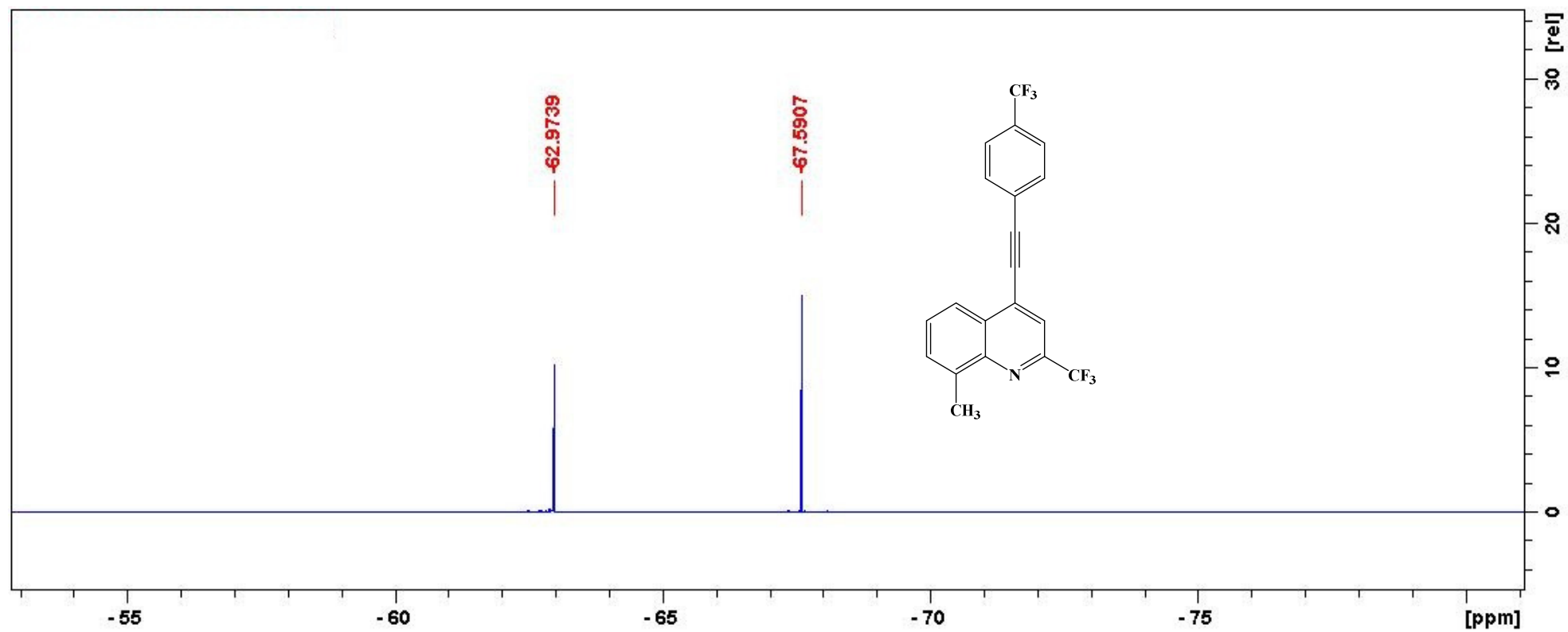
SA26

MS_Direct_151211_47 43 (0.201) Cm (35:44)

1: TOF MS ES+
2.53e4

¹H NMR spectrum of **4g**

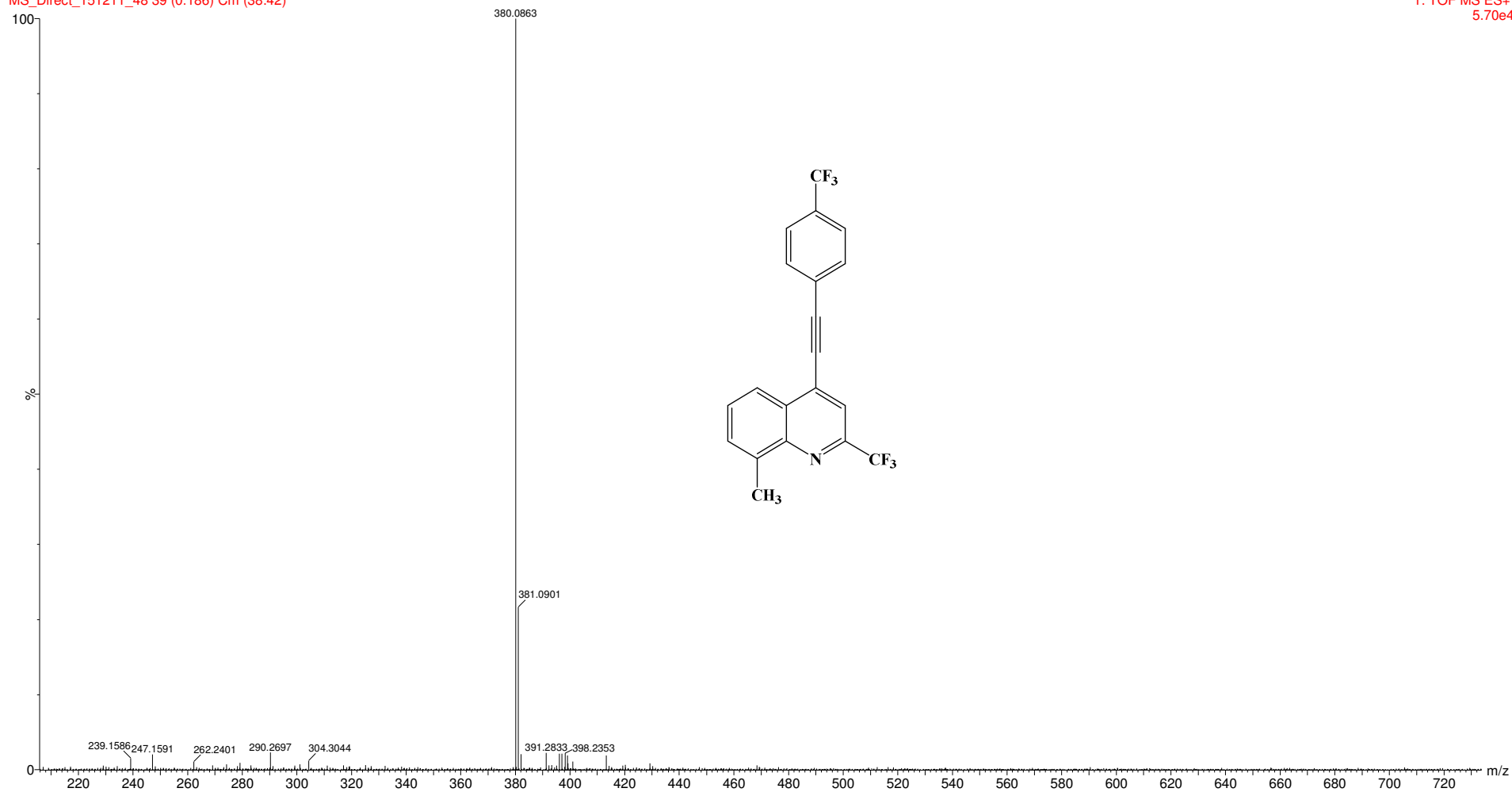
^{13}C NMR spectrum of **4g**

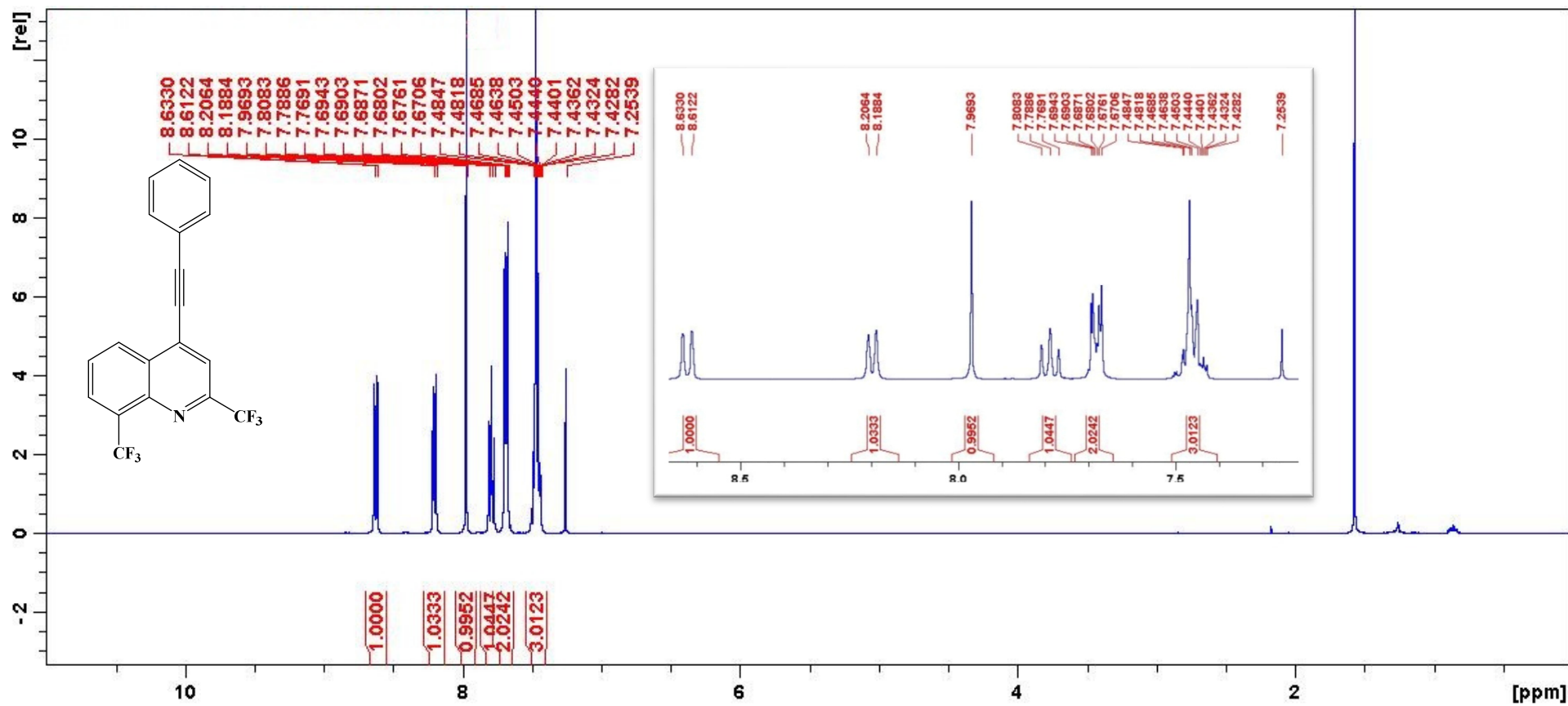
^{19}F NMR spectrum of **4g**

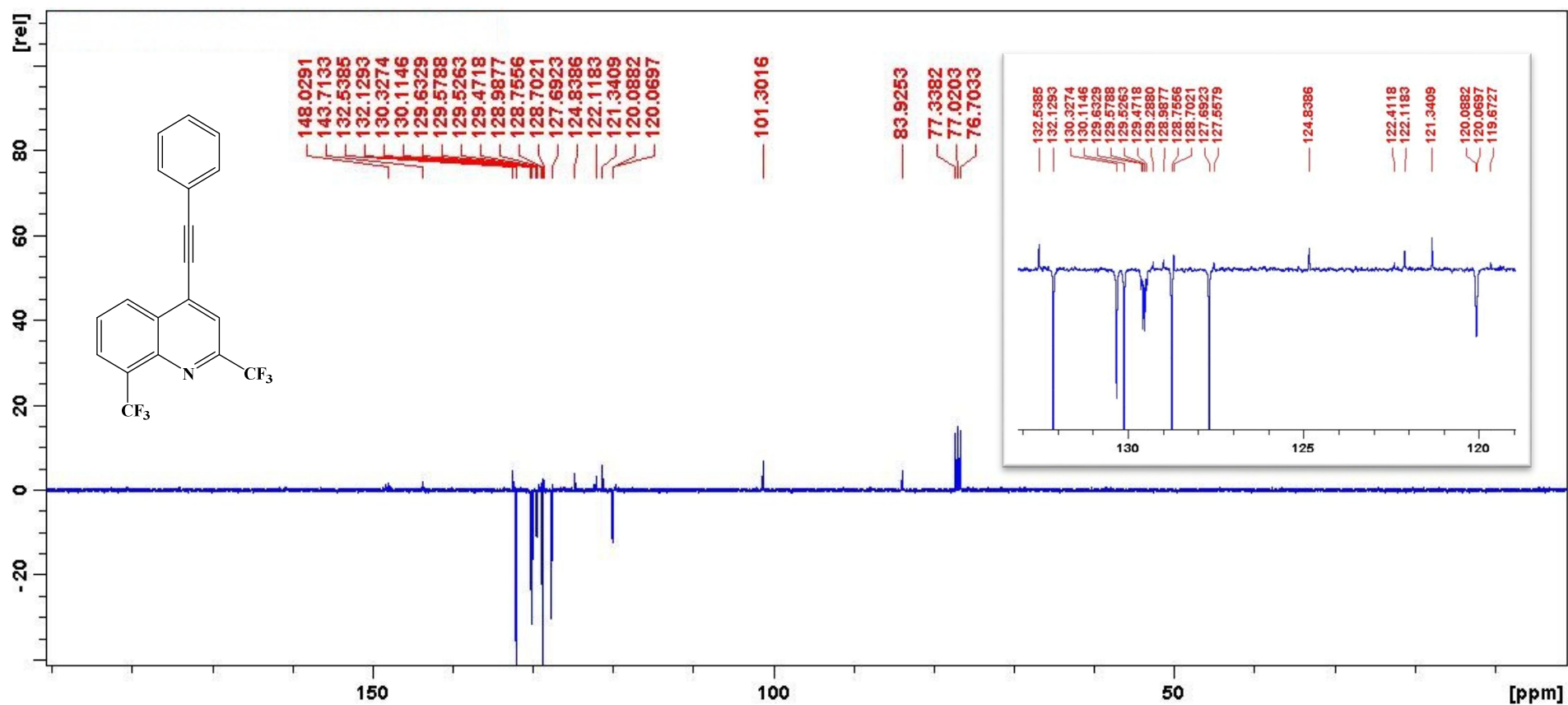
HRMS of 4g

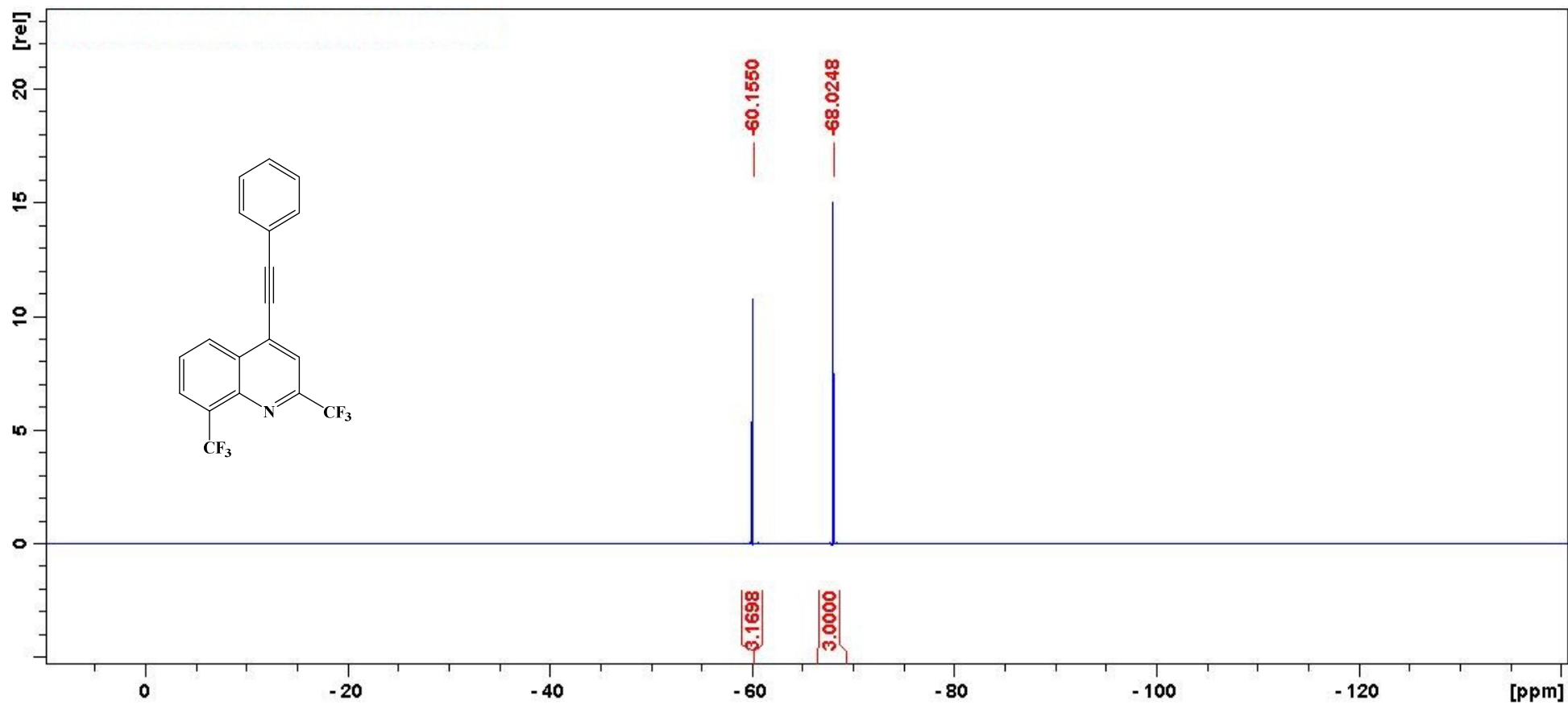
SA27

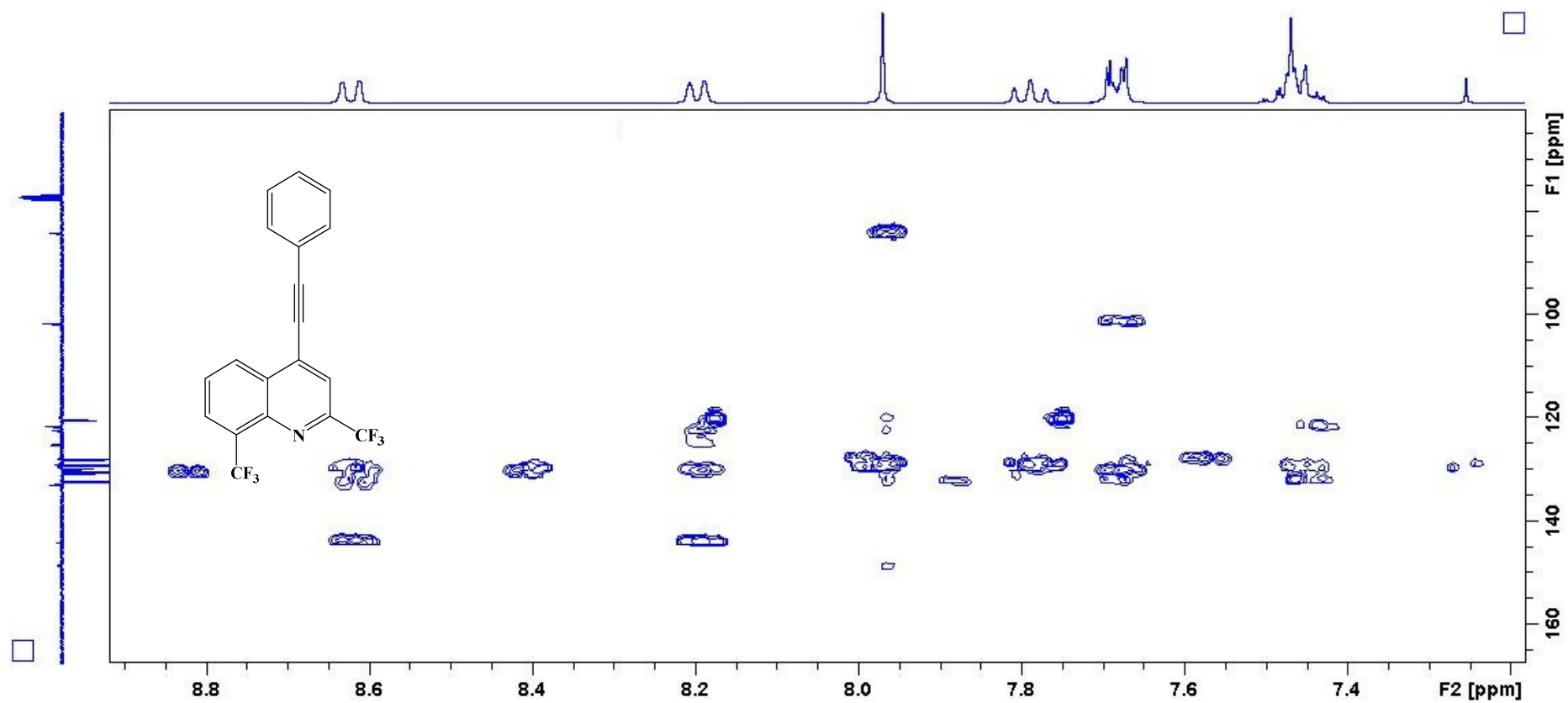
MS_Direct_151211_48 39 (0.186) Cm (38:42)

1: TOF MS ES+
5.70e4

¹H NMR spectrum of **4h**

^{13}C NMR spectrum of **4h**

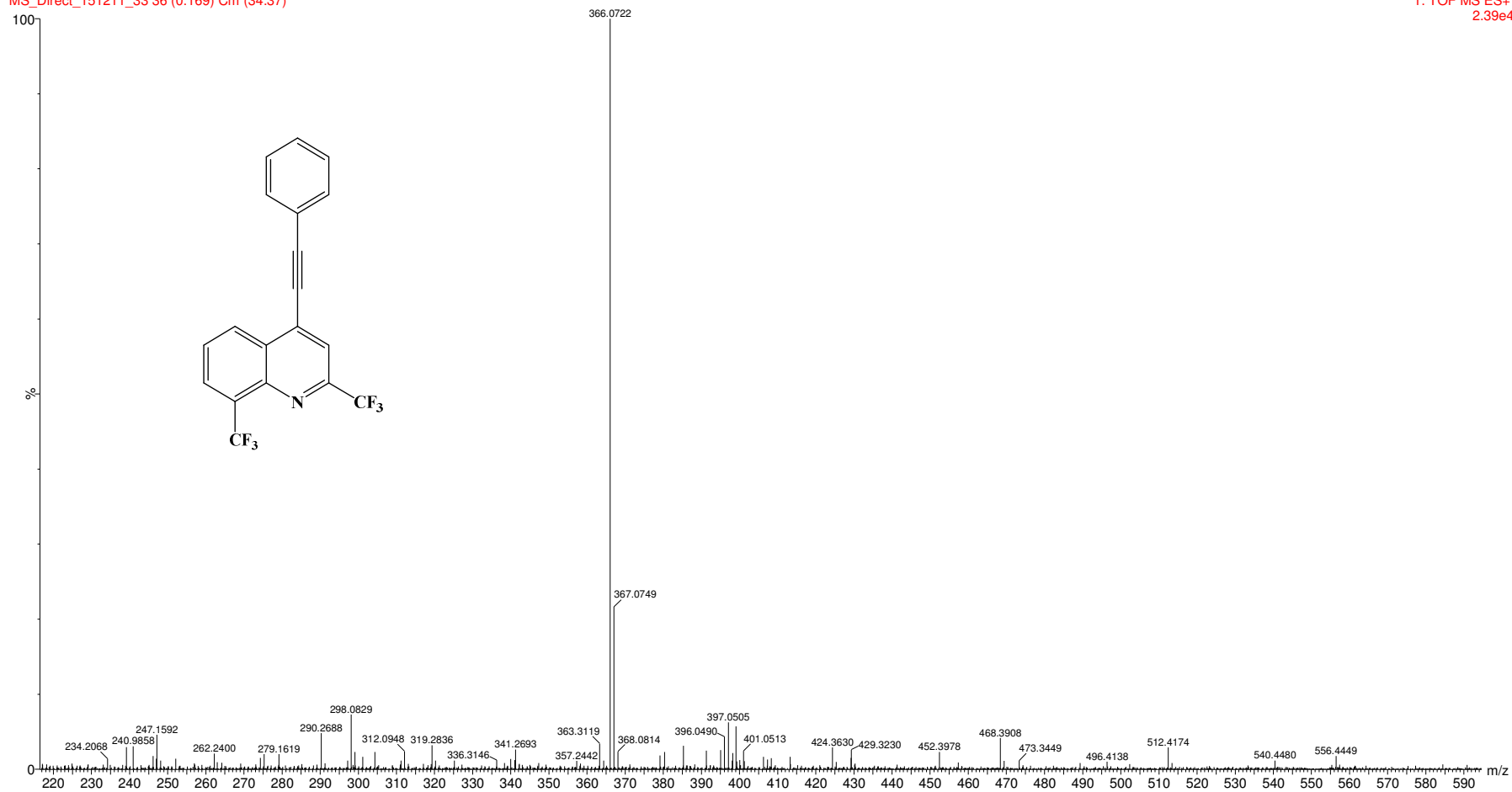
¹⁹F NMR spectrum of **4h**

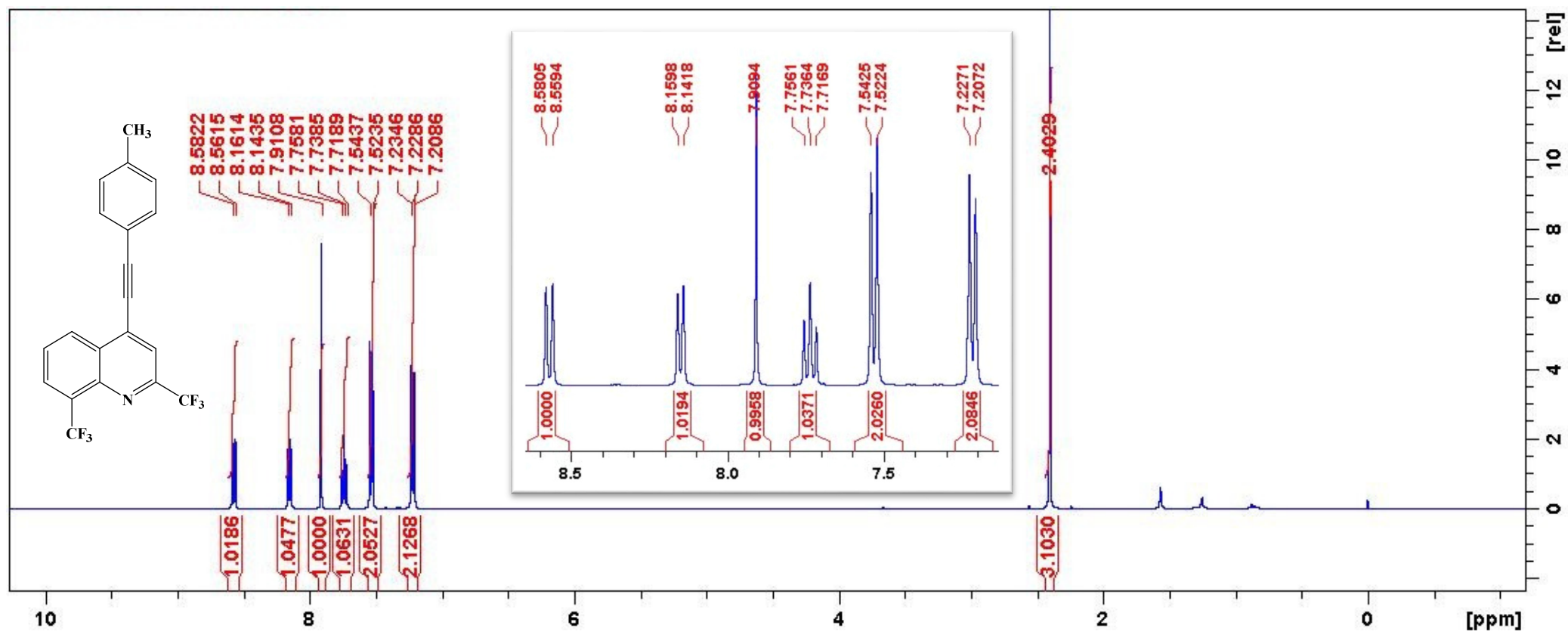
HMBC spectrum of **4h**

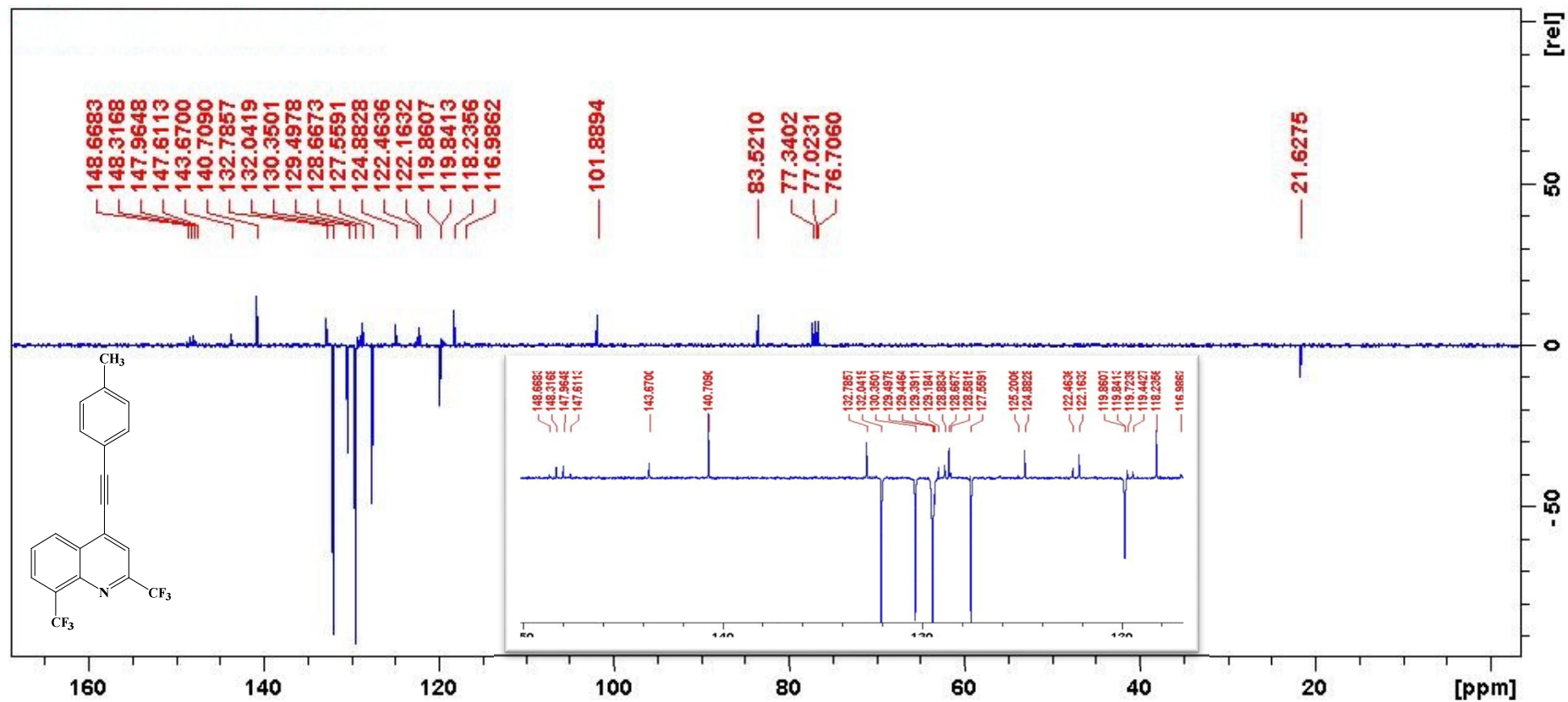
HRMS of **4h**

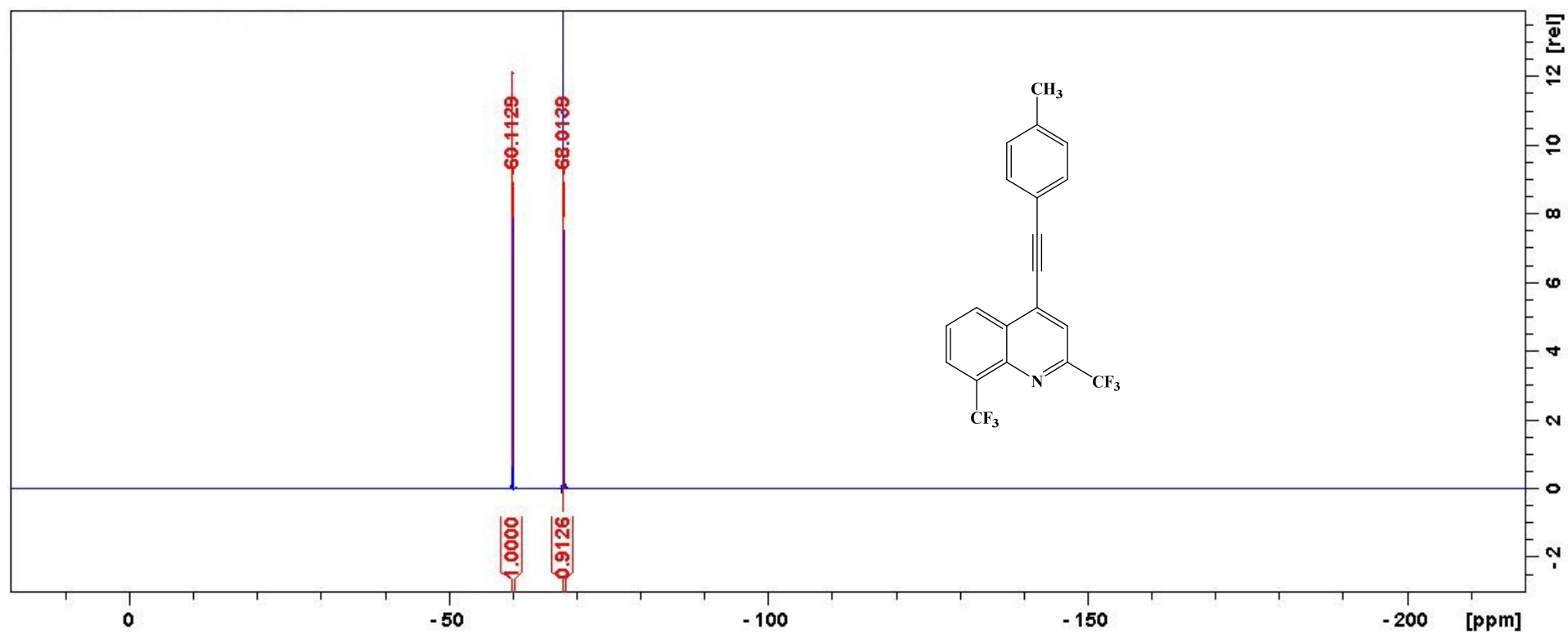
SA3

MS_Direct_151211_33_36 (0.169) Cm (34:37)

1: TOF MS ES+
2.39e4

¹H NMR spectrum of **4i**

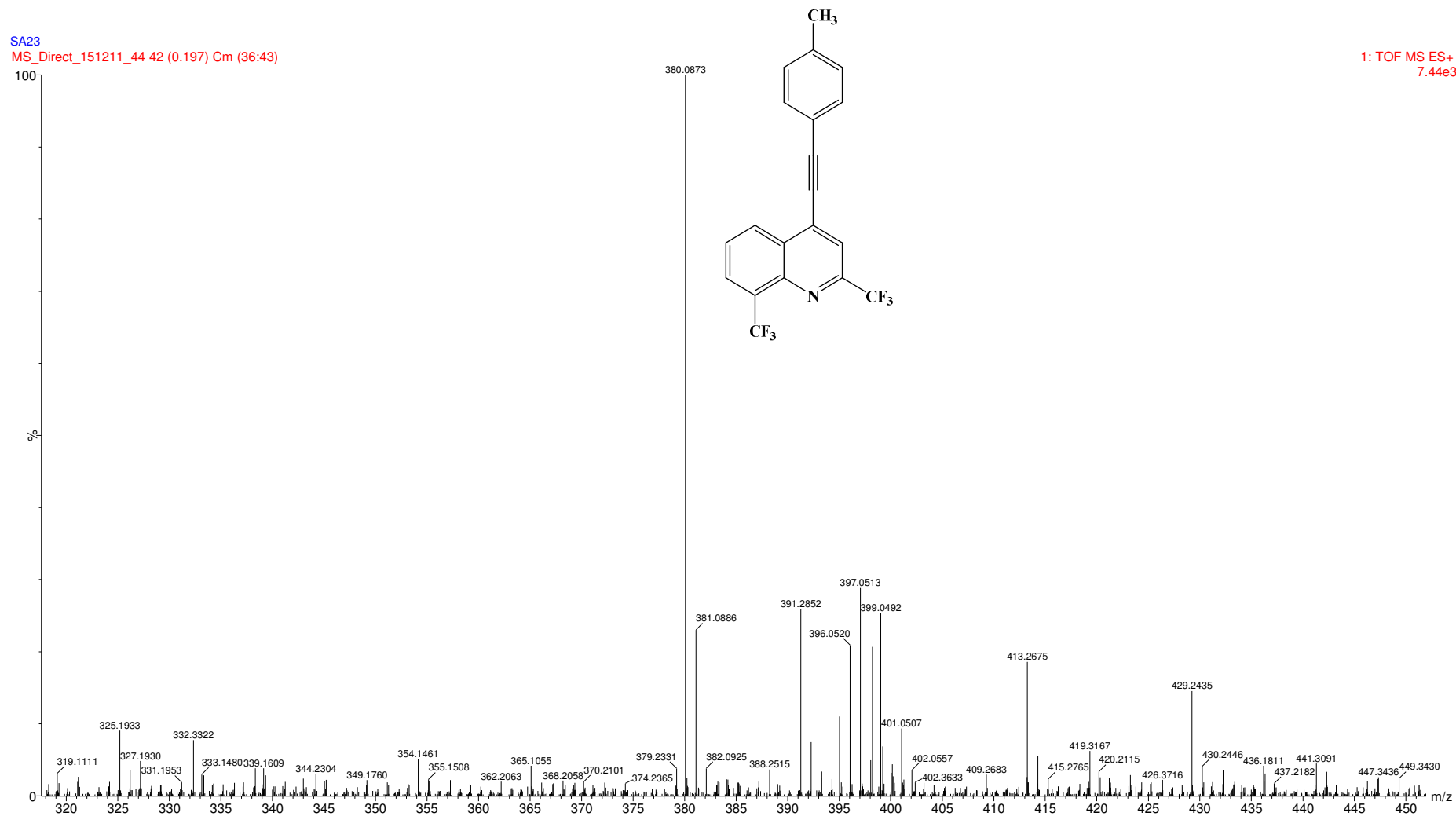
^{13}C NMR spectrum of **4i**

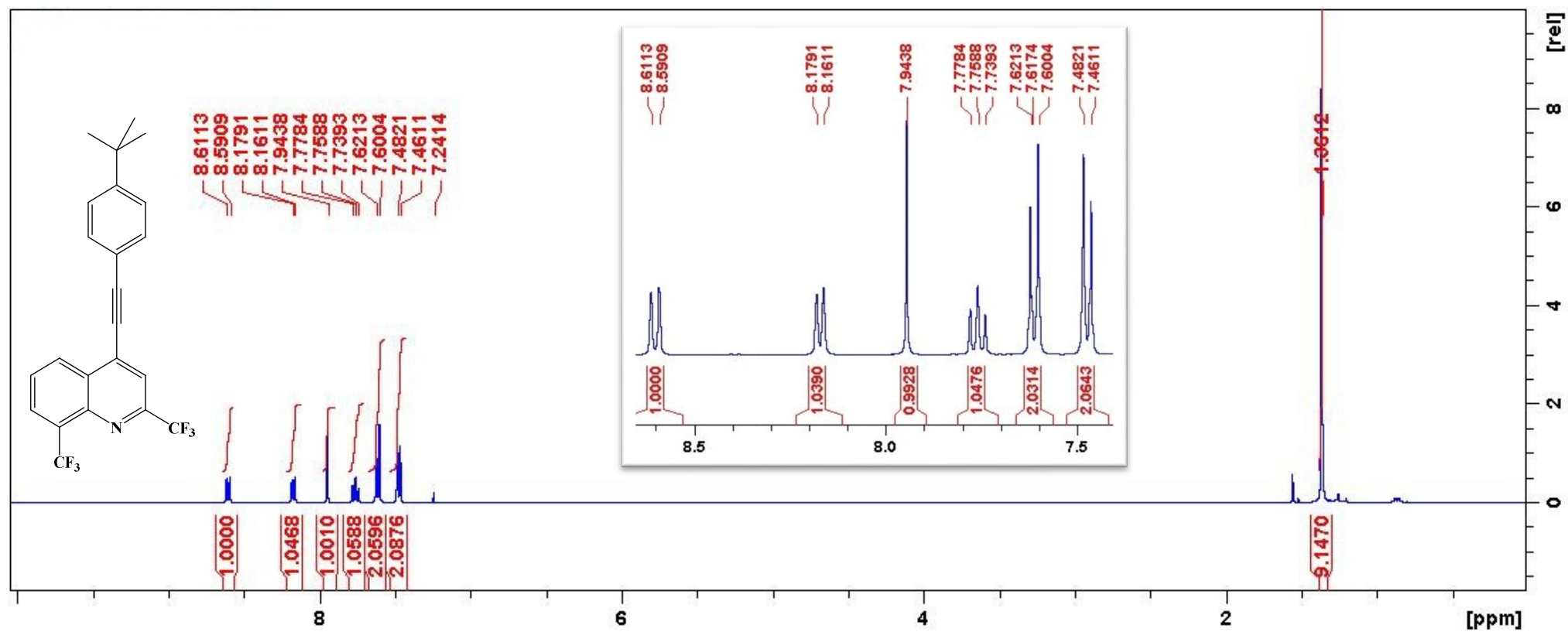
^{19}F NMR spectrum of **4i**

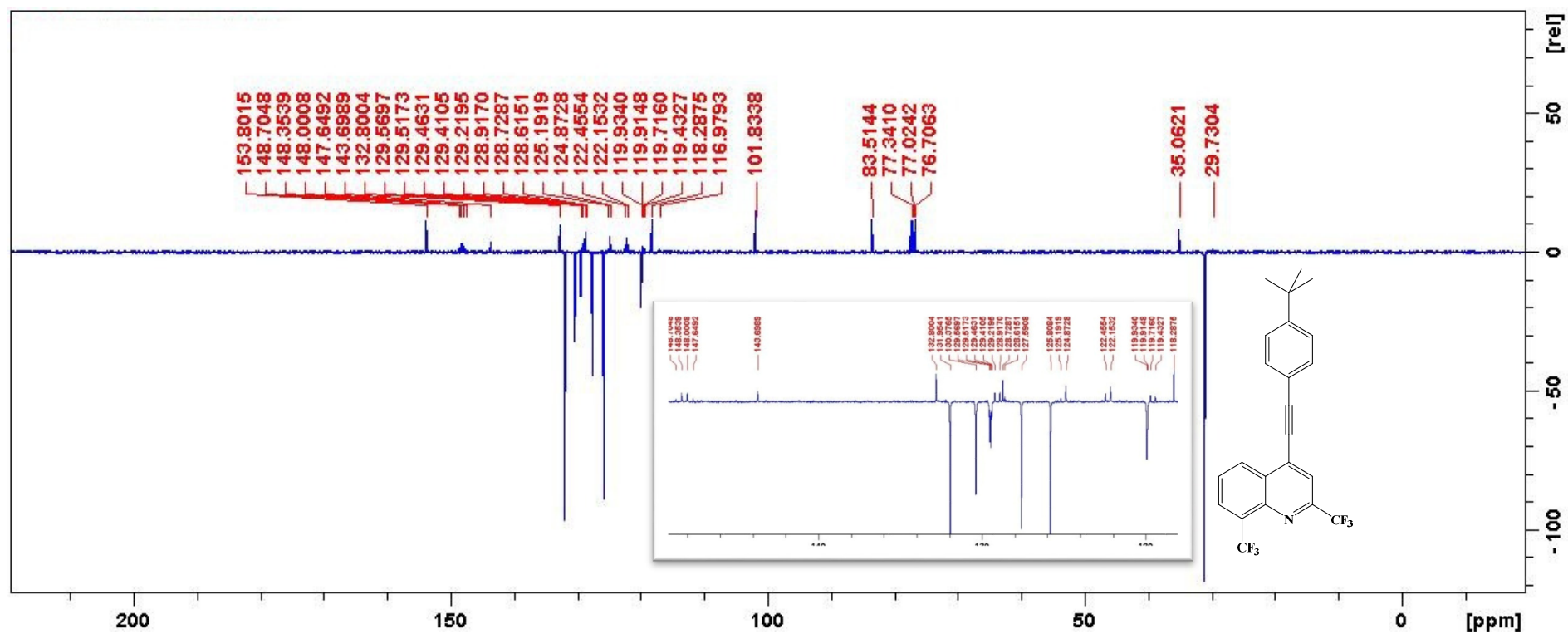
HRMS of 4i

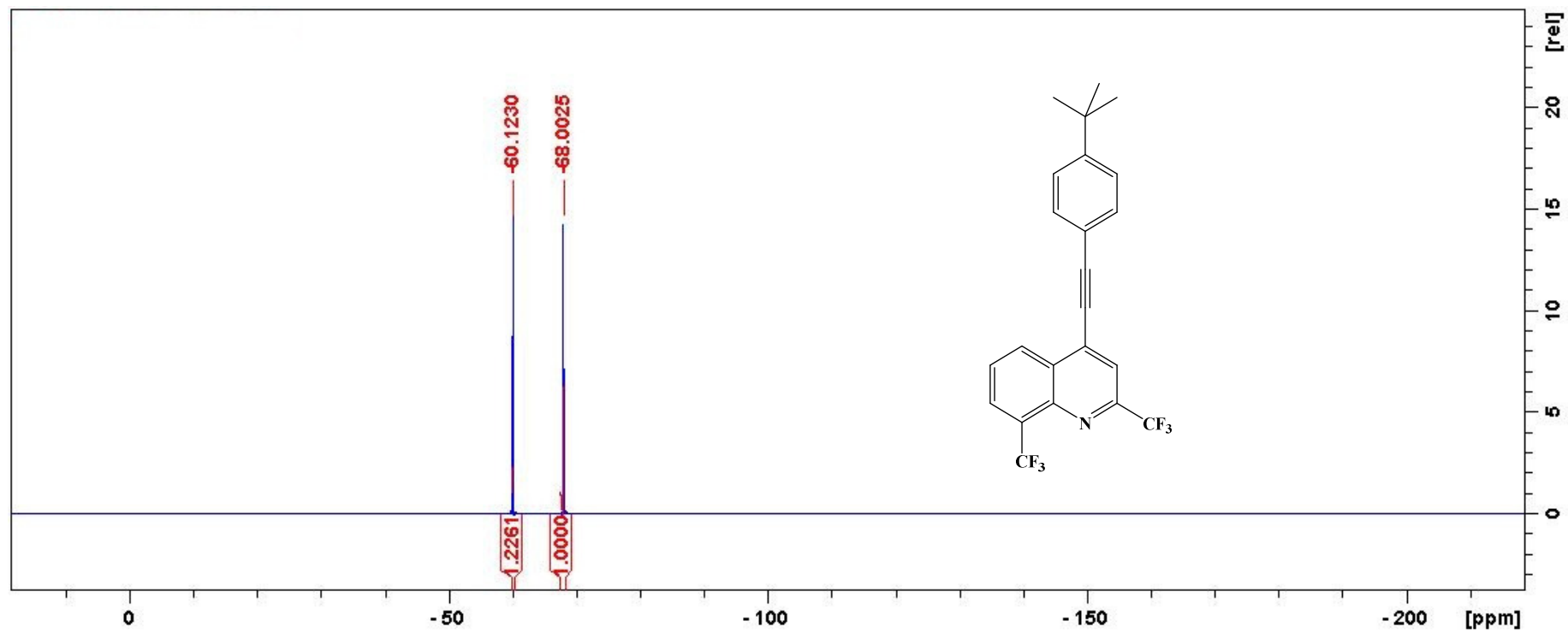
SA23

MS_Direct_151211_44 42 (0.197) Cm (36:43)

1: TOF MS ES+
7.44e3

¹H NMR spectrum of 4j

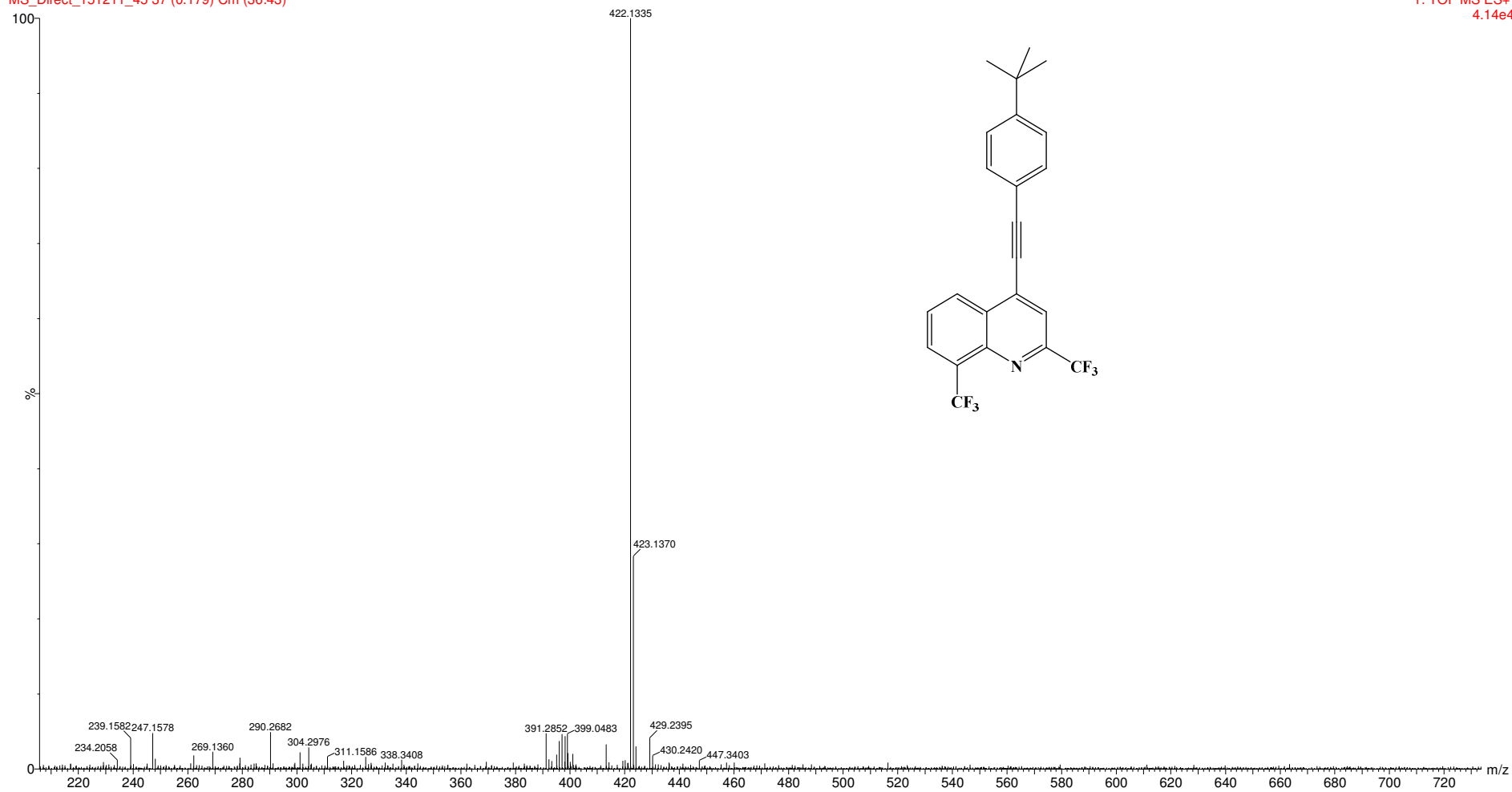
^{13}C NMR spectrum of **4j**

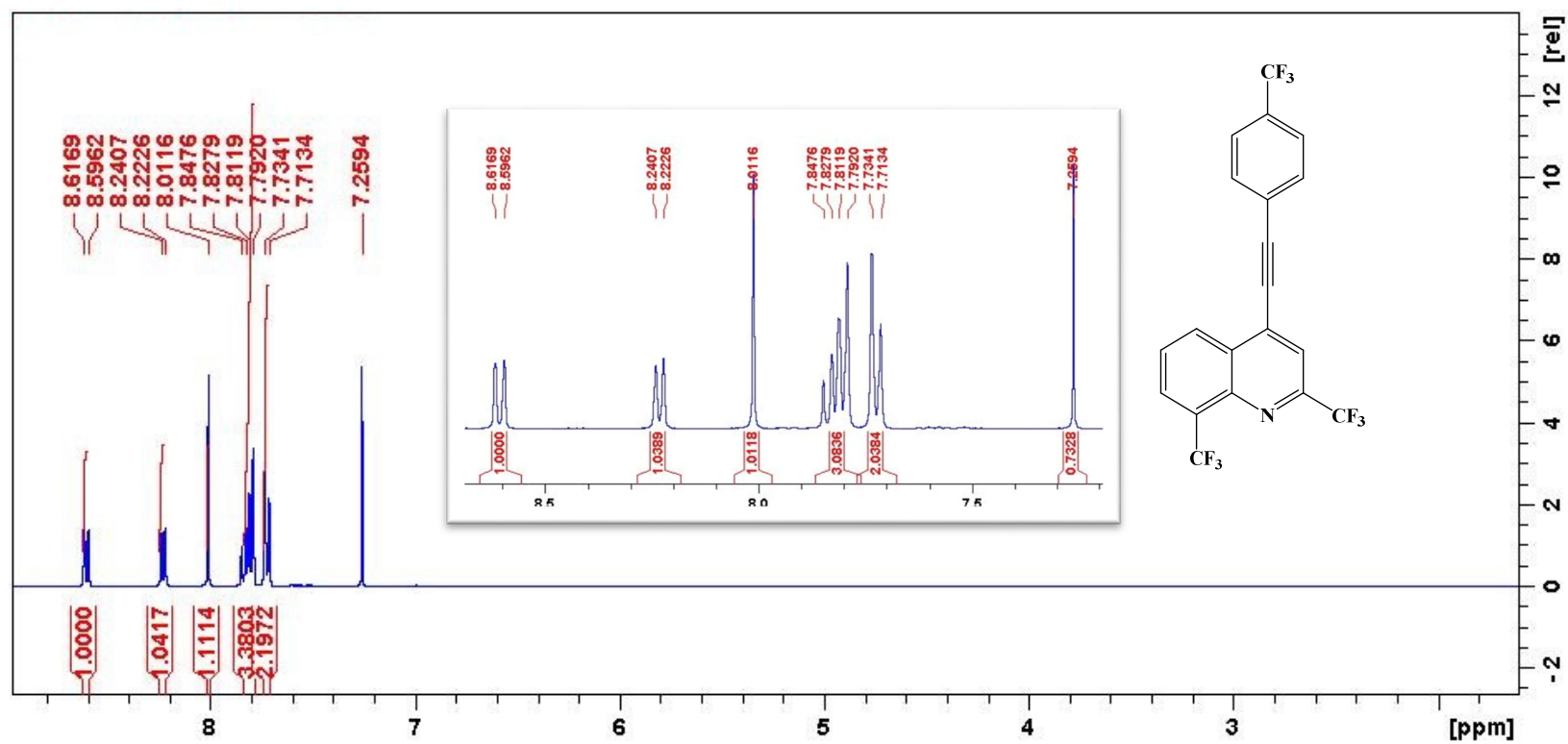
¹⁹F NMR spectrum of **4j**

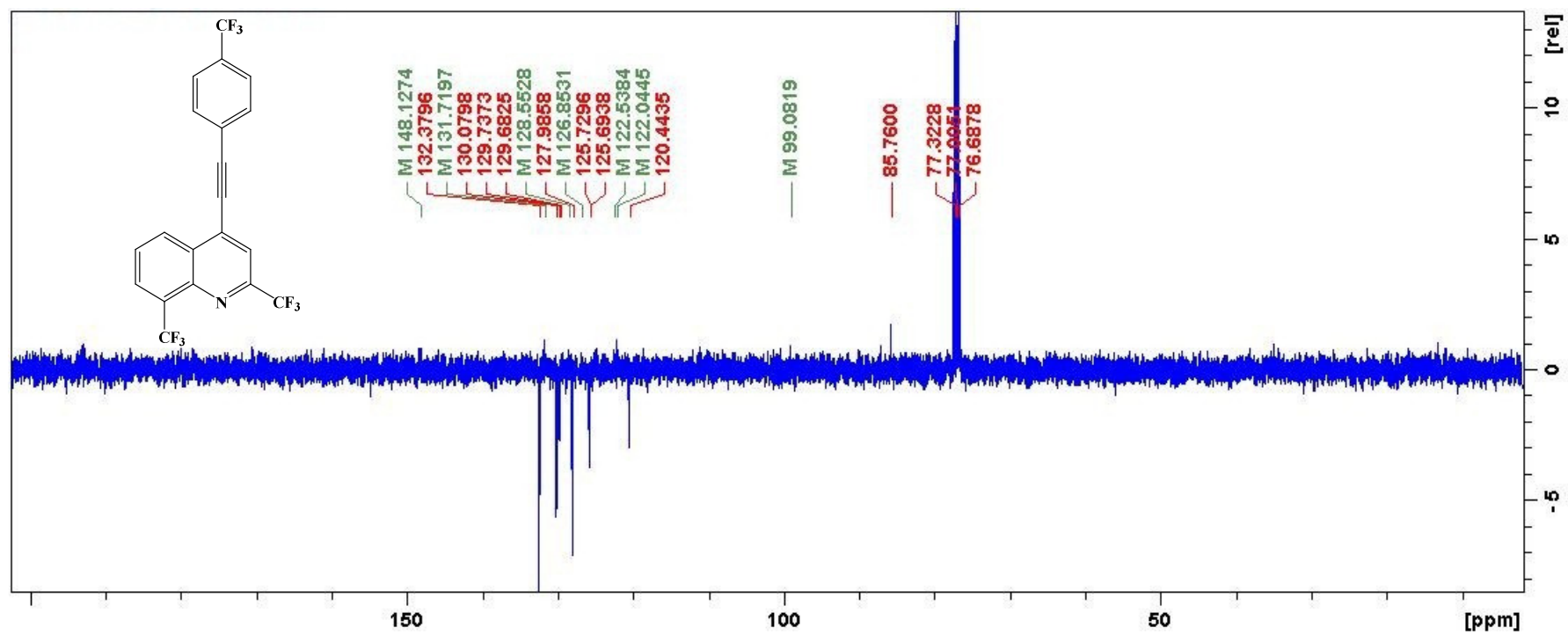
HRMS of 4j

SA24

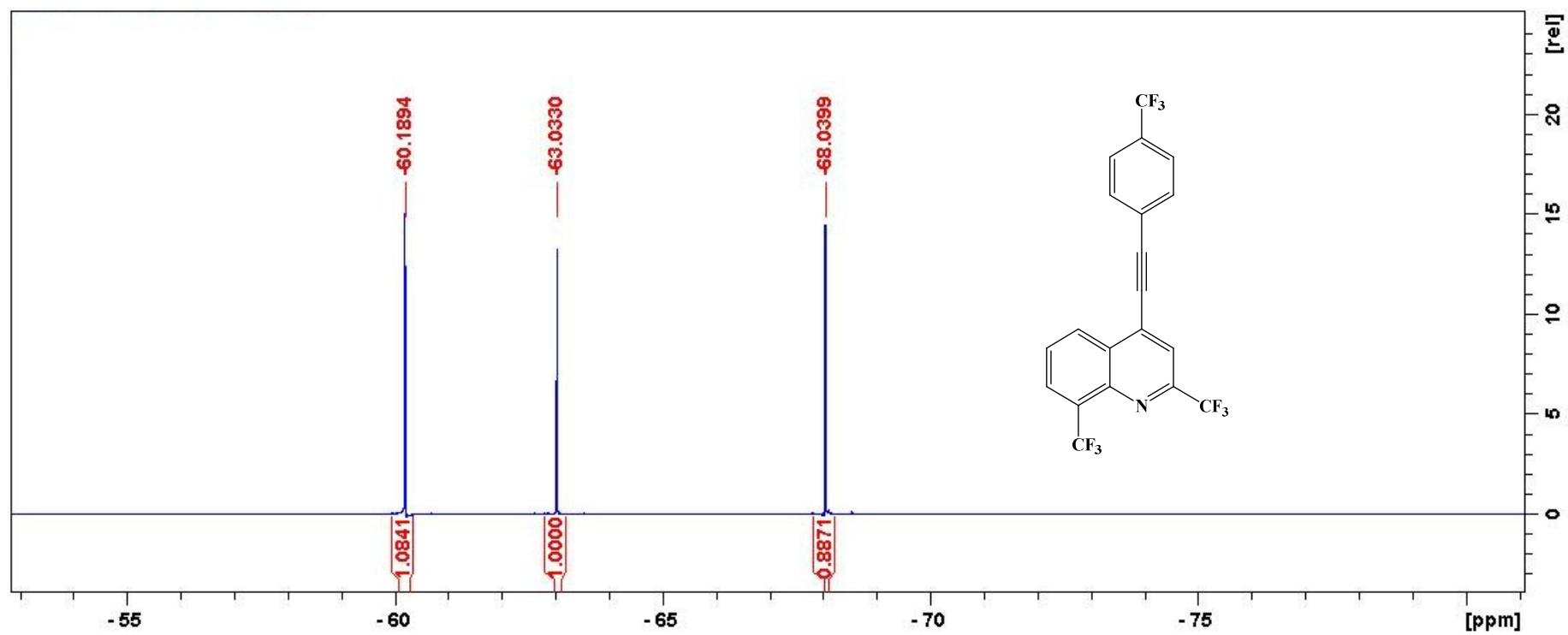
MS_Direct_151211_45 37 (0.179) Cm (36:43)

1: TOF MS ES+
4.14e4

¹H NMR spectrum of **4k**

^{13}C NMR spectrum of **4k**

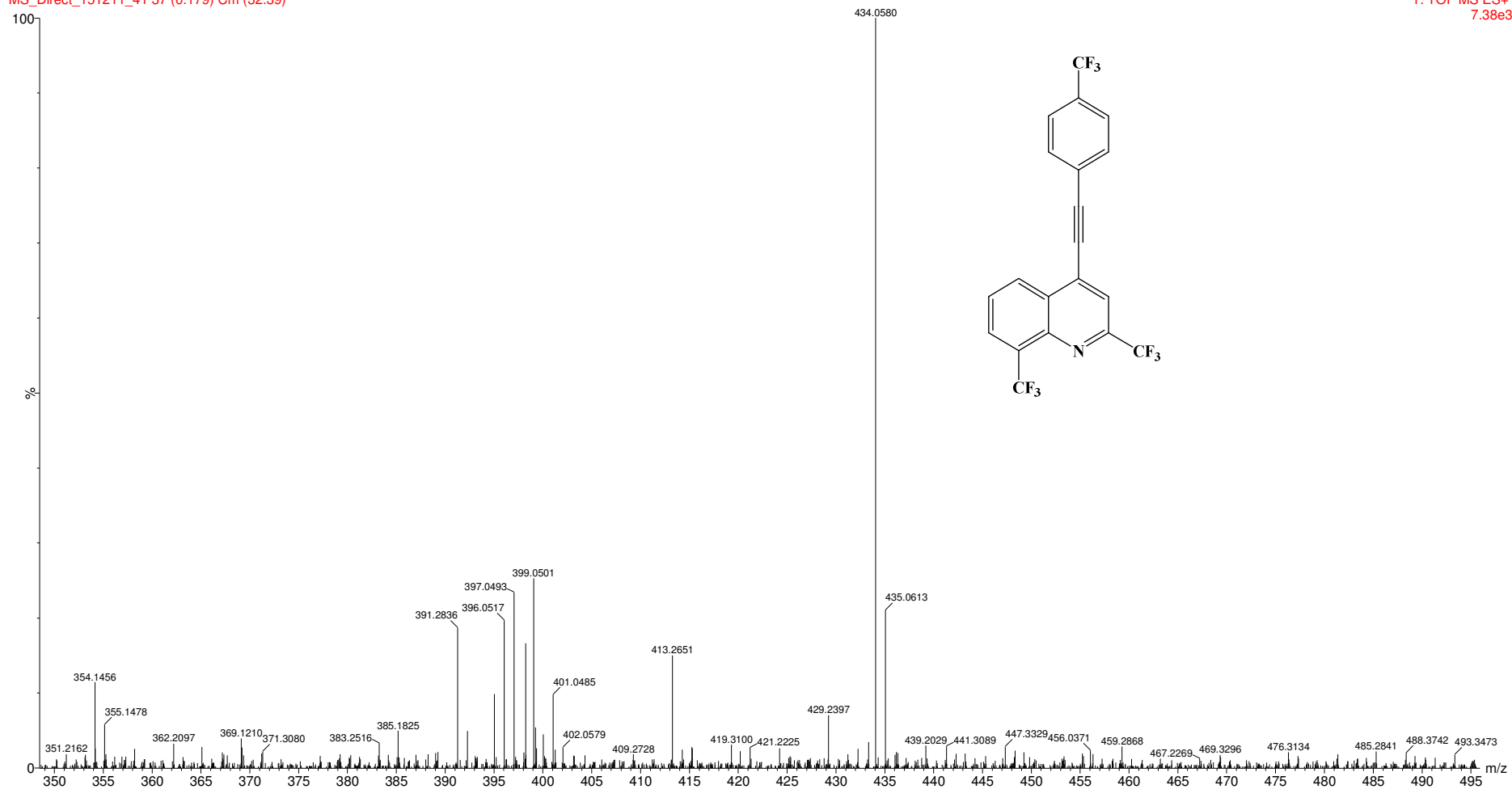
^{19}F NMR spectrum of **4k**

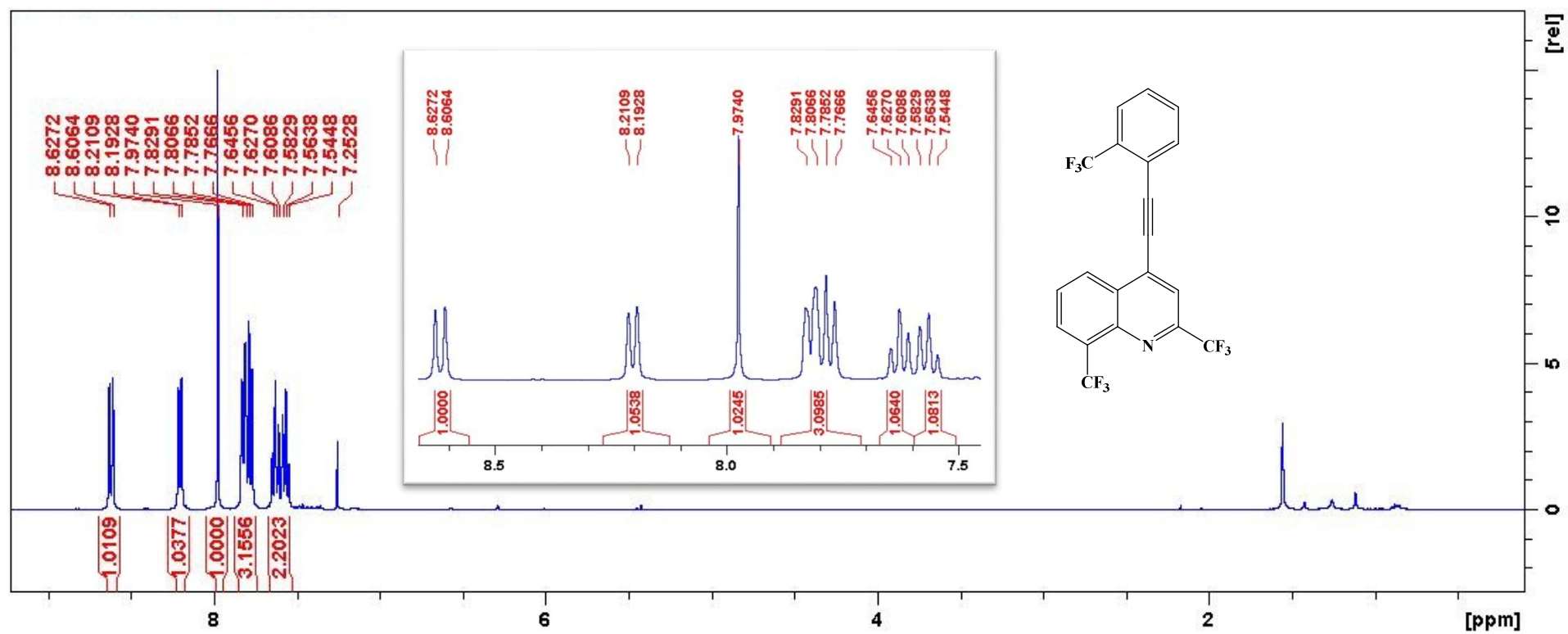


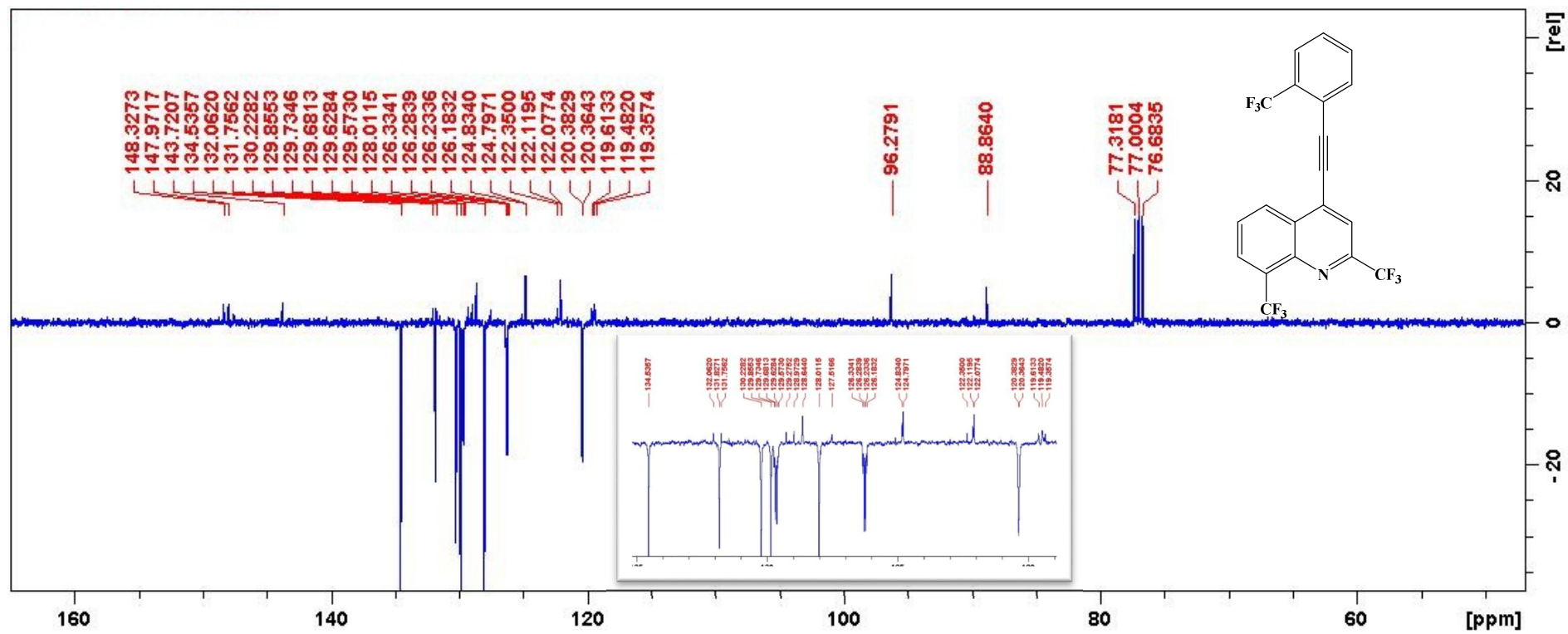
HRMS of 4k

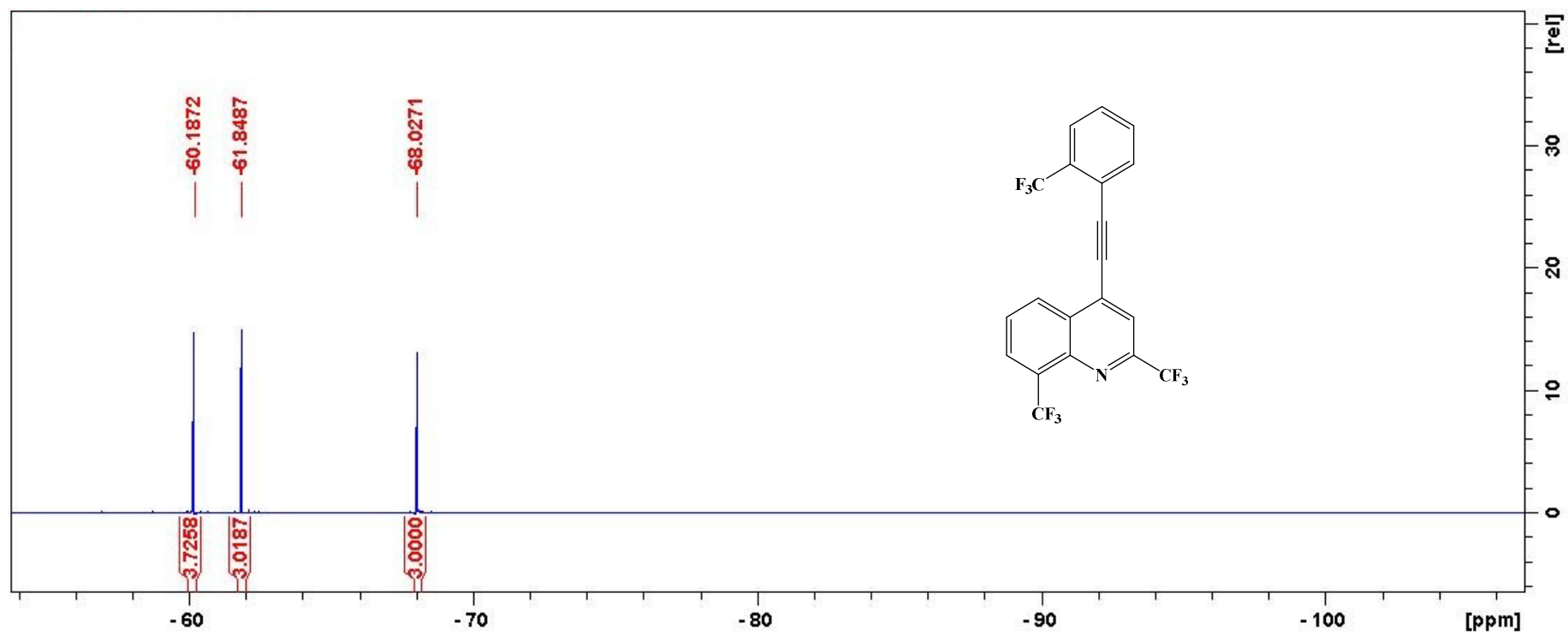
SA18

MS_Direct_151211_41 37 (0.179) Cm (32:39)

1: TOF MS ES+
7.38e3

¹H NMR spectrum of **4l**

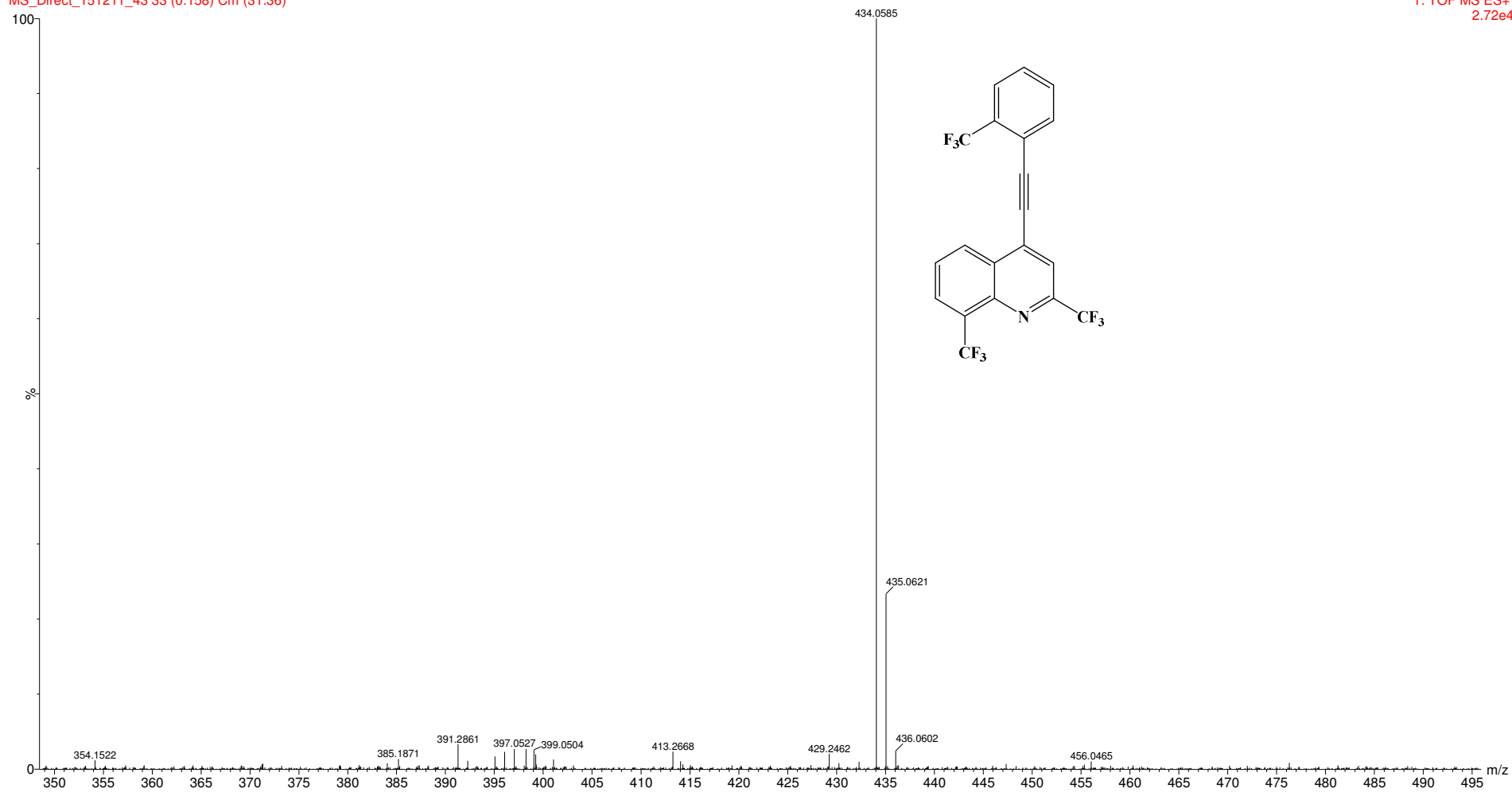
¹³C NMR spectrum of **4l**

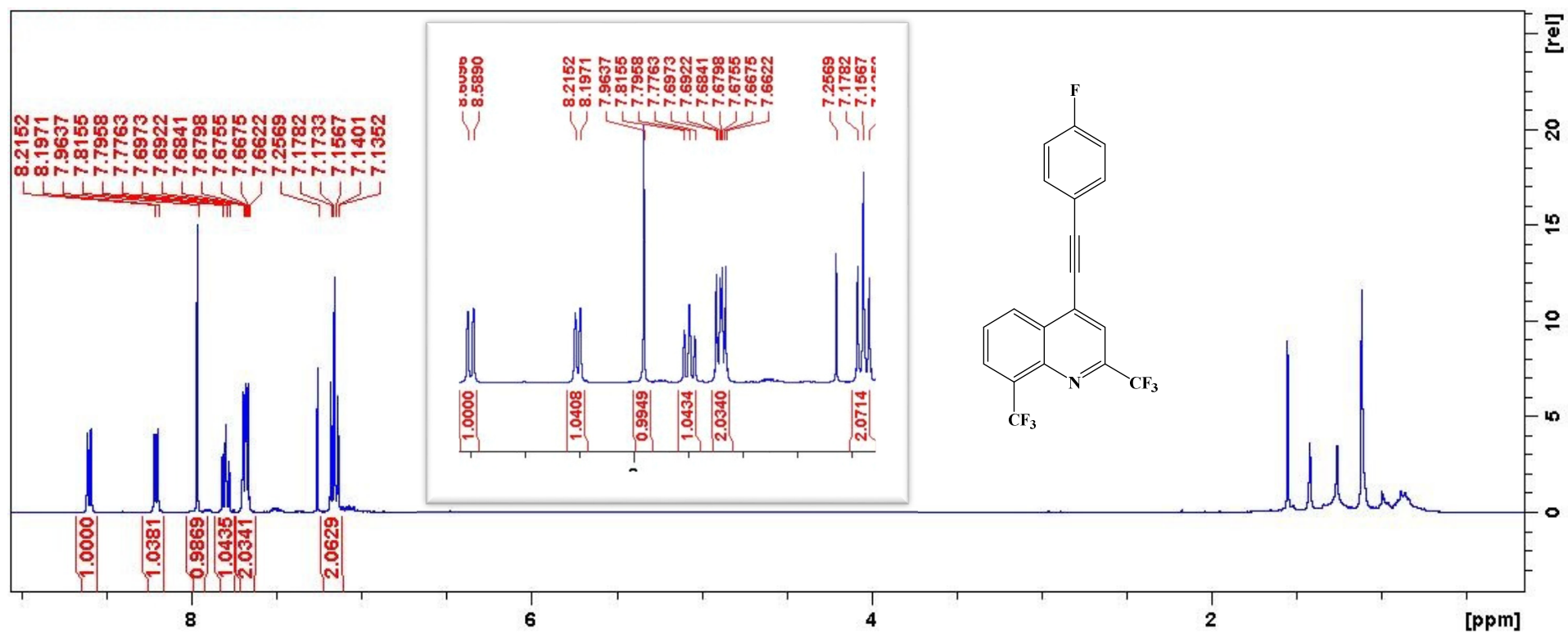
¹⁹F NMR spectrum of **41**

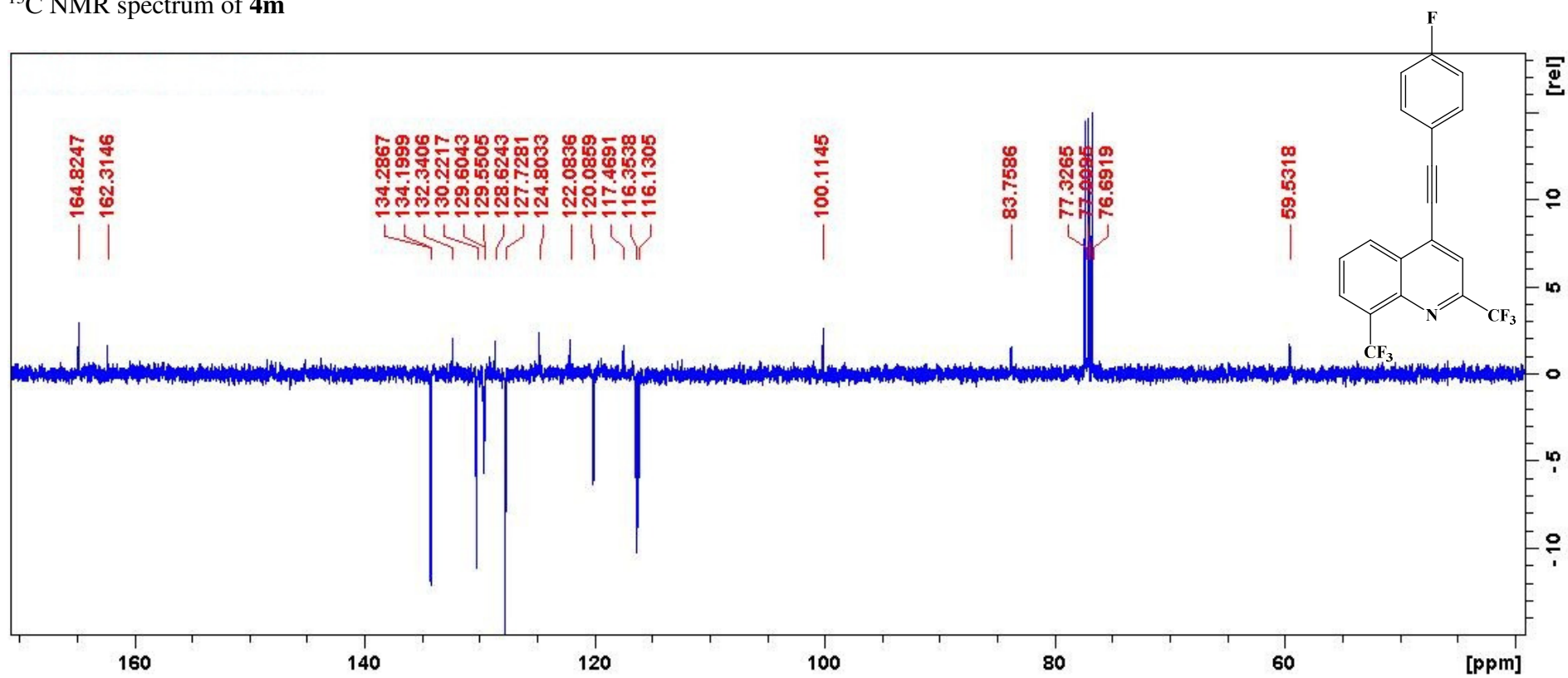
HRMS of **4l**

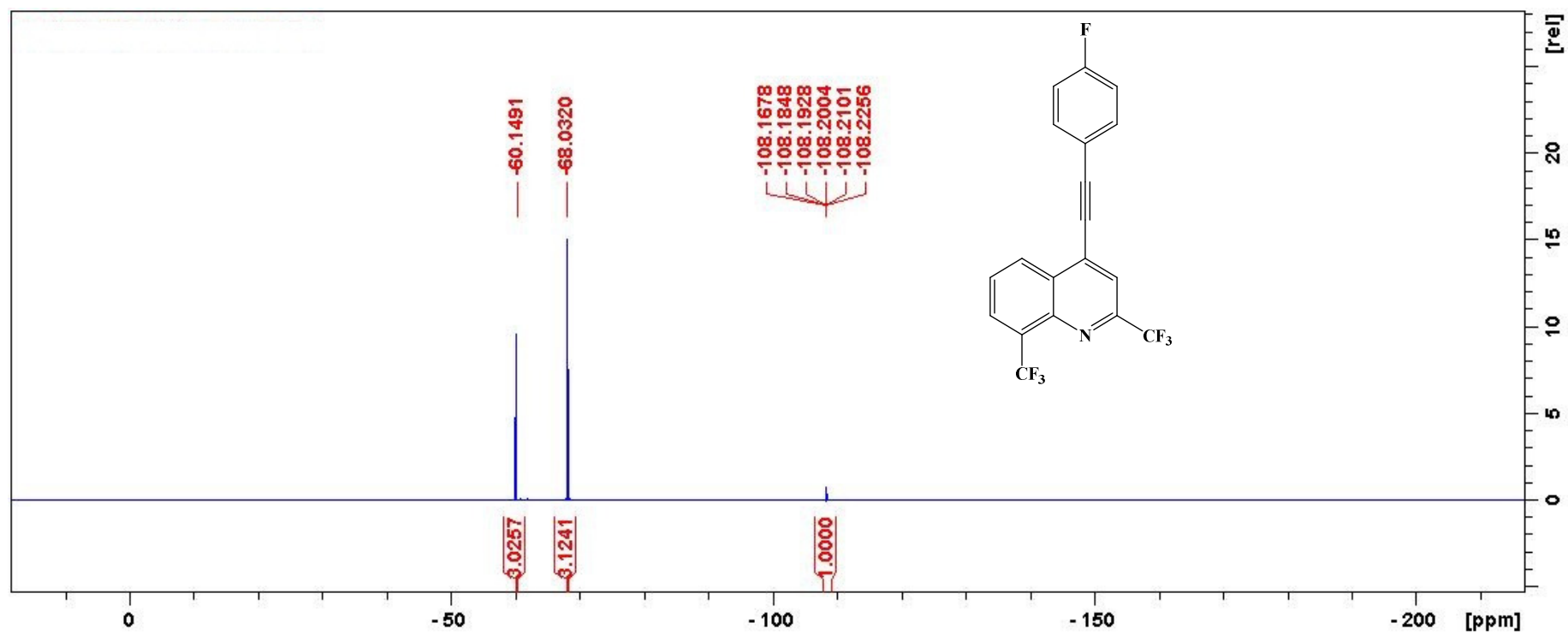
SA21

MS_Direct_151211_43 33 (0.158) Cm (31:36)

1: TOF MS ES+
2.72e4

¹H NMR spectrum of **4m**

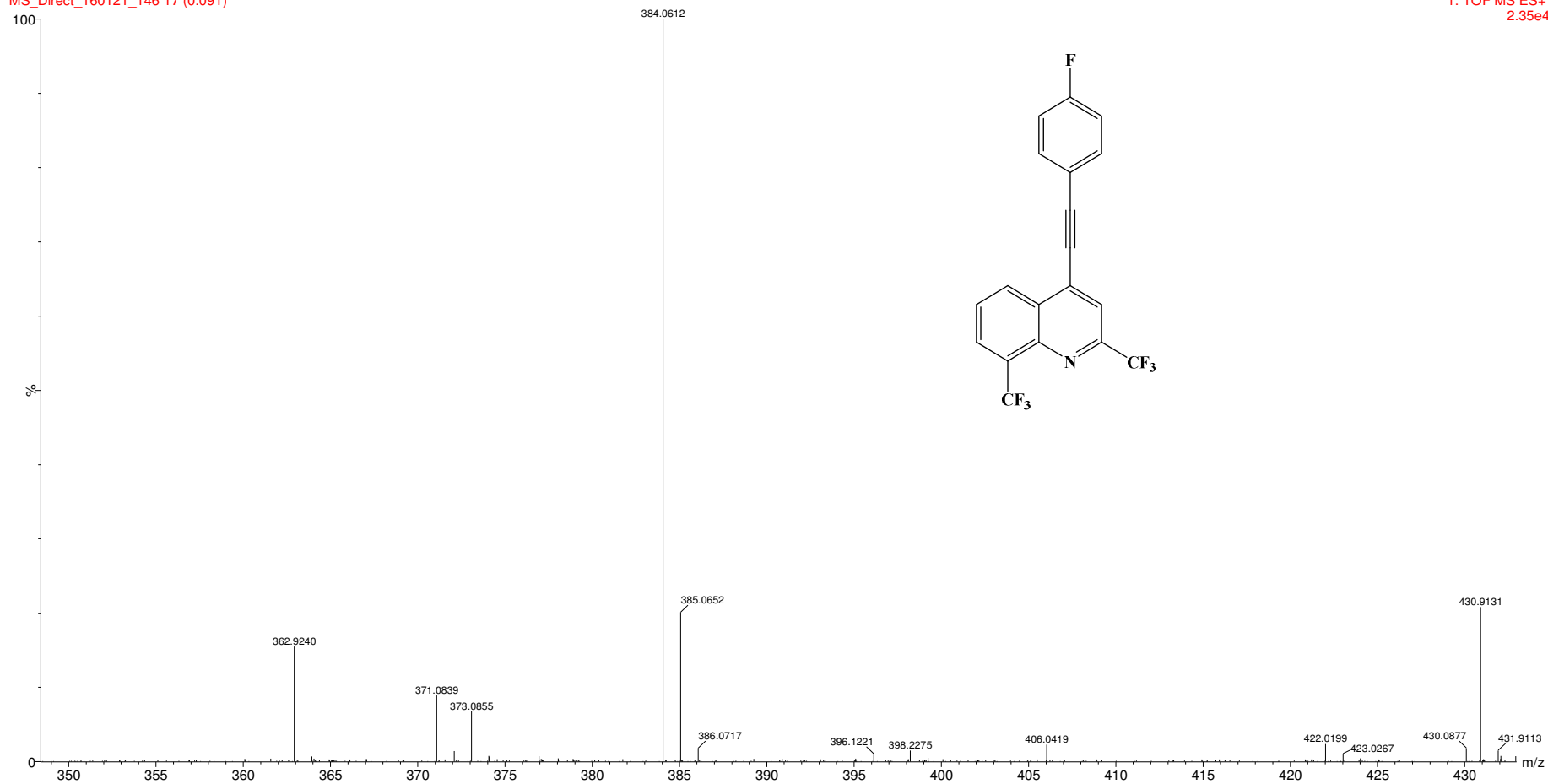
^{13}C NMR spectrum of **4m**

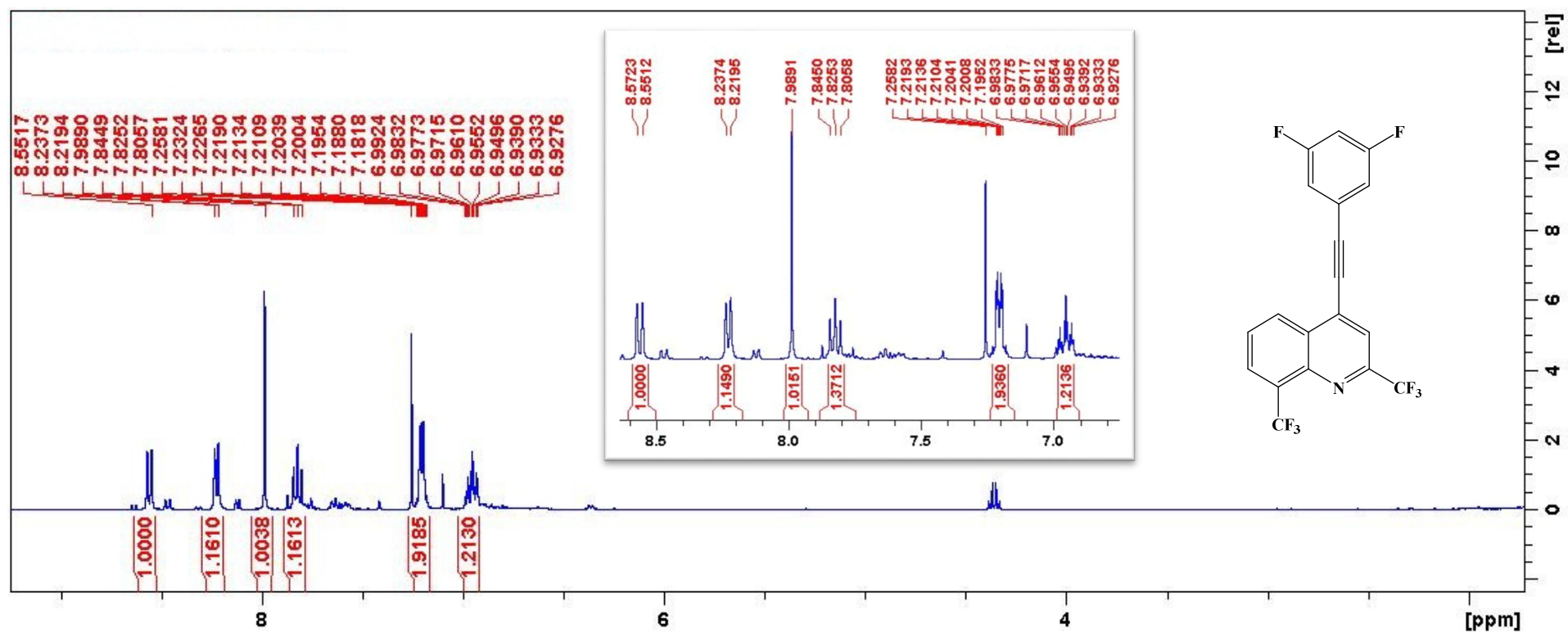
^{19}F NMR spectrum of **4m**

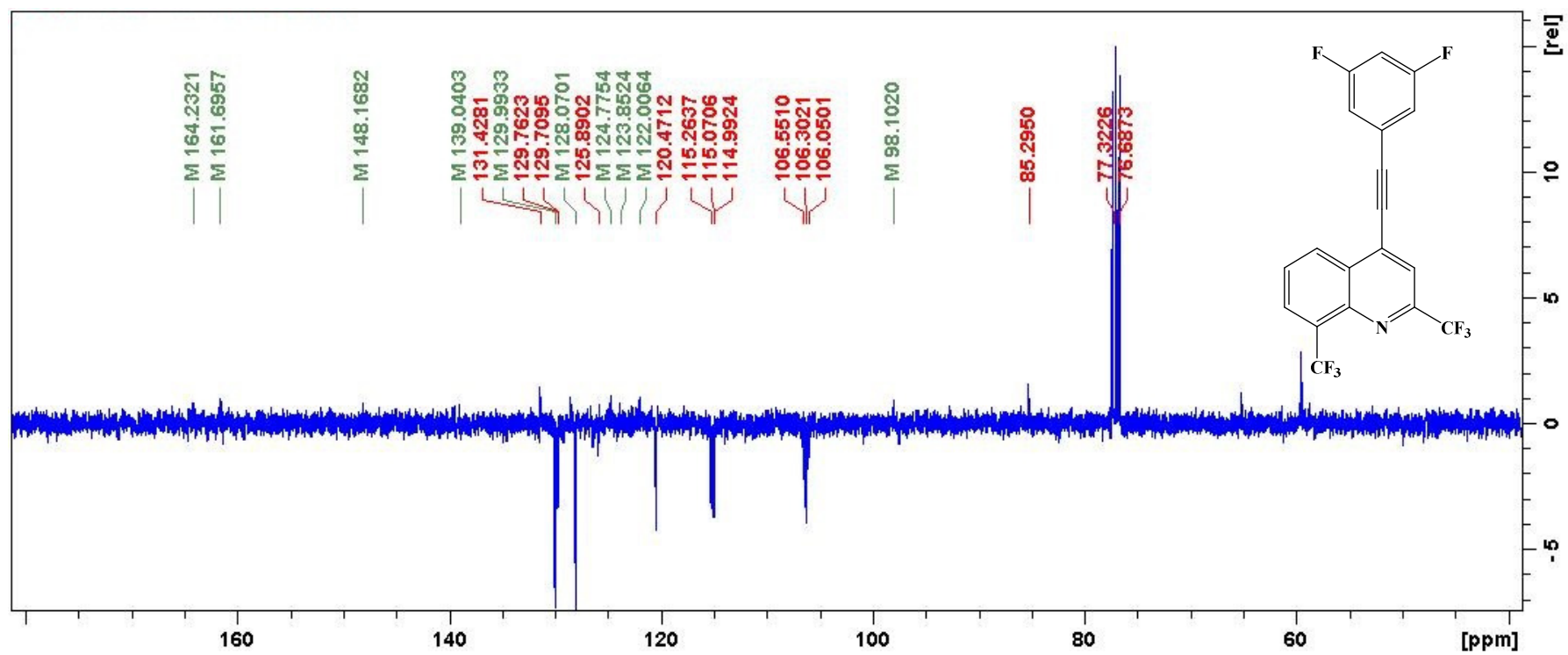
HRMS of 4m

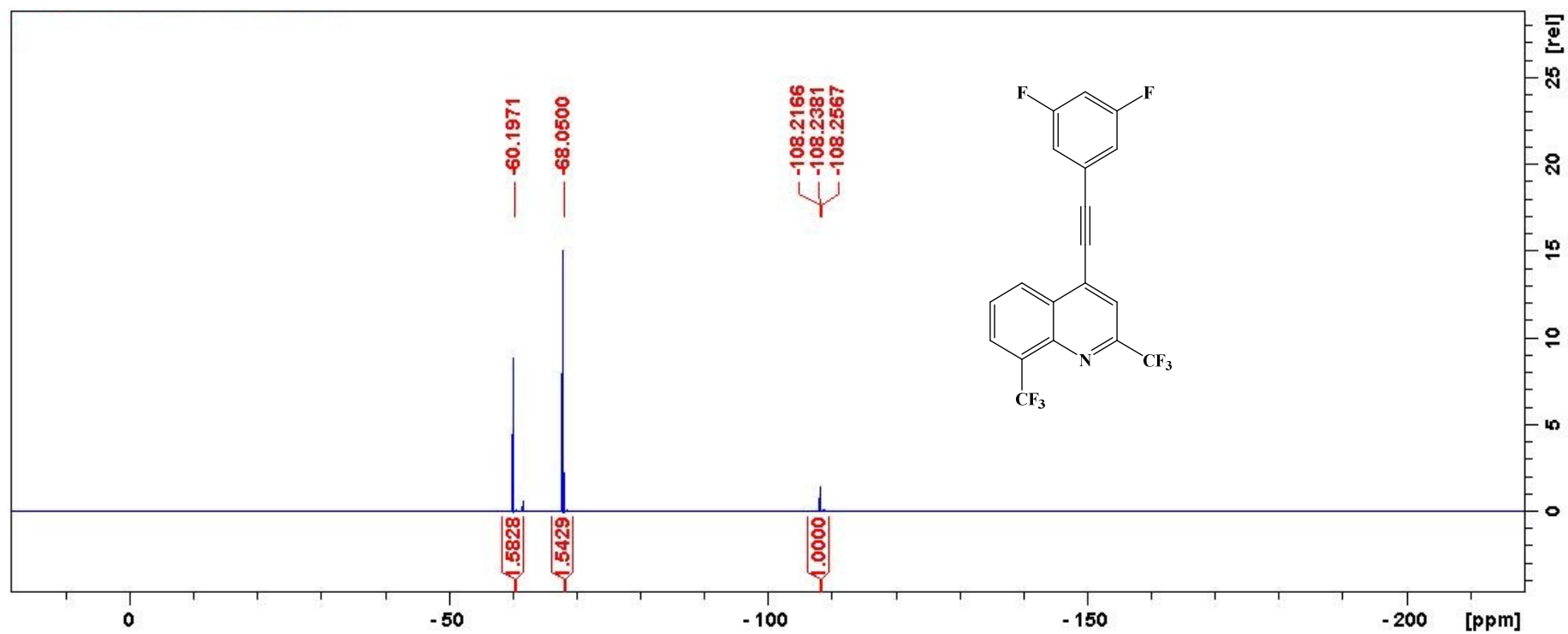
NO 17

MS_Direct_160121_146 17 (0.091)

1: TOF MS ES+
2.35e4

¹H NMR spectrum of **4n**

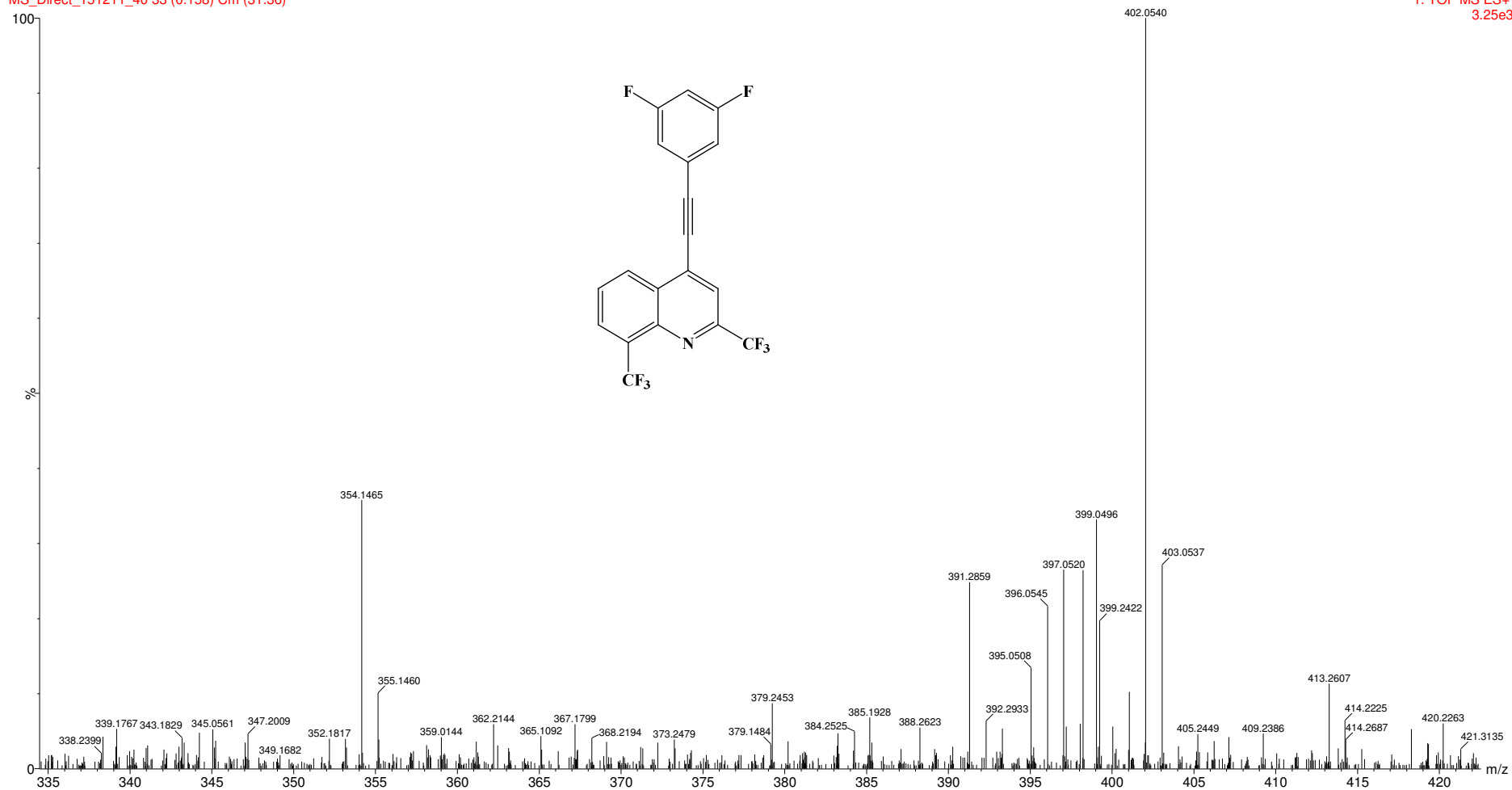
^{13}C NMR spectrum of **4n**

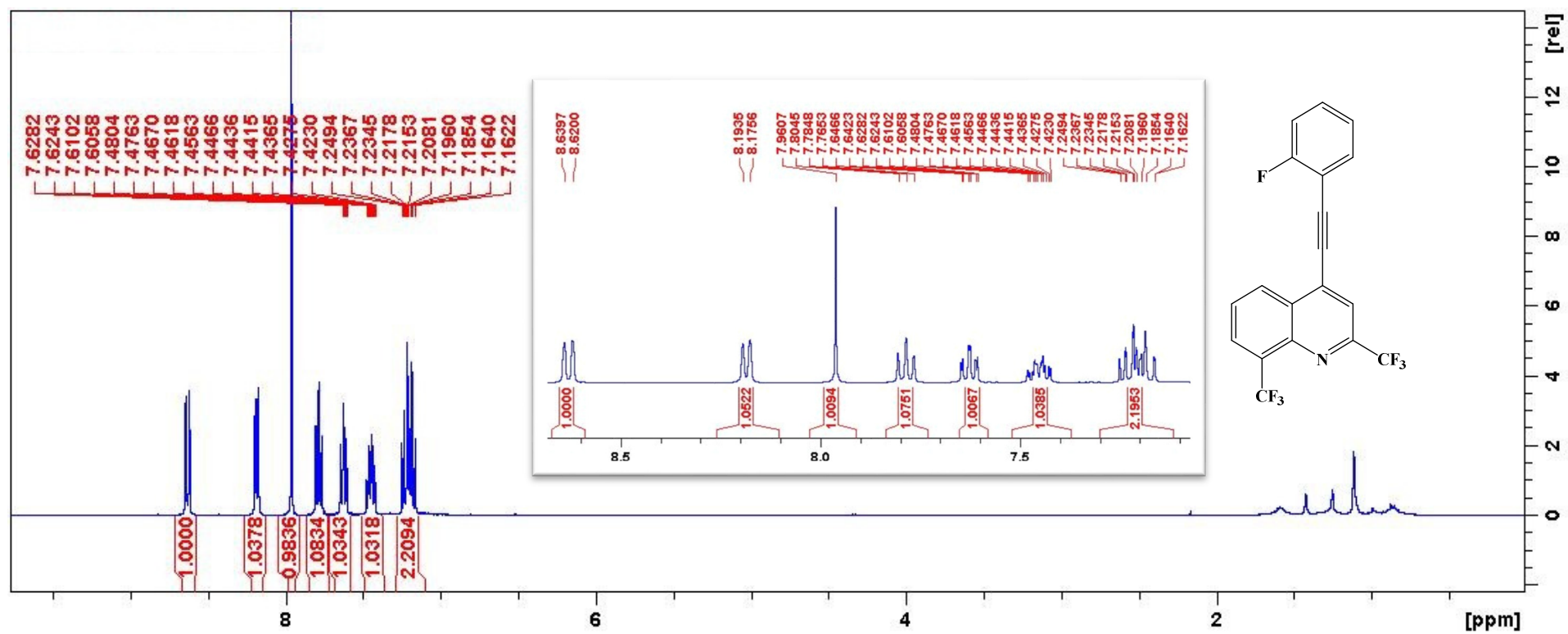
^{19}F NMR spectrum of **4n**

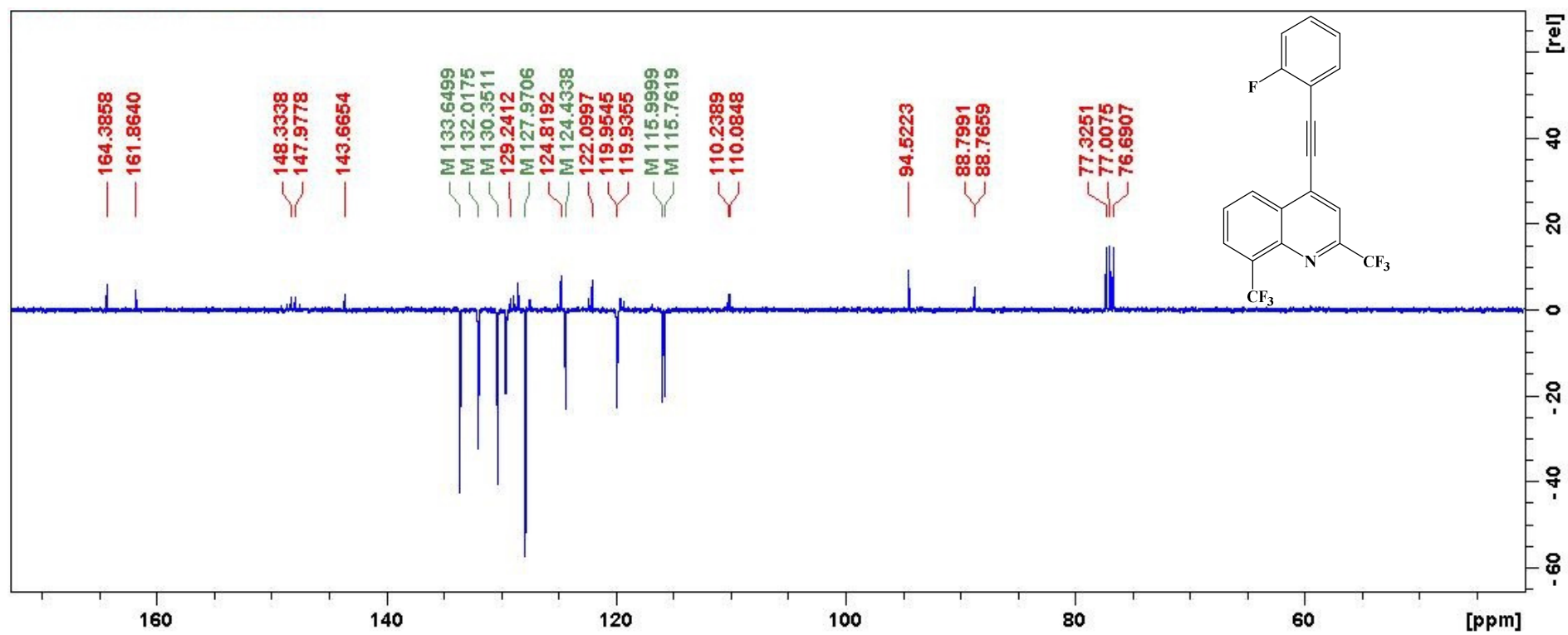
HRMS of 4n

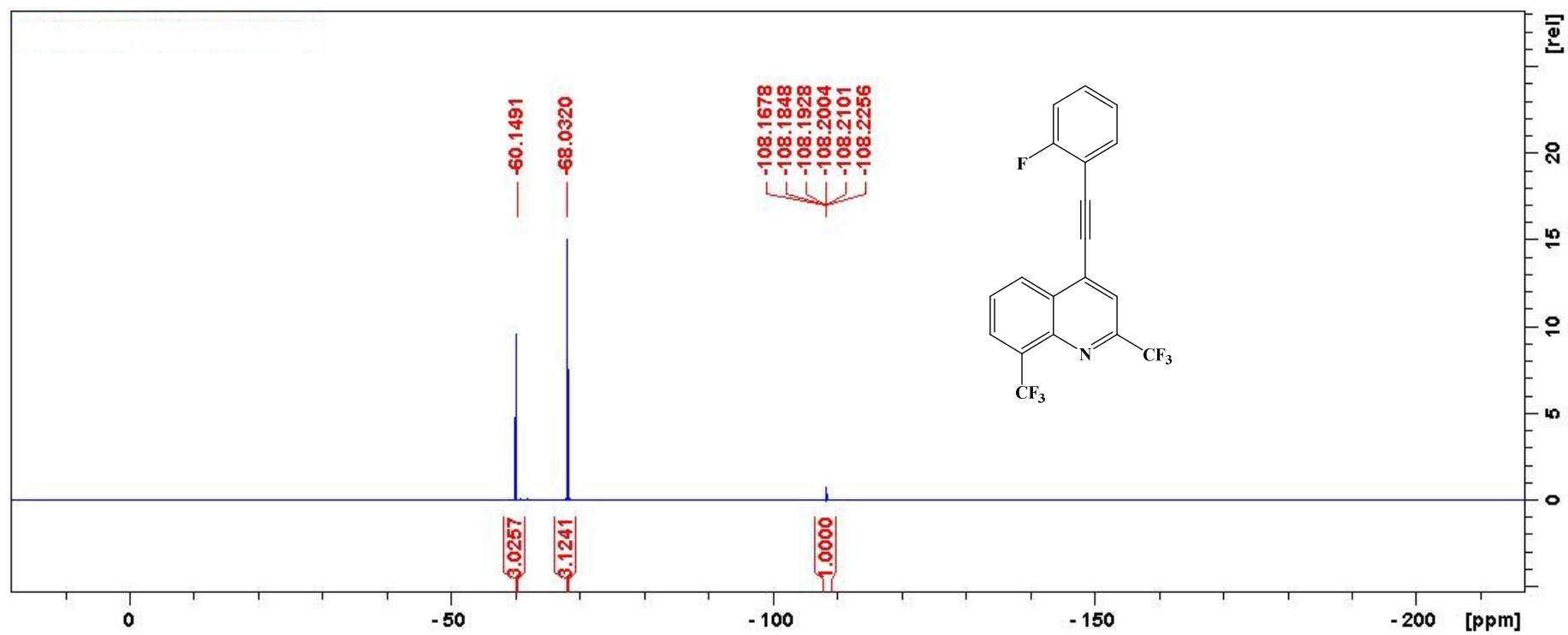
SA16

MS_Direct_151211_40 33 (0.158) Cm (31:36)

1: TOF MS ES+
3.25e3

¹H NMR spectrum of **4o**

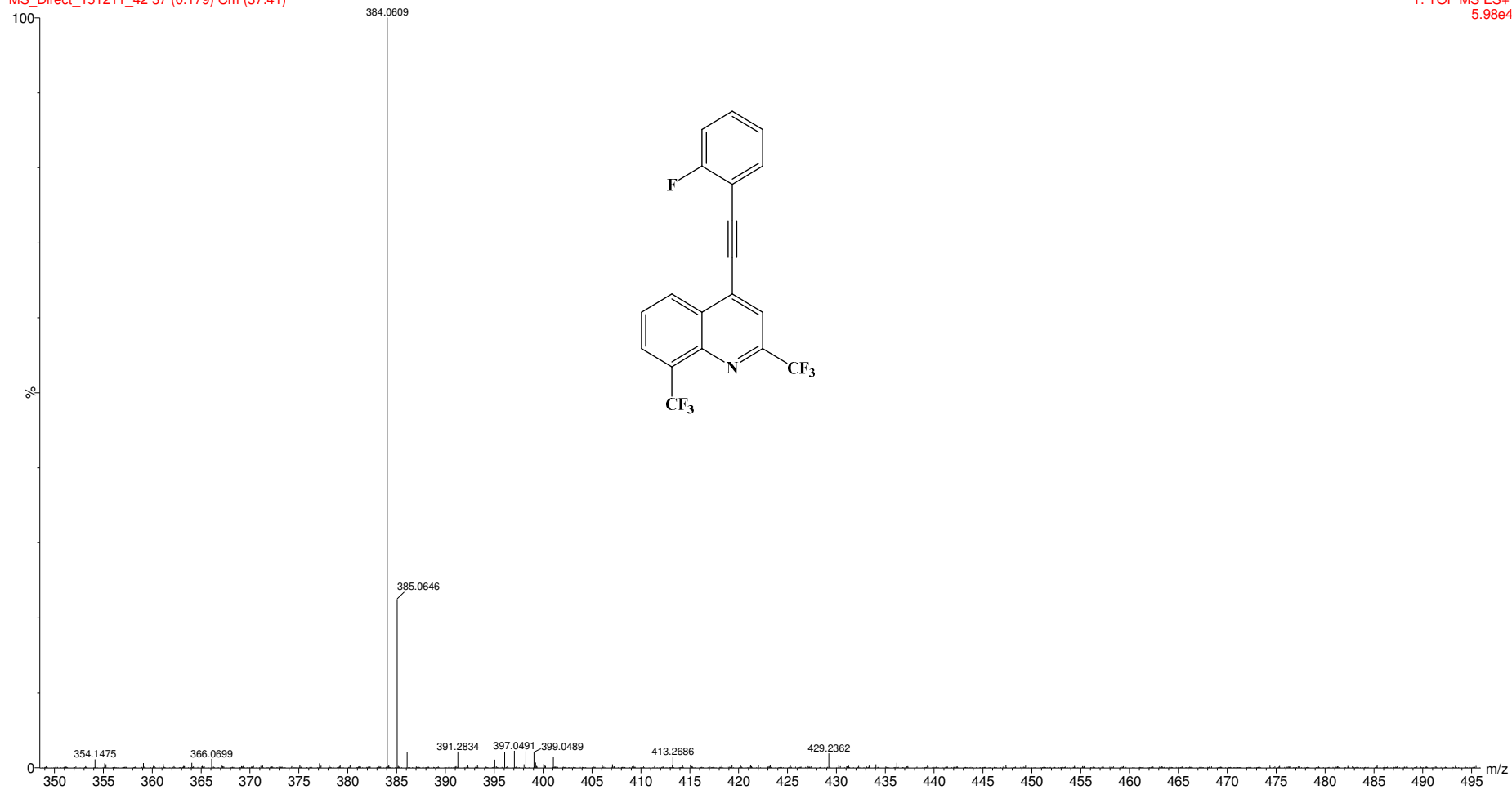
^{13}C NMR spectrum of **4o**

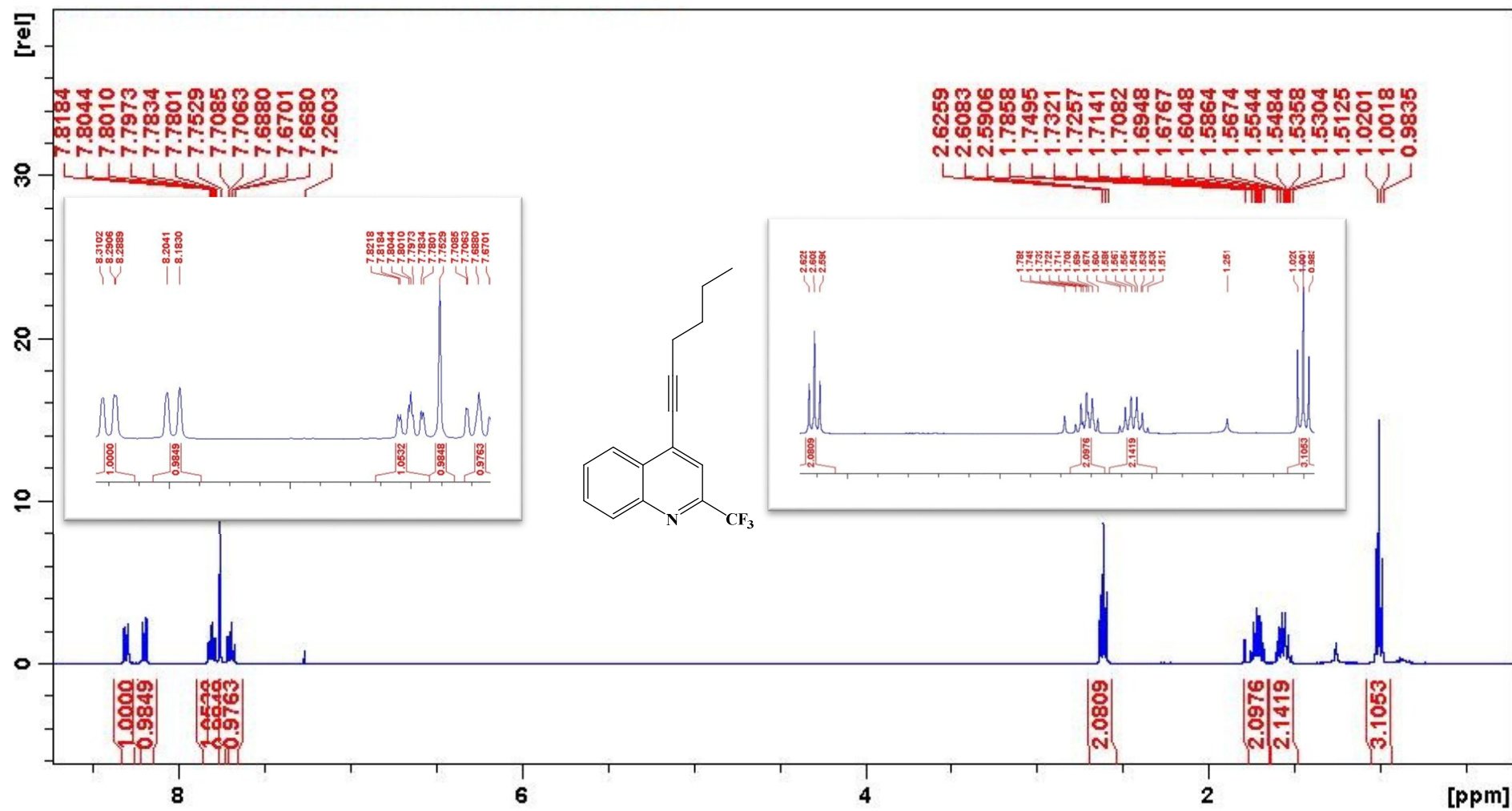
^{19}F NMR spectrum of **4o**

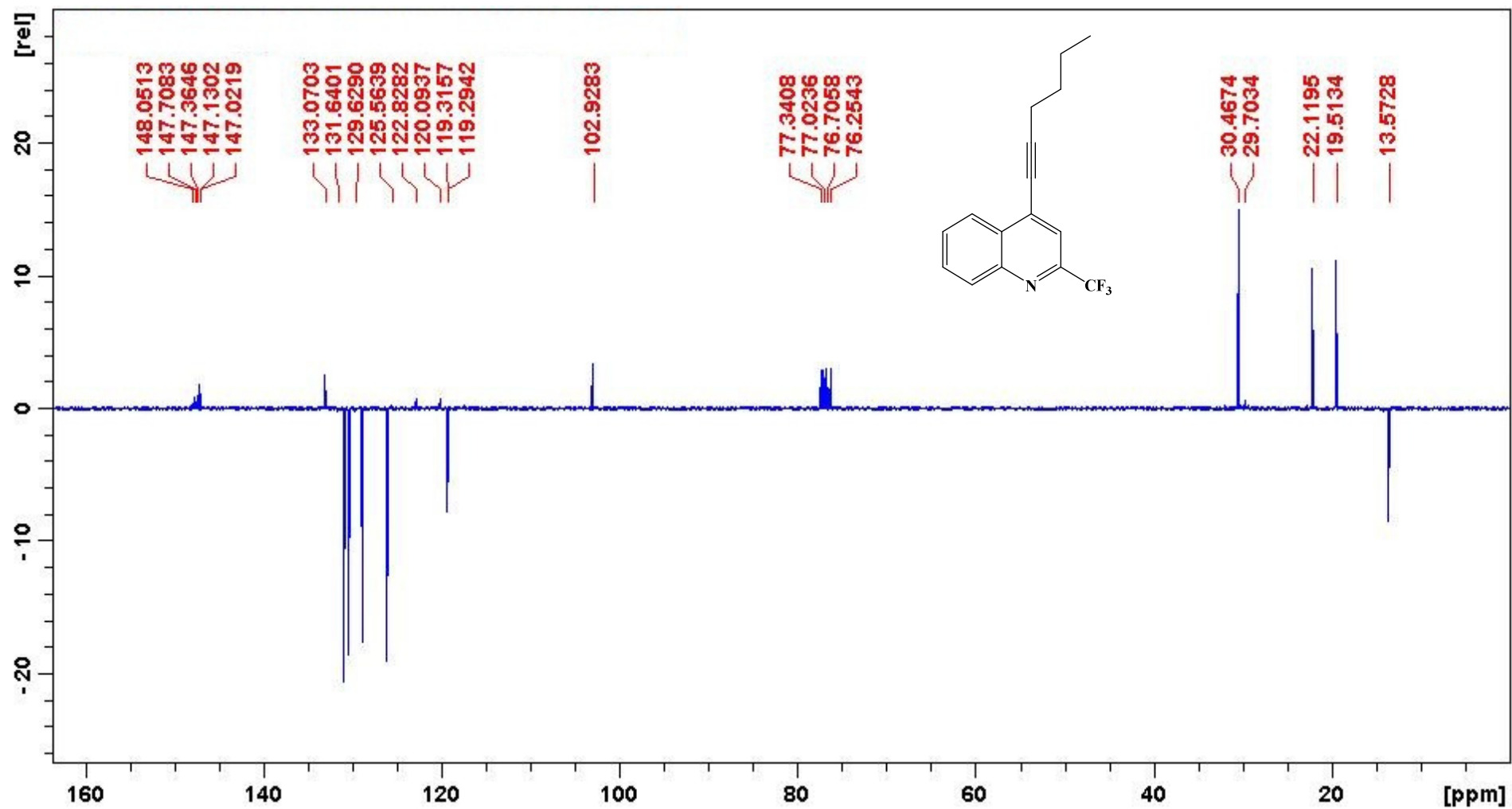
HRMS of **4o**

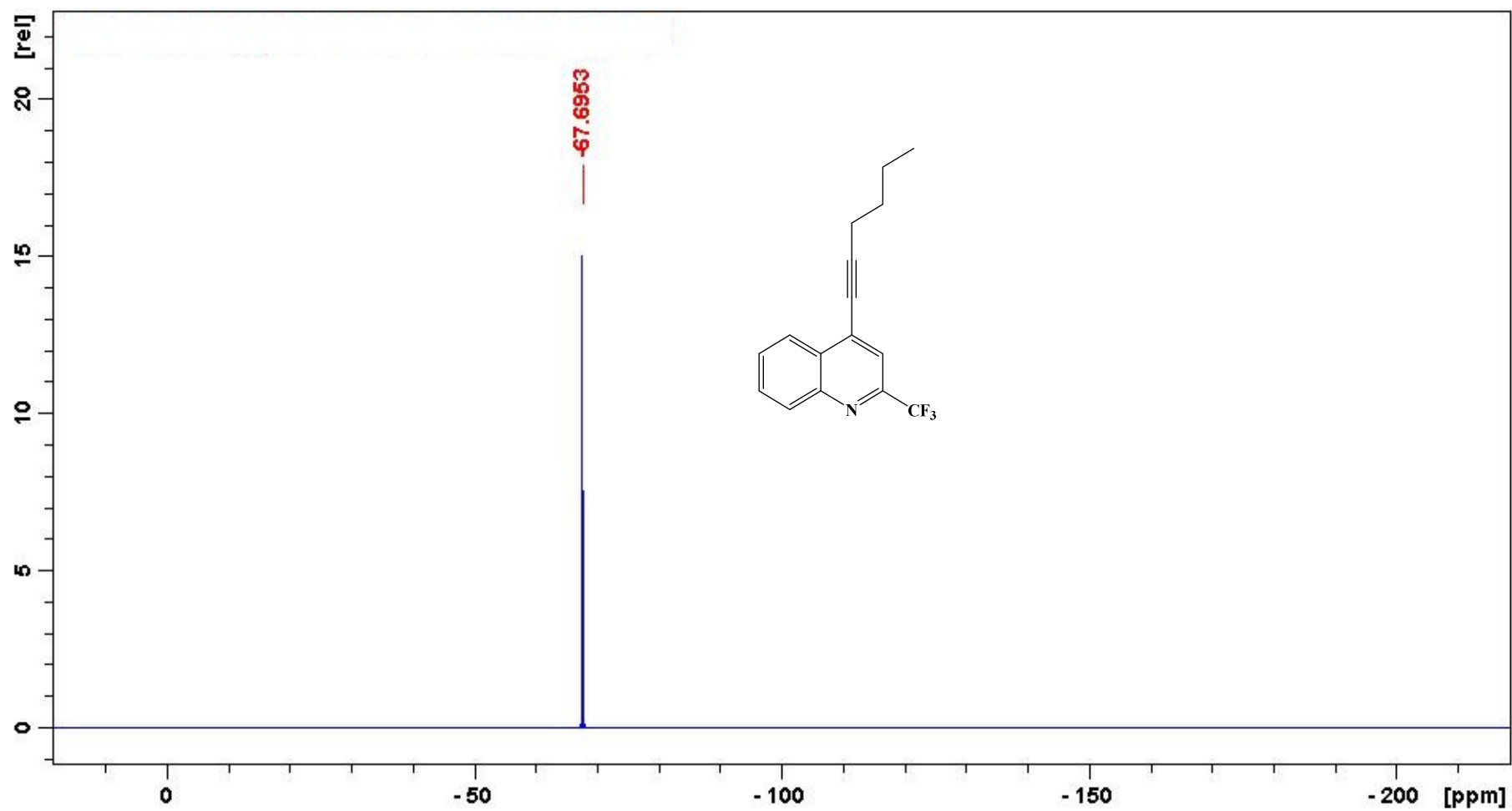
SA20

MS_Direct_151211_42 37 (0.179) Cm (37:41)

1: TOF MS ES+
5.98e4

¹H NMR spectrum of **4p**

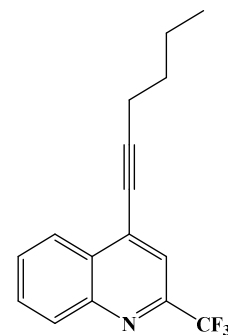
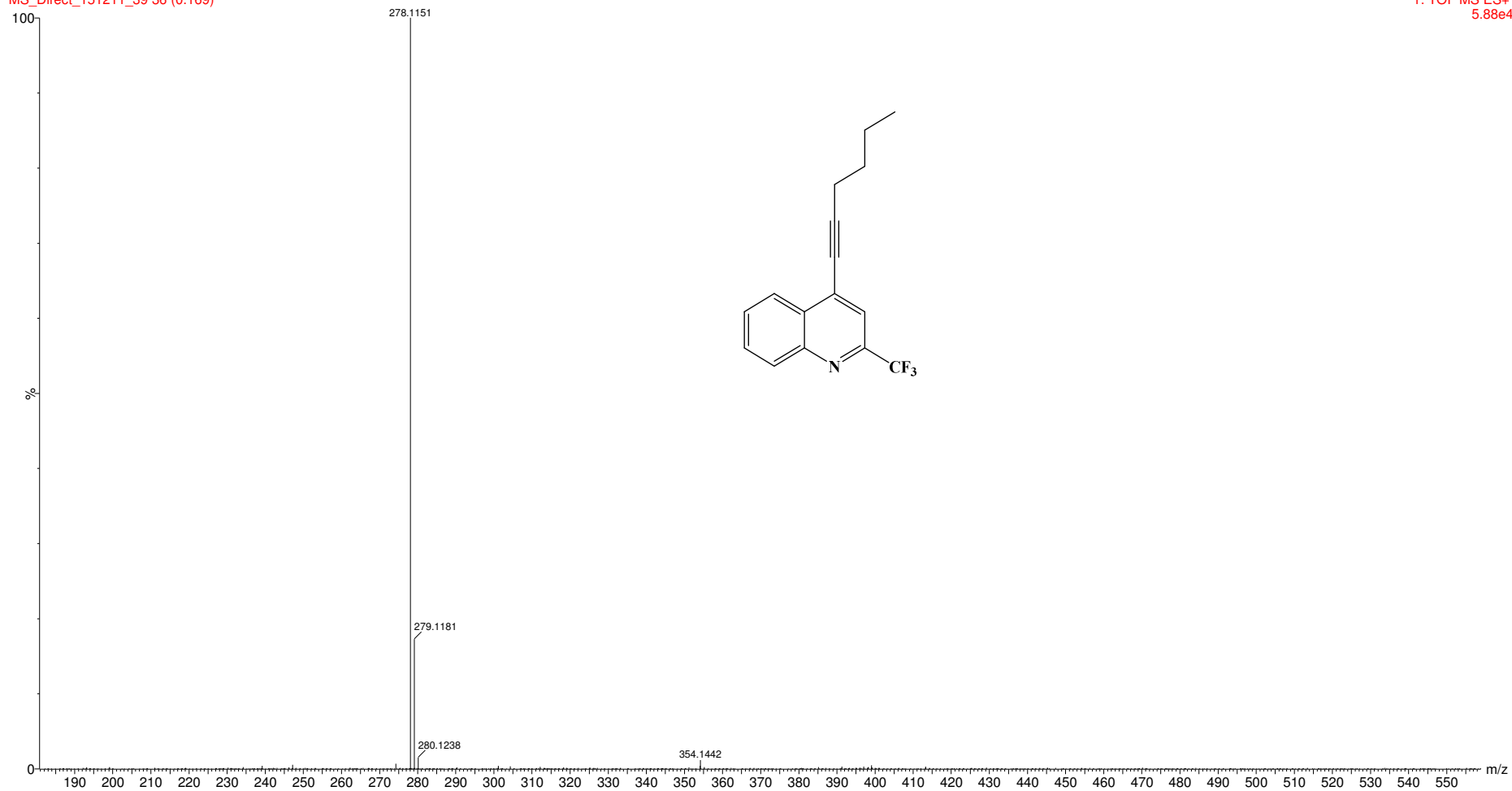
^{13}C NMR spectrum of **4p**

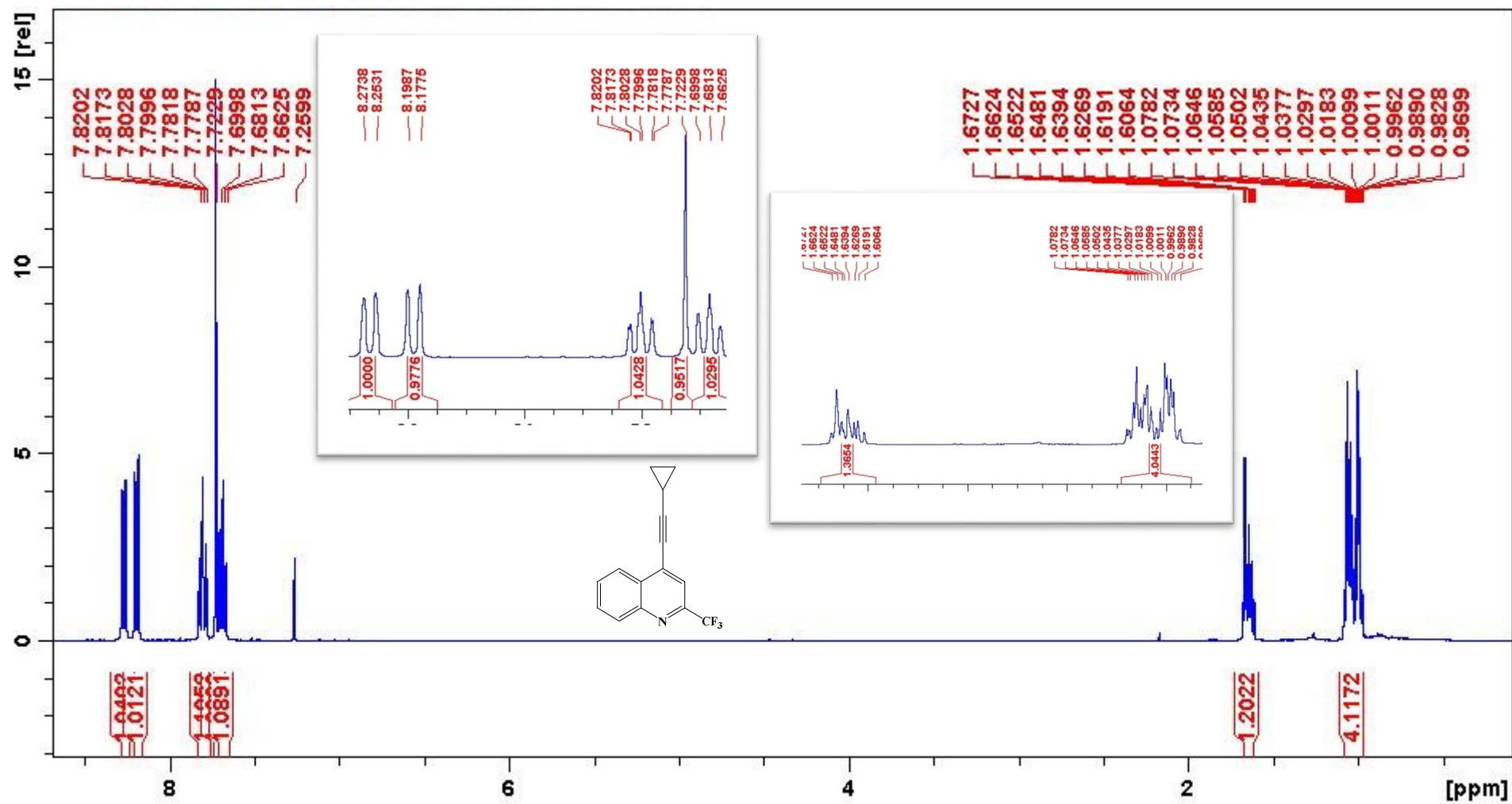
¹⁹F NMR spectrum of **4p**

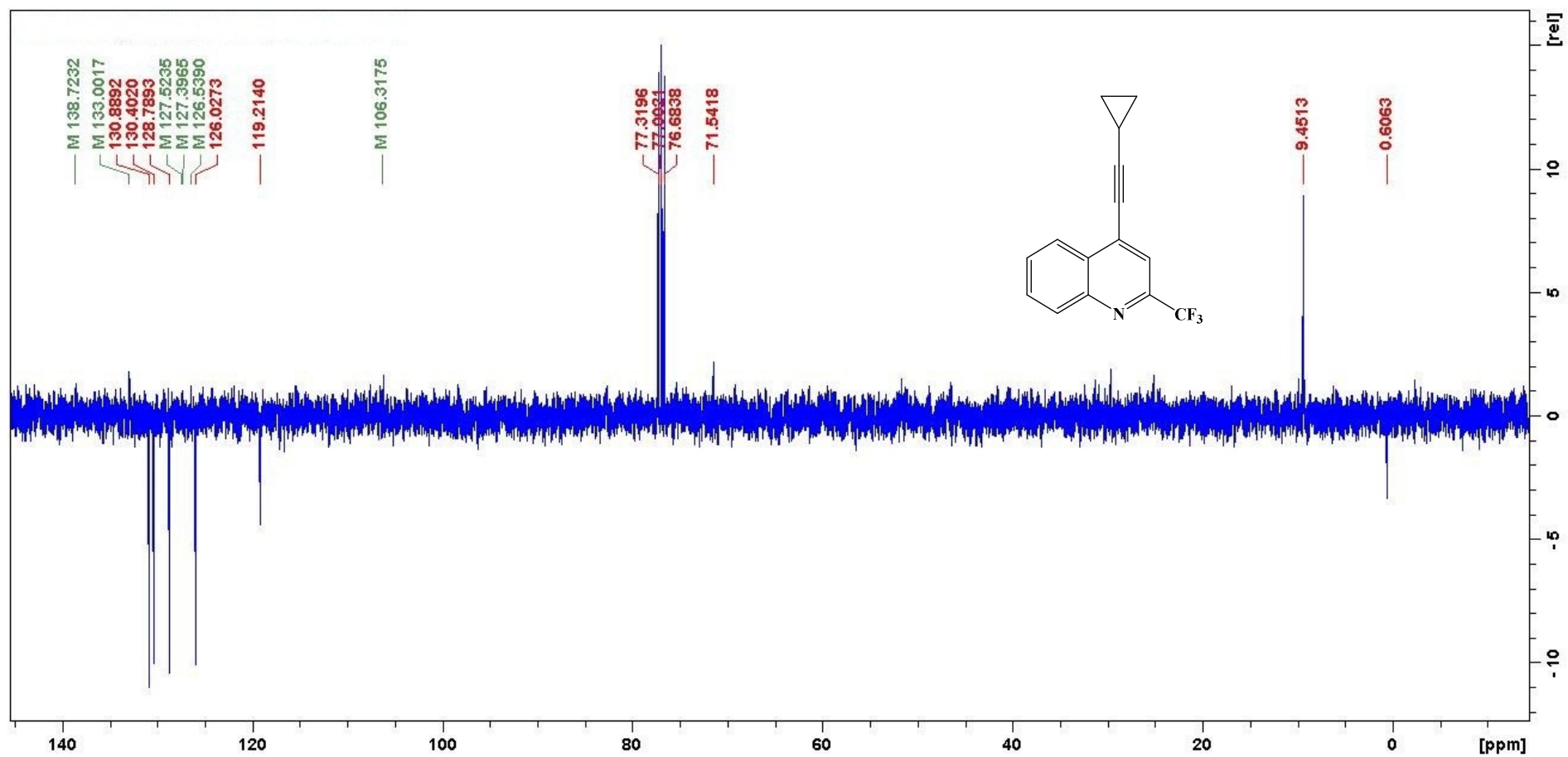
HRMS of 4p

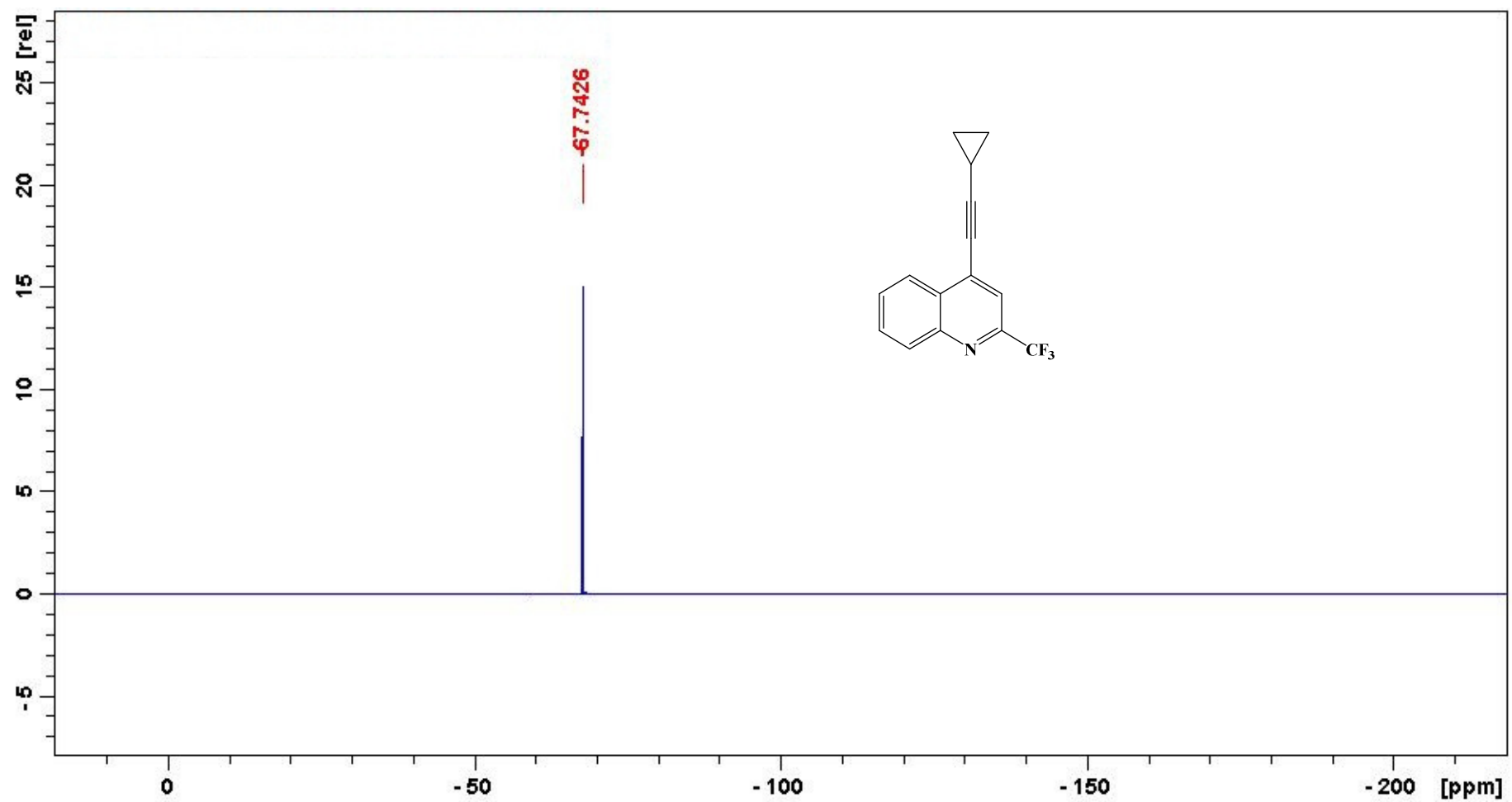
SA10

MS_Direct_151211_39 36 (0.169)

1: TOF MS ES+
5.88e4

¹H NMR spectrum of **4q**

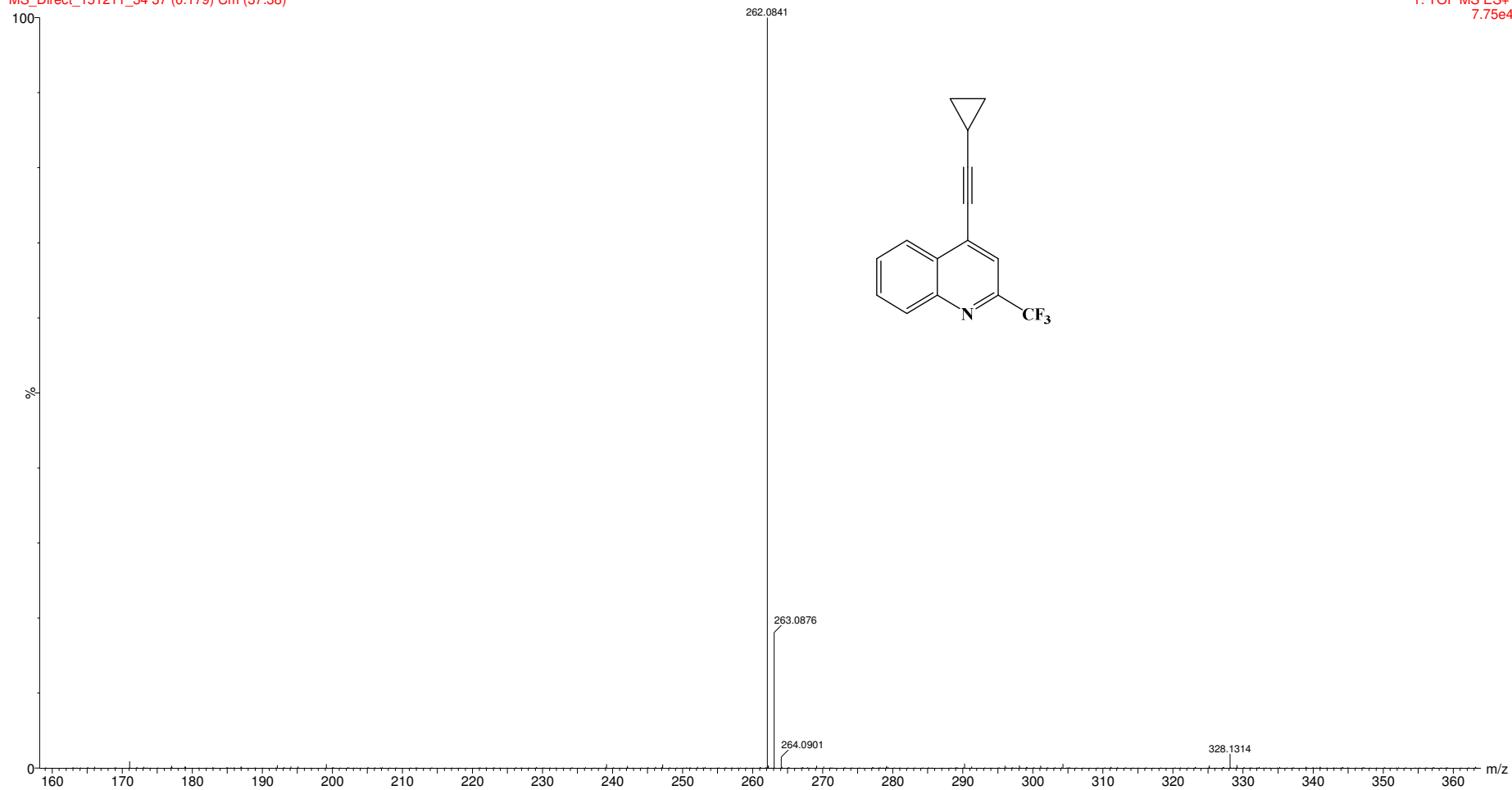
^{13}C NMR spectrum of **4q**

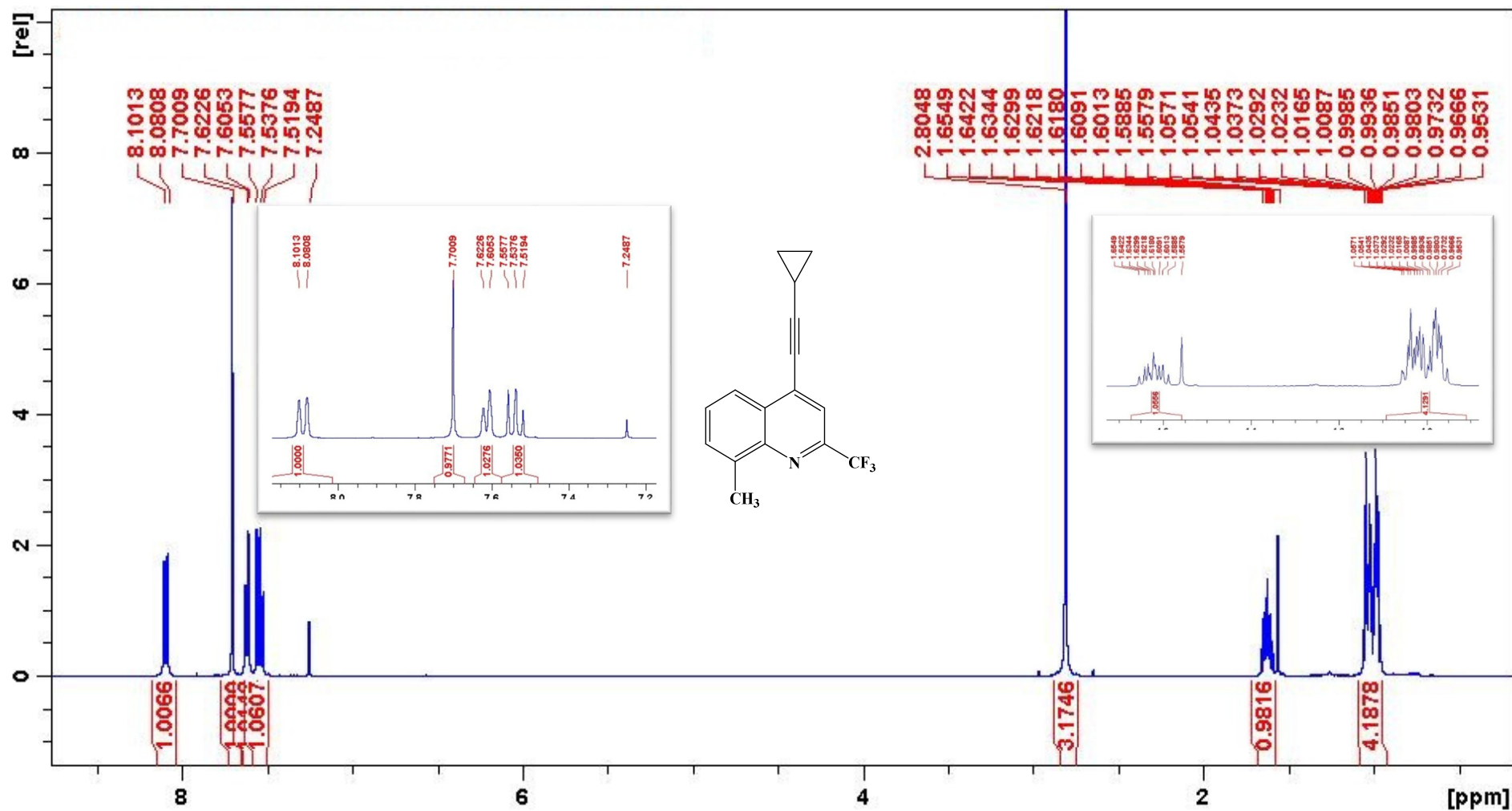
¹⁹F NMR spectrum of **4q**

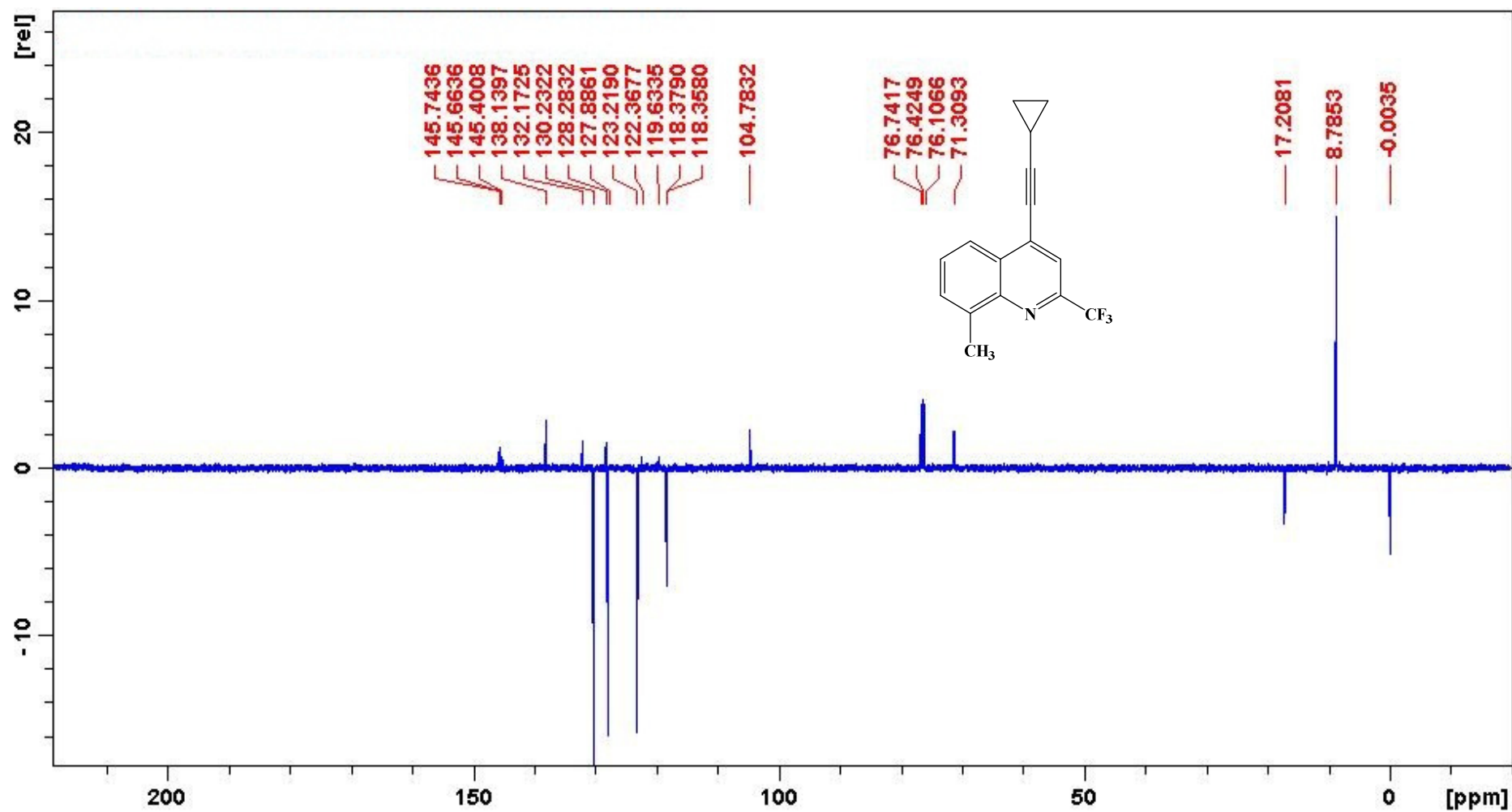
HRMS of **4q**

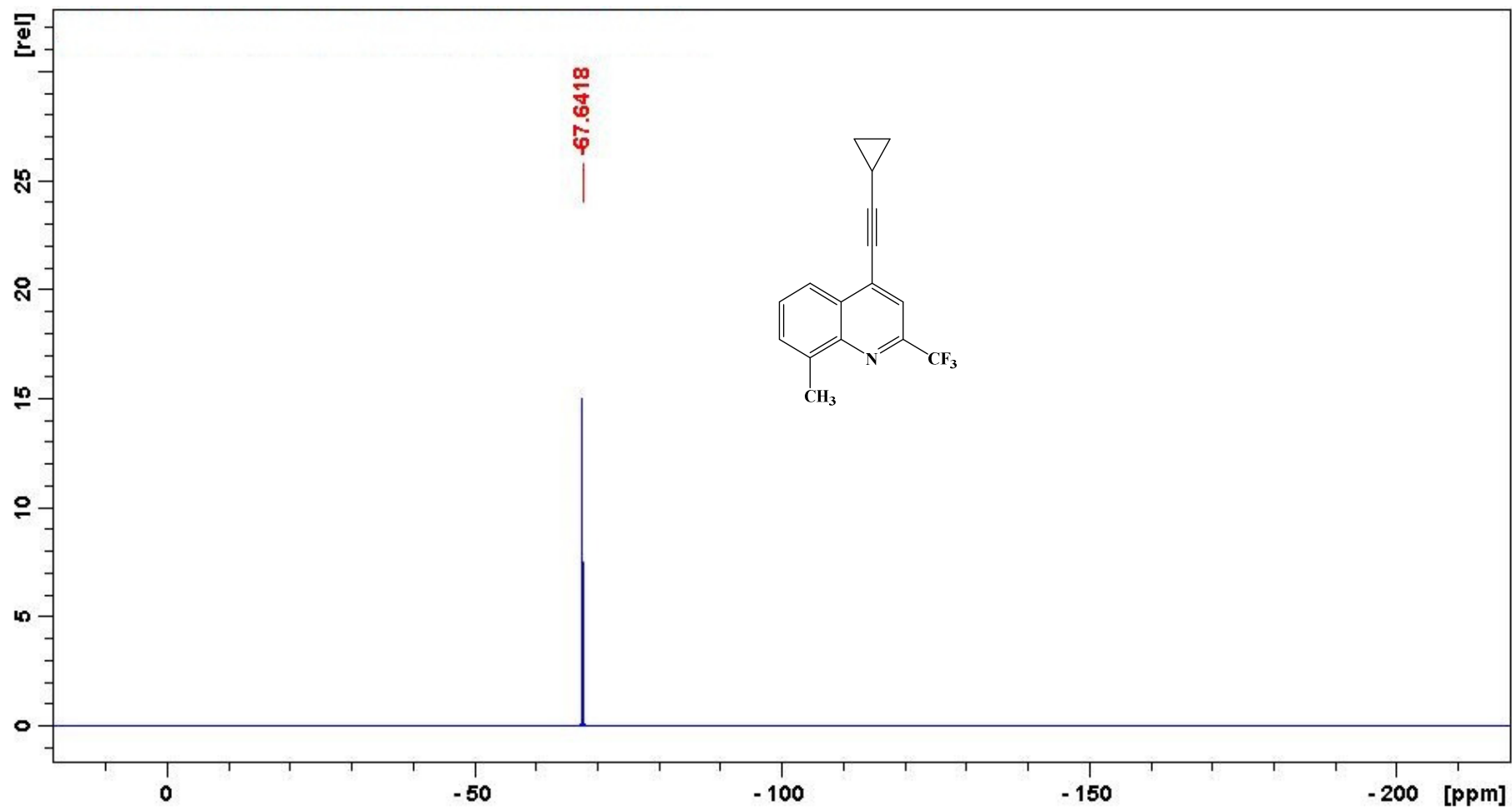
SA4

MS_Direct_151211_34 37 (0.179) Cm (37:38)

1: TOF MS ES+
7.75e4

¹H NMR spectrum of 4r

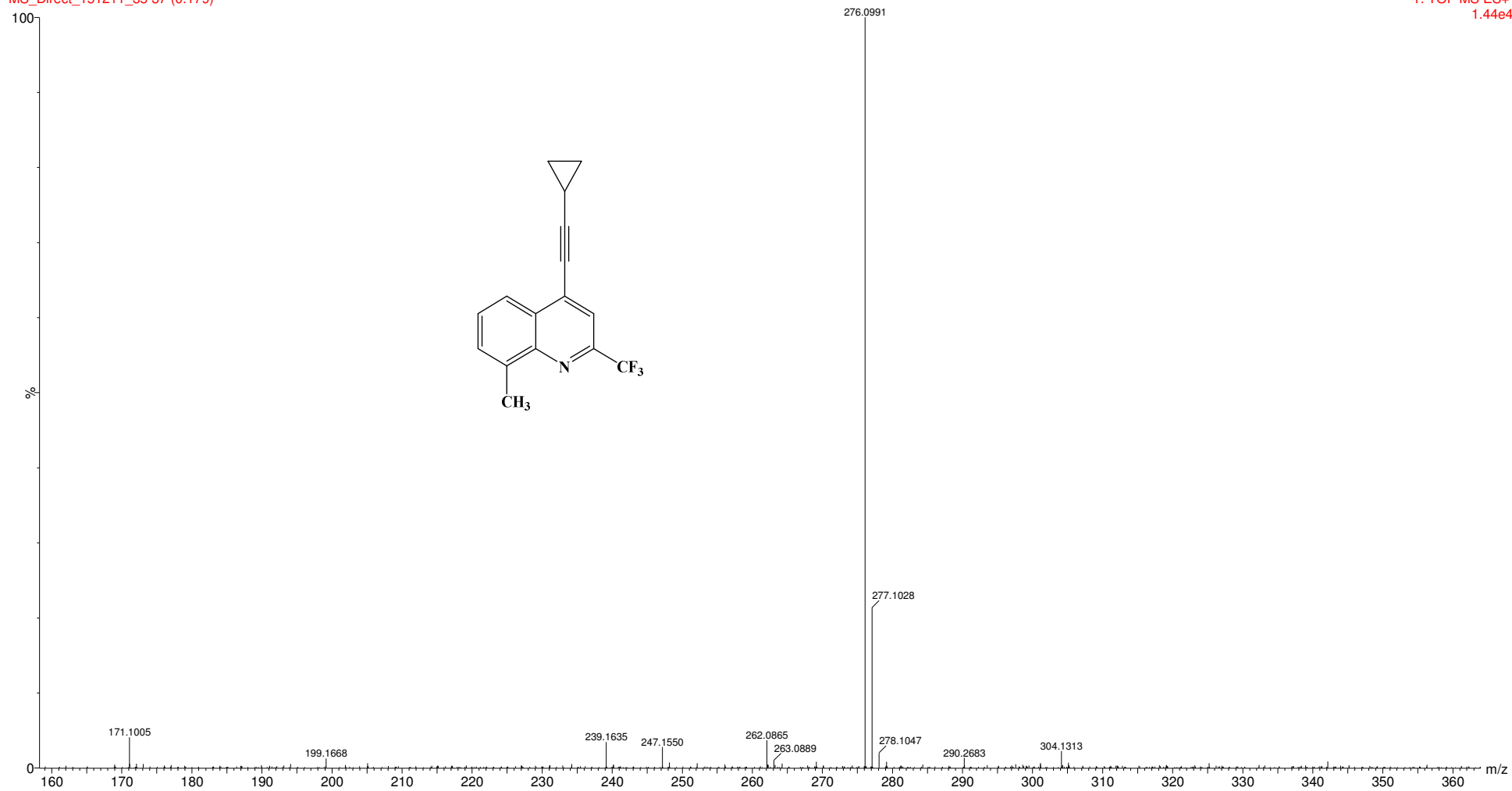
¹³C NMR spectrum of **4r**

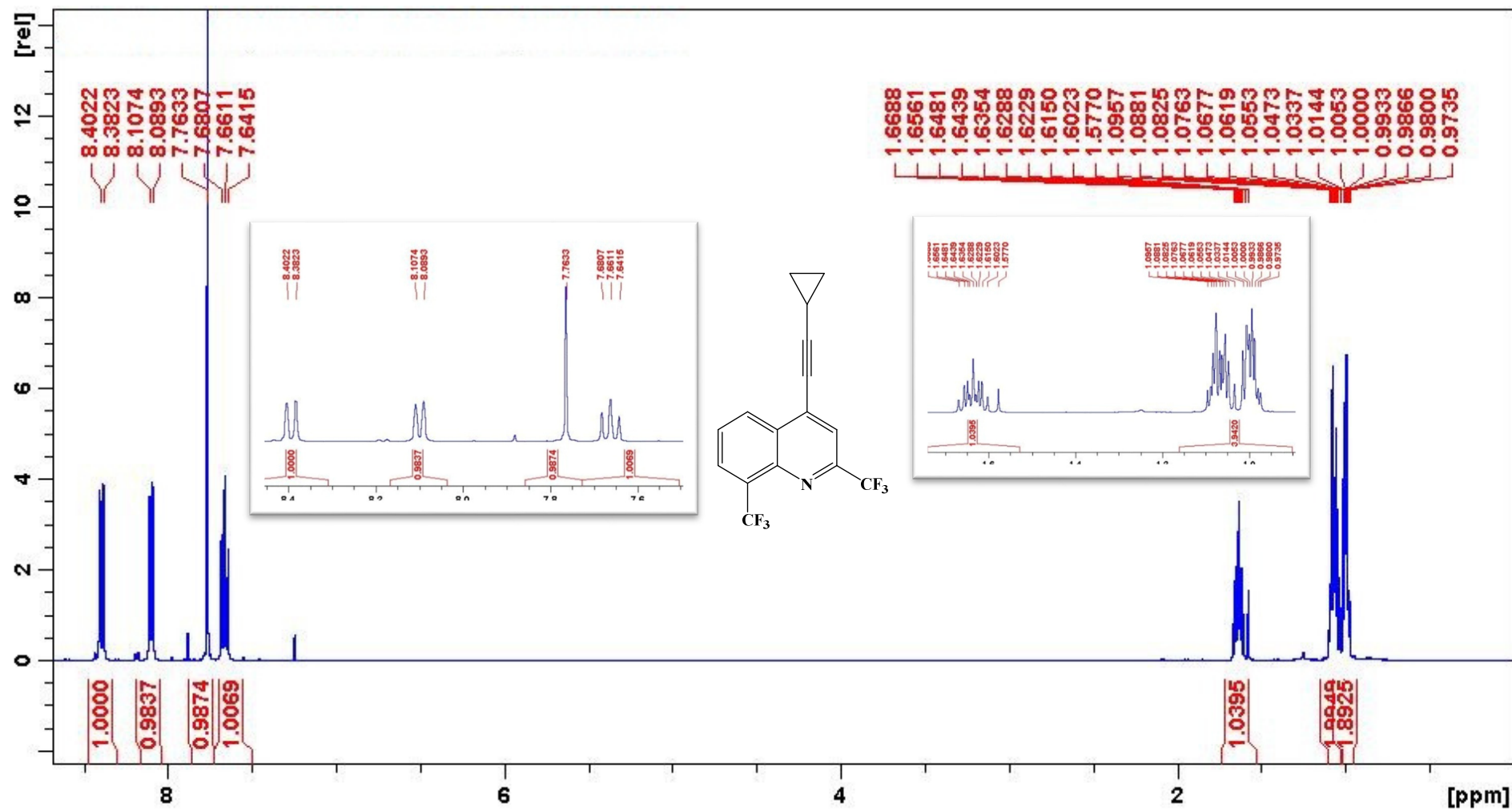
¹⁹F NMR spectrum of **4r**

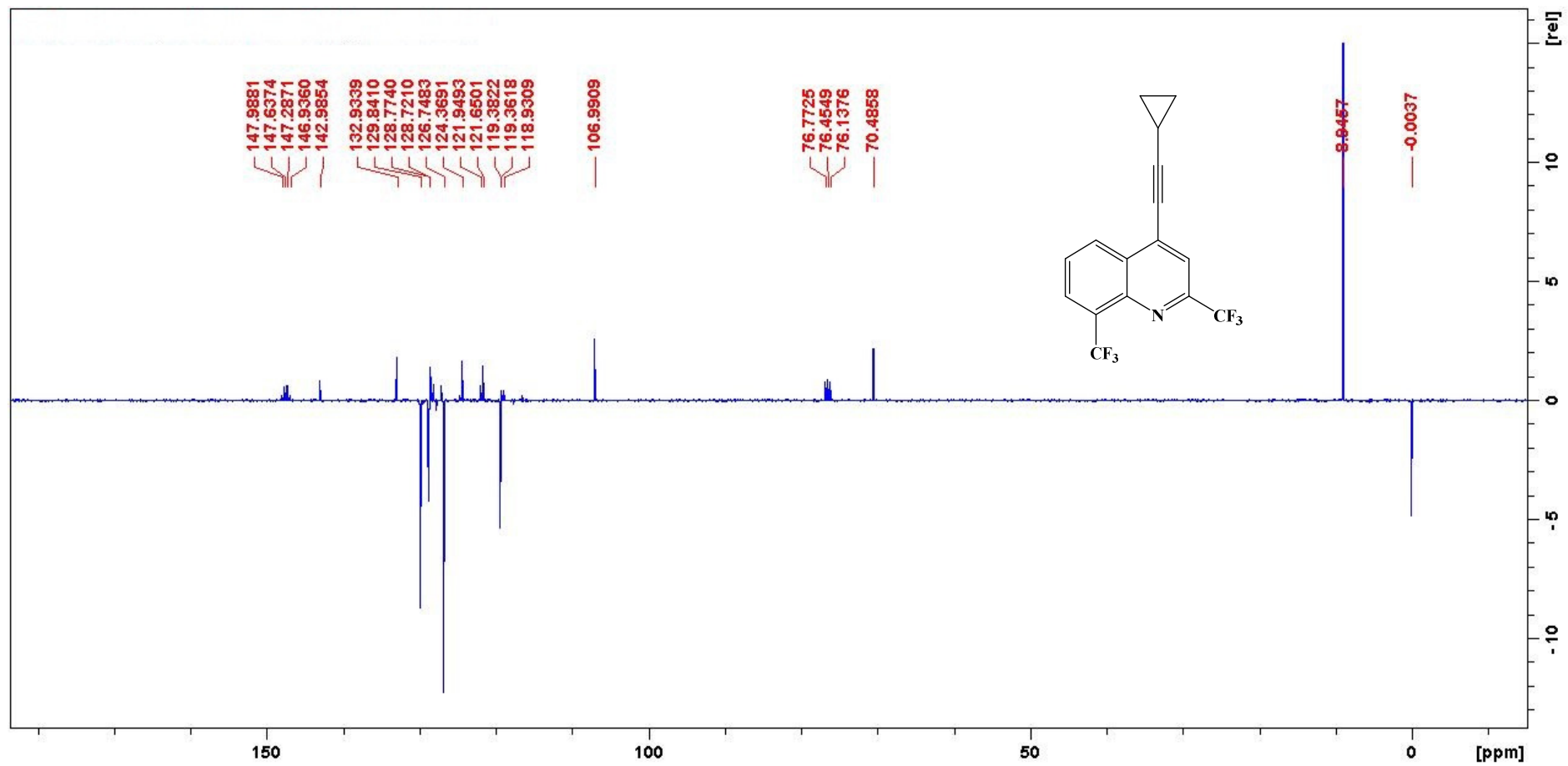
HRMS of 4r

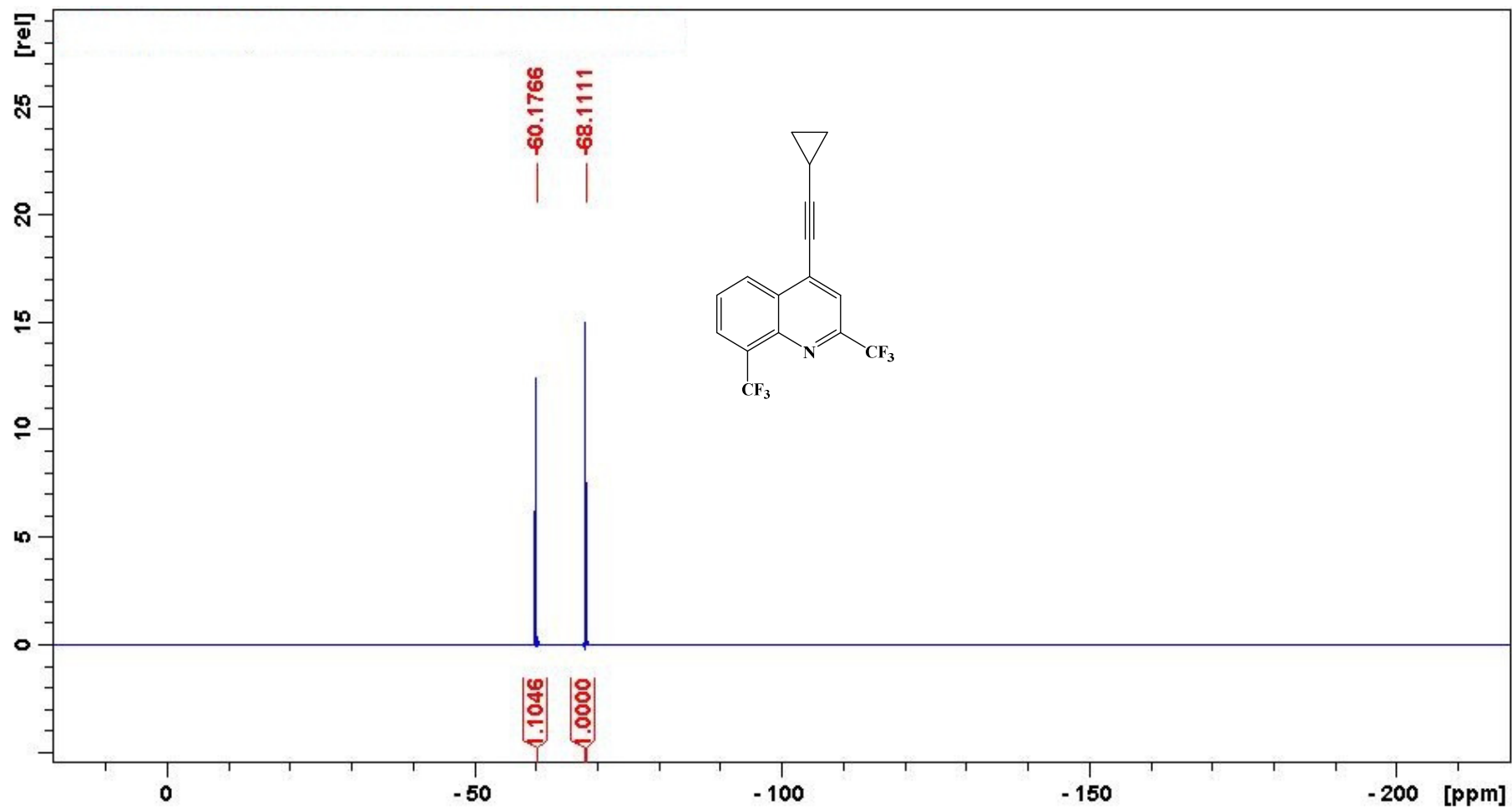
SA5

MS_Direct_151211_35 37 (0.179)

1: TOF MS ES+
1.44e4

¹H NMR spectrum of **4s**

^{13}C NMR spectrum of **4s**

¹⁹F NMR spectrum of **4s**

HRMS of 4s

SA6

MS_Direct_151211_36 35 (0.165) Cm (35:36)

1: TOF MS ES+
1.34e4